An investigation into the role of T follicular helper cells in follicular lymphoma

Phillips, Beth

Awarding institution:
King's College London

An Investigation into the Role of T Follicular Helper Cells in Follicular Lymphoma

Elizabeth Phillips

Student number: 1581408

A thesis submitted for the degree of MD(Res) in Cancer Studies

King's College London

March 2020

First supervisors: Dr Andrea Pepper and Dr Piers Patten

Second supervisor: Prof Stephen Devereux

DECLARATION

I hereby declare that I alone composed this thesis and the work is my own, except where stated otherwise.

Elizabeth Phillips, March 2020

ABSTRACT

Follicular lymphoma (FL) is the most common form of indolent lymphoma in northern Europe, with approximately 2000 cases diagnosed each year in the UK. It is a malignancy derived from germinal centre (GC) B-lymphocytes and is critically dependent on non-malignant immune cells within the tumour microenvironment (TME) for growth and survival. FL retains a follicular structure similar to reactive GCs and, like its non-malignant counterparts, is infiltrated by T follicular helper cells (T_{FH}). T_{FH} are a specialised subset of $CD4^+$ T-cells that are essential for supporting proliferation, affinity maturation and differentiation of healthy GC B-cells. In FL, T_{FH} appear to create a tumour-permissive environment that supports FL growth, although the mechanisms by which FL B-cells and T_{FH} provide mutual support are not known.

The aim of this thesis is to investigate the hypothesis that T_{FH} play a key role in driving FL growth and progression. Here, the nature of interactions between T_{FH} and FL B-cells, both in *in vitro* culture and in archival FL tissue, are explored using novel imaging techniques.

Firstly, it is shown that T_{FH} are identifiable within FL lymph node (LN) tissue and fine needle aspirate, comprising just over a quarter (28.6%) of all $CD4^+$ T-cells. Secondly, it is demonstrated that these FL cell suspensions can be used to explore the mutual role of T_{FH} and FL B-cells on cell survival and activation *in vitro.* Attempts were made to overcome the limited availability of LN tissue by generating T_{FH} from peripheral blood T-cells. However, it was not possible to successfully obtain cells with a true T_{FH} phenotype from either $CXCR5^+CD4^+$ T-cells or naïve T-cells.

In culture studies, expression of the activation markers CD86 and HLA-DR on FL B-cells was enhanced by co-culture with T_{FH}, but not by other, non-T_{FH} $CD4^+$ T-cells. FL B-cell survival was also higher in the presence of FL T-cells, including T_{FH}. Conversely, ICOS-L expression was lower on FL B-cells that were cultured with T_{FH}, compared to without, indicating the formation of active ICOS/ICOS-L interactions. ICOS stimulation is known to be critical for T_{FH} survival. Accordingly, co-culture with FL B-cells increased survival of T_{FH} and supported persistence of the T_{FH} phenotype *in vitro*. FL B-cells also increased expression of the activation marker CD69 on T_{FH}. These results demonstrate dynamic, mutually supportive interactions between T_{FH} and FL B-cells.

In FL tissue, there was a close spatial correlation between T_{FH} and expression of MYC in FL B-cells by confocal immunofluorescence microscopy. However, accurate characterisation of complex cell populations in FL tissue requires highly multiplexed imaging techniques. Use of imaging

mass cytometry (IMC) was explored as a novel method to assess spatial interactions of T_{FH} within the FL TME. This technique allowed assessment of 20 antigens within the same tissue section and could identify T_{FH} in archival FL tissue. It was possible to replicate previously published findings with confocal imaging by demonstrating a very close correlation between T_{FH} and FL proliferation. This novel imaging technique holds the ability to greatly enhance our knowledge of spatial interactions within FL tissue and potentially identify prognostic networks within the FL TME in future.

This thesis provides insights into the mechanisms by which T_{FH} and FL B-cells co-operate to provide mutual support and promote FL growth. T_{FH} therefore represent an exciting potential therapeutic target in FL. Given the critical role that the TME plays in supporting FL growth, better understanding of these interactions will assist in developing novel therapeutic strategies to improve patient outcomes.

ACKNOWLEDGEMENTS

First and foremost, I thank my supervisors, Dr Andrea Pepper, Dr Piers Patten and Prof Stephen Devereux, for inspiring and supporting this work throughout. It was their knowledge, experience and encouragement that made this work possible. My other colleagues within the lymphoma group provided hugely valuable support and advice, especially Dr Eve Coulter.

I am grateful to many colleagues at Kings College Hospital and Kings College London for their assistance throughout this research, in particular:

- The Lymphoma Team at Kings College Hospital for support in obtaining patient samples
- Dr Robert Marcus for his support, mentorship and helping us to obtain funding for this project
- Dr Jon Salisbury and the histopathology team at Kings College Hospital for providing archival tissue and histology advice
- Dr George Chennell at the Wohl Cellular Imaging Centre for providing microscopy training and guidance
- The entire team at the BRC Flow Core at Guys Hospital for their help with imaging mass cytometry and flow sorting, particularly Drs Katrina Todd, Richard Ellis and Ned Petryalko
- Prof Jo Spencer and Dr Thomas Tull at Kings College London for assistance with tissue processing and culture facilities
- Dr Thomas Seidl for keeping our laboratory and flow cytometer running in the face of numerous obstacles
- Drs Alan Ramsay and Benedetta Apollonio for their advice and technical support

I am also grateful to my other colleagues at University College London for providing me with financial support throughout this work and allowing flexibility in my job to allow this part-time research to succeed. I am particularly grateful to Dr Laura Clifton-Hadley, Professor David Linch and Paul Smith for their support and mentorship.

I am grateful to the British Society for Haematology for awarding an Early Stage Research Grant to support this thesis in its initial stages. F. Hoffman-La Roche supported this work in its latter stages through an unrestricted educational grant.

I am particularly thankful to the patients who altruistically donated samples and underwent fine needle aspirate to support these studies.

Finally, I thank my husband, Joe, for a sense of perspective, endless patience, excellent catering skills and unwavering support.

CONTENTS

Abstract 1
Acknowledgements 4
List of Abbreviations 10
List of Figures 13
List of Tables 15
Chapter 1: Introduction 16
1.1. T Follicular Helper Cells in Health and Disease 16
1.1.1. The Normal Germinal Centre Reaction 16
1.1.2. Affinity Maturation and AID 17
1.1.3. T Follicular Helper Cells 18
1.1.4. T_{FH} and GC B-cell Maturation 19
1.1.5. B-Cell Support for T_{FH} 20
1.1.6. T_{FH} Regulation and Homeostasis 20
1.1.7. T_{FH} Memory and Circulating T_{FH} 22
1.1.8. T_{FH} and Malignancy 22
1.2. Clinical Features of Follicular Lymphoma 23
1.2.1. Presentation and Natural History 23
1.2.2. Prognostic Factors 25
1.2.3. Histopathological Characteristics 26
1.3. Pathogenesis of Follicular Lymphoma 27
1.3.1. t(14;18) translocation 27
1.3.2. Epigenetic Dysregulation in FL 28
1.3.3. Other Genomic Aberrations in FL 29
1.3.4. Drivers of Genomic Instability in FL 30
1.3.5. Tumour Microenvironment in FL 31
1.3.6. Role of T-cells in FL 32
1.3.7. T Follicular Helper Cells in FL 33
1.3.8. Modulation of T_{FH} Activity in FL 35
1.3.9. Co-operation Between T_{FH} and the Wider Tumour Microenvironment 36
1.3.10. T_{FH} and Novel Therapies 37
1.4. Summary 40
1.5. Aims 41
Chapter 2: Materials and Methods 42
2.1. Patient Samples and Ethics 42
2.2. Peripheral Blood and Bone Marrow Mononuclear Cell Isolation 42

2.3. Fine Needle Aspiration 43
2.4. Lymph Node Disaggregation 44
2.5. Immunomagnetic Cell Selection 44
2.6. Cell Culture 45
2.7. Flow Cytometry 45
2.7.1. Viability Staining 45
2.7.2. Cell Surface Staining 46
2.7.3. Intranuclear Staining 46
2.7.4. Annexin V Staining 46
2.7.5. Sample Analysis by Flow Cytometry 47
2.7.6. Cell Counting 49
2.7.7. Control Samples and Other Considerations 50
2.7.8. Fluorescence-Activated Cell Sorting 52
2.8. Histology Studies 53
2.8.1. Tissue Sectioning and Deparaffinisation 53
2.8.2. Antigen Retrieval and Blocking 53
2.8.3. Primary Antibody Incubation 54
2.8.4. Secondary Antibody Incubation 55
2.8.5. Peroxidase and Haematoxylin Staining 56
2.8.6. Control Samples 57
2.8.7. Assessment of IHC staining 57
2.8.8. Confocal Immunofluorescence Microscopy 57
2.8.9. Confocal Image Analysis 59
2.8. Statistical Considerations 61
Chapter 3: Identifying T_{FH} in Follicular Lymphoma Tissue 63
3.1. Introduction and Aims 63
3.2. Identifying T_{FH} in Lymph Node Tissue 64
3.2.1. Background 64
3.2.2. Methods 65
3.2.3. Lymph Node Samples and Patient Characteristics 66
3.2.4. T_{FH} in FL LN Cell Suspensions 66
3.2.5. Characterisation of FL LN T_{FH} 70
3.2.6. Cell Yield 73
3.2.7. Reproducibility 75
3.2.8. Discussion 76
3.3. Characterisation of Peripheral Blood and Bone Marrow T-cells 76

3.3.1. Background 76
3.3.2. Bone Marrow T-Cells 77
3.3.3. Peripheral Blood T-Cells in Follicular Lymphoma and Healthy Controls 77
3.3.4. Discussion 80
3.4. Generating T_{FH}-like Cells from Naïve T-Cells 81
3.4.1. Background 81
3.4.2. Results 82
3.4.3. Discussion 83
Chapter 4: *In Vitro* Characterisation of T_{FH}:B-Cell Interactions in Follicular Lymphoma 87
4.1. Introduction 87
4.2. Methods 88
4.3. Results 89
4.3.1. Patients and Lymph Node Samples 89
4.3.2. Effect of T-Cell Depletion on FL Survival 91
4.3.3. Effect of T-Cell Depletion on FL B-Cell Phenotype 94
4.3.4. Effect of FL B-Cells on T_{FH} Survival 98
4.3.5. Effect of FL B-Cells on the T_{FH} Phenotype 101
4.4. Discussion 105
Chapter 5: Insights from Confocal Immunofluorescence Microscopy Studies 109
5.1. Introduction 109
5.2. Tissue Sections and Patient Characteristics 111
5.3. MYC and T_{FH} 112
5.3.1. Results 112
5.3.2. Discussion 117
5.4. Regulatory T-cells and T_{FH} 118
5.4.1. Results 118
5.4.2. Discussion 125
Chapter 6: Imaging Mass Cytometry as a Tool to Explore the Follicular Lymphoma Tumour Microenvironment 127
6.1. Introduction 127
6.2. Methods 128
6.2.1. Tissue Processing and Primary Antibody Staining 128
6.2.2. Antibody Selection, Optimisation and Panel Design 130
6.2.3. Controls 132
6.2.3. Image Acquisition and Analysis 133
6.3. Results 135
6.3.1. Multiparameter Assessment of FL Tissue and Identification of T_{FH} 135

6.3.2. Correlation with Confocal Imaging Results 139
6.4. Discussion 140
Chapter 7: Conclusions and Future Work 142
Appendix: Antigen Retrieval Buffers for FFPE Tissue 145
References 146

LIST OF ABBREVIATIONS

AID	Adenosine-induced cytidine deaminase
AITL	Angioimmunoblastic T-cell lymphoma
BCL2	B-cell lymphoma 2
BCL6	B-cell lymphoma 6
BCR	B-cell receptor
BMA	Bone marrow aspirate
BMMC	Bone marrow mononuclear cells
BTLA	B and T lymphocyte attenuator
CCR-	C-C chemokine receptor
CD	Cluster of differentiation
CD40L	CD40-ligand
CVP	Cyclophosphamide, vincristine and prednisolone chemotherapy
CHOP	Cyclophosphamide, hydroxydaunorubicin, vincristine (Oncovin) prednisolone
CIFM	Confocal immunofluorescence microscopy
CIITA	Class II transactivator
CLL	Chronic lymphocytic leukaemia
CREBBP	CREB binding protein
CSR	Class switch recombination
CXCR-	C-X-C motif chemokine receptor
DAB	Diaminobenzidine
DAPI	4’,6-diamino-2-phenylindole
DLBCL	Diffuse large B-cell lymphoma
DMSO	Dimethyl sulfoxide
DPBS	Dulbecco’s phosphate-buffered saline
EDTA	Ethylenediaminetetraacetic acid
FBS	Foetal bovine serum
FDC	Follicular dendritic cell
FFPE	Formalin-fixed, paraffin-embedded
FITC	Fluorescein isothiocyanate
FMO	Fluorescence minus one

FRC	Fibroblast reticular cell
FL	Follicular lymphoma
FLIPI	Follicular lymphoma international prognostic index
FNA	Fine needle aspirate
FFPE	Formalin fixed paraffin embedded
FoxP3	Forkhead box P3
g	Gravity
GC	Germinal centre
HLA-DR	Human leukocyte antigen DR isotype
ICOS	Inducible co-stimulator (CD278)
ICOS-L	Inducible co-stimulator ligand (CD275; B7-H2)
IF	Immunofluorescence
IFN	Interferon-γ
Ig	Immunoglobulin
IgH	Immunoglobulin heavy chain
IHC	Immunohistochemistry
IL-	Interleukin
IMC	Imaging mass cytometry
IU	International Units
KMT2D	Lysine methyltransferase 2D
LAG3	Lymphocyte-activating gene-3
LN	Lymph node
MFI	Median fluorescence intensity
MHC	Major histocompatibility complex
MSC	Mesenchymal stromal cell
NHL	Non-Hodgkin lymphoma
NRES	National Research Ethics Service
OS	Overall survival
PB	Peripheral blood
PBMC	Peripheral blood mononuclear cell
PBS	Phosphate-buffered saline

PD-1	Programmed death 1 (CD279)
PD-L1	Programmed death ligand 1 (CD278)
PD-L2	Programmed death ligand 2 (CD273)
PE	Phycoerythrin
PI3K	Phosphoinositide 3-kinase
psi	Pounds per square inch
rpm	Revolutions per minute
RPMI	RPMI-1640 culture medium (Roswell Park Memorial Institute)
RT	Room temperature
SAP	Signalling lymphocyte activation marker (SLAM)-associated protein
SHM	Somatic hypermutation
STAT	Signal transducer and activator of transcription
TCR	T-cell receptor
T_{FH}	T-follicular helper cells
T_{FR}	T-follicular regulatory cells
TGFβ	Transforming growth factor-β
Th-	T-helper cell
Tim3	T-cell immunoglobulin and mucin-domain containing-3
T_{reg}	Regulatory T-cell
TME	Tumour microenvironment
TNF	Tumour necrosis factor

LIST OF FIGURES

1.1. Diagrammatic representation of the germinal centre reaction 17

2.1. Identification of viable lymphocytes 49

2.2. Identification of counting beads by flow cytometry 50

2.3. Identification of $CD10^+$ germinal centre B-cells 51

2.4. Primary antibody optimisation 54

2.5. Fluorochrome excitation spectra and emission spectra 58

2.6. Confocal image analysis and binary image generation 60

2.7. Generation of intersection binary layers 61

3.1. Expansion of $CD19^+CD10^+$ germinal centre B-cells in FL 66

3.2. Identification of T_{FH} and T_{regs} in FL LN cell suspensions..... 68

3.3. PD-1 and ICOS identify a discrete population of $CXCR5^+$ T_{FH} FL LN tissue..... 69

3.4. Comparison of $CD4^+$ T-cell subsets in FL FNA and LN tissue 70

3.5. Comparison of gating strategies to identify T_{FH} 71

3.6. Prevalence of T_{regs} within T_{FH} subsets 72

3.7. BCL6 expression in FL LN $CD4^+$ T-cells 73

3.8. Absolute cell counts obtained from FL FNAs 74

3.9. Absolute B-cell numbers obtained from FL FNAs 75

3.10. Phenotype of bone marrow-derived T-cells 78

3.11. Comparison between $CD4^+$ T-cell subsets in FL patients and healthy controls 79

3.12. Median fluorescence intensity of T_{FH} markers in PB T-cells 80

3.13. Expression of T_{FH} markers following naïve T-cell stimulation 83

3.14. Effect of stimulation with T_{FH} cytokines on naïve T-cell phenotype 84

4.1. Gating strategy for fluorescence-activated cell sorting 91

4.2. Assessment of FL B-cell apoptosis by flow cytometry 92

4.3. Effect of T-cell depletion on FL B-cell viability 93

4.4. Expression of B-cell activation markers during in vitro culture 94

4.5. CD86 expression on FL B-cells in co-culture studies 95

4.6. HLA-DR expression on FL B-cells in co-culture studies 96

4.7. Influence of T-cells on ICOS-L expression in FL B-cells 97

4.8. Influence of FL B-cells on $CD4^+$ T-cell composition 98

4.9. Effect of B-cell depletion on T-cell survival 99
4.10. Influence of FL B-cells on T_{FH} viability 100
4.11. FL B-cells support maintenance of the T_{FH} phenotype 102
4.12. Influence of FL B-cells on T_{FH} phenotype 103
4.13. FL B-cells induce activation of T_{FH} 104
4.14. Influence of FL B-cells on T_{FR} 105
5.1. Immunofluorescence panel for assessment of T_{FH} and MYC expression 113
5.2. MYC expression in FL B-cells 114
5.3. Distribution of T_{FH} and MYC expression 115
5.4. Spatial interaction between T_{FH} and MYC^+ B-cells 116
5.5. Relationship between T_{FH} and MYC expression 117
5.6. Immunofluorescence panel for visualisation of T_{FH} and T_{regs} 119
5.7. $FoxP3^+$ cells are $CD4^+$ T-cells 120
5.8. Distribution of T_{FH} and T_{regs} in FL tissue 121
5.9. Correlation between T_{FH} and T_{FR} in FL tissue 122
5.10. Correlation between T_{FR} and clinical outcomes in FL 123
5.11. Clinical outcomes according to the balance between follicular T_{FH} and T_{reg} 124
6.1. Overview of Imaging Mass Cytometry 128
6.2. Antibody validation after metal tagging 131
6.3. Imaging Mass Cytometry analysis and cell segmentation 134
6.4. Multiparameter assessment of FL tissue by IMC 136
6.5. Follicular PD-1 staining by Imaging Mass Cytometry 137
6.6. Identification of T-cells and proliferating B-cells by IMC 138
6.7. Relationship between T_{FH} and proliferating B-cells 139
6.8. Correlation between T_{FH} numbers by CIFM and IMC 140

LIST OF TABLES

1.1. Histological grading in FL 26
2.1. List of antibodies for flow cytometry 47
2.2. Primary antibodies for immunohistochemistry and immunofluorescence studies 55
2.3. Secondary antibodies for immunohistochemistry and immunofluorescence studies 56
2.4. Filters used for confocal immunofluorescence microscopy 58
3.1. Baseline patient characteristics 67
3.2. Reproducibility of FNA results 75
4.1. Patient characteristics 90
5.1. Patient characteristics 111
6.1. List of metal-conjugated antibodies for IMC 129
6.2. Metal isotope purity matrix 132

CHAPTER 1: INTRODUCTION

The principal role of B lymphocytes is to produce a diverse and specific range of antibodies that provide humoral immunity against a large range of pathogens. In order to achieve this, maturing B-lymphocytes undergo rapid proliferation and a series of genomic changes that enhance their affinity for target pathogens. This requires support from a specialised subset of T-cells: T-follicular helper cells (T_{FH}). However, these processes are error-prone and can lead to the development of malignant lymphoma. Follicular lymphoma (FL) is a malignancy derived from germinal centre (GC) B-cells. It is characteristically infiltrated by T_{FH}, which play a key role in supporting FL growth and progression. This chapter first details the role of T_{FH} within normal lymphoid tissue, before outlining the clinical features of FL and lastly describing the role of T_{FH} in the pathogenesis of FL.

1.1. T Follicular Helper Cells in Health and Disease

1.1.1. The Normal Germinal Centre Reaction

The germinal centre (GC) is a specialised structure within secondary lymphoid tissue that is responsible for B lymphocyte maturation, leading to the generation of highly specific, affinity-matured antibody responses. GCs form a niche where B lymphocytes are able to form antigen-dependent interactions with T-cells, supported by follicular dendritic cells (FDCs) and other stromal cells, which induce GC B-cell survival, proliferation and maturation. Normal GCs show evidence of polarisation, with 'light zones', where B-cells interact with cognate (antigen-specific) T-cells, and 'dark zones' comprised primarily of rapidly proliferating B-cells, known as 'centroblasts' (Figure 1.1) (De Silva and Klein 2015).

T follicular helper cells (T_{FH}), are a specialised subset of $CD4^+$ T-cells that are resident solely within secondary lymphoid tissue and are responsible for providing help to maturing B-cells. T_{FH} are the rate-limiting step in the GC reaction that determines B-cell fate and proliferation (Gitlin*, et al* 2014). Competition for T_{FH} support ensures that survival and proliferation signals are only provided to GC B-cells expressing high-affinity immunoglobulins (Ig) in a process known as positive selection. Interaction with T_{FH} is also necessary to initiate class switch recombination (CSR) and somatic hypermutation (SHM) in GC B-cells, the two essential processes required for Ig affinity maturation (Crotty 2014). Interactions with T_{FH} in the light zone trigger migration of GC B-cells into the dark zone, where they undergo rapid clonal proliferation and SHM. GC B-cells then return to the light zone, where they receive further T_{FH} support, which determines

whether they undergo additional cycles of proliferation or differentiate (Luo, *et al* 2018). This GC reaction is essential for generating an effective humoral immune response and creating B-cell memory for long term immunity.

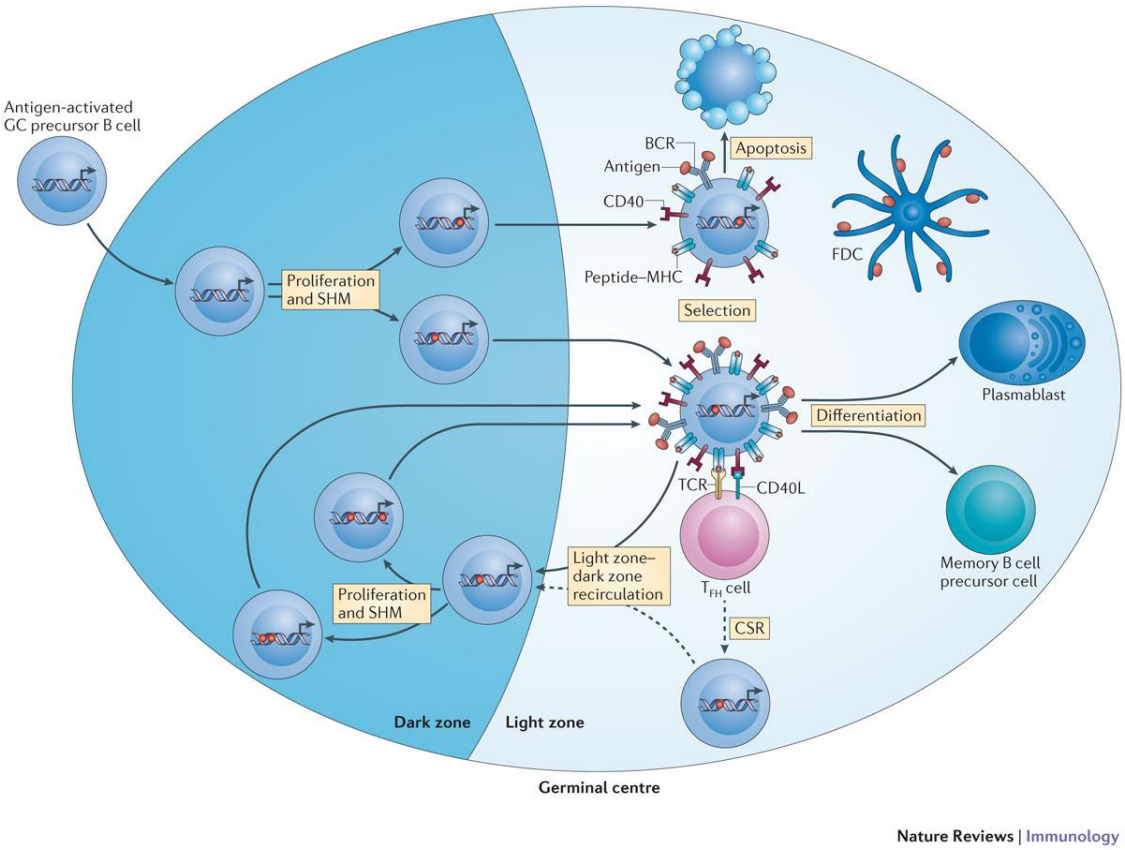

***Figure 1.1*. Diagrammatic representation of the germinal centre reaction**. *T_{FH} (pink) provide B-cell support to drive B-cell proliferation, differentiation, CSR and SHM. Reprinted by permission from Springer Nature: Dynamics of B-cells in Germinal Centres, De Silva and Klein, Nature Reviews Immunology 2015;15:137-148 ©.*

1.1.2. Affinity Maturation and AID

During CSR, double-stranded DNA breaks are introduced to allow switching of the Ig heavy chain locus and production of Ig isotypes other than IgM, appropriate to the anatomical location and pathogen. SHM is a process of targeted mutagenesis within the Ig variable region genes (*IgV*) that alters affinity for the target antigen. Both CSR and SHM are processes critically dependent on the action of the DNA-modifying enzyme activation-induced cytosine deaminase (AID) (Muramatsu, *et al* 2000, Revy, *et al* 2000). AID directly induces targeted mutagenesis of Ig genes through deamination of cytosine residues and replacement by uracil on single-stranded DNA in

proliferating lymphocytes. This leads to base pair transitions and transversions, as well as the double-stranded DNA breaks that facilitate CSR. AID-related mutations are identifiable by their predilection for WRCY base pair sequences (Martin*, et al* 2002).

These processes allow generation of highly-specific antibodies against a diverse range of pathogens but the unique DNA remodelling events that occur during B-cell maturation also make B-lymphocytes susceptible to developing deleterious mutations and chromosomal translocations involving Ig genes. Physiological AID-related mutations within the Ig genes are described as 'on-target', however aberrant or 'off-target' action of AID on other genes has been implicated in lymphomagenesis (Alexandrov*, et al* 2013, Pasqualucci*, et al* 2008, Ramiro*, et al* 2004).

1.1.3. T Follicular Helper Cells

T_{FH} are crucial for all stages of the GC reaction. In the absence of T_{FH}, GCs do not form, and B-cells cannot undergo CSR or SHM. Patients carrying mutations that block critical steps in T_{FH} maturation and/or function exhibit marked defects in humoral immunity and lose the ability to produce non-IgM, affinity-matured antibodies or B-cell memory in response to pathogens or vaccination (Ma and Deenick 2014).

Providing help to developing B-cells was the first known functions of T-cells and it has been known for over 50 years that antibody production requires the presence of T-cells (Crotty 2015). The existence of a specialised subset of T-helper (Th) cells responsible for B-cell help was first postulated two decades ago, and identified as a subset of $CD4^+$ T-cells expressing high levels of the chemokine receptor CXCR5 (C-X-C Motif Chemokine Receptor-5) that were able to greatly amplify IgG production (Schaerli*, et al* 2000). These cells were shown to have an effector memory T-cell phenotype, lack expression of CD62-ligand and CCR7 (C-C chemokine receptor 7), and were highly activated, expressing the activation markers CD69, Human Leukocyte Antigen-DR (HLA-DR) and inducible co-simulator (ICOS). It is now known that CXCR5 expression, together with downregulation of CCR7, is required for T_{FH} migration and entry into the GC (Lu*, et al* 2011). CXCL13 (C-X-C Motif Ligand-13) is the main chemoattractant responsible for recruiting $CXCR5^+$ T_{FH} and B-cells to the GC, and is released by T_{FH}, FDCs and other stromal cells.

The identification of BCL6 (B-cell lymphoma-6) as the lineage-defining T_{FH} transcription factor greatly amplified interest and advanced study in the field of T_{FH} biology (Johnston*, et al* 2009, Nurieva*, et al* 2009). BCL6 is the master regulator of the GC phenotype and is expressed in both

T_{FH} and GC B-cells. BCL6 is an obligate repressor of gene expression and co-operates with multiple other transcription factors to maintain the GC transcription programme (Crotty 2019). It also represses expression of Blimp1 (B lymphocyte-induced maturation protein-1), a selective inhibitor of T_{FH} differentiation that reprograms T-cells towards alternative cell fates (Johnston*, et al* 2012, Johnston*, et al* 2009).

1.1.4. T_{FH} and GC B-cell Maturation

The basic requirements to support GC B-cell maturation are CD40-ligand (CD40L) signalling, Interleukin (IL)-4 and IL-21, all of which are primarily supplied by T_{FH} within the GC niche (Crotty 2015). CD40 is expressed on activated T-cells and is a critical regulator of B-cell survival. CD40 plays a key role in positive selection of high-affinity B-cells and directly promotes the development of plasmablasts in a dose-dependent manner (Ise*, et al* 2018). CD40 signalling is required for expression of MYC, a key cell cycle regulator and mediator of positive selection, which initiates shuttling of GC B-cells to the dark zones and B-cell proliferation (Dominguez-Sola*, et al* 2012, Luo*, et al* 2018). CD40L is also necessary to initiate CSR. Patients lacking CD40 or CD40L develop hyper-IgM syndrome, an immunodeficiency characterised by the absence of GC formation, Ig class switching and antibody responses to T-cell dependent antigens, which leads to early, recurrent bacterial infections (Ma and Deenick 2014).

T_{FH} provide cytokine-mediated help to GC B-cells through release of IL-4 and IL-21. T_{FH} characteristically release extremely small quantities of cytokines, providing a very constrained resource in order to facilitate positive selection (Dan*, et al* 2016). Although not specific to T_{FH}, IL-21 is considered the signature T_{FH} cytokine and is a potent inducer of B-cell proliferation, AID expression and plasma cell differentiation, particularly when combined with CD40 stimulation (Eto*, et al* 2011, Konforte*, et al* 2009). IL-21 also upregulates CD86 expression on GC B-cells, which in turn provides positive feedback and vital co-stimulation to T_{FH} (Attridge*, et al* 2014). IL-4 is expressed later in T_{FH} maturation and co-cooperates with IL-21 to provide maximum B-cell support (McGuire*, et al* 2015, Weinstein*, et al* 2016).

Stable cell adhesion, mediated through the signalling and lymphocyte activation molecule (SLAM) family of receptors, is required for effective interactions between T_{FH} and B-cells within the GC. In particular, the absence of SLAM-associated protein (SAP) expression on T-cells leads to the complete absence of GC formation with a virtual absence of both T_{FH} and GC B cells (Crotty 2014, Lu*, et al* 2011, Qi*, et al* 2008).

1.1.5. B-Cell Support for T_{FH}

T_{FH} are dependent on reciprocal B-cell support for their development and survival under physiological conditions (Choi*, et al* 2013). GC B-cells provide key T-cell activation signals through both cognate T-cell receptor (TCR) interactions and CD28-mediated co-stimulation. Sustained cognate TCR stimulation, either from B-cells or other antigen presenting cells, is necessary for T_{FH} maturation, proliferation and persistence (Deenick*, et al* 2010, Johnston*, et al* 2009). The CD28 ligands CD80 and CD86 are both expressed on activated B-cells and are essential for T_{FH} formation and development of GCs (Wing*, et al* 2014). CD86 appears to be the more potent and specific inducer of T_{FH} differentiation, with minimal effect on development of other Th subsets (Salek-Ardakani*, et al* 2011). *CD80* knockout in mice also results in reduced T_{FH} numbers, loss of the T_{FH} phenotype and reduced cytokine synthesis (Good-Jacobson*, et al* 2012).

B-cells also provide vital inducible co-stimulator (ICOS) stimulation, which is essential for maintenance of the T_{FH} phenotype (Choi*, et al* 2011). ICOS ligation upregulates BCL6 and CXCR5 expression in T_{FH} through activation of phosphoinositide 3-kinase-δ (PI3Kδ). Blockade of ICOS results in rapid and near complete loss of T_{FH} phenotype, with downregulation of BCL6 and upregulation of other transcription factors that reprogram cells away from a T_{FH} phenotype (Stone*, et al* 2015, Weber*, et al* 2015). Patients with homozygous *ICOS* deficiency have marked hypogammaglobulinaemia, reduced circulating B-cells and $CD4^{+}CXCR5^{+}$ T-cells (Bossaller*, et al* 2006, Grimbacher*, et al* 2003).

Bi-directional ICOS/ICOS-ligand (ICOS-L) interactions between T_{FH} and GC B-cells are mutually beneficial. Following TCR ligation, T_{FH} induce increased ICOS-L expression in cognate B-cells through both CD40/CD40L signalling and by release of the neurotransmitter dopamine, which stimulates very rapid translocation of ICOS-L to the surface membrane. This feed-forward loop strengthens the immune synapse between T_{FH} and GC B-cells, thus enhancing CD40/CD40L signalling and is necessary for the selection of high-affinity B-cells (Liu*, et al* 2014, Papa*, et al* 2017).

1.1.6. T_{FH} Regulation and Homeostasis

Given the critical role of T_{FH} in determining the rate of B-cell proliferation, tight control of T_{FH} activity is required to ensure GC homeostasis. Excess or indiscriminate T_{FH} activity results in increased survival of low-affinity B-cells, impaired quality of antibody responses and has been

implicated in the development of immune and inflammatory disorders (Fu*, et al* 2018). T follicular regulatory cells (T_{FR}) are a subset of regulatory T-cells that reside primarily within GCs and are responsible for limiting T_{FH} and GC B-cell activity (Linterman*, et al* 2011). T_{FR} share many characteristics with T_{FH}, including BCL6, CXCR5, ICOS and PD-1 expression, but can be differentiated by expression of CD25 and the regulatory transcription factor Forkhead Box P3 (FoxP3). Both regulatory T-cells (T_{regs}) and T_{FR} can restrict generation of T_{FH} and GC formation, principally through CTLA4 (Cytotoxic T-lymphocyte-associated protein 4)-mediated downregulation of the co-stimulatory molecules CD80 and CD86 (Wang*, et al* 2015, Wing*, et al* 2014).

Very high levels of the inhibitory receptor PD-1, encoded by the *Pdcd1* gene, are unique to T_{FH}, and are thus postulated to play a key role in regulating T_{FH} function (Crotty 2014). PD-1 signalling dampens CD3 and CD28 signalling and reduces numbers of T_{FH}. The PD-1 ligands- PD-L1 and PD-L2- are variably expressed by B-cells, macrophages and dendritic cells. Overexpression of PD-L1 impairs IL-21 expression and Ig production (Cubas*, et al* 2013, Hams*, et al* 2011). However, the effects of PD-1 on T_{FH} function are complex. PD-1 modulates chemotaxis in response to CXCR5 signalling and promotes the localisation of T_{FH} within GCs (Shi*, et al* 2018a). PD-1 signalling is also necessary for IL-21 expression; mice with homozygous *Pdcd1* knockout have impaired production of IL-21 and IL-4, a reduction long-lived plasma cells and lower serum Ig levels, despite an overall increase in T_{FH} numbers (Good-Jacobson*, et al* 2010). Therefore, in addition to the known inhibitory effects, PD-1 signalling can enhance T_{FH} function and promote high-affinity antibody production.

HVEM (Herpes virus entry modulator; also known as TNFRSF14) is a member of the TNF (tumour necrosis factor) receptor superfamily, which, in conjunction with its inhibitory co-partner BTLA (B and T lymphocyte attenuator), functions as a negative regulator of lymphocyte activation and proliferation (Vendel*, et al* 2009). Both BTLA and HVEM are variably expressed on normal B- and T-lymphocytes, and T_{FH} characteristically express high levels of BTLA. In normal GCs, BTLA engagement on T_{FH} by HVEM inhibits TCR signalling and subsequent upregulation of CD40L, thereby limiting the provision of help to GC B-cells. HVEM-deficient GC B-cells have increased proliferation and a competitive advantage over HVEM-replete B-cells, which is dependent on the presence of T_{FH} (Mintz*, et al* 2019).

1.1.7. T_{FH} Memory and Circulating T_{FH}

Memory T_{FH} cells exist within secondary lymphoid tissue that can be adoptively transferred and re-establish a full, active T_{FH} phenotype upon antigen rechallenge (Choi*, et al* 2011, Hale*, et al* 2013). $CD4^+CXCR5^+$ T-cells in the peripheral blood (PB) have been postulated as the circulating counterpart of memory T_{FH}. The differentiation of such PB T_{FH}-like cells (PB-T_{FH}) requires transient BCL6 expression and ICOS stimulation but does not require exposure to GCs, as they are preserved in patients with profound GC T_{FH} defects such as SAP deficiency (He*, et al* 2013), therefore the extent to which they represent bona fide memory T_{FH} is unclear. They also have marked phenotypic differences from effector T_{FH}, with absent BCL6 and ICOS expression, increased CCR7 expression and variable expression of PD-1 (Schmitt*, et al* 2014b). Nevertheless, PB-T_{FH} demonstrate enhanced ability to support IgG production and plasmablast differentiation, compared with CXCR5-negative PB T-cells (Morita*, et al* 2011). The ability of PB-T_{FH} to provide B-cell help can be predicted according to expression of additional chemokine receptors. PD-1^+CCR7^{lo} PB-T_{FH} are more polarised towards a full T_{FH} phenotype and possess enhanced ability to provide B-cell help compared with PD-1^- or $CCR7^+$ PB-T_{FH} (He*, et al* 2013). PB-T_{FH} that co-express CXCR3 have reduced ability to stimulate Ig secretion and are skewed towards expression of Th1 (type 1 T helper cells) cytokines, such as interferon-γ (IFNγ) (Morita*, et al* 2011).

1.1.8. T_{FH} and Malignancy

T_{FH} are present within a range of solid organ malignancies, including breast, colorectal cancer and lung adenocarcinomas, although their role in these malignancies has not yet been fully explored. In general, higher numbers of intra-tumoural T_{FH} and increased expression of T_{FH} genes both correlate with less advanced tumour stage and improved survival (Bindea*, et al* 2013, Gu-Trantien*, et al* 2013). T_{FH} in these cancers are associated with formation of ectopic GC-like lymphoid structures and correlate with neoantigen load, therefore improved outcomes are likely to reflect organised anti-tumour immunity rather than any direct interaction between T_{FH} and malignant cells *per se* (Ng*, et al* 2018). However, there are conflicting reports on the role of T_{FH} in anti-tumour immunity, potentially due to different methods of identifying and defining T_{FH} within malignant tissue. For example, IL-21 is reported to enhance CD8-mediated anti-tumour responses, albeit derived from $CXCR5^+$ 'T_{FH}' that were described as PD-1-negative (Shi*, et al* 2018b), whilst T_{FH}-derived IL-4 has been reported to inhibit anti-tumour immunity (Shirota*, et al* 2017).

T_{FH} are the postulated cell of origin for a range of aggressive T-cell lymphomas, now defined under the entity 'nodal peripheral T-cell lymphoma with T_{FH} phenotype', which includes angioimmunoblastic T-cell lymphoma (AITL) (Swerdlow*, et al* 2016). These lymphomas are closely related to T_{FH}, both in terms of gene expression profile and surface phenotype, with expression of BCL6, CXCR5, PD-1, ICOS, SAP and CXCL13. AITL is characterised by a dense infiltrate of proliferating B-cells and FDCs, forming GC-like 'follicles' (de Leval*, et al* 2007, Swerdlow*, et al* 2008). A recurrent G17V mutation in the *RHOA* gene occurs in 68-70% of AITLs and drives development of a T_{FH} phenotype (Sakata-Yanagimoto*, et al* 2014). Similar to their non-malignant counterparts, *RHOA* G17V^{+} lymphomas show a dependence on ICOS signalling, which is provided by ICOS-L-expressing non-neoplastic cells within the tumour microenvironment (TME) (Cortes*, et al* 2018). The importance of CD28 signalling in these lymphomas is highlighted by the occurrence of recurrent translocations and activating mutations, which increase binding affinity to CD86 (Rohr*, et al* 2016, Yoo*, et al* 2016).

Conversely, follicular lymphoma (FL) is a malignancy of GC B-cells that characteristically forms neoplastic follicles enriched with non-malignant T_{FH} and FDCs, and is also dependent on survival signals from its non-malignant tumour microenvironment (TME) (Ame-Thomas and Tarte 2014). The role of T_{FH} in the pathobiology of FL is the focus of this thesis and is described in further detail below.

1.2. Clinical Features of Follicular Lymphoma

1.2.1. Presentation and Natural History

FL is the most common form of indolent non-Hodgkin lymphoma (NHL) in the UK, with an incidence of 3-4 persons per 100,000/year, equating to approximately 2200 new cases occurring per year. The incidence rises with age, with a median age at diagnosis of 65 years (Smith*, et al* 2015). FL has a striking geographical distribution; it is one of the predominant forms on lymphoma in Europe and North America but is relatively rare amongst Asian communities (Anderson*, et al* 1998).

Whilst FL can arise within almost any tissue in the body, usual sites of involvement are secondary lymphoid organs and the bone marrow. Typical presenting features include painless lymphadenopathy and/or 'B-symptoms' (weight loss, night sweats and/or fevers) related to increased metabolic activity. A smaller proportion of patients present with anaemia or other cytopenias related to bone marrow infiltration, or obstructive symptoms due to the bulk effect

of large tumour masses. FL is increasingly diagnosed as an incidental finding in asymptomatic patients, following investigation for other medical conditions.

For the small proportion of patients (approximately 10%) that present with localised (stage I) disease, radiotherapy alone confers long-term disease-free survival rates of 40-50%, potentially signifying disease cure (Guadagnolo*, et al* 2006, Mac Manus and Hoppe 1996, Petersen*, et al* 2004). However, for the majority of patients that present with widespread disease, FL is ultimately incurable with conventional immunochemotherapy regimens. The aim of treatment is therefore to achieve prolonged clinical remission and therapy is usually deferred until patients become symptomatic or develop high tumour bulk (Brice*, et al* 1997). Choice of frontline chemotherapy regimen is a matter of considerable debate but usually comprises either bendamustine, CVP (cyclophosphamide, vincristine, prednisolone) or CHOP (CVP plus doxorubicin) (Hiddemann*, et al* 2018, Rummel*, et al* 2013). The addition of anti-CD20-directed monoclonal antibody therapy to chemotherapy has markedly improved progression-free survival in FL and is standard of care, principally with either rituximab or obinutuzumab (Hiddemann*, et al* 2005, Marcus*, et al* 2017, Marcus*, et al* 2008). Following immunochemotherapy 'induction', treatment usually continues with single agent anti-CD20 'maintenance' treatment for 2 years, to prolong duration of remission (Salles*, et al* 2011). Allogeneic stem cell transplantation is the only therapy that is potentially curative for those with advanced stage (widespread) disease but, due to significant transplant-related mortality and morbidity, it is usually reserved for multiply relapsed or refractory cases and is only available to a select few FL patients, considering patient age and comorbidities (Sureda*, et al* 2018).

Median overall survival (OS) has increased with modern treatment regimens to an estimated 15-20 years (Junlen*, et al* 2015, Sant*, et al* 2014). Despite a prolonged clinical course and favourable long-term survival rates, progressive resistance to immunochemotherapy usually occurs with successive lines of treatment. FL remains the leading cause of death, with half of FL patients dying of their primary disease (Sarkozy*, et al* 2017). The clinical heterogeneity of FL is well recognised; an estimated 20% of patients with FL never require treatment (Ardeshna*, et al* 2003), whilst a further 20% progress rapidly and have significantly shortened survival. For patients that progress within 5 years of initial immunochemotherapy, the 5-year OS rate is only 50%, compared with 90% for all other FL patients (Casulo*, et al* 2015). In addition, transformation to forms of aggressive NHL, largely diffuse large B-cell lymphoma (DLBCL), which is associated with inferior outcomes, occurs in an estimated 1-3% of FL patients per year, necessitating treatment with intensive chemotherapy (Link*, et al* 2013, Sarkozy*, et al* 2016).

1.2.2. Prognostic Factors

Developing strategies to prospectively identify and effectively treat patients with a more aggressive clinical course is a major priority in FL. Clinical scoring systems, including the follicular lymphoma prognostic index (FLIPI), FLIPI2 and PRIMA prognostic index have prognostic value (Bachy*, et al* 2018, Federico*, et al* 2009, Solal-Céligny*, et al* 2004) but lack sufficient accuracy to predict those likely to develop early progression or disease transformation (Casulo*, et al* 2015, Jurinovic*, et al* 2016). Tumour parameters on baseline ^{18}FDG-PET (18-fluorodeoxyglucose positron emission tomography) imaging, such as metabolic tumour volume and maximum standardised uptake value (SUV_{max}), can potentially predict outcomes after immunochemotherapy but require validation and remain research tools at present (Cottereau*, et al* 2016, Meignan*, et al* 2016).

A number of secondary treatment endpoints can identify patients with residual disease after treatments that have inferior outcomes. This may warrant treatment with novel agents, entry intro clinical trials or treatment intensification. Prognostic markers include ^{18}FDG-PET response (Trotman*, et al* 2011) and minimal residual disease (MRD) negativity in the blood and bone marrow (Pott*, et al* 2016) after induction immunochemotherapy. Early relapse is also a very strong predictor of adverse outcomes, whether assessed by progression-free survival at 12 or 24 months or measured by the presence of ongoing complete remission at 30 months post-treatment (Casulo*, et al* 2015, Maurer*, et al* 2016, Shi*, et al* 2017). However, none of these measures are able to prospectively identify those with aggressive disease at the time of diagnosis.

Current prognostic indicators are imperfect as they do not reflect the underlying disease biology. A number of groups have tried to address this by developing clinico-biological risk scores. These include the M7-FLIPI and POD24-PI, both of which incorporate mutational analysis of up to 7 genes alongside clinical variables and correlate well with progression-free survival at 24 months (Jurinovic*, et al* 2016, Pastore*, et al* 2015). A risk score based on expression of 23 genes can also predict early relapse in FL patients receiving R-CHOP or R-CVP chemotherapy (Huet*, et al* 2018). However, the prognostic value of these clinico-biological risk scores is strongly influenced by the nature of any treatment given; for example, gene expression profiling does not predict outcomes for the increasing number of patients receiving frontline bendamustine chemotherapy (Bolen*, et al* 2019). Furthermore, it is unclear how many of the genes included in these risk scores contribute to FL pathogenesis. The cellular pathways that drive aggressive

disease and high-grade transformation are incompletely understood, which ultimately limits our ability to predict disease behaviour or improve outcomes by developing targeted biological therapy for these high-risk patients.

1.2.3. Histopathological Characteristics

FL is a malignancy of GC B-lymphocytes, expressing B-cell and GC markers, including CD19, CD20, CD22, CD79a, surface immunoglobulin, CD10 and BCL6. Unlike their benign counterparts, FL B-cells characteristically ectopically express the anti-apoptotic protein BCL2 (Marafioti*, et al* 2013, Swerdlow*, et al* 2008). FL retains organised FDC networks, expressing CD21 and CD23, which support GC-like structures known as malignant follicles, along with variable numbers of macrophages, stromal cells., T_{FH} and other T-cells. Unlike reactive GCs, FL follicles lack zonation; small condensed 'centrocytic' B-cells, which usually predominate in reactive GC light zones, are mixed with larger centroblasts that resemble proliferating dark-zone B-cells (Swerdlow*, et al* 2008).

Histological grading is based on the number of centroblasts visible per high-powered microscope field (Table 1.1). FL grade correlates with tumour proliferation fraction, but this does not reflect the clinical phenotype or translate to a difference in survival (Klapper*, et al* 2007). The exception is grade 3B FL, which is comprised of sheets of centroblasts, without centrocytes. Grade 3B FL frequently contains areas of high-grade B-cell lymphoma, has poorer outcomes compared with grades 1-3A and is usually considered a transformed lymphoma, rather than indolent FL (Wahlin*, et al* 2012).

Table 1.1. Histological grading in FL. *HPF: high-powered field*

Grade	Definition
1	0-5 centroblasts per HPF
2	6-15 centroblasts per HPF
3A	>15 centroblasts per HPF with centrocytes present
3B	Solid sheets of centroblasts

1.3. Pathogenesis of Follicular Lymphoma

Acquisition of the t(14;18) *IgH-BCL2* translocation is widely recognised as the founder event that initiates the development of FL. Other key pathobiological hallmarks of FL are: 1) alterations in epigenetic modifiers, 2) acquisition of somatic mutations and 3) dependence on non-malignant immune cells within the TME. None of these aspects occur in isolation, and FL genotype has a clear influence on disease phenotype that links epigenetic, genomic and TME changes. The following section describes how these key factors contribute to the pathogenesis of FL, whilst highlighting the interplay between genomic changes, T_{FH} and the wider TME.

1.3.1. t(14;18) translocation

The t(14;18) translocation is a hallmark of FL and brings the *BCL2* gene under the influence of the constitutively activated immunoglobulin heavy chain (*IgH*) enhancer region, leading to overexpression of the anti-apoptotic protein BCL2. This translocation arises during defective RAG (recombination activating gene)-mediated V(D)J gene recombination early in B-cell development, and *IgH* and *BCL2* breakpoints are highly conserved in FL, consistent with t(14;18) as a founding event in FL (Green*, et al* 2015, Jäger*, et al* 2000, Tsujimoto*, et al* 1985). In normal GC B-cells, BCL6 represses BCL2 expression, but in t(14;18)-translocated B-cells this negative feedback is interrupted. Constitutive expression of BCL2 confers a selective advantage by allowing rescue of GC B-cells expressing low affinity B-cell receptors (BCR) that would otherwise undergo apoptosis (Sungalee*, et al* 2014). It also permits survival of cells that acquire additional genomic alterations, within a GC environment that facilitates genomic instability. However, expression of a high-affinity BCR is still required to differentiate and exit the GC reaction, therefore t(14;18)$^+$ B-cells are unable to mature beyond GC B-cells and continue to express BCL6. Characteristic features of (14;18)$^+$ cells include evidence of ongoing SHM, reflecting multiple cycles of GC re-entry, and persistent expression of surface IgM/IgD, despite evidence of CSR, the so-called 'allelic paradox' (Sungalee*, et al* 2014). IgG-expressing t(14;18)$^+$ B-cells do not repeatedly cycle through GCs, thus IgM$^+$ cells may have a selective advantage in FL (Sungalee*, et al* 2014).

The *IgH-BCL2* translocation is insufficient for lymphomagenesis in isolation. Low levels of t(14;18) are detectable in the peripheral blood in up to 70% of healthy individuals, a large proportion of whom do not develop NHL after prolonged periods of observation (Dolken*, et al* 1996, Limpens*, et al* 1995, Liu*, et al* 1994). Indeed, 10-20% FL patients lack this characteristic

translocation. Furthermore, in murine models, only a small proportion of mice with the t(14;18) translocation develop lymphoma, which usually resembles high-grade lymphoma and is accompanied by additional genomic changes (McDonnell and Korsmeyer 1991, Strasser*, et al* 1993). Finally, responses to pharmacological agents targeting BCL2 have been very poor, suggesting that FL is not critically dependent on BCL2 expression (Davids*, et al* 2017). Additional genomic and epigenetic alterations, accompanied by changes in non-neoplastic immune cells, are necessary to facilitate the development of FL (Ame-Thomas and Tarte 2014, Dave*, et al* 2004, Okosun*, et al* 2014).

1.3.2. Epigenetic Dysregulation in FL

Epigenetic dysregulation is a defining feature of FL and its importance in the pathogenesis of FL is emphasised by the finding that over 70% FL patients harbour somatic mutations in more than 1 histone-modifying gene (Green*, et al* 2015, Okosun*, et al* 2014). Mutations in the histone acetyltransferase *CREBBP* (CREB binding protein) are detectable in around 60% of patients and mutations in the histone methyltransferase *KMT2D* (lysine-specific methyltransferase 2D; MLL2) are present in approximately 80%, many of whom harbour multiple mutations (Green*, et al* 2013, Green*, et al* 2015, Morin*, et al* 2011, Okosun*, et al* 2014). Characteristically, clonal changes in epigenetic regulators are dominant and are conserved over time, identifying them as key early driver mutations (Green*, et al* 2013, Green*, et al* 2015, Okosun*, et al* 2014). As transactivators and repressors of multiple genes regulating a broad range of cellular functions, epigenetic modification is likely to have a significant influence on cellular biology and lymphomagenesis.

Targets of CREBBP include the *CIITA* (class II transactivator) gene, which upregulates transcription of class II MHC (major histocompatibility complex) genes. Inactivating mutations of *CREBBP* result in a marked reduction in class II MHC expression, which facilitates immune evasion by FL cells and leads to a reduction in $CD4^+$ and $CD8^+$ T-cell infiltration (Green*, et al* 2015), highlighting the interplay between genomic/epigenetic change and the TME.

KMT2D is a tumour suppressor that is usually inactivated by somatic mutations in FL. KMT2D regulates expression of multiple genes that influence cytokine/chemokine signalling, lymphocyte migration and plasma cell differentiation (Ortega-Molina*, et al* 2015, Zhang*, et al* 2015). KMT2D-deficient B-cells have increased resistance to apoptosis induced by CD40 and BCR overstimulation, and enhanced proliferation in response to CD40, IL-4 and IL-21 signalling, which suggest that *KMT2D* inactivation allows FL B-cells to derive exaggerated benefit from T_{FH} support (Ortega-Molina*, et al* 2015, Zhang*, et al* 2015). Loss of KMT2D expression co-operates

with both *IgH-BCL2* and AID to facilitate development of lymphoma in mouse models of BCL2- and AID-induced lymphomagenesis (Ortega-Molina*, et al* 2015, Zhang*, et al* 2015).

The histone methyltransferase EZH2 (enhancer of zeste homologue 2) is responsible for maintaining the GC gene expression programme and inhibits B-cell differentiation (Beguelin*, et al* 2013). Activating *EZH2* mutations, which occur in 12-25% of FL patients (Green*, et al* 2015, Okosun*, et al* 2014), are sufficient to initiate development of follicular hyperplasia and accelerate lymphomagenesis in animal models (Beguelin*, et al* 2013). *EZH2* mutations are associated with a favourable prognosis and are pharmacologically targetable, although *EZH2* mutations are predominantly subclonal and thus non-driver mutations (Huet*, et al* 2017)

1.3.3. Other Genomic Aberrations in FL

HVEM is frequently downregulated through a variety of mechanisms, highlighting the importance of this tumour suppressor gene in the pathogenesis of FL. After t(14;18), the most common chromosomal alterations in FL involve the 1p36 locus, which contains the *HVEM* gene, resulting in deletion or uniparental disomy of *HVEM* in up to two-thirds of patients (Cheung*, et al* 2010, Launay*, et al* 2012). Direct *HVEM* mutations are present in over a quarter of FL cases (Boice*, et al* 2016). In addition, *HVEM* and its inhibitory co-partner *BTLA* (B and T lymphocyte attenuator) are both regulated by KMT2D, with reduced expression in *KMT2D*-mutated lymphoma (Ortega-Molina*, et al* 2015). Downregulation of HVEM reduces inhibitory BTLA signalling in T_{FH}, which increases CD40L expression and potentially enhances the ability of FL T_{FH} to provide help to FL B-cells (Mintz*, et al* 2019). Loss of HVEM also indirectly facilitates T_{FH} recruitment by enhancing the ability of FL B-cells to activate stromal cells, which secrete CXCL13. As a result, HVEM-deficient lymphomas have increased numbers of infiltrating T_{FH} and higher levels of IL-4 and IL-21 (Boice*, et al* 2016). In animal models, loss of HVEM/BTLA signalling promotes accumulation of $BCL2^+$ GC B-cells and accelerates lymphomagenesis (Mintz*, et al* 2019).

Recurrent mutations involving the Janus Kinase (JAK) and Signal Transducer and Activator of Transcription (STAT) pathways, which play a key role in mediating cytokine signalling, are present in 20% of FL cases (Okosun*, et al* 2014). These mutations primarily involve the STAT6 signalling pathway, which mediates B-cell signalling in response to IL-4- a key T_{FH}-derived cytokine. Activating mutations in *STAT6* result in heightened responses to exogenous IL-4 stimulation, as well as increased basal transcription of STAT6-mediated genes (Yildiz*, et al* 2015).

Although only present in a small minority of FL patients at diagnosis (6%), *TP53* mutations are the only genomic changes that are independently associated with inferior OS (O'Shea*, et al* 2008, Pastore*, et al* 2015). Tumour protein 53 (p53) primarily controls genes that promote the DNA damage response, cell cycle arrest and apoptosis, however, it also regulates a large number of genes involved in anti-tumour immunity. p53 increases expression of surface MHC, PD-1 and PD-L1 in response to genotoxic stress (Munoz-Fontela*, et al* 2016). *TP53* mutations in FL are known to correlate with expression of a TME-related gene expression signature that is associated with inferior prognosis and reflects a predominance of macrophage and dendritic cell-related genes (Dave*, et al* 2004, O'Shea*, et al* 2008).

Mutations in the *CIITA*, *B2M* (encoding β_2-microglobulin) and *CD58* genes are all associated with high-grade transformation of FL. These mutations alter MHC expression and/or tumour recognition by T-cells and thus facilitate immune evasion (Pasqualucci*, et al* 2014). Other gene mutations that are implicated in FL transformation involve *MYC*, *CDKN2A/B* and *TP53*, genes that influence cell cycle progression and/or the DNA damage response (Pasqualucci*, et al* 2014).

1.3.4. Drivers of Genomic Instability in FL

Expression of AID within normal GCs intentionally creates genomic instability to facilitate acquisition of advantageous mutations within Ig genes. In malignant FL follicles, this genomic instability combined with BCL2-mediated resistance to apoptosis can result in deleterious mutations that contribute to disease pathogenesis. In animal models, development of BCL6-related GC B-cell lymphomas is dependent on expression of AID (Pasqualucci*, et al* 2008). The development of lymphoma in t(14;18)$^+$ B-cells is hypothesised to result from recurrent activation of AID through repeated cycles of GC entry in order to acquire additional genomic changes. The high levels of intraclonal variation seen within *IGHV* genes in FL is consistent with persistent exposure of t(14;18)$^+$ B-cells to AID-mediated SHM over time (Loeffler*, et al* 2014, Sungalee*, et al* 2014). A notable feature of FL is the accumulation of on-target SHM-related mutations within *IGHV* genes that create glycosylation motifs terminating in high mannose residues, which are present in approximately 80% patients. These unusual sequences provide key survival signals to FL cells by enabling constitutive antigen-independent BCR signalling through interaction with C-type lectins on myeloid cells (Cha*, et al* 2013, Coelho*, et al* 2010).

Studies of paired biopsies at FL diagnosis and relapse have consistently identified AID-mediated aberrant SHM as a driver of genomic change in FL. However, studies differ in their interpretation of AID-mediated tumour evolution. Loeffler *et al* reported high rates of aberrant SHM at

diagnosis, but did not find a correlation between genomic divergence and time, suggesting that AID plays a major role in disease pathogenesis (Loeffler*, et al* 2014). However, Green *et al* found that most somatic mutations at diagnosis do not contain an AID-related signature but are enriched at FL relapse, suggesting that AID facilitates tumour progression (Green*, et al* 2013, Green*, et al* 2015). Studies agree that AID-related change is enriched at disease transformation within *BCL2*, *MYC* and a number of other off-target genes (Correia*, et al* 2015, Pasqualucci*, et al* 2014).

AID is expressed in the vast majority of FL and correlates with increased mutational load in the majority of FLs that express surface IgM (Hardianti*, et al* 2004, Scherer*, et al* 2016). The *Aicda* gene itself is unmutated and elevated AID expression levels are not required for AID-induced lymphomagenesis (Pasqualucci*, et al* 2008). However, AID activity is tightly regulated at multiple levels and acquisition of off-target mutations in FL may involve a yet unidentified defect in guidance of AID to target genes (Zan and Casali 2013). The pathways involved in upregulation of AID in response to CD40, IL-4 and IL-21 signalling are all either intact or enhanced in FL, suggesting that T_{FH} may play a key role in stimulating AID expression in FL. Although direct evidence demonstrating that T_{FH} can enhance AID expression in FL is lacking, T_{FH} are seen to co-localise and maintain direct cell contact with proliferating, AID-expressing B-cells in FL tissue (Townsend*, et al* 2019). T_{FH} may thus provide a key link between genomic change and the TME, as part of a positive feedback loop where T_{FH} encourage genomic instability and acquisition of mutations that create a supportive microenvironment and further enhance T_{FH} recruitment. The role of T_{FH} and the wider TME in the pathogenesis of FL will be discussed in the following sections.

1.3.5. Tumour Microenvironment in FL

The ability to evade recognition by the immune system is one of the hallmarks of cancer (Hanahan and Weinberg 2011). Spontaneous regressions without treatment can occur in some FL patients, demonstrating the potential of anti-tumour immune responses to exert disease control. FL has developed multiple strategies to evade anti-tumour immunity, such as downregulation of MHC and HVEM expression. However, it is also able to selectively co-opt elements of the normal immune system to support its growth and survival. Indeed, FL is a malignancy that is critically dependent on the TME for survival, illustrated by the fact that maintenance of FL cells *in vitro* is reliant on external support from stromal cells, T-cells, cytokines

and/or CD40L for survival (Ame-Thomas*, et al* 2012, Kagami*, et al* 2001, Smeltzer*, et al* 2014, Travert*, et al* 2008).

The importance of the TME in FL was emphasised by a seminal study in 2004, suggesting that survival in FL could be predicted by a gene expression signature that reflected the composition of non-malignant tumour-infiltrating immune cells, rather than malignant FL B-cells (Dave*, et al* 2004). Two signatures were identified: an 'immune response 1' signature reflected increased expression of certain T-cell and macrophage genes and was associated with a good prognosis, whereas an 'immune response 2' signature, predominantly consisting of stromal and other macrophage-related genes, was associated with a poor prognosis (Dave*, et al* 2004). One important caveat is that this study was performed on a heterogeneously-treated population in the pre-rituximab era. Macrophages mediate rituximab-induced phagocytosis, therefore use of rituximab abrogates the prognostic effect of macrophages in FL (Canioni*, et al* 2008, Taskinen*, et al* 2007). Nevertheless, gene expression studies in the rituximab era confirm that the non-malignant TME influences prognosis (Tobin*, et al* 2019).

However, the extent to which individual immune cell subsets contribute to these observations remains unclear. A large number of studies have used single- or dual-parameter immunohistochemistry (IHC) to investigate the association between individual cell markers and prognosis and have yielded inconsistent and often conflicting results (Ame-Thomas and Tarte 2014). These studies were varied in their methodology, assessed different clinical endpoints and, importantly, lacked the resolution to assess the contribution of complex cell subtypes within the TME.

1.3.6. Role of T-cells in FL

FL has generally been thought to create an environment that suppresses T-cell activity, with a higher proportion of functionally exhausted T-cells in FL than in healthy lymphoid tissue. Both $CD4^+$ and $CD8^+$ tumour-infiltrating lymphocytes (TILs) have defective cytokine production, reduced motility and an impaired ability to form immune synapses (Gravelle*, et al* 2016, Kiaii*, et al* 2013, Ramsay*, et al* 2009). These defects are directly induced by FL B-cells and also occur in healthy donor T-cells co-cultured with FL B-cells (Kiaii*, et al* 2013, Ramsay*, et al* 2009). Approximately 30-40% of intra-tumoural $CD4^+$ and $CD8^+$ T-cells in FL express exhaustion markers such as TIM3 (T-cell immunoglobulin and mucin-domain containing-3) and LAG3 (Lymphocyte-activating gene-3) (Yang*, et al* 2012). These phenotypically-exhausted T-cells are highly heterogeneous, and their origin is not clear; a small proportion express the transcription factors

Tbet and FoxP3, but most do not express known Th lineage markers. These cells predominantly reside in interfollicular areas and express low levels of PD-1 (Yang*, et al* 2015a). They are distinct from T_{FH} by nature of their distribution, phenotype (lower levels of PD-1 expression, absence of CXCR5 and BCL6) and reduced cytokine and intracellular STAT signalling (Yang*, et al* 2012, Yang*, et al* 2015a). Importantly, the proportion of both $TIM3^+$ and $LAG3^+$ T-cells correlates with survival in FL (Yang and Zhang 2017, Yang*, et al* 2015a).

Regulatory T-cells account for a larger proportion of $CD4^+$ T-cells in FL compared to reactive LN, tonsillar tissue and other B-cell lymphomas (Ame-Thomas*, et al* 2012, Le*, et al* 2016, Myklebust*, et al* 2013). In co-culture studies, FL B-cells are able to directly enhance T_{reg} generation in unselected FL TILs (Le*, et al* 2016). FL-derived T_{regs} possess enhanced ability to suppress proliferation and cytokine release in both autologous and allogeneic T-cells, compared with reactive T_{regs} (Hilchey*, et al* 2007). However, whilst FL T_{regs} potentially suppress anti-tumour immunity, they also inhibit FL B-cell activation (Le*, et al* 2016). The net effect of T_{regs} on overall FL phenotype is therefore unclear and there are conflicting data on the prognostic significance of T_{regs} in the FL TME. In some studies, FoxP3 expression, particularly in interfollicular areas, has been associated with a poor prognosis (Blaker*, et al* 2016, Carreras*, et al* 2009), whilst others have correlated intrafollicular FoxP3 expression with favourable outcomes (Wahlin*, et al* 2010), or have found no prognostic association (Richendollar*, et al* 2011).

It is clear, however, that many $CD4^+$ T-cells in FL are neither functionally exhausted nor inactive. FL contains a higher proportion of activated $CD4^+$ T-cells expressing the activation marker CD69 than reactive LN (Hilchey*, et al* 2011). $CD4^+$ T-cells are necessary for the engraftment of FL-like lymphoma in animal models and therefore provide active support for FL survival *in vivo* (Burack*, et al* 2016, Egle*, et al* 2004b). Indeed, the appearance of T-cell anergy may, in part, reflect the nature of T-cell subsets present, rather than an FL-induced defect in T-cell function. For example, FL T-cells have reduced STAT phosphorylation in response to multiple cytokines, when compared with healthy donor T-cells or reactive LN tissue, but the same patterns are replicated in reactive tonsillar tissue, which has a very similar T-cell composition to FL (Myklebust*, et al* 2013). One of the striking features characterising both tonsillar and FL tissue is a preponderance of T_{FH}.

1.3.7. T Follicular Helper Cells in FL

T_{FH} comprise almost a third of all $CD4^+$ T-cells in FL, which is similar to reactive tonsillar tissue and greater than levels seen in reactive LNs or other B-cell lymphomas (Ame-Thomas*, et al*

2012). Studies using multiparameter confocal immunofluorescence microscopy have demonstrated that the number of T_{FH} and their interaction with FL B-cells closely mirrors patterns seen within reactive GCs (Townsend*, et al* 2019). Similar to reactive LN tissue, very high levels of PD-1 expression differentiate FL T_{FH} from exhausted cells expressing lower levels of PD-1 (Yang*, et al* 2015a). FL T_{FH} have an activated phenotype: they express co-stimulatory ligands, such as OX40 and CD70 and lack expression of exhaustion markers, such as TIM3 and LAG3 (Yang*, et al* 2015a). T_{FH} are also functionally active: they have the ability to form immune synapses with FL B-cells and secrete IL-4, IL-21 and CXCL13 (Ame-Thomas*, et al* 2012, Myklebust*, et al* 2013, Townsend*, et al* 2019).

Importantly, FL T_{FH} are able to provide support to FL B-cells. Multiple studies have shown that co-culture with T_{FH} protects FL B-cells from apoptosis *in vitro* (Ame-Thomas*, et al* 2012, Yang*, et al* 2015a). Stimulation with IL-4 and CD40 is often used to enhance the survival of FL cells *in vitro* and protects from apoptosis through CD40L-mediated upregulation of pro-survival proteins, such as BCL-XL (Travert*, et al* 2008). The addition of autologous T_{FH} alone to FL B-cell culture is able to provide the same level of protection against apoptosis (Amé-Thomas*, et al* 2015). T_{FH} promote activation of FL B-cells, reflected by increased expression of the activation marker CD86, which in turn provides important reciprocal co-stimulation to T_{FH} (Ame-Thomas*, et al* 2012, Yang*, et al* 2015a).

There are key differences between T_{FH} derived from FL and reactive tonsillar tissue, with notable differences in gene expression and cytokine release (Ame-Thomas*, et al* 2012). FL T_{FH} have markedly increased IL-4 expression, which induces high basal levels of STAT6 phosphorylation in FL B-cells and increased transcription of IL-4 target genes (Amé-Thomas*, et al* 2015, Calvo*, et al* 2008, Pangault*, et al* 2010). CD10 expression on T_{FH} correlates with an increased capacity to secrete IL-4, and is expressed by a higher proportion of FL T_{FH} than in reactive tonsillar tissue (Amé-Thomas*, et al* 2015). CD40L expression is also higher in FL T_{FH}, potentially signifying an increased capacity to provide support to FL B-cells (Ame-Thomas*, et al* 2012, Travert*, et al* 2008). CD40 signalling reduces the threshold needed for BCR activation and may contribute to the exaggerated BCR signalling responses seen in FL (Irish*, et al* 2006). CD40 signalling through NFκB is able to bypass the need for BCR signalling altogether in the minority of FL B-cells that have impaired B-cell signalling, and heightened responses to CD40L stimulation are associated with inferior survival (Irish*, et al* 2010).

It has not yet been determined whether T_{FH} are able to recapitulate their role in reactive GCs by inducing proliferation or AID expression in FL B-cells. There are no animal models that accurately

recapitulate the indolent behaviour of FL and it is notoriously difficult to stimulate FL proliferation *in vitro* under any conditions; AID expression is predominantly limited to proliferating cells. However, imaging studies of FL tissue demonstrate a very close spatial association between T_{FH} and proliferating and AID-expressing B-cells *in situ*. In addition, the number of T_{FH} closely correlates with the number of proliferating FL B-cells, suggesting that T_{FH} may influence the rate of FL proliferation (Townsend*, et al* 2019).

FL B-cells express co-stimulatory molecules and it is inferred that they actively support the presence and survival of T_{FH} within the FL TME. However, functional data demonstrating this are lacking. It is unclear whether T_{FH} derive the same level of support from FL B-cells as they do from reactive GC B-cells. In normal GCs, maintenance and proliferation of T_{FH} is critically dependent on cognate TCR stimulation; whether this holds true for FL T_{FH} is not known. However, intrafollicular T-cells have increased TCR clonality compared to extrafollicular T-cells in FL, suggesting that T_{FH} expansion may be antigen-dependent (Townsend*, et al* 2019). The nature of any potential antigenic stimulus remains unclear.

Despite evidence demonstrating that T_{FH} have a pro-tumoural effect and can support FL survival *in vitro*, it remains unclear whether the presence of T_{FH} has an adverse prognostic effect *in vivo.* Increased intrafollicular PD-1, CD57 and CD4 expression, which largely reflect the presence of T_{FH}, have all been associated with an increased risk of transformation (Blaker*, et al* 2016, Glas*, et al* 2007). Some studies have demonstrated an inverse correlation between intrafollicular PD-1 expression and survival (Farinha*, et al* 2008, Richendollar*, et al* 2011), whilst other studies have associated intrafollicular PD-1 expression with favourable outcomes (Smeltzer*, et al* 2014, Sohani*, et al* 2015, Wahlin*, et al* 2010). It is therefore unknown whether T_{FH} can influence the clinical phenotype of FL.

1.3.8. Modulation of T_{FH} Activity in FL

It has been postulated that the balance between T_{FH} and T_{FR} in FL may dictate the disease phenotype, although the role of T_{FR} in FL has been relatively underexplored and data to support this hypothesis are lacking (Brady*, et al* 2014). Similar to reactive LN tissue, T_{FR} represent a minority of follicular T-cells, comprising around 10% of $CD4^{+}CXCR5^{hi}ICOS^{hi}$ T-cells (Brady*, et al* 2014). FL T_{FR} are able to directly suppress proliferation of autologous T_{FH} and reduce activation of FL B-cells (Tarte*, et al* 2017). T_{FR} correlate in number with T_{FH} in FL, reflecting their migration in response to similar stimuli, such as CXCL13 (Ame-Thomas*, et al* 2012, Hilchey*, et al* 2011). There is evidence of overlap and plasticity between T_{FH} and T_{FR} in FL; there is significant overlap

in their TCR repertoire and up to 10% of FL T_{FH} co-express BCL6 and FoxP3 (Hilchey*, et al* 2011, Tarte*, et al* 2017). There is also evidence that FL T_{FH} can convert to T_{FR}, although the extent to which this occurs *in vivo* and contributes to disease pathogenesis is unclear (Brady*, et al* 2014).

PD-L1 is largely expressed by non-malignant immune cells within the TME (Laurent*, et al* 2015, Myklebust*, et al* 2013). FL B-cells generally do not express PD-L1, although weak expression is detectable in a small minority (<10%) of FL tissue (Menter*, et al* 2016). Expression of PD-1 ligands is likely to exert a homeostatic effect on FL T_{FH} but will also alter the activity of other PD-1^+ T-cells in the TME. The net effect of PD-L1 expression on FL biology is unknown and tissue expression of PD-L1 does not appear to correlate with clinical outcomes (Blaker*, et al* 2016).

Data on tissue expression of PD-L2 is lacking, partly due to the lack of robust, commercially-available primary antibodies to facilitate assessment of PD-L2 protein expression. Available data suggest that PD-L2 is variably expressed on a minority of FL B-cells as well as other immune cells within the TME (Laurent*, et al* 2015). At an mRNA level, PD-L2 gene expression correlates with improved clinical outcomes, independently of established clinical and genetic prognostic scores (Tobin*, et al* 2019). The authors of this study observed that reduced PD-L2 expression was associated with a general downregulation of the intra-tumoural immune response and hypothesised that reduced anti-tumour immunity accounts for this prognostic effect, however reduced PD-L2 within the TME may alter and potentially enhance T_{FH} activity.

1.3.9. Co-operation Between T_{FH} and the Wider Tumour Microenvironment

The majority of FL B-cells maintain BCR expression, are dependent on BCR signalling and have exaggerated signalling responses to BCR stimulation (Irish*, et al* 2006). BCR stimulation is independent from T_{FH}-derived support and requires the presence of other non-malignant cells within the TME, such as macrophages and stromal cells. None of these non-malignant cells act in isolation and there is a high degree of interplay between stromal cells, macrophages and T_{FH} in the TME that regulates the behaviour of FL.

FL tumour-associated macrophages (TAM) express the surface receptor DC-SIGN (dendritic cell–specific intercellular adhesion molecule-3–grabbing nonintegrin), which binds to and triggers sustained activation of highly-mannosylated IgM BCRs. T_{FH}-derived IL-4 and, to a lesser extent, IL-21 play a key role in promoting recruitment and differentiation of DC-SIGN-expressing macrophages, as well as increasing surface IgM expression on FL B-cells (Amin*, et al* 2015). IL-4 also plays a key role in polarising FL macrophages away from a pro-inflammatory phenotype

towards a more immunoregulatory 'M2' phenotype. M2 TAMs aid in creating a tumour-permissive microenvironment by expressing inhibitory receptors, such as PD-L1, and releasing cytokines that enhance recruitment of T_{regs} to the TME (Yang and Zhang 2017).

The contribution of stromal cells to the pathogenesis of FL has been relatively understudied, in part due to the difficulty in isolating and culturing these cells (Mourcin*, et al* 2012). Nevertheless, available data suggest that stromal cells play a significant role in orchestrating the FL niche. FL mesenchymal stem cells (MSCs) can also induce conversion of macrophages towards an immunoregulatory M2 phenotype and enhance macrophage recruitment through overexpression of CCL2 (Guilloton*, et al* 2012). FL-derived stromal cells (both FDCs and fibroblast reticular cells (FRCs)) are able to support the survival of FL cells *in vitro* (Ame-Thomas*, et al* 2007, Kagami*, et al* 2001). FDCs and FRCs can also support the survival of T_{FH} *in vitro* and enhance T_{FH} recruitment through secretion of CXCL13 (Boice*, et al* 2016). Stromal cell-derived IL-6 promotes T_{FH} differentiation and enhances IL-21 production (Brady*, et al* 2014). However, MSCs can also upregulate FoxP3 expression and are able to induce conversion of T_{FH} into T_{FR}, although the extent to which this occurs *in vivo* and influences T_{FH} activity is unclear (Brady*, et al* 2014).

There is extensive interplay and co-operation between T_{FH} and stromal cells in FL creating a positive feedback loop that enhances tumour survival and proliferation. T_{FH}-derived IL-4 enhances secretion of CXCL12 by FL stromal cells, which in turn stimulates recruitment and activation of FL B-cells (Pandey*, et al* 2017). FL B-cells secrete a number of TNF-family cytokines that encourage growth of FDC networks, induce differentiation of MSCs into tumour-supportive FRCs and activate stromal cells within the TME, which in turn release CXCL13 to promote further T_{FH} recruitment (Ame-Thomas*, et al* 2007, Boice*, et al* 2016).

Macrophages and stromal cells in FL therefore promote the development of an immunomodulatory, pro-tumour microenvironment. This requires multidirectional crosstalk with both FL B-cells, T_{FH} and T_{regs}, to create the FL tumour niche, which ultimately facilitates immune evasion and tumour growth.

1.3.10. T_{FH} and Novel Therapies

An expanding number of novel agents are in clinical trials for FL, some of which are licensed for the treatment of refractory/relapsed FL and are now moving into the frontline setting. Interest in these agents is rapidly increasing, in order to expand the treatment arsenal for patients with relapsed disease and to pursue the goal of 'chemotherapy-free' treatment. The ultimate aim is

to be able to deliver precision medicine with agents that directly target the underlying biology of FL. Many novel agents have the potential to alter T_{FH} function, but the effects of these agents on the TME have not been fully assessed and are poorly understood. This section discusses the key novel agents that are currently in clinical use and how they may promote or inhibit T_{FH} activity.

Anti-CD20 therapy with rituximab has been established in FL for more than a decade and was the first of an ever-expanding portfolio of immune therapies to come into clinical practice. However, despite universal CD20 expression by FL B-cells, there is no evidence that rituximab therapy is curative or improves overall survival. T_{FH} may potentially facilitate rituximab resistance: the combination of IL-4 and CD40L, both of which are derived from T_{FH} within malignant follicles, can rescue FL B-cells from direct rituximab-induced apoptosis (Ame-Thomas*, et al* 2012). The number of T_{FH} within the LN and PB of FL patients is not altered by rituximab treatment, therefore FL-derived T_{FH} can potentially support re-establishment of malignant follicles following treatment (Wallin*, et al* 2014).

T_{FH} may also play a key role in resistance to BCL2-targeted therapy. Despite constitutive expression of BCL2 in almost cases of FL, clinical results with the BCL2 inhibitor venetoclax have been disappointing (Davids*, et al* 2017). *In vitro* studies in chronic lymphocytic leukaemia (CLL) suggest that the TME can rescue malignant B-cells from venetoclax-mediated apoptosis. Stimulation with CD40L, IL-4 and, to a lesser extent, IL-21 result in upregulation of additional anti-apoptotic proteins such as BCL-XL, which protected against venetoclax-induced apoptosis (Thijssen*, et al* 2015). Similarly, CD40 stimulation by T_{FH} in FL increases BCL-XL expression and is likely to confer venetoclax resistance (Travert*, et al* 2008).

Other novel agents are likely to downregulate T_{FH} activity. Both the PI3Kδ inhibitor idelalisib and the PI3Kδγ inhibitor duvelisib, have shown clinical efficacy in FL (Flinn*, et al* 2016, Gopal *, et al* 2014). Multiple PI3K isoforms are present in T-cells but, importantly, PI3Kδ is a key mediator of ICOS signalling and is therefore essential for the maintenance and function of GC T_{FH} (Weber*, et al* 2015). Indeed, PI3Kδ expression in T-cells, but not B-cells, plays a key role in supporting the normal GC reaction, thus modulation of T_{FH} activity may contribute to the efficacy of PI3K inhibition in FL (Rolf*, et al* 2010).

Bruton tyrosine kinase (BTK) inhibitors, such as ibrutinib, have modest clinical efficacy in FL and are now being evaluated in combination with other agents (Gopal*, et al* 2018). BTK inhibitors irreversibly inhibit interleukin-2-inducible kinase (ITK), which is an important component of T-cell receptor signalling and is a downstream mediator of ICOS signalling via PI3K (Dubovsky*, et*

al 2013, Nurieva*, et al* 2007). ITK is expressed by T_{FH}-related T-cell lymphomas, in which there is pre-clinical evidence to suggest ibrutinib reduces proliferation and can induce downregulation expression of T_{FH} markers (Mamand*, et al* 2019). Therefore, BTK inhibitors are likely to inhibit T_{FH} function.

The effects of other novel agents on T_{FH} function are more difficult to predict. Lenalidomide targets the E3 ubiquitin ligase cereblon and is one of the most promising novel agents in FL (Fowler*, et al* 2014, Leonard*, et al* 2019). Recently, the RELEVANCE clinical trial demonstrated that frontline lenalidomide in combination with rituximab has similar efficacy to immunochemotherapy (Morschhauser*, et al* 2018) and this regimen is now approved in the United States for frontline treatment of FL as part of a 'chemotherapy-free' approach. Lenalidomide has wide-ranging immunomodulatory effects, facilitates pro-inflammatory cytokine release and augments T-cell activation and proliferation (Chiu*, et al* 2019, Gribben*, et al* 2015). Lenalidomide can also restore defective T-cell immune synapse formation in FL (Ramsay*, et al* 2009). FL patients treated with lenalidomide-rituximab have a marked early reduction in intra-tumoural $CD4^+$ T-cell infiltration but the Th subsets accounting for this observation are not known (Fowler*, et al* 2014). Whilst lenalidomide-induced changes in cytokine profile, such as increased IL-2 and reduced IL-6 expression, may create a less T_{FH}-supportive environment, the specific effects of lenalidomide on T_{FH} are unknown.

Monoclonal antibodies against PD-1 have also shown clinical efficacy in FL and are presumed to work by enhancing anti-tumour immunity, particularly through $CD8^+$ T-cell-mediated cytotoxicity (Lesokhin*, et al* 2016, Westin*, et al* 2014). The majority of commercially-available PD-1 inhibitors are IgG4 antibodies that bind to T-cells and block interaction of PD-1 with its ligands but do not stimulate antibody-dependent cytotoxicity (Fessas*, et al* 2017). These antibodies are therefore likely to reduce PD-1 signalling in T_{FH} and increase T_{FH} proliferation, activation and cytokine expression (Cubas*, et al* 2013). However the effects of PD-1 on T_{FH} function are complex and complete blockade of PD-1 signalling may also impair cytokine signalling (Good-Jacobson*, et al* 2010). PD-1 is also expressed by T_{FR}, T_{regs} and exhausted T-cells (Yang*, et al* 2019, Yang*, et al* 2015a); PD-1 inhibitors may have indirect effects on T_{FH} activity by modulating T_{FR} activity (Sage*, et al* 2013).

In summary, T_{FH} are a potential therapeutic target in FL and may contribute to the efficacy of certain agents but can also mediate treatment resistance. A better appreciation of the effect of novel agents on T_{FH} and other T-cell subsets is necessary to understand their mechanism of action, predict treatment responses and aid rational design of targeted combination treatments.

1.4. Summary

FL is a GC B-cell-derived malignancy that retains multiple features in common with its non-neoplastic GC counterparts, including an abundance of functionally-active T_{FH}. FL is critically dependent on its TME and T_{FH} appear to play a key role in creating a tumour-permissive environment that supports FL growth. The importance of T_{FH} is highlighted by the ability of FL to harness the advantageous functions of T_{FH}, by enhancing expression of CD40L and IL-4, whilst evolving mechanisms to evade their inhibitory effects, such as downregulation of HVEM expression.

T_{FH} have been implicated in multiple stages of lymphomagenesis and can potentially facilitate FL progression by:

- Promoting development of lymphoma in $t(14;18)^{+}$ precursors through repeated cycles of GC re-entry
- Supporting survival, activation and proliferation of FL within malignant follicles
- Interacting with other TME cells to orchestrate development of the tumour-supportive FL niche
- Promoting the acquisition of genomic changes that support FL progression and transformation
- Conferring resistance to treatment

Data to date therefore strongly suggest that T_{FH} promote the growth and progression of FL. However, there are numerous unanswered questions regarding the role of T_{FH} in FL. First and foremost, it is unclear whether the tumour-supportive effects of T_{FH} have an influence on the clinical behaviour and natural history of FL. FL is a clinically heterogenous disease in which the mechanisms that drive development of more aggressive disease are unknown. It is not yet known, for example, whether T_{FH} can directly induce FL proliferation or are directly responsible for inducing AID expression and driving genomic change. Secondly, the mechanisms through which FL B-cells and T_{FH} interact to provide mutual support are not yet clear. It has not yet been shown that FL B-cells are able to independently support T_{FH} survival. In addition, are FL B-cells able to form cognate interactions with T_{FH} and, if so, what is the nature of the antigens providing this stimulus? Thirdly, very little is known about the regulation- or dysregulation- of T_{FH} activity in FL. For example, the significance of T_{FR} and PD-1 ligands in FL and their effect on T_{FH} activity in FL is unclear. Finally, the influence of both standard and novel therapeutics on T_{FH} biology has

not been fully explored. With the rapid introduction of novel agents into clinical practice, there is an urgent need to better understand T_{FH} biology and the pathways within the FL TME that support the pathogenesis of FL.

1.5. Aims

The overarching aim of this research is to investigate the hypothesis that T_{FH} play a key role in driving the growth and progression of FL. Specifically, this thesis aims to address the following questions:

1. Do T_{FH} activate FL B-cells and promote their survival?
2. Conversely, are FL B-cells directly able to support the survival and activation of T_{FH}?
3. Is there a spatial relationship between FL B-cell proliferation, MYC expression and T_{FH}?
4. Does the balance between T_{FH} and T_{FR} influence clinical phenotype?

This work will use a combination of *in vitro* culture studies, to provide information about functional cellular interactions, and tissue imaging studies, to assess the *in situ* relationship between T_{FH} and FL B-cells. In order to achieve these aims, the first results section (Chapter 3) focusses on methods of identifying and generating FL T_{FH} for further *in vitro* study.

Conventional imaging methods used to investigate cellular interactions within FL tissue are limited by their ability to assess only a limited number of histological markers and inability to fully identify complex cell populations within FL tissue. A subsidiary aim is to explore the feasibility of a novel imaging technique, imaging mass cytometry, to facilitate highly multiplexed assessment of interactions between T_{FH} and other complex cell types within the FL TME.

CHAPTER 2: MATERIALS AND METHODS

2.1. Patient Samples and Ethics

Patient with untreated or relapsed FL were identified from King's College Hospital lymphoma clinic lists. Patients with suspected reactive lymphadenopathy or low-grade lymphoma were identified via King's College Hospital neck lump clinic. Patients with known HIV, hepatitis C and active hepatitis B were excluded. Samples obtained included peripheral blood (PB), lymph node (LN) fine needle aspirates (FNA), disaggregated fresh LN tissue and bone marrow aspirates (BMA). Informed patient consent was obtained prior to obtaining any tissue for research purposes in accordance with the Declaration of Helsinki. All samples and linked clinical data were pseudonymised. Institutional ethical approval was obtained under King's College Hospital (National Research Ethics Service (NRES) reference: 13/NS/0039) and King's College London (NRES reference: 18/NE/0141).

For histology studies, archival formalin-fixed paraffin-embedded (FFPE) tissue was obtained from patients who had undergone LN excision biopsy for lymphoma or reactive lymphadenopathy between January 2007 and August 2014, with at least 2 years of clinical follow-up. Samples were identified through the King's College Hospital histopathology database. All tissue was deemed surplus to diagnostic requirements. Tissue blocks and linked clinical data were pseudonymised. Written consent was not deemed necessary for use of this archival tissue from both alive and deceased patients. Ethical approval was granted under King's College Hospital (NRES reference: 13/NW/0040).

2.2. Peripheral Blood and Bone Marrow Mononuclear Cell Isolation

Fresh PB and BMA samples were collected and anticoagulated in either sodium ethylenediaminetetraacetic acid (EDTA) or lithium heparin. BMAs were first diluted 1:1 with sterile phosphate-buffered saline (PBS). Peripheral blood mononuclear cells (PBMC) and bone marrow mononuclear cells (BMMC) were then isolated by density gradient centrifugation: equal volumes of PB or diluted BMA were gently layered over 10-15mls of Histopaque-1077 (Sigma-Aldrich, Missouri, USA) at room temperature (RT) in a 50ml conical centrifuge tube, then spun in a swinging bucket centrifuge at 1800 rpm for 25 minutes with the brake removed. The lymphocyte film at the interface of the Histopaque and serum layers, containing PBMCs or BMMCs, was carefully pipetted off and washed twice in warm, sterile PBS (Sigma-Aldrich).

For cryopreservation, samples were resuspended in equal volumes of freezing medium (80% foetal bovine serum (FBS) plus 20% dimethyl sulfoxide (DMSO)) and RPMI-1640 medium (Roswell Park Memorial Institute; all Sigma-Aldrich) to give a final DMSO concentration of 10% and cell concentration of up to 1-5 x 10^7 cells/ml. Samples were transferred into cryogenic vials, placed in an isopropanol freezing box then transferred to -80°C for a minimum of 3 hours before storage in liquid nitrogen. When required for use, samples were rapidly thawed in a 37°C water bath and washed twice in warm RPMI medium or sterile PBS to remove any residual DMSO.

2.3. Fine Needle Aspiration

FL patients with palpable, enlarged, superficial LNs were selected for FNA without ultrasound guidance. Patients receiving therapeutic anticoagulation or with suspected/known disease transformation were excluded.

Suitable superficial LN sites were selected by clinical examination with the aid of prior imaging studies to confirm sites of disease involvement, where available. FNA was performed under aseptic technique, using 2% chlorhexidine to sterilise the surrounding skin. A 21-gauge needle attached to a 10ml syringe was passed through the lymph node mass under gentle suction (approx. 0.5cm^3). The needle was rinsed at least 5 times with media to dislodge cells. Samples were collected and stored in McCoy's medium supplemented with L-glutamine and penicillin/streptomycin. This process was repeated a further 2-3 times from the same LN to obtain sufficient cells.

FNAs were processed fresh where possible, or after storage at 5°C for up to 18 hours. Samples were centrifuged at 1200 rpm for 10 minutes then resuspended for further use. Where not required for immediate use, cells were cryopreserved as described above.

Most FNA cell pellets had visible red cell contamination. Removal of red cells is reported to enhance antibody staining quality and simplify data acquisition by removing superfluous events. Therefore, an additional red cell lysis step was performed, where possible, using an eBiosciences red cell lysis buffer (eBiosciences), which uses ammonium chloride to disrupt erythrocyte membranes whilst exerting minimal effect on viable lymphocytes. Cells were suspended in 1-5ml lysis buffer and incubated at room temperature (RT) for 10 mins. At least 3 volumes of sterile PBS were then added to terminate the lysis reaction and cells were centrifuged at 1200 rpm for 10 minutes before further use.

For all 5-day culture experiments, FNAs were processed fresh and used without freezing or red cell lysis, in order to preserve cell viability and minimise processing/washes when working with low cell numbers.

2.4. Lymph Node Disaggregation

Surgical LN specimens were collected in RPMI-1640 medium or sterile 0.9% NaCl. Samples were immediately transferred for histopathology assessment, where they evaluated and sectioned under aseptic conditions to remove sufficient tissue for diagnostic purposes. Any remaining tissue was divided with a scalpel into small sections (<5mm) and dissociated by mechanical disruption through a cell dissociation sieve (Sigma-Aldrich). Gentle pressure was applied with a pestle to push the tissue through a 60-mesh screen (opening size 230μm). The filter and cells were rinsed with warm RPMI then centrifuged at 1200rpm for 10 minutes. Cells were then frozen at a concentration of up to 5 x10^7 cells/ml, as detailed in section 2.2. After thawing, cells were either subject to density gradient centrifugation to isolate the mononuclear cell layer or, if cell numbers were low, filtered through a 35μm cell strainer (Corning, New York, USA) to remove cell clumps prior to further use.

2.5. Immunomagnetic Cell Selection

Immunomagnetic negative selection was used to purify naïve CD45RA$^+$ T-cells for culture using an EasySep Human Naïve CD4+ T-cell Isolation Kit. To remove T-cell and B-cells from cell cultures, EasySep Human CD3 and CD19 Positive Selection Kits II were used, respectively (all Stem Cell Technologies, Vancouver, Canada). Immunomagnetic selection was performed according to manufacturer's instructions. In brief, unselected cells were suspended at a concentration of up to 1 x 10^8 cells/ml in sterile PBS containing 2% FBS and 1mM EDTA in a 5ml round-bottomed tube. Cells were incubated with the requisite biotinylated selection or isolation cocktail for 5 minutes, before adding streptavidin-coated magnetic RapidSpheres and incubating for a further 5 minutes. Cells were then placed into an EasySep magnet for 5 minutes and the supernatant was carefully decanted for further use, then placed through the magnet a second time to ensure maximum depletion of unwanted cells. Flow cytometry was performed to confirm >95% enrichment or depletion of the target cell population.

2.6. Cell Culture

Cells were cultured in RPMI-1640 medium (Sigma-Aldrich), supplemented in all instances with 10% FBS (Gibco/ThermoFisher Scientific, Massachusetts, USA), penicillin 100 IU/ml, streptomycin 100 µg/ml and 2mM L-glutamine (all Sigma-Aldrich). Lymphocytes were cultured at a concentration of 1 x 10^6/ml, except where stated, in either round-bottomed plates or flat-bottomed plates that were tilted during incubation in order to maximise cell-cell contact. Cells were maintained in a CO_2 incubator at 37°C, with a humidity of 95% and 5% CO_2 for up to 5 days.

To obtain approximate viable cell counts, aliquots of cell suspensions were mixed with equal volumes of 0.4% trypan blue. Viable cells lacking trypan blue uptake were counted on a haematocytometer slide.

For naïve T-cell experiments, initial T-cell stimulation was provided by adding 10µl/ml of Human T-Activator CD3/CD28 Dynabeads (ThermoFisher Scientific) for 16 hours. Samples were then vortexed and Dynabeads were removed by placing the sample in a DYNAL DynaMag2 magnet (ThermoFisher Scientific) for 2 minutes. Subsequently, naïve T-cell suspensions were supplemented with 1 µg/ml anti-CD28 (clone CD28.2, eBiosciences) and were transferred to 24-well tissue culture plates (Greiner Bio-One, Gloucestershire, UK) that had been pre-coated with 5µg/ml anti-CD3 overnight (clone OKT3, eBiosciences) and washed twice with sterile PBS, to provide a gentler level of T-cell stimulation. Cells were then incubated for 96 hours either without cytokines, or with the addition of interleukin (IL)-12 (1ng/ml), IL-1β (10ng/ml), IL-6 (25ng/ml) and transforming growth factor (TGF)-β (5ng/ml; all Peprotech, London, UK).

2.7. Flow Cytometry

2.7.1. Viability Staining

Fixable Viability Dye eFluor 780 (eBiosciences) exploits the more porous nature of cell membranes to penetrate dead cells and bind to intracellular amines, thus distinguishing between live and dead cells. For each sample, 1-10 x 10^5 cells were resuspended in 1ml PBS in 5ml round-bottomed tubes. Fixable Viability Dye was diluted 1:6 in PBS and 1µl/ml was added to each tube, then gently vortexed to mix. From this point onwards up until data acquisition, samples were protected from light to limit photobleaching. Samples were incubated at RT for 10 minutes, then washed at least once in 2ml PBS and centrifuged at 1500 rpm for 5 minutes.

2.7.2. Cell Surface Staining

After centrifugation, the supernatant was decanted, and cell pellets were gently vortexed to resuspend cells in the residual volume of PBS (approximately 100µl). For panels where 2 or more brilliant violet fluorochromes were used together, an additional 50µl Brilliant Stain Buffer (BD Biosciences, New Jersey, USA) was added to each sample to prevent brilliant violet dye interactions. Except where stated, 2.5µl of fluorochrome-conjugated antibody targeted against the cell surface antigen/s of interest was added to each tube and gently vortexed to mix. For a full list of antibodies used for flow cytometry see Table 2.1. Samples were incubated at 5°C for 30 minutes, then washed twice in at least 2ml PBS and centrifuged at 1500 rpm for 5 minutes. Cells were either resuspended in 150-400µl PBS, dependent on cell number, for flow cytometry, or subject to further processing for intracellular or annexin V staining, where applicable.

2.7.3. Intranuclear Staining

Cell fixation and permeabilisation was performed after cell surface staining using a FoxP3/Transcription Factor Staining Buffer Set (eBiosciences) according to manufacturers' instructions. Cells were resuspended in 1ml of formaldehyde-containing FoxP3 Fixation/Permeabilization working solution and incubated at room temperature for 30-60 mins. 2ml Permeabilization Buffer was added and cells were centrifuged at 450g for 5 minutes. Cells were resuspended in the residual volume of buffer (approximately 100µl) and non-specific antibody binding was blocked by adding 2µl rat serum (or other serum from the same species as the relevant primary antibody) for 15mins. Without washing, 2.5µl of fluorochrome-conjugated antibody directed against transcription factor/s of interest was added to each tube. Samples were gently vortexed and incubated at RT for 45mins, following which they were washed twice in Permeabilization Buffer and centrifuged at 450g for 5 minutes. Samples were resuspended in 100-500µl PBS, dependent on cell number to give a final concentration of up to 2×10^6/ml.

2.7.4. Annexin V Staining

Annexin V binds to extracellular phophatidylserine residues, which only become exposed on cell surface membranes during the intermediate stages of apoptosis. Up to 1×10^6 cells were resuspended in 100µl of Annexin V Binding Buffer (Biolegend, California, USA) to provide a source of calcium to facilitate Annexin V binding. 5µl fluorescein isothiocyanate (FITC)-conjugated annexin V (Biolegend) was then added to each tube. Cells were incubated at RT for

15mins. A further 100-300µl Annexin V Binding Buffer was then added to each tube, dependent on cell number, and samples were immediately analysed by flow cytometry.

Table 2.1. List of antibodies for flow cytometry

Antigen	Clone	Fluorochrome	Channel	Manufacturer
BCL6	7D1	APC	R670	Biolegend
CCR7	G043H7	PE	YG586	Biolegend
CD3	OKT3	Alexa Fluor 700	R730	Biolegend
CD4	RPA-T4	PerCP-Cy5.5	B710	Biolegend
CD8	RPA-T8/SK1	BV510	V525	Biolegend
CD10	HI10a	PE	YG586	BD Biosciences
CD19	HIB19	BV421	V450	Biolegend
CD20	L27	FITC	B530	BD Biosciences
CD25	BC96	PE	YG586	Biolegend
CD25	M-A251	BB515	B530	BD Horizon
CD45RA	HI100	BV510/Alexa Fluor 488	V525/B530	Biolegend
CD69	FN50	PE-Dazzle	YG610ish	Biolegend
CD86	IT2.2	PE-Cy7	YG780	Biolegend
CD127	A019D5	BV605	V610	Biolegend
CXCR3	G025H7	Alexa 488	B530	Biolegend
CXCR5	J252D4	APC/BV605	R670/V610	Biolegend
FoxP3	PCH101	eFluor450	V450	eBiosciences
HLA-DR	L243	BV605	V610	Biolegend
ICOS	C398.4A	BV421/PE	V450/YG586	Biolegend
ICOS-L	2D3	APC	R670	Biolegend
PD-1	EH12.2H7	PE/Cy7	YG780	Biolegend

2.7.5. Sample Analysis by Flow Cytometry

Data were acquired using a BD LSRFortessa flow cytometer (BD Biosciences) with 4 lasers: blue, red, violet and yellow-green. The cytometer passes cells in a fine, rapidly-following, single-cell stream through these lasers. Fluorochromes are identified by their ability to become excited by lasers producing light at specific wavelengths (excitation spectra) and then emit light at different wavelengths (emission spectra), that are able to pass through specific filters and are detectable by photomultiplier tubes.

Although fluorochromes have unique excitation and emission spectra, there is some overlap between the emission spectra of certain fluorochromes, and some fluorochromes are excited by multiple lasers. To correct for this spectral overlap, mathematical corrections, or compensations, need to be electronically applied to the optical signals in order to accurately differentiate between colours. Compensations were evaluated using BD FACSDiva software. Before data acquisition, the spillover for each colour was quantified using Anti-Mouse Igκ/Negative Control Compensation Particles (BD Biosciences) stained with each fluorochrome-conjugated antibody, according to the manufacturer's protocol. For viability and annexin V staining, compensations were performed using PBMCs. To ensure sufficient numbers of dead cells, half were subjected to heat shock at 64°C for 5 mins then cooled on ice for 5 mins to induce apoptosis. These were then re-combined with untreated cells and underwent viability or annexin V staining as described above. Whilst it was technically feasible to use up to 18 colours simultaneously on the BD Fortessa cytometer, a maximum of 10 colours were used here to avoid difficulties with data compensation and the need for excessive numbers of control samples.

Data were analysed with FlowJo v10 software (BD Biosciences). In all cases, cells were first gated according to forward scatter (FSC) and side scatter (SSC) to identify the lymphocyte population (Figure 2.1A). Lymphocytes were then gated to exclude cell doublets followed by non-viable cells, except where stated (Figure 2.1B-C). Viable cells were then gated according to expression of B- and T-cell markers, dependent on the cell population of interest.

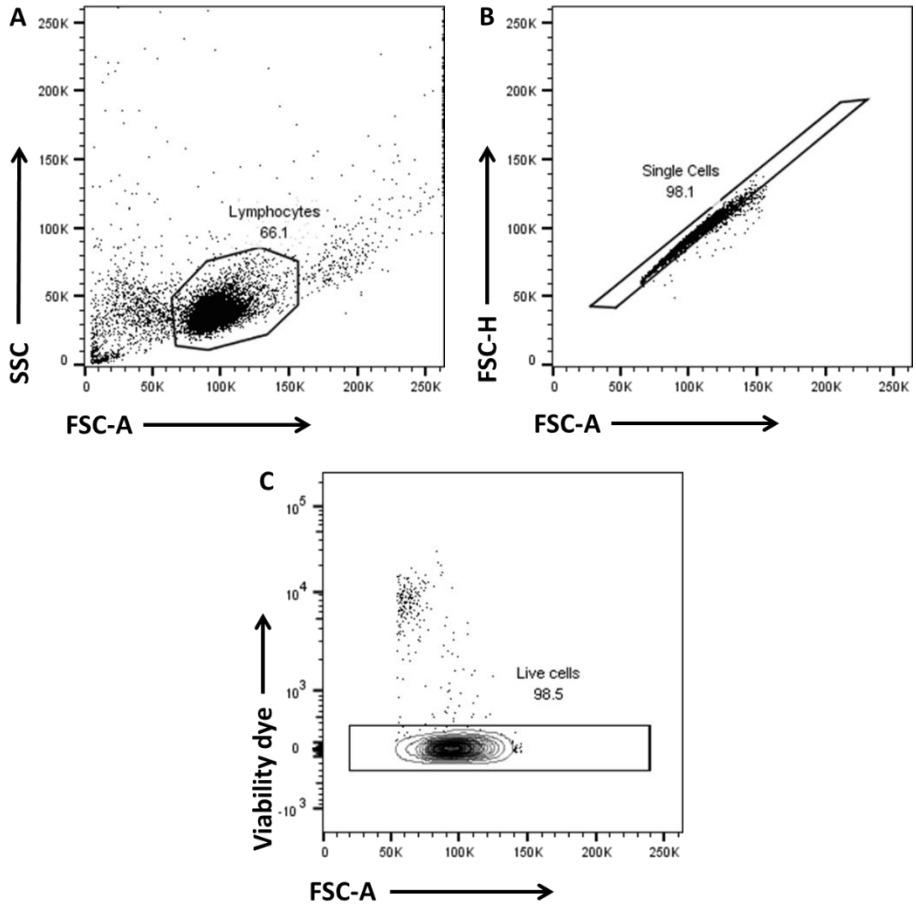

Figure 2.1. Identification of viable lymphocytes. A) *Representative flow plots show FL LN cell suspension gated according to forward (FSC-A) and side scatter (SSC) to identify lymphocytes (gated).* ***B)*** *Lymphocytes were gated according to forward scatter properties- area (FSC-A) and height (FSC-H)- to identify single cells.* ***C)*** *Viable lymphocytes (gated) were then identified by the lack of uptake of fixable viability dye.*

2.7.6. Cell Counting

Cells were resuspended in at least 150µl PBS and the total sample volume was measured with calibrated pipettes. 123Count eBead Counting Beads (eBiosciences) were vortexed for at least 30 seconds then 50µl of beads was carefully pipetted to each tube and vortexed again. Data were acquired as described above. Bead counts were obtained by gating on a low forward scatter, high side scatter population, which was clearly distinct from the lymphocyte population, and recording the number of events with strong fluorescence in both B530 and V450 channels (Figure 2.2). The number of events corresponding to the cell population of interest was also recorded. Absolute counts of the cell population of interest were then calculated using the following formula:

$$Absolute\ count\ (cells/\mu l) = \frac{(cell\ count\ \times\ eBead\ volume)}{(eBead\ count\ \times\ cell\ volume)} \times eBead\ concentration$$

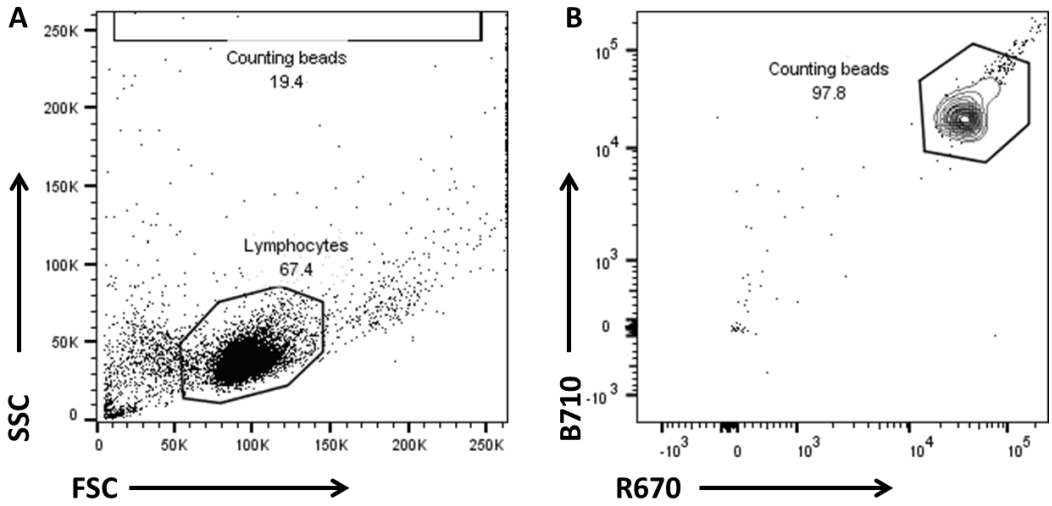

Figure 2.2. Identification of counting beads by flow cytometry. A) *Representative flow plot shows a FL LN cell suspension with counting beads added. Counting beads are identified by very high side scatter, higher than the scale visualised here.* ***B)*** *High side-scatter events were then gated on B710 and R670 channels. Counting beads are identified by high levels of fluorescence in both channels.*

2.7.7. Control Samples and Other Considerations

For each sample, test cells were run in tandem with unstained cells as a negative control for background autofluorescence. In addition, a proportion of cells were stained with viability dye only, and with only basic B- and T-cell markers (CD3, CD4, CD8, CD19) to exclude significant autofluorescence in the cell populations of interest and facilitate placement of positive/negative gates for other antigens.

As a result of compensation for spectral overlap between fluorochromes, there is an inevitable element of data spread, which may influence interpretation of minor shifts in antigen expression and placement of positive/negative cell gates. To adjust for this, fluorescence minus one (FMO) controls were used, in which cells were stained with all antibodies apart from the one directed against the antigen of interest, which illustrated the extent of data spread in the relevant channel. This allowed for accurate gating of negative/positive cell populations in stained

samples. FMOs were used for all antigens that were weakly expressed and where there were minor shifts in expression levels, such as intranuclear transcription factors and ICOS-ligand.

To control for non-specific antibody uptake when performing intranuclear staining, isotype-matched control samples were also used. Isotype-matched controls are fluorochrome-conjugated antibodies that lack target specificity but are otherwise matched to the relevant targeted antibody in terms of immunoglobulin isotype, host species and fluorochrome. Equivalent concentrations of isotype-matched control antibody were added to FMO controls when assessing transcription factor expression, i.e. FoxP3 and BCL6. It is feasible that isotype-matched controls can label cells non-specifically on occasions where target antibodies do not. However, in all cases, staining patterns with isotype-matched controls were similar to unstained controls and lower than staining with target antibodies.

FMOs were not used in instances where cell populations were easily separated, as was the case for all cell lineage markers and for PD-1/ICOS. In some cases, internal negative controls within the same sample could be used to guide gating of cells, for example, positive CD10 expression could be identified on CD19-positive B cells by setting a gate that excluded most of the CD10-negative non-B cell population (Figure 2.3).

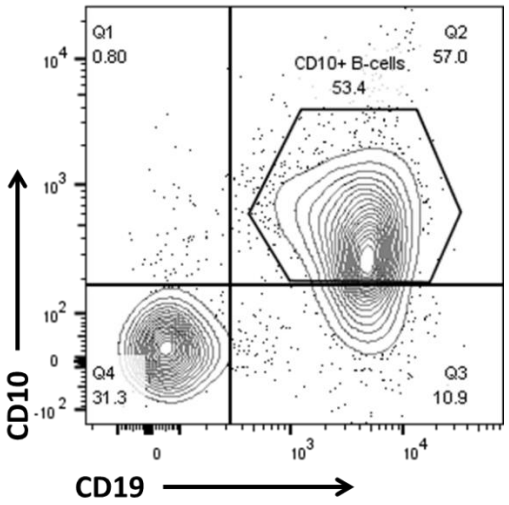

Figure 2.3. Identification of CD10$^+$ germinal centre B-cells. *Representative flow plot shows viable FL lymphocytes. FL B-cells are identified as CD19$^+$CD10$^+$. As expression of CD10 was weak, the level of CD10 expression in CD19-negative cells was used to set the threshold for CD10 positivity.*

Positive controls were required to confirm whether primary antibody staining had been successful in certain instances where staining of test samples was weak. This was the case for intranuclear BCL6 expression, where the Burkitt lymphoma cell line Ramos was used to confirm BCL6 positivity.

Fluorochromes were chosen according to fluorescence intensity and potential for spectral overlap. Strong antigens were paired with less intense fluorochromes (e.g. CD3 and Alexa Fluor 700), whilst weakly-expressed antigens were paired with stronger fluorochomes (e.g. CD25 and phycoerythrin (PE)). Antibody panels were designed such that where there was the potential for higher levels of spectral overlap, for example between BV510 and BV605, there was no co-expression of the respective target antigens on the cell population of interest, wherever possible. For example, CD8-positive T-cells (BV510) were usually excluded from analyses where CD127 and HLA-DR expression were assessed using BV605.

2.7.8. Fluorescence-Activated Cell Sorting

Mechanically-disaggregated LN cells were thawed and washed twice in RPMI-1640 medium. Cells were then rested at a concentration of 5-10 x 10^6 cells/ml for 1-2 hours before further manipulation. Cells were centrifuged at 1000 rpm for 10 minutes then resuspended in sterile PBS supplemented with 2% FBS and 1mM EDTA (staining buffer) and passed through a 35µm cell strainer to remove cell clumps. From this point onwards, cells were kept at RT to avoid frequent temperature fluctuations and preserve cell viability. Viability staining was performed as described in section 2.6.1. Cells were washed once then resuspended in staining buffer at 50 x 10^6 cells/ml. 25µl/ml of primary antibodies were added and incubated for 15 minutes, protected from light. No formal antibody titrations were undertaken but starting concentrations were based on the manufacturer's instructions and recommendations of experienced colleagues and produced the expected staining pattern on flow. Cells were washed twice in staining buffer and resuspended at 50 x 10^6 cells/ml.

Cells were sorted on a BD-FACS Aria III (BD Biosciences). In brief, cells were passed through a 70µm nozzle into a fine, rapidly-moving stream, which was then broken into single-cell droplets. Dependent on the characteristics of each cell, detected by standard flow cytometry, a differential electric charge was activated and applied to each droplet. An electrostatic deflection system then separated the droplets based on their charge profile into collection tubes. Cells were collected in RPMI-1640 medium (plus residual flow sheath fluid) in 5ml tubes. Assistance

with cell sorting and operation of the BD-FACS Aria III were provided by Drs Rianne Wester and Anna Rose at the Biomedical Research Council Flow Core facility at Guys' Hospital, London.

2.8. Histology Studies

2.8.1. Tissue Sectioning and Deparaffinisation

FFPE tissue blocks were cooled on ice for 1 hour. Tissue sections were cut to a thickness of 4µm using a Rotary Cut 4060 microtome (Slee Mainz, Mainz, Germany). Sections were floated on a water bath at 40°C and mounted onto poly-L-lysine coated microscope slides (VWR International, Pennsylvania, USA). Samples were dried on a heat block at 70°C for 30 minutes then at RT for at least 24 hours.

Samples were deparaffinised by immersion in 100% xylene for 5-10 minutes, repeated twice. Slides were transferred into 100% ethanol for 10 minutes then rehydrated through graded ethanol solution at 96% (twice), 70% and 50% ethanol for 5 minutes each and finally rinsed with tap water.

2.8.2. Antigen Retrieval and Blocking

For immunohistochemistry only, samples were first blocked with 0.5% hydrogen peroxide (Sigma-Aldrich) in PBS for 10 minutes, then washed briefly in PBS.

Antigen retrieval was performed in either sodium citrate buffer (pH 6.1) or tris-EDTA buffer (pH 9.0), both with 0.05% Tween-20, except where stated (Appendix 1). One litre of buffer was added to a pressure cooker and heated to 120°C on a portable hotplate. The slides were lowered into the buffer once boiling and pressure-cooked at 15 psi for 3 minutes. Slides were then cooled and washed with distilled water for 10-15 minutes.

Samples were blocked with serum from the same species in which the secondary antibodies were raised, to prevent non-specific antibody binding. The area surrounding the tissue section was carefully dried with low-lint tissues (Kimberly-Clark, Texas, USA), taking care not to allow the tissue itself to dry out at any point, and the tissue was encircled by hydrophobic barrier pen (Dako/Agilent Technologies, California, USA). Up to 400µl 5% serum in PBS was added to each slide, dependent on the size of the tissue section, and incubated for at least 1 hour at RT. For immunohistochemistry only, 150µl/ml avidin solution (Vector Laboratories, California, USA) was

also added to the serum blocking solution. Immunohistochemistry samples were subsequently blocked with 150µl/ml biotin solution in PBS for 15 minutes.

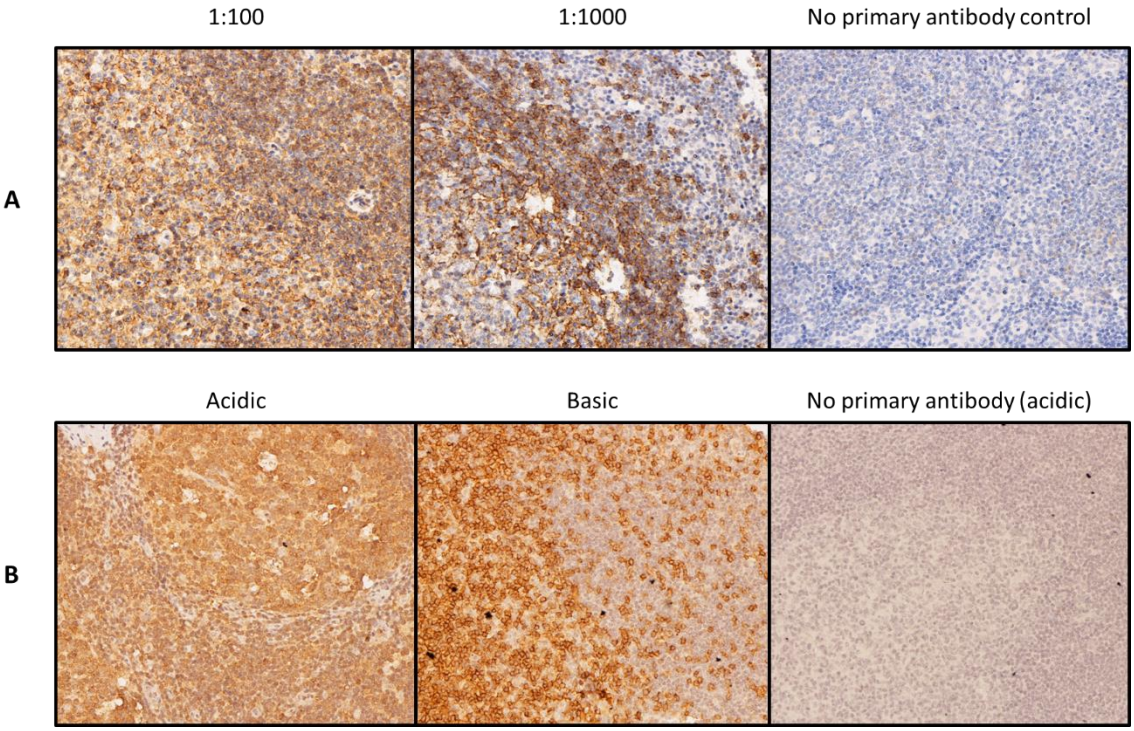

Figure 2.4: Primary antibody optimisation. A) *IHC images show CD23 assessment in reactive LN tissue, using a range of antibody concentrations. At high antibody concentrations (1:100), there is a lack of specific staining, with high levels of background uptake. Lower antibody concentrations (1:1000) gave expected staining characteristics, outlining FDCs and follicular B-cells.* ***B)*** *IHC images show CD4 staining in reactive tonsillar tissue under acidic (pH 6.1) and basic (pH 9.0) antigen retrieval conditions. Expected staining patterns were only seen with basic antigen retrieval. All images were taken with a x20 objective lens.*

2.8.3. Primary Antibody Incubation

Primary antibodies were made up to at a dilution of 1:50-1:1000 in PBS. Antibody concentrations, staining protocols and antigen retrieval conditions for most primary antibodies had been previously optimised in our laboratory (Townsend*, et al* 2019). New antibodies were tested first using immunohistochemistry on tissue known to be positive for the antigen in question, at a range of concentrations, and usually under both acidic and basic antigen retrieval conditions, to determine the optimum staining conditions (Figure 2.4). For multiparameter confocal immunofluorescence microscopy (CIFM), 3 or 4 primary antibodies were combined.

Primary antibodies are listed in Table 2.2. The blocking serum was poured off the tissue sections and, without rinsing, up to 400µl primary antibody solution was added to each slide. Slides were then placed in a humidified box at 4°C overnight. Slides were then washed 3 times with PBS, each for at least 5 minutes.

Table 2.2: Primary antibodies for immunohistochemistry and immunofluorescence studies

Antigen	Antibody clone	Species/Isotype	Manufacturer	Dilution
AID	ZA001	Mouse IgG1	Invitrogen	1:200
CD3	CD3-12	Rat IgG1	Abcam	1:200
CD4	4B12	Mouse IgG1	Leica Biosystems	1:50
CD8	EP1150Y	Rabbit	Abcam	1:400
CD20	L26	Mouse IgG2a	Dako	1:200
CD21	EP3093	Rabbit	Abcam	1:1000
CD23	Polyclonal	Goat IgG	R&D	1:1000
Cleaved Caspase-3	Polyclonal	Rabbit	Cell Signaling	1:200
FoxP3	236A/E7	Mouse IgG1	Abcam	1:100
ICOS	SP98	Rabbit	Abcam	1:100
MYC	Y69	Rabbit	Abcam	1:200
PD-1	Polyclonal	Goat IgG	R&D	1:50
PD-L1	E1L3N	Rabbit	Cell Signaling	1:100
PD-L2	176611	Mouse IgG2b	R&D	1:20-1:1000
Pax5	1H9	Rat IgG2a	EMD Merck	1:200
Tbet	EPR9302	Rabbit	Abcam	1:200
Pax5	1H9	Rat IgG2a	Biolegend	1:200

2.8.4. Secondary Antibody Incubation

For immunohistochemistry, biotinylated secondary antibodies (Vector Laboratories) were used at a dilution of 1:100 in PBS. Up to 400µl was added to each tissue section, including control slides, then incubated for 1 hour at RT for immunohistochemistry and 2 hours for CIFM. For CIFM, slides were protected from light this point onwards. Slides were then washed 3 more times with PBS for at least 5 minutes per wash.

For CIFM, fluorochrome-conjugated donkey anti-species secondary antibodies were used (Jackson ImmunoResearch, Pennsylvania, USA) at a concentration of 1:200 in PBS, or 1:400 if

using Dylight 405-conjugated antibodies, to reduce background staining (Table 2.3). Up to 400µl was added to each tissue section, including control slides, then incubated for 2 hours at RT. Slides were protected from light this point onwards to prevent photobleaching. Slides were then washed 3 more times with PBS for at least 5 minutes per wash, then partially dried for approximately 20 minutes before adding a drop of aqueous Prolong Gold Antifade mountant (Invitrogen, California, USA) plus a coverslip. Slides were left to dry at RT for a further 24 hours then stored for up to 2 weeks at 5°C prior to image acquisition.

Table 2.3: Secondary antibodies for immunohistochemistry and immunofluorescence studies

Target	Species	Fluorochrome	Subclass	Manufacturer	Dilution
Goat	Donkey	Cy3	IgG	Jackson Immunoresearch	1:200
Mouse	Donkey	Alexa 647	IgG	Jackson Immunoresearch	1:200
Rabbit	Donkey	Alexa 488	IgG	Jackson Immunoresearch	1:200
Rat	Donkey	Dylight 405	IgG	Jackson Immunoresearch	1:400

2.8.5. Peroxidase and Haematoxylin Staining

For immunohistochemistry, samples were next coated with peroxidase-containing avidin/biotin complex solution for 30 minutes using the Vectastain Peroxidase Standard Kit PK-400 (Vector Laboratories), according to manufacturer's instructions, then washed 3 more times with PBS for 5 minutes each.

Immunohistochemistry was performed using 3,3'-diaminobenzidine (DAB) as a peroxidase substrate with the ImmPact DAB Kit for Peroxidase (Vector Laboratories). One drop of DAB solution was added to per ml of supplied diluent and vortexed to mix. Up to 400µl was applied to each tissue section for between 30 seconds and 10 minutes, until the desired degree of brown colour change was observed. Slides were then washed in tap water to quench the peroxidase reaction for at least 5 minutes. Samples were counterstained with haematoxylin (Vector Laboratories) for 30 seconds, to dye cellular nuclei blue, and washed again with tap water.

Slides were dehydrated through graded ethanol solutions (50%, 70%, 96%, 96% then 100%) for 2 minutes each, and then placed in 100% xylene for 20 minutes. Tissue sections were then partially dried and mounted with xylene-based Eukitt quick-hardening mounting medium (Sigma-Aldrich) and a coverslip.

2.8.6. Control Samples

Negative control tissue slides were produced in parallel for all tissue sections in order to exclude the presence of significant non-specific background staining and, for CIFM, tissue autofluorescence. Control slides were processed in the same way as test sections, except during primary antibody incubation, where control sections were covered with PBS only, i.e. lacking any primary antibody. For multiparameter CIFM, additional control slides were produced, which were stained with each individual primary antibody in isolation, to assess for the presence of fluorescence spillover into adjacent channels.

Positive control slides were used to confirm that the expected staining pattern was produced with certain primary antibodies where expression was low or absent on test slides, or when testing new primary antibodies. Choice of control tissue depended on the antigen in question but was usually reactive lymphoid or Burkitt lymphoma tissue. These slides were stained in exactly the same way as test slides.

2.8.7. Assessment of IHC staining

IHC slides were visualised by light microscopy using x10, x20 and x40 objective lenses. Negative control slides were visualised first, and test samples were excluded if an excess of non-specific background rendered staining patterns uninterpretable. In most cases, areas of brown DAB staining were visible within cell nuclei, cytoplasm or cell membranes, corresponding to known staining patterns for the antigen in question. Positive control slides were used where staining was weak or absent. Again, test samples were excluded if parallel positive control samples failed to produce a clear positive result.

2.8.8. Confocal Immunofluorescence Microscopy

Images were acquired with a Nikon Eclipse Ti A1R inverted microscope and confocal imaging system (Nikon, Tokyo, Japan). Four lasers were used: blue, yellow-green, red and far red. The excitation and emission spectra of the fluorochromes used is shown in Figure 2.5 and the filters used for image acquisition are shown in Table 2.4. In theory, up to 6 different fluorochromes can be assessed simultaneously but for this work a maximum of 4 channels were used. This was partly due to the lack of diversity of commercially-available primary antibodies in terms of host species and immunoglobulin isotype, such that it was not possible to find sufficient primary-secondary antibody combinations to assess a larger number of antigens. In addition, our wider

group has encountered issues with spectral overlap and increased background fluorescence when assessing more than 4 antigens, which can confound image analysis.

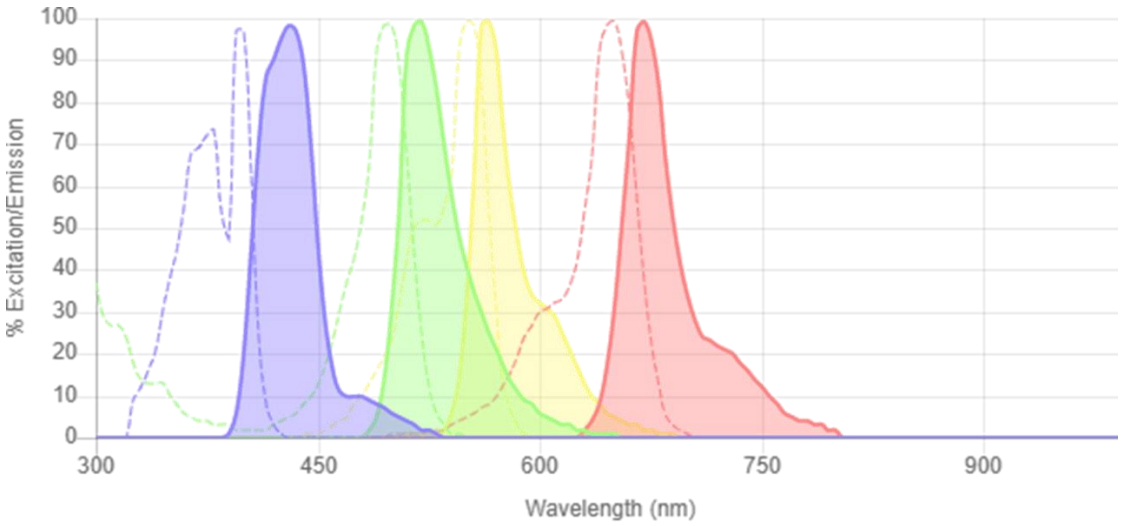

Figure 2.5: Fluorochrome excitation spectra and emission spectra. *Graph illustrates the excitation spectra (dotted line) and emission spectra (solid colour) of fluorochromes used in CIFM studies. Blue: Dylight405; green: Alexa Fluor 488; yellow: Cy3; red: AlexaFluor 647. Image produced using the Jackson ImmunoResearch Spectra Viewer*

Table 2.4. Filters used for confocal immunofluorescence microscopy

Channel	Excitation filter (nm)	Dichroic mirror cut-off (nm)	Emission filter (nm)	Fluorophore
Blue	325 – 375	400	405 – 485	Dylight 405
	426 – 446	*455*	*460 – 500*	*not used*
	450 – 490	*495*	*500 – 575*	*not used*
Yellow-green	490 – 510	515	520 – 550	Alexa Fluor 488
Red	540 – 580	585	598 – 662	Cy3
Far red	608 – 648	660	672 – 712	Alexa Fluor 647

Microscope settings were kept constant wherever possible to facilitate image comparison; filter settings, pin hole size, pixel dwell time and optical section thickness were identical for all imaged tissue sections. Laser power and photomultiplier tube (PMT) gain had to be adjusted for each tissue section due to natural variations in tissue quality (for example due to tissue fixation, size and age) and therefore staining intensity. Positively-stained areas of tissues were visualised,

and the power/gain settings were optimised to find a threshold where only a few pixels were oversaturated, which ensured the widest image detection range whilst preventing overexposure and fluorochrome bleaching. Laser offset was generally maintained at zero, except in instances where there was high image background. After imaging tissue samples, all settings (including laser power and PMT gain) were left unchanged when imaging paired negative control tissue (see below).

Low power images were first acquired using a 20x Plan Apo VC objective lens. High-power images were acquired using a 60x Plan Apo oil immersion lens (both Nikon).

2.8.9. Confocal Image Analysis

Images were analysed using NIS-Elements Advanced Research software version 4.2. Contrast optimisation was performed using the look-up table function of the NIS-Elements software. NIS-Elements image files (ND2 format) were directly exported as tiff files. Some images have also been cropped for presentation, where appropriate, but no digital image manipulation has occurred.

Binary images were created for each laser channel to identify areas of positive antigen expression and facilitate image analysis. These were overlaid onto the original image, without altering the image file itself. In order to produce binary layers, fluorescence intensity thresholds were set at a level that clearly differentiated between positive and negative expression, without picking up aberrant positivity in negative control sections (Figure 2.6). The threshold was adjusted for each tissue section where necessary, due to varying levels of staining intensity and background fluorescence between samples. When differentiating between high and low levels of antigen expression, internal tissue controls were used to set thresholds; for example, the threshold to define high levels of PD-1 expression was set at a level that excluded the majority of extrafollicular T-cells (Figure 2.6). Identical binary thresholds were applied to paired negative control images for each sample, to ensure that background autofluorescence was not present at a level that would obscure image interpretation.

NIS-Elements software tools enabled binary image refinement. Restrictions were set according to object size to exclude very small objects (e.g. <2μm) that are likely to represent artefact or very large objects (e.g. >50μm) that may represent fluorescence from vessels or connective tissue. Non-cellular objects that clearly represented artefact or connective tissue could be manually deleted, if required. It was possible to smooth binary layer contours and fill holes in

circular objects, although these functions were not used where binary image area was used as part of the image analysis. Binary layers from 2 or more channels could be combined to identify areas of co-expression and then generate secondary 'intersection' binary layers (Figure 2.7).

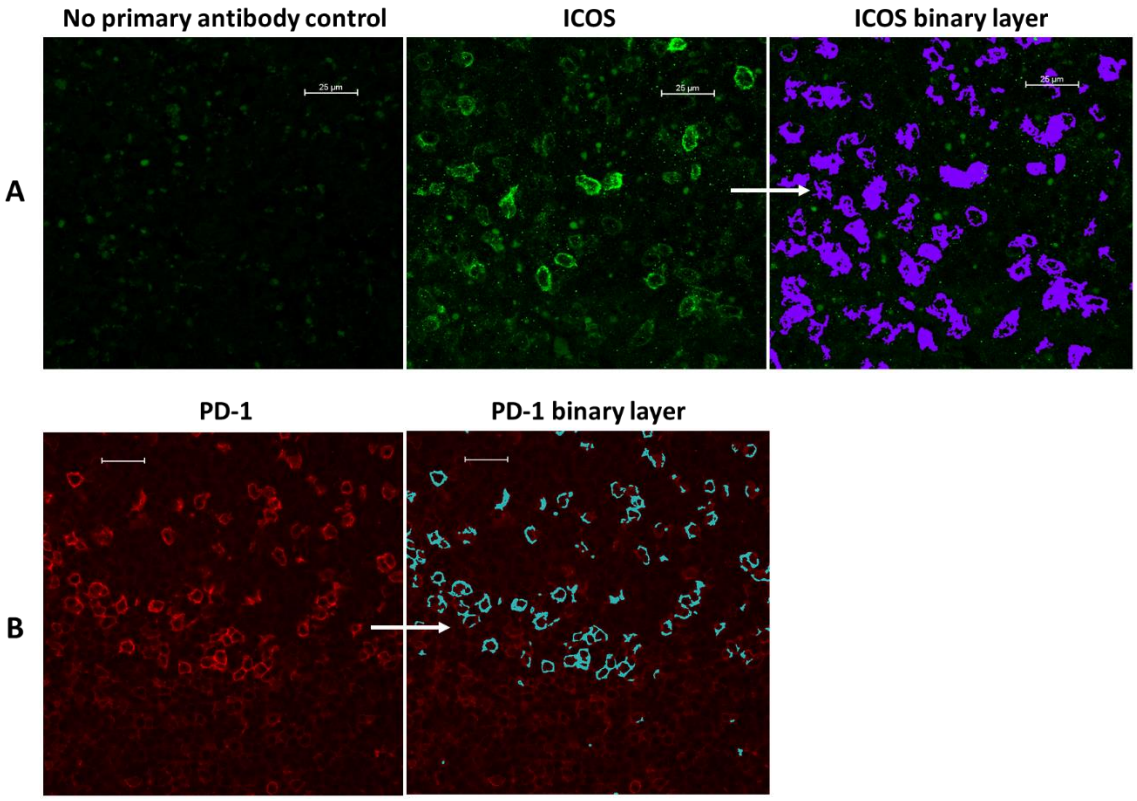

Figure 2.6. Confocal image analysis and binary image generation. A) *Image of FL tissue shows high levels of autofluorescence in the yellow-green channel in negative control samples (no primary antibody), which is also visible when assessing ICOS expression in the same channel. A binary layer was generated to identify low levels of ICOS expression (right panel), which excluded background autofluorescence by setting appropriate fluorescence thresholds and excluding objects <2µm in size. The same binary settings were applied to negative control tissue, which confirmed that autofluorescence did not give a false positive signal.* ***B)*** *Representative image shows expression of PD-1 in the perifollicular area of FL tissue (left). The binary layer defining PD-1 expression was set at a level that excluded the majority of interfollicular T-cells with weaker PD-1 expression (right). No background fluorescence was seen in the red laser channel (not shown). All images were taken with a x60 objective lens and scale bars measure 25µm.*

NIS-Elements software calculated the area of binary layers. Automated cell counting was also potentially feasible, but this required accurate separation of cells/nuclei into discrete objects. Due to the closely packed nature of lymphoid tissue in FL, it was not feasible to accurately separate objects either manually or using the NIS-Elements automated object separation tool. Therefore, cell counts were performed manually for a representative area of the tissue image. Image analysis is discussed in more detail in Chapter 5.

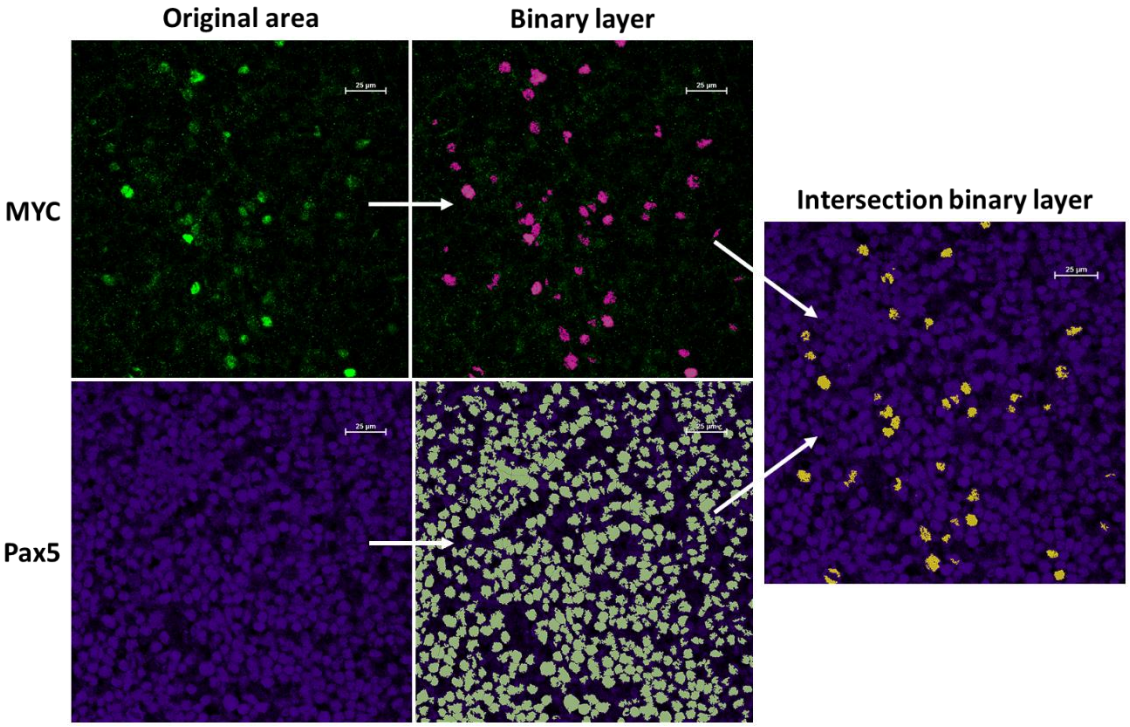

Figure 2.7. Generation of intersection binary layers. *Images of FL tissue show the original confocal images and binary layers for MYC (top) and Pax5 (bottom). The panel on the right shows areas of overlap between the MYC and Pax5 binary layers in yellow, generated as a new 'intersection' binary layer. All images were taken with a x60 objective lens and scale bars measure 25µm.*

2.8. Statistical Considerations

All statistics were calculated using FlowJo v10 and GraphPad Prism software v7 (GraphPad, California, USA).

Data are reported as mean values ± standard error, except where specifically stated. Median values and ranges are reported for data that are clearly not normally distributed or where outlying results skewed mean values.

Samples were tested for normality (d'Agostino-Pearson omnibus normality test) and, where appropriate, sample means were compared using either paired or unpaired t-tests. When the sample failed the normality test an appropriate non-parametric test was performed: Mann-Whitney U for independent samples and Wilcoxon signed rank for paired samples. A 2-sided significance level of 0.05 was used. Correlation between normally-distributed variables was evaluated using Pearson's correlation coefficients.

CHAPTER 3: IDENTIFYING T_{FH} IN FOLLICULAR LYMPHOMA TISSUE

3.1. Introduction and Aims

Studies using archival FL tissue have provided significant insights into the biology of follicular lymphoma, allowing assessment of genomic change and overall patterns of gene expression in FL tissue as a whole. Tissue imaging studies have provided insights into the spatial interactions between FL B-cells and non-neoplastic cells within the TME. Such studies demonstrate apparent immune synapse formation between T_{FH} and FL B-cells and imply a close relationship between T_{FH} and FL proliferation (Townsend*, et al* 2019). However, two-dimensional imaging studies of tightly-packed, cell-dense FL tissue cannot easily tease out the contributions of individual cells from that of the surrounding microenvironment. These findings are hypothesis-forming but cannot definitively demonstrate a direct relationship between T_{FH} and FL growth. Functional studies are required to explore the interactions between FL B-cells and T_{FH} in greater detail.

T_{FH} are primarily resident within secondary lymphoid tissue, therefore obtaining T_{FH} from human subjects poses a challenge. Much of our knowledge of the biology of T_{FH} in the normal GC reaction is derived from animal models, particularly murine studies (Crotty 2014). However, there are no animal models that accurately recapitulate the indolent behaviour of FL. Murine models of BCL2, BCL6 and AID-driven lymphomagenesis usually develop aggressive B-cell lymphomas, or otherwise display significant alterations in T-cell number and function (Egle*, et al* 2004a, Pasqualucci*, et al* 2007). In patient-derived xenograft models, there is preferential expansion of non-neoplastic B-cells and most FL B-cells rapidly differentiate into plasmablasts (Burack*, et al* 2017).

Alternative options include the use of surrogate models to mimic T_{FH} stimulation. For example, multiple groups have successfully maintained GC B-cells *in vitro* for up to 10 days by co-culturing with CD40L-transfected fibroblasts or FDCs, in combination with selected cytokines to mimic T_{FH} support (Caeser*, et al* 2019). Recently, modified FDCs that express CD40L and secrete IL-21 have been shown to induce both proliferation and long-term survival of healthy GC B-cells (Caeser*, et al* 2019). These effects were enhanced when GC B-cells were modified to constitutively express BCL2. However, it is not yet clear whether this be reproduced with primary FL cells and it is not possible to tease out the relative contributions of the stromal cells themselves versus any acquired T_{FH}-like capabilities. Fibroblasts and FDCs cannot recapitulate the full T_{FH} phenotype (e.g. IL-4, ICOS and SAP expression), nor can they be used to assess the bi-directional influence that FL B-cells have on T_{FH} phenotype and survival. Therefore, to investigate functional

interactions between FL-T_{FH} and FL B-cells requires human FL tissue to facilitate *in vitro* culture experiments.

Disaggregated FL cells from fresh LN excision biopsies are the ideal source of T_{FH} and FL B-cells but are difficult to obtain, primarily due to an increasing reliance on less invasive core needle biopsy for lymphoma diagnosis, where the scant volume of tissue is usually all required for diagnostic purposes (Johl*, et al* 2016). In the increasingly rare instances that excision biopsies are performed, the primary diagnosis is often not yet known, and patients are frequently under the care of other medical teams (i.e. non-haematology). Thus, it is challenging to prospectively identify potential FL patients and ensure that tissue is processed fresh and in a timely manner, without coming into contact with formalin or other fixative that would preclude later cell culture. It was therefore necessary to explore other means of obtaining T_{FH} and FL B-cells.

The following sources were considered, and are described in greater detail in the sections below:

1. LN fine needle aspirate (FNA)
2. Peripheral blood and bone marrow aspirates
3. In-vitro transformation of naïve T-cells into T_{FH}

The aim of this preliminary work was to assess whether T-cells corresponding to a T_{FH} phenotype could be readily identified or generated from FL patients using these sources, and in sufficient numbers to enable further co-culture studies.

3.2. Identifying T_{FH} in Lymph Node Tissue

3.2.1. Background

LN FNA is a less invasive method of obtaining LN single cell suspensions than surgical or core biopsy and can easily be performed in the outpatient clinic. FNA cytology has been used to diagnosis and classify low-grade non-Hodgkin lymphoma (Cozzolino*, et al* 2016), and our group has previously demonstrated the utility of FNAs for assessing the TME in CLL (Pasikowska*, et al* 2016). FNAs have also been successfully used to study T_{FH} in reactive LNs of non-human primates (Havenar-Daughton*, et al* 2016).

It was not clear whether this technique could be successfully applied to the study of the TME in FL, a tissue more heterogeneous in its composition than CLL, and whether the lymphocyte subsets obtained would accurately reflect those present in the entire LN. Presuming that T_{FH}

could be identified, it was also unclear whether they would be present in sufficient numbers to facilitate culture studies.

The aims of this section were:

1) To characterise and compare lymphocyte subsets in FL cell suspensions derived from disaggregated LN tissue (acquired on rare occasions) and FNA

2) To quantify T_{FH} and FL B-cell yield from FL FNA and assess the feasibility of using FL for culture studies

3.2.2. Methods

LN FNA, tissue disaggregation and flow cytometry were performed as described in Sections 2.3, 2.4 and 2.7, respectively. No single antigen is specific to T_{FH} or able to accurately identify T_{FH} within $CD4^+$ T-cells in isolation. Optimal protocols for identifying human T_{FH} cells have been published (Espeli and Linterman 2015), incorporating combinations of the following antigens:

$CD3^+$ $CD4^+$ PD-1^{hi} $CXCR5^+$ $ICOS^+$ $BCL6^+$ $CD57^+$ $CD200^+$ $CD25^-$ $CD45RA^-$ $CCR7^-$ $FoxP3^-$

All experiments throughout this thesis used a basic antibody panel to identify T_{FH} consisting of T-cell markers (CD3 and CD4) and T_{FH}-associated markers (PD-1, ICOS and CXCR5; see Table 2.1). These markers have most consistently been used to identify T_{FH} across published studies and are the most functionally relevant; high levels of PD-1 expression have been shown to identify functionally active T_{FH} within FL (Yang*, et al* 2015a), whilst ICOS and CXCR5 are essential for T_{FH} function (Crotty 2019). CD25 together with CD127 was used to identify any cells that possessed $CD127^{lo}CD25^+$ T_{reg} or T_{FR} phenotype. Disaggregated reactive LN tissue was available from a patient with toxoplasmosis lymphadenitis and was initially used as a positive control to ensure that *bona fide* T_{FH} were identified in FL LN cell suspensions. CD19 and CD10 were used to identify the malignant GC B-cell population. CD10 expression is confined to a relatively small population of GC B-cells in reactive LNs but is usually diffusely expressed in FL (Figure 3.1). Whilst a small minority of $CD19^+CD10^+$ FL B-cells may be non-malignant, it has already been shown that the vast majority of B-cells in FL tissue are neoplastic, their phenotype is complex and no single antigen can adequately distinguish malignant from non-malignant B-cells (Le*, et al* 2016, Wogsland*, et al* 2017). Concurrent assessment of Ig light chain clonality or intracellular markers, such as BCL2, would not completely exclude non-malignant B-cells but would increase flow panel complexity and difficulty in performing compensations.

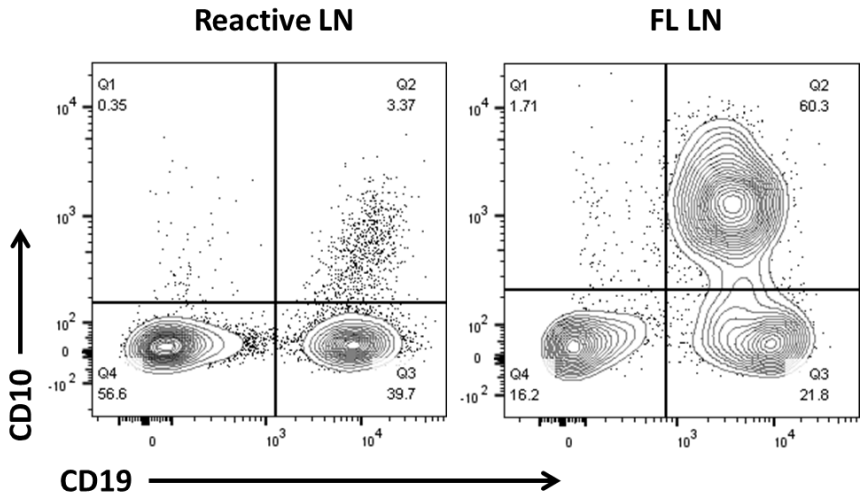

Figure 3.1. Expansion of CD19⁺CD10⁺ germinal centre B-cells in FL. *Representative flow plots show expression of CD19 and CD10 viable lymphocytes isolated from reactive lymph node (left) and FL FNA (right)*

3.2.3. Lymph Node Samples and Patient Characteristics

Samples obtained included FL FNAs (n=17, from 12 patients) and disaggregated FL LN tissue (n=5; 4 from whole LN excision biopsy, 1 from needle core biopsy). The baseline demographics and disease characteristics of these patients are outlined in Table 3.1. Median age was 64.0 years (range 36.7 – 78.2). Twelve patients (70.6%) had not received any prior lymphoma treatment. Five patients were at 1st or 2nd disease relapse and had not received treatment for a median of 34 months (range 6 – 84). None had received prior bendamustine or purine analogue therapy, which can induce prolonged lymphopenia. Only 1 patient had high-risk disease, defined by progression of disease within 24 months of initial immunochemotherapy.

3.2.4. T_{FH} in FL LN Cell Suspensions

The gating strategy used to identify T-cell subsets in FL LN is shown in Figure 3.2. There was a discrete population of PD-1^{hi}ICOS^{+}CD4^{+} T-cells in disaggregated FL LN tissue that were CXCR5^{+} and lacked CCR7 and CD45RA expression, corresponding to a T_{FH} phenotype (Figure 3.3). The same PD-1^{hi}ICOS^{+} T-cell population was also present in reactive LN control tissue, where T_{FH} accounted for a very small proportion of CD4^{+} T-cells (3.2%), consistent with published literature (Ame-Thomas*, et al* 2012).

Table 3.1. Baseline patient characteristics

Patient ID	Sample	Age (years)	Sex	Stage	Grade	Treatment
FL001	FNA*	59.5	F	4	3A	Pre-treatment
FL004	FNA	70.1	M	4	Unk	W&W
FL005	FNA*	36.7	M	3	2	First relapse
FL006	FNA*	40.3	F	3	2	W&W
FL009	FNA	64	F	1	2	Pre-treatment
FL010	FNA*	52.4	F	4	1	W&W
FL013	FNA	67.7	F	Unk	1	First relapse
FL018	FNA	78	M	1	2	First relapse
FL023	FNA	54	M	4	3A	Second relapse
FL024	FNA	74.2	M	4	Unk	First relapse
FL026	FNA†	69.1	M	3	2	W&W
FL028	FNA	55.4	F	4	2	Pre-treatment
FL014	LN	60.9	M	4	1	W&W
FL021	LN	54.3	F	4	1	Pre-treatment
FL022	LN	71.4	F	3	3A	Pre-treatment
FL025	LN	71.8	F	3	3A	Pre-treatment
FL027	LN	78.2	M	3	1	W&W

** denotes patients that underwent FNA on more than one occasion*

† *failed to obtain LN cells from FNA*

FNA: fine needle aspirate; LN: lymph node; Pre-treatment: prior to first-line immunochemotherapy; unk: unknown; W&W: watch and wait

PD-1^{hi}ICOS^{+} T_{FH} were also readily identifiable in 16 of 17 FNAs (94%; Figure 3.3A); only one FNA did not have any T_{FH}. The same sample also lacked FL B-cells, therefore the FNA is likely to have either missed affected LN tissue, in the absence of ultrasound guidance, or sampled a rare necrotic area.

The lymphocyte composition of disaggregated LN tissue and FNAs was then compared to assess whether these sources of LN cell suspensions were similar and could be used within the same experiments. FL is a heterogeneous tissue and it is not possible to assume that lymphocytes from both follicular and interfollicular areas are equally easy to aspirate. Many FNAs also contain some visible red cell contamination, therefore the presence of PB lymphocytes may skew T-cell composition.

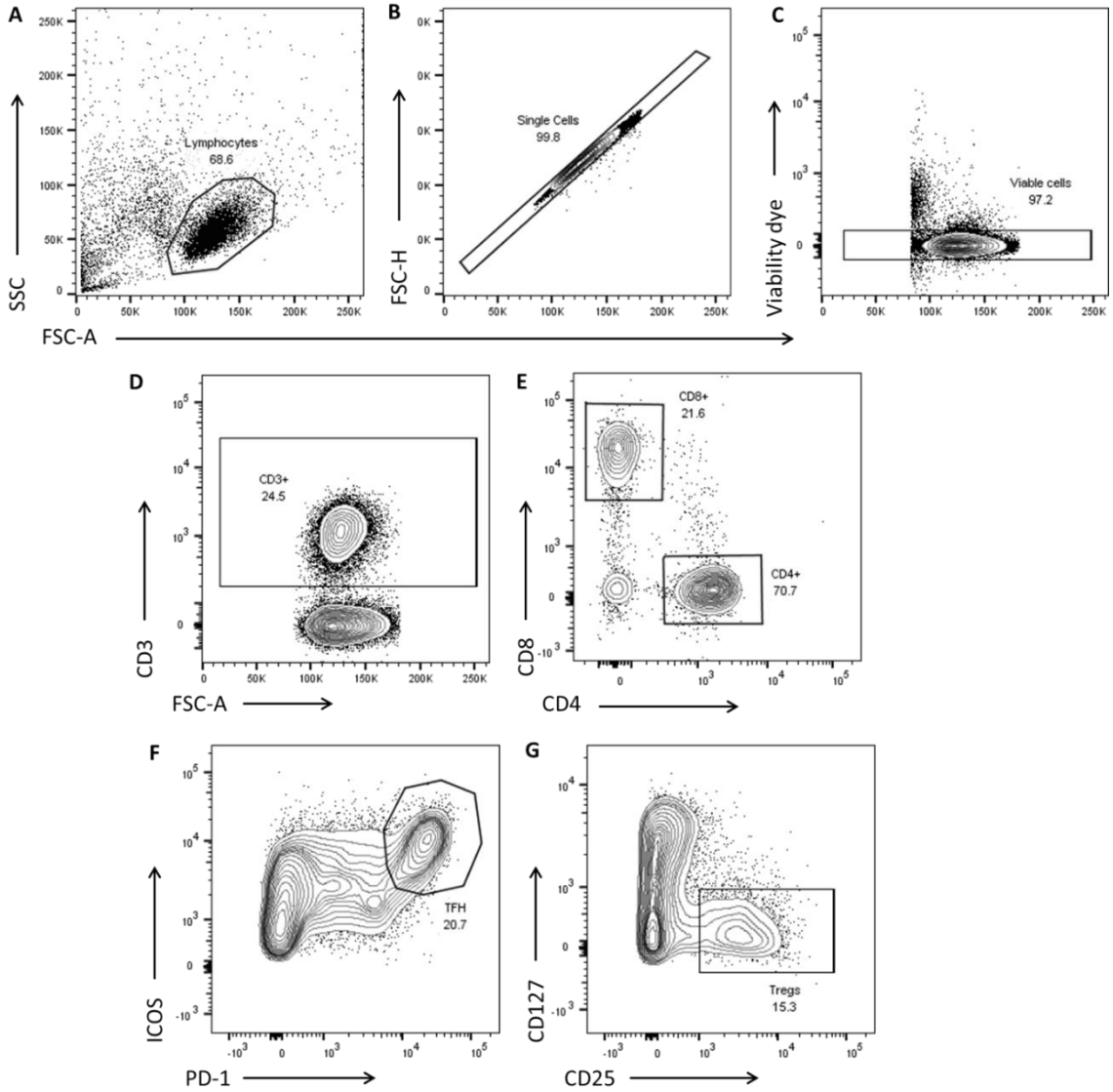

***Figure 3.2**. Identification of T_{FH} and T_{regs} in FL LN cell suspensions. Representative flow plots show cells sequentially gated according to **A)** forward and side scatter, **B)** doublet exclusion (forward scatter area vs height), **C)** cell viability, **D)** CD3 and **E)** CD4 and CD8 expression. $CD4^+$ T-cells were gated accordingly and high ICOS and PD-1 expression used to identify T_{FH} **(F)**, and CD127 and CD25 expression used to identify T_{regs} **(G)**.*

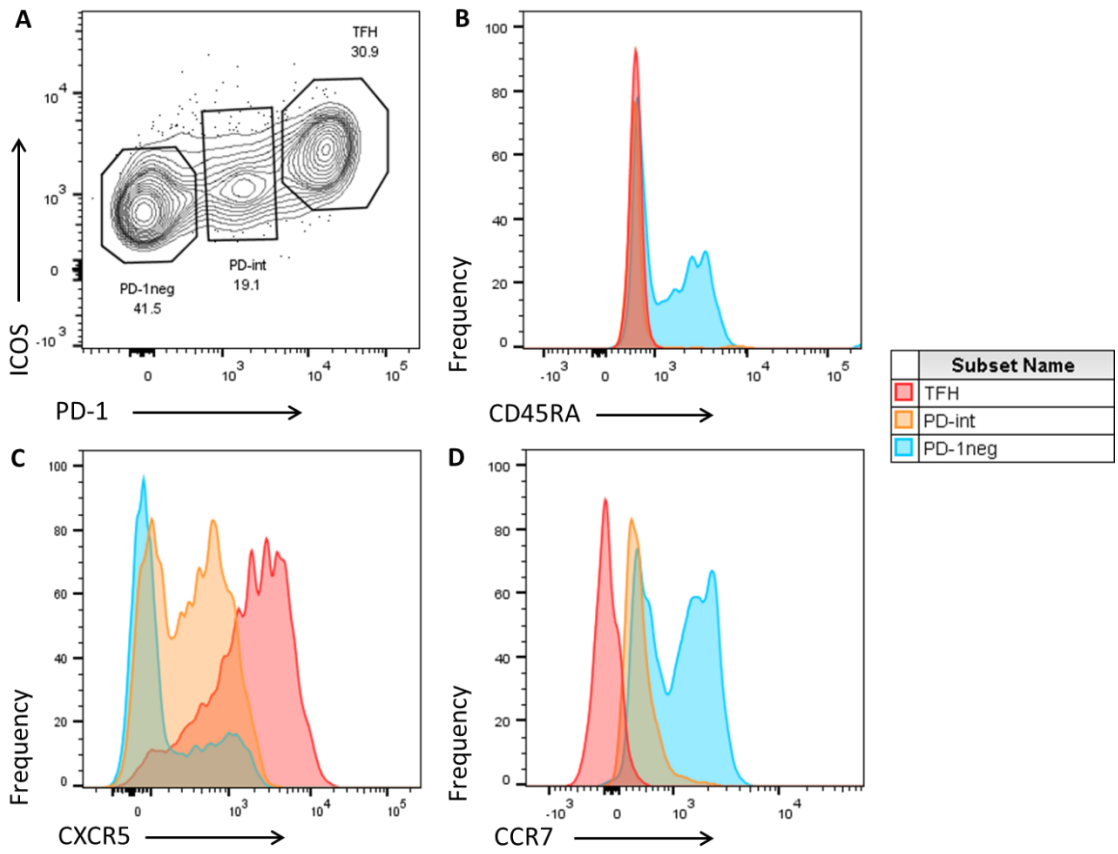

Figure 3.3. PD-1 and ICOS identify a discrete population of CXCR5⁺ T_{FH} FL LN tissue. A) *Representative flow plot show A) identification of PD-1^{hi}ICOS⁺ T_{FH} in gated CD4⁺ T-cells from a LN FNA. Histograms compare* ***B)*** *CD45RA,* ***C)*** *CXCR5 and* ***D)*** *CCR7 expression in CD4⁺ T-cell subsets according to PD-1 and ICOS expression.*

T_{FH} accounted for a similar proportion of CD4⁺ T-cells in LN cell suspensions from both sources: 28.6 ± 3.8% in FL LN FNAs (n=12) and 29.2 ± 6.1% in disaggregated FL LNs tissue (p=0.68; n=5, Figure 3.4). Both are consistent with other studies using disaggregated FL LN tissue, which have reported that T_{FH} represent 26.6 – 35.0% of CD4⁺ T-cells in FL (Ame-Thomas*, et al* 2012, Pangault*, et al* 2010, Yang*, et al* 2015a). Other lymphocyte subsets were also similar in both sources. The median ratio of B-cells to T-cells was 1.98 (range 0.19 – 7.99) in disaggregated LN and 2.20 (range 0.16 – 4.14) in FNAs (p>0.99). CD4⁺ T-cells comprised 74.0 ± 5.4% of all CD3⁺ lymphocytes in disaggregated LN and 77.5 ± 2.6% in FNA (p=0.55). The proportion of CD4⁺ T-cells that had a CD127^{lo}CD25⁺ T_{reg} phenotype, which usually predominate in interfollicular areas, was also similar: 23.7 ± 3.0% in FNAs and 24.4 ± 6.8% in disaggregated LN (p=0.84).

These data show that the lymphocyte composition of disaggregated FL LNs and FNAs are very similar. Therefore, cell suspensions from both sources were used interchangeably from this point onwards

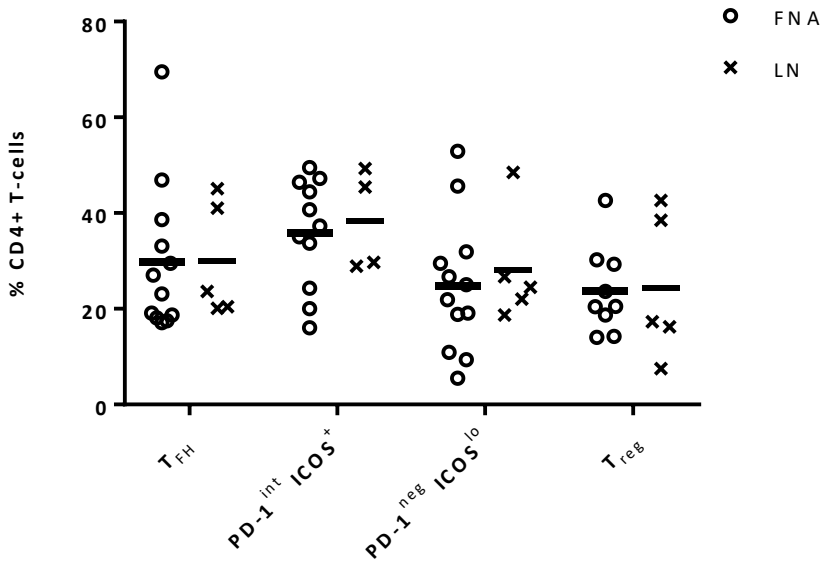

Figure 3.4. Comparison of CD4⁺ T-cell subsets in FL FNA and LN tissue. *Graph shows the proportion of viable CD4⁺ T-cells that possessed the phenotypes indicated. Horizontal bars represent mean values. p=NS for all FNA and LN comparisons*

3.2.5. Characterisation of FL LN T_{FH}

Different combinations of T_{FH} markers have been used to identify T_{FH} across the published literature, variously defining T_{FH} as CXCR5^{hi}ICOS^{+}, PD-1^{hi}ICOS^{+}, PD-1^{hi}CXCR5^{hi} or CXCR5^{hi}CCR7^{lo}. These gating strategies were compared in FL LN tissue to assess their feasibility and ability to identify bona fide T_{FH}.

The proportion of cells identified as 'T_{FH}' was very similar by all 4 methods (see Figure 3.5). However, PD-1 and ICOS together most consistently identified T_{FH} as a discrete population that was easy to identify and gate reproducibly.

Another important consideration was whether cells identified as T_{FH} included regulatory T-cells. T_{FR} have an identical phenotype to T_{FH} but express T_{reg} markers including CD25 and FoxP3. Gating strategies that incorporated PD-1 along with either ICOS or CXCR5 included the lowest proportion of T_{FR}-like cells with a T_{reg} phenotype: only 6.73 ± 1.5% of PD-1^{hi}ICOS^{+} cells were

$CD25^{+}CD127^{lo}$, compared with 20.2 ± 3.4% $CXCR5^{hi}ICOS^{hi}$ cells (p=0.002; n=12; Figure 3.6). This is consistent with published data identifying high PD-1 expression as a key marker of functionally-active T_{FH} in FL (Yang*, et al* 2015a). It also highlights that different gating strategies are not interchangeable and can incorporate functionally diverse groups of cells.

Lastly, PD-1 and ICOS are almost solely expressed by T-lymphocytes, whereas CXCR5 is also expressed by FL B-cells, therefore the latter is not useful for assessing T_{FH} in tissue imaging studies. Thus, for consistency, and to link with confocal imaging studies (see Chapter 5), T_{FH} are defined as $CD4^{+}PD\text{-}1^{hi}ICOS^{+}$ T-cells throughout this thesis.

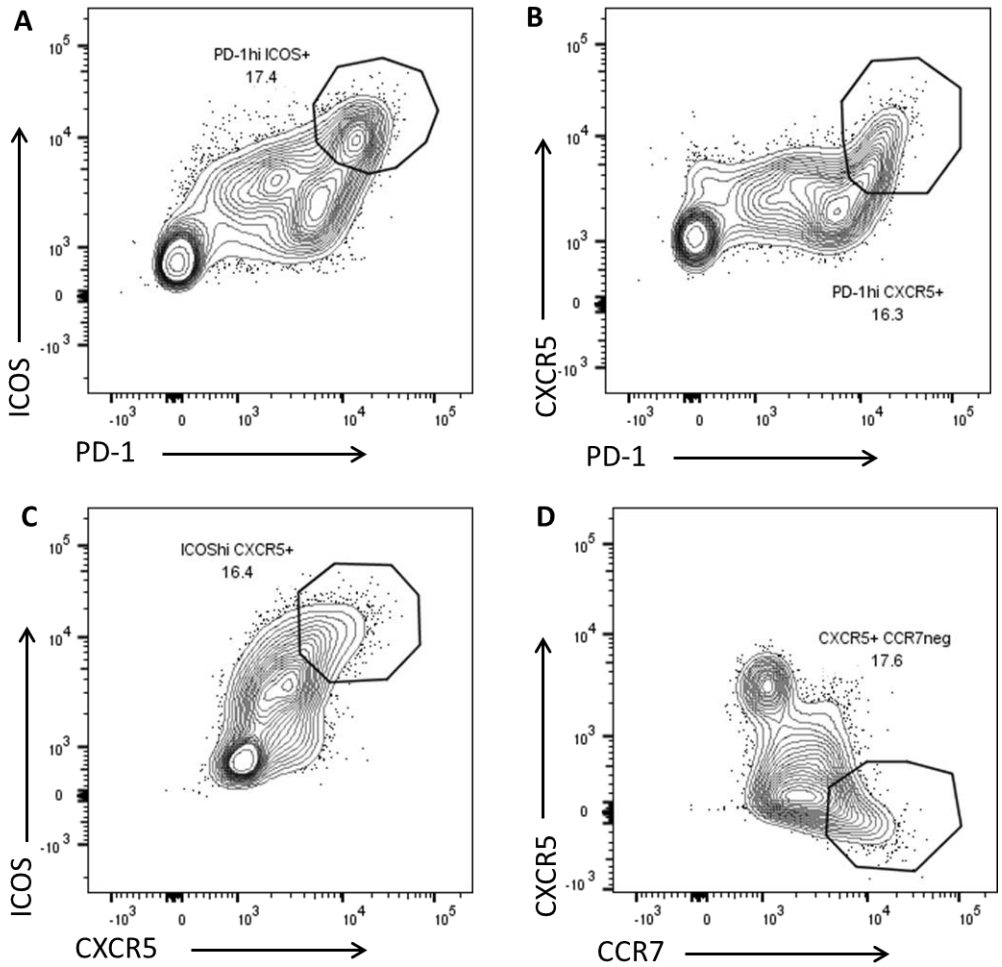

Figure 3.5. Comparison of gating strategies to identify T_{FH}. *Representative flow plots show expression of T_{FH} markers in viable $CD4^{+}$ T-cells from a disaggregated reactive LN. Gated cells on each plot indicate cells with a T_{FH} phenotype.*

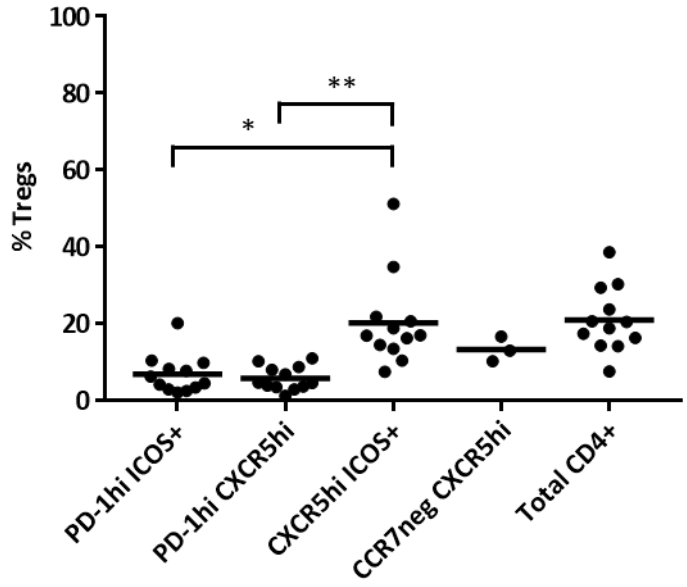

Figure 3.6. Prevalence of T_{regs} within T_{FH} subsets. *Different flow gating strategies were applied to FL LN $CD4^+$ T-cells to identify T_{FH}-like cells (x axis). Graph shows the proportion of these T_{FH}-like cells that had a $CD127^{lo}CD25^+$ regulatory phenotype. Horizontal bars represent mean values. *p=0.002; **p<0.001*

We then considered whether PD-1 and ICOS were sufficient to identify T_{FH} in isolation, or if additional markers are needed. $CD4^+PD\text{-}1^{hi}ICOS^+$ T-cells were almost universally CXCR5-positive (96.3 ± 1.1% were $CXCR5^+$) and CCR7-negative (96.88 ± 1.4% were $CCR7^-$; n=6), consistent with a T_{FH} phenotype. Therefore, neither of these markers were deemed essential and CCR7 was not included in most subsequent flow experiments.

Expression of the T_{FH}-defining transcription factor BCL6 was assessed by intracellular flow cytometry (Section 2.7.3). Only small shifts were seen in BCL6 expression, compared with either isotype-matched or unstained negative controls, even in Ramos positive-control cells and using a strong fluorochrome (APC; Figure 3.7). As a result, only a minority of $PD\text{-}1^{hi}ICOS^+$ T_{FH} (32.5 ± 9.9%) had detectable BCL6 expression. However, as expected, T_{FH} were more likely to express BCL6 than other $CD4^+$ T-cells: only 10.9 ± 4.9% of $PD\text{-}1^{int}ICOS^+$ T-cells and 10.1 ± 4.4% of $PD\text{-}1^{neg}$ $ICOS^{lo}$ cells were $BCL6^+$ (p=0.03 for both, n=6). The most likely explanation for the lack of BCL6 expression in most $PD\text{-}1^{hi}ICOS^+$ T_{FH} is that intracellular flow cytometry is not sensitive enough. BCL6 expression is known to be weaker in T_{FH} than in GC B-cells (such as Ramos cells) and other studies have shown similar results by flow cytometry but much higher rates of BCL6 expression at a transcriptional level (Schmitt*, et al* 2014c). Methodological factors may be contributory, such as the primary antibody clone used or fixation/permeabilization method.

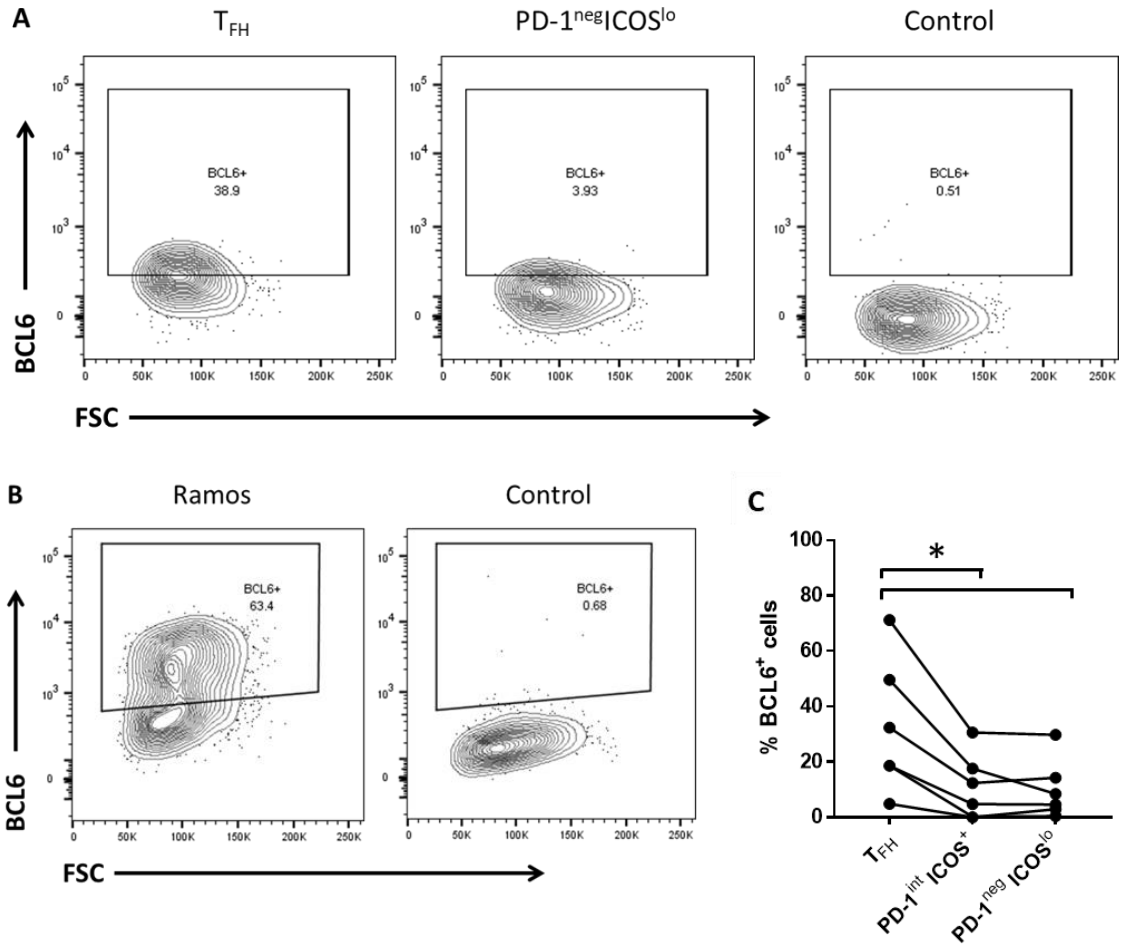

Figure 3.7. BCL6 expression in FL LN CD4⁺ T-cells. A) *Representative flow plots show BCL6 expression in subsets of CD4⁺ T-cells.* ***B)*** *Flow plots show expression of BCL6 in Ramos positive-control cells and isotype-matched negative controls.* ***C)*** *Proportion of BCL6⁺ cells in CD4₊ T-cell subsets*

3.2.6. Cell Yield

Fresh LN tissue was obtained from 5 patients over a period of 3 years. Two of these were large LN biopsies that yielded at least 10^8 cells and could be used for multiple experiments, including flow sorting. However, the other 3 were very small tissue sections that provided <20 x 10^6 cells, with lower cell counts after freeze-thawing, and could only be used for a limited range of experiments. This emphasised the need to find alternative sources of FL B-cells and autologous T_{FH}.

For FNAs used fresh, without freeze-thawing, the median total number of viable cells obtained was 2.99 x 10^6 (range 0.39 – 4.34; n=11), counting cells lacking trypan blue uptake on a haemocytometer slide as an approximate measure of total viable cell count.

By flow cytometry with counting beads, the median absolute number of $CD4^+$ T-cells and T_{FH} obtained per FNA were 30.6 x 10^4 (range 1.05 – 77.6) and 9.9 x 10^4 (range 0.58 – 44.8), respectively (n=8; Figure 3.8). Four of the 8 FNAs assessed had fewer than 10^5 T_{FH}.

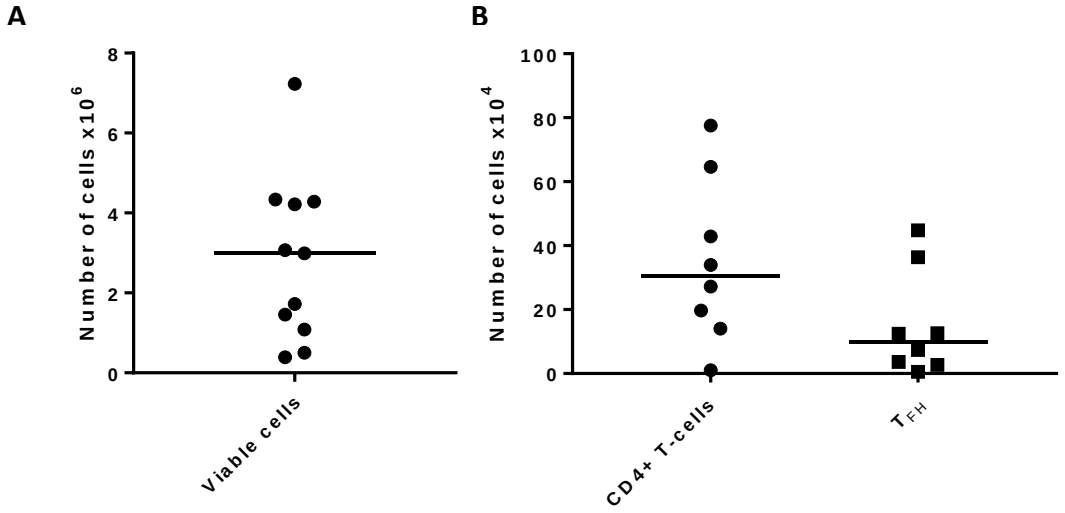

Figure 3.8. Absolute cell counts obtained from FL FNAs. A) *total viable cell count by trypan blue exclusion.* ***B)*** *T-cell subsets quantified by flow cytometry with counting beads. Horizontal bars represent median values.*

The majority of lymphocytes in FNAs were GC B-cells. The median total number of $CD19^+$ B-cells obtained per FNA was 97.6 x 10^4 (range 3.7 – 356.3; n=8), of which a median of 78.3% were $CD10^+$ FL B-cells (range 11.1 – 95.1; Figure 3.9). CD10 expression can be heterogeneous or even absent in some FL cases (Swerdlow*, et al* 2008). In 1 patient only 11% of B-cells were $CD10^+$, where the FNA was taken from a biopsy-proven area of relapsed FL with heterogeneous CD10 expression; CD19 alone was used as the sole B-cell marker for this patient.

For comparison, core needle biopsies were also obtained from 3 patients with suspected lymphoma during this study (2 patients with DLBCL and 1 FL). These were of various size and quality and yielded a median of 2.6 x 10^6 cells (range 1 – 12 x 10^6). Therefore, there was not felt to be an advantage in using core needle biopsies over FNAs, as they are slightly more invasive and usually require local anaesthetic and imaging guidance. Even if extra cores were taken specifically for the purpose of research, there was also concern that this could not be deemed surplus to diagnostic requirements, where the amount of tissue obtained is usually so small.

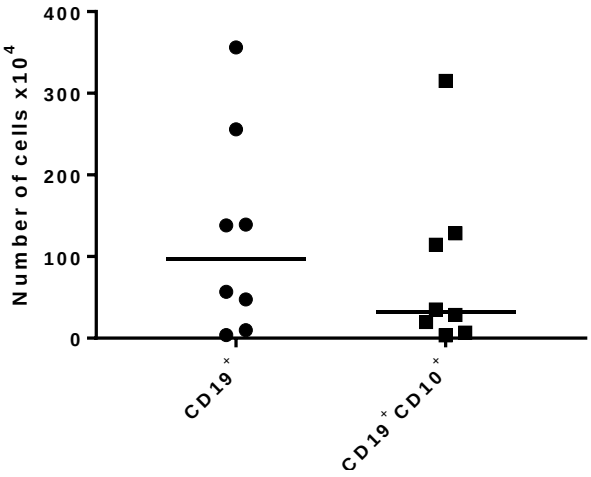

Figure 3.9. Absolute B-cell numbers obtained from FL FNAs. *Viable $CD19^+$ and $CD10^+$ lymphocytes were quantified by flow cytometry using counting beads. Horizontal bars represent median values*

3.2.7. Reproducibility

FNA was repeated on at least 1 occasion in 4 patients, 3 of whom had not received treatment in the intervening period (Table 3.2). The proportion of $CD4^+$ T-cells that had a T_{FH} phenotype varied by 8.0 – 9.7% for consecutive FNAs, indicating an element of intrapatient heterogeneity. There are multiple factors that may account for this variability, including differences in LN site and storage conditions (i.e. used fresh or freeze-thawed). There is likely to be an element of sampling variation; FL tissue is not homogeneous, and the density of follicles may vary throughout an involved LN. Heavy PB contamination may also skew the lymphocyte composition.

Table 3.2: Reproducibility of FNA results. *Table shows the proportion of $CD4^+$ T-cells that had a T_{FH} phenotype for patients undergoing repeated FNA*

Patient number	% T_{FH}			Lymph node site	Time interval (months)	Clinical status
	FNA 1	FNA 2	FNA 3			
FL005	29.5*	20.2	-	Same	14.1	Stable indolent disease
FL006	27.4*	19.4	19.8	Different	29.2	Stable indolent disease
FL010	23.0	32.7	-	Different	3.4	Progression at FNA2

**indicates use of freeze-thawed samples*

3.2.8. Discussion

These data demonstrate that T_{FH} can readily be aspirated and identified within FL FNAs. The proportion of T_{FH} and other lymphocyte subsets obtained by FNA was very similar to disaggregated FL LN tissue, demonstrating that FNAs adequately reflect the lymphocyte composition of the wider LN TME and can be used alongside disaggregated LN tissue.

The number of T_{FH} is a limiting factor in experiments using FNAs: half of the FNAs contained less than 10^5 T_{FH} in total. This precludes complex culture studies involving multiple different conditions or requiring more than basic cell manipulation, for example, flow sorting. Nevertheless, FNAs are a viable and representative source of FL T-cells, therefore are suitable for further studies of T_{FH} in FL.

3.3. Characterisation of Peripheral Blood and Bone Marrow T-cells

3.3.1. Background

FL infiltration in the BM is present in approximately 40% of patients (Federico*, et al* 2009), whilst PB involvement is present in 4-23% (Beltran*, et al* 2013). Both can be used as sources of FL cells for culture studies, with the potential to obtain greater cell numbers than FNA. PB and BM can also be obtained in conjunction with routine diagnostic procedures, thus are relatively non-invasive. However, the potential for these sources to produce autologous T_{FH} is less clear.

Although T_{FH} almost exclusively reside within secondary lymphoid tissue in healthy individuals, it is known that follicular structures with ectopic FDC networks can form within in the bone marrow when infiltrated by FL (Swerdlow*, et al* 2008). The T-cell composition of these BM follicular structures has not been well characterised.

T_{FH}-like cells are present within the PB of healthy individuals (PB-T_{FH}). However, in contrast to LN T_{FH}, PB-T_{FH} are typically defined by CXCR5 expression alone and the majority of these cells have low or absent PD-1 and ICOS expression (Schmitt*, et al* 2014a). The presence of leukaemic disease in FL can alter PB T-cell phenotype. PB T-cells from FL patients with leukaemic involvement, but not those without, have impaired immune synapse formation, mimicking the behaviour of LN-derived FL T-cells (Ramsay*, et al* 2009). PB-T_{FH} have not been characterised in FL, although in other leukaemic B-cell neoplasms, such as CLL, circulating $CD4^+CXCR5^+$ PB-T_{FH} cells are increased in number (Ahearne*, et al* 2013).

PB-T_{FH} and naïve T-cells from healthy donors are both able to adopt T_{FH}-like properties and provide B-cell help under appropriate experimental conditions (Locci*, et al* 2016, Morita*, et al*

2011, Schmitt*, et al* 2014c). To assess whether either can potentially be used as a source of autologous T_{FH} in FL patients first requires characterisation of these T-cell subtypes. FL patients are reported to have reduced numbers of $CD4^+$ and naïve T-cells compared with age-matched controls (Christopoulos*, et al* 2011). Age has a major influence on circulating immune cells and the median age of FL patients at presentation is 65 years. Older patients are also known to have a reduced proportion of naïve T-cells, higher levels of T_{regs} and PB-T_{FH}, diminished antibody responses to vaccination and elevated levels of ICOS and PD-1 expression (Lefebvre and Haynes 2012, Zhou*, et al* 2014).

The aims of this work were to:

1) To investigate the feasibility of obtaining T_{FH} from FL-derived PB and BM tissue
2) To characterise the circulating $CD4^+$ T-cell subsets in FL, compared to age-matched healthy controls.

3.3.2. Bone Marrow T-Cells

Bone marrow T-cells were assessed in 2 untreated FL patients with known, extensive bone marrow involvement. Neither patient had a discrete identifiable population of T_{FH}. One patient had LN material available for comparison: only 5.8% of BM $CD4^+$ T-cells were PD-$1^{hi}ICOS^+$, compared with 16.4% in the LN, and the majority of these (58.2%) were CXCR5-negative (Figure 3.10). Other groups investigating the role of T_{FH} in FL also confirmed that T_{FH} were not present in BMMC (K Tarte, personal communication), therefore this avenue was not explored further. It is known that BM disease in FL has a lower proliferation rate and less aggressive phenotype than LN disease (Bognar*, et al* 2005, Rajnai*, et al* 2012). The BM microenvironment is likely to exert a strong influence on the phenotype of marrow disease, although whether the absence of T_{FH} contributes to this observation is unknown.

3.3.3. Peripheral Blood T-Cells in Follicular Lymphoma and Healthy Controls

PBMCs were obtained from 12 FL patients (n=12) and 8 age-matched healthy controls (n=8), as described in section 2.2. The median age was 59.4 years (range 36.7 – 77.7) in FL patients and 57.6 years (range 43.6 – 69) in healthy controls. Three FL patients (25%) had received previous immunochemotherapy; none had received prior purine analogue-based therapy, and all had been off treatment for at least 6 months. Three FL patients (25%) had elevated total lymphocyte counts with evidence of leukaemic involvement.

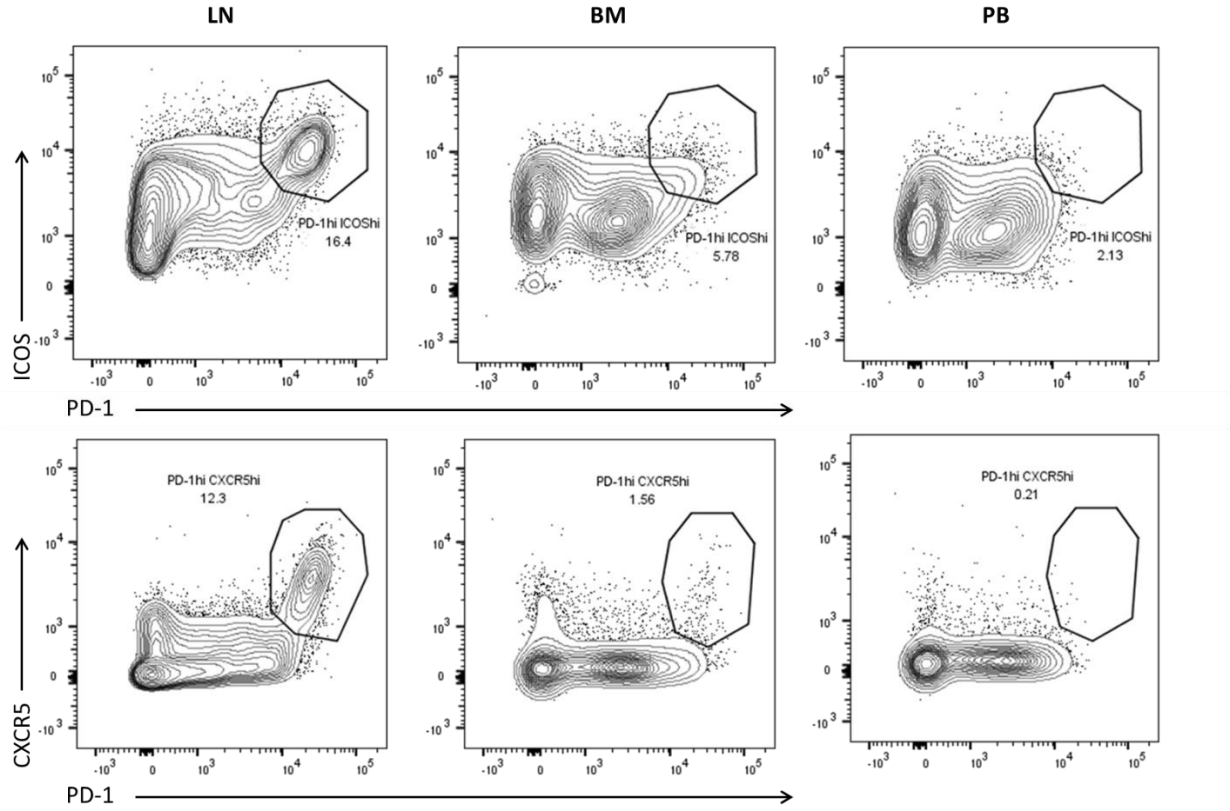

Figure 3.10: Phenotype of bone marrow-derived T-cells: *Flow plots show PD-1, ICOS and CXCR5 expression in viable LN, BM and PB CD4⁺ T-cells from the same patient*

PB-T_{FH}, defined by CXCR5 expression, were present in all patients but formed a minority of PB T-cells, comprising 13.7% ± 1.6% of $CD4^+$ T-cells in FL patients and 10.5% ± 3.0 in healthy controls (p=0.08; Figure 3.11). Naïve $CD45RA^+$ T-cells accounted for a greater proportion of $CD4^+$ T-cells: 33.3 ± 7.21% in FL patients and 46.2 ± 8.8% in healthy controls (p=0.46). There was no detectable difference in the proportion of PB-T_{FH} or naive T-cells between FL patients or healthy controls, although greater patient numbers are required to exclude small differences.

Expression of T_{FH} and other T-cell markers can reflect the potential of $CXCR5^+$ PB-T_{FH} to adopt T_{FH}-like properties. In particular, expression of PD-1 and the absence of CXCR3 expression both signify an increased capacity to support class-switching and IgG production in healthy B-cells (He*, et al* 2013, Morita*, et al* 2011). FL patients had significantly higher levels of PD-1 expression in PB-T_{FH} compared to healthy controls, with $PD\text{-}1^+$ cells comprising 63.0 ± 5.8% of PB-T_{FH} in FL patients compared to 27.7 ± 3.3% of controls (p<0.001). The increase in PD-1 expression was not specific to PB-T_{FH}: 41.1 ± 7.1% of CXCR5-negative $CD4^+$ T-cells were $PD\text{-}1^+$ in FL patients

compared to 13.0 ± 2.5% in controls (p=0.002; Figure 3.12), therefore it is not clear whether increased PD-1 expression necessarily correlates with increased T_{FH} potential. There was no difference in the proportion of more functionally-active $CXCR3^-$ PB T_{FH}: 27.4 ± 4.8% PB T_{FH} expressed CXCR3 in FL compared to 27.0 ± 3.0% in controls (p=0.43). There was also no difference in expression of ICOS, CCR7 or intensity of CXCR5 in PB-T_{FH} between FL patients and healthy controls (Figure 3.12).

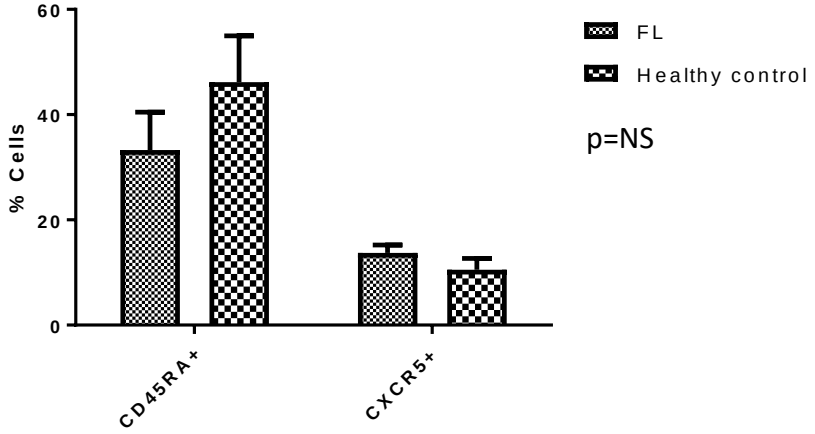

Figure 3.11. Comparison between $CD4^+$ T-cell subsets in FL patients and healthy controls. *Graph shows the proportion of $CD3^+CD4^+$ PB lymphocytes that expressed CD45RA (naïve T-cells) and CXCR5 (PB-T_{FH}) by flow cytometry. Columns represent mean values and error bars represent standard error*

PB-T_{FH} had higher PD-1 expression than $CXCR5^{neg}$ or $CD8^+$ PB T-cells in both FL patients and healthy controls, although this did not reach the levels of PD-1 expression seen in LN T_{FH}. Eight FL patients had paired LN and PBMCs available for comparison; 63.0 ± 5.8% of PB-T_{FH} were PD-1-positive but only 5.7 ± 2.6% were PD-1^{hi}, with levels of PD-1 expression comparable to LN T_{FH} (Figure 3.10). Although the majority (98.8% ± 0.33) of PB-T_{FH} expressed ICOS to some extent, only 15.4 ± 3.9% expressed ICOS to the same levels as LN T_{FH}. Overall, only 3.0 ± 1.3% of PB-T_{FH} had a phenotype similar to LN T_{FH}, therefore it is not possible to assume that FL PB-T_{FH} have the same functional capacity as LN T_{FH}.

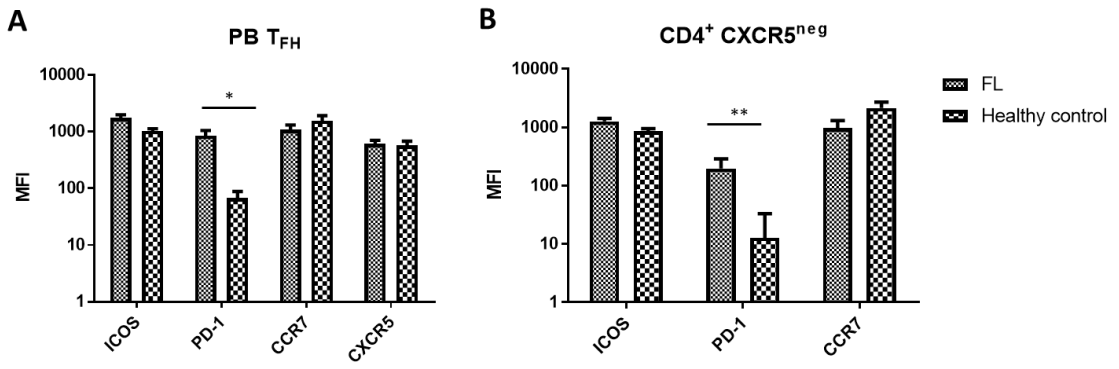

Figure 3.12. Median fluorescence intensity of T_{FH} markers in PB T-cells. *Graphs shows expression of T_{FH} antigens by flow cytometry in:* ***A)*** *$CD4^+CXCR5^+$ PB-T_{FH} and* ***B)*** *$CD4^+CXCR5^{neg}$ T-cells in the PB of FL patients and healthy controls. Columns represent mean values and error bars represent standard error. *p=0.002, **p=0.01*

There was no overt difference between FL patients with leukaemic involvement (n=3) and those without (n=9), either with respect to the proportion of PB-T_{FH} or levels of ICOS, PD-1 and CXCR5 expression (data not shown), although the small number of patients with leukaemic disease precluded formal comparison.

3.3.4. Discussion

There are several advantages to using PB-T_{FH} to study interactions between T_{FH} and FL B-cells: firstly, all FL patients had detectable $CXCR5^+$ PB-T_{FH}, which are much more accessible than LN-derived T_{FH}. Secondly, compared with naïve T-cells, PB-T_{FH} are more differentiated and have some T_{FH} polarisation. However, these data demonstrate that PB-T_{FH} comprise a minority of circulating $CD4^+$ T-cells and do not have the same phenotype as LN-derived T_{FH}. These results are consistent with published data, showing that 5-10% of PB $CD4^+$ T-cells are $CXCR5^+$ (Ahearne*, et al* 2013, Morita*, et al* 2011). However, there are also no commercial kits available to facilitate T_{FH} isolation, therefore flow sorting would be required, which can reduce cell viability during subsequent co-cultures. In addition, given that the intensity of CXCR5 expression in PB-T_{FH} was low, stricter gating strategies would be required to ensure only pure $CXCR5^+$ cells are isolated, leading to the inevitable loss of a proportion of true PB-T_{FH}. It is therefore clear that PB-T_{FH} are not present in sufficient numbers to facilitate culture studies. $CD45RA^+$ naïve T-cells formed a much larger proportion of PB $CD4^+$ T-cells (33.7 ± 5.0%) and, using commercial immunomagnetic selection kits, are much easier to isolate for further culture and differentiation experiments.

The higher expression of PD-1 expression in PB T-cells in FL replicates findings in other B-cell malignancies, such as CLL (Brusa*, et al* 2013). Whether the increase in PD-1 reflects a polarisation towards more activated T_{FH} in FL, or a higher proportion of exhausted T-cells in FL is unclear; this requires correlation with additional markers of T-cell exhaustion and functional studies. It has been shown that PB T-cells from FL patients have increased proliferation in response to CD3/CD28 stimulation and increased capacity to secrete IL-4 compared with healthy controls (Christopoulos*, et al* 2011), which may reflect a degree of T_{FH} polarisation. However, we did not observe an overt difference in the expression of other antigens that contribute to the PB-T_{FH} phenotype, particularly CCR7, which is usually downregulated in PD-1^+ T_{FH} (He*, et al* 2013).

One caveat is that absolute T-cell numbers were not quantified in this study. It is therefore unclear whether PD-1^+ T-cells are increased in number in FL, or unchanged with a relative reduction in other $CD4^+$ T-cells. It is also unclear whether absolute numbers of circulating naïve T-cells or PB-T_{FH} are altered in FL patients. Higher sample numbers would be required to identify subtle differences in T-cell composition between FL patients and healthy controls.

There are a number of key unanswered questions. Firstly, what is the origin of PB-T_{FH} in FL; are they clonally related to LN T_{FH}? This would imply a common origin, implicate PB-T_{FH} in the pathogenesis of FL and support the use of PB-T_{FH} in culture studies. Secondly, can PB-T_{FH} adopt a full T_{FH} phenotype when cultured with autologous FL B-cells? The latter question would need to be addressed if considering use of PB-T_{FH} as a surrogate for LN-derived T_{FH}. Given the low cell numbers and additional validation required, we elected not to pursue investigation into the use of PB-T_{FH} for this thesis.

3.4. Generating T_{FH}-like Cells from Naïve T-Cells

3.4.1. Background

Multiple groups have demonstrated that particular cytokines can induce naïve T-cells from healthy individuals to develop a T_{FH}-like phenotype (Locci*, et al* 2016, Ma*, et al* 2009, Schmitt*, et al* 2014c). IL-12 has been consistently identified as a factor in T_{FH} development but in isolation induces a Th1 phenotype (Locci*, et al* 2016, Ma*, et al* 2009). IL-6 is important for early T_{FH} polarisation (Crotty 2014) and TGFβ promotes human T_{FH} development and CXCR5 expression (Schmitt*, et al* 2014c).

Schmitt *et al* demonstrated that T_{FH}-like cells can be generated from human naïve T-cells, which have the ability to provide B-cell help and enhance IgG production (Schmitt*, et al* 2014c). This study has been hailed as describing the 'most successful conditions yet' for T_{FH} generation by a leading expert within the field (Crotty 2014). A wide range of cytokines were assessed and the combination of IL-12, IL-1β, IL-6 and TGFβ1 induced the highest levels of ICOS, CXCR5 and BCL6 expression (Schmitt*, et al* 2014c). We investigated whether we could reproduce these results to generate T_{FH}-like cells from naïve T-cells.

3.4.2. Results

PBMCs were isolated from treatment-naïve FL patients (n=3) and healthy individuals (n=3; not age-matched). Except where stated, data from FL patients and healthy controls were analysed together (n=6). The protocol for cell culture and cytokine stimulation is detailed in Section 2.6. $CD4^+CD45RA^+$ naïve T-cells were isolated by immunomagnetic negative selection with an average purity of 94.6% (range 92.6 – 96.9%). Naïve T-cell phenotype was assessed after 4 days of CD3/CD28 stimulation, either without additional cytokines or with the addition of IL-12, IL-1β, IL-6 and TGFβ1 for the final 72 hours of culture.

Schmitt *et al* reported that IL-12, IL-1β, IL-6 and TGFβ1 were together able to induce a 5-fold and 2-fold increase in the intensity of ICOS and CXCR5 expression, respectively. By contrast, our data showed only a very modest increase in ICOS expression in cytokine-stimulated naïve T-cells, compared with non-specific CD3/CD28 stimulation alone (21.5 ± 8.2%; p=0.03; Figures 3.13 and 3.14A). There was no significant difference in CXCR5 expression; with an increase of 20.4 ± 10.1% compared with control samples (p=0.22). Similarly, there was no overt difference in PD-1 expression, with a mean increase of 53.8 ± 29.4% (p=0.31; Figure 3.14). Therefore, even though sample numbers are small, the magnitude of change in T_{FH} markers was modest and insufficient to suggest a major phenotypic shift in naïve T-cells following cytokine stimulation. Unexpectedly, the most striking change was in CCR7 intensity, suggesting polarisation away from a T_{FH} phenotype. CCR7 expression doubled in in cytokine-stimulated cells, with a relative increase of 107.4 ± 44.2% compared with CD3/CD28-stimulated control cells (p=0.03; Figure 3.14).

Although numbers and age differences do not allow for formal comparison between FL patients and healthy controls, CXCR5 expression was lower in the 3 FL patients (Figure 3.14). There were no overt differences in PD-1, ICOS or CCR7 expression.

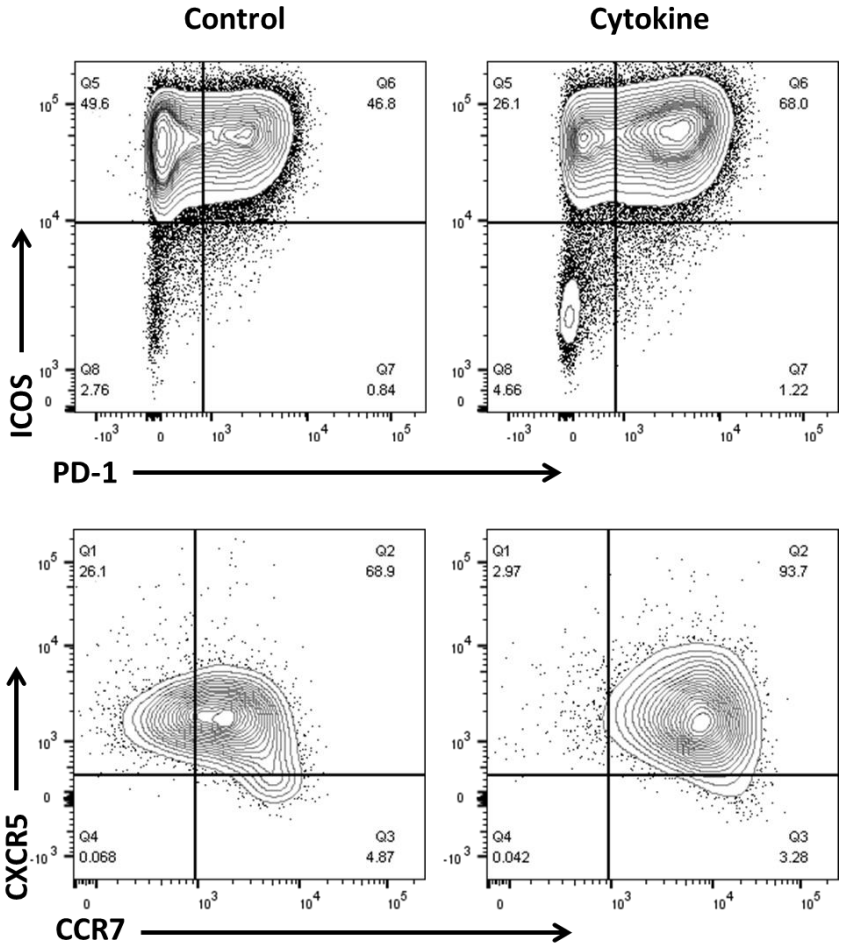

Figure 3.13. Expression of T_{FH} markers following naïve T-cell stimulation. *Representative flow plots show the phenotype of naïve $CD4^+$ T-cells following stimulation with anti-CD3 and anti-CD28, either with or without the addition of T_{FH} cytokines (IL-12, IL-1β, IL-6 and TGFβ1) for 72 hours*

3.4.3. Discussion

The combination of IL-12, IL-1β, IL-6 and TGF-β was only able to induce very minor shifts in ICOS, CXCR5 and PD-1 expression in naïve T-cells, over and above the effect of non-specific CD3/CD28 stimulation alone. It was therefore not possible to generate cells with sufficient evidence of T_{FH} polarisation to facilitate T_{FH} co-culture studies. The study by Schmitt *et al* focussed on CXCR5 and ICOS expression as markers of the T_{FH} phenotype, but did not describe expression of other important T-cell markers, such as PD-1 and CCR7 (Schmitt*, et al* 2014c). Paradoxically, the most prominent change in cytokine-stimulated cells was a near 2-fold increase in CCR7 expression. CCR7 expression is usually lost in effector memory T-cells, including T_{FH}, and precludes GC entry.

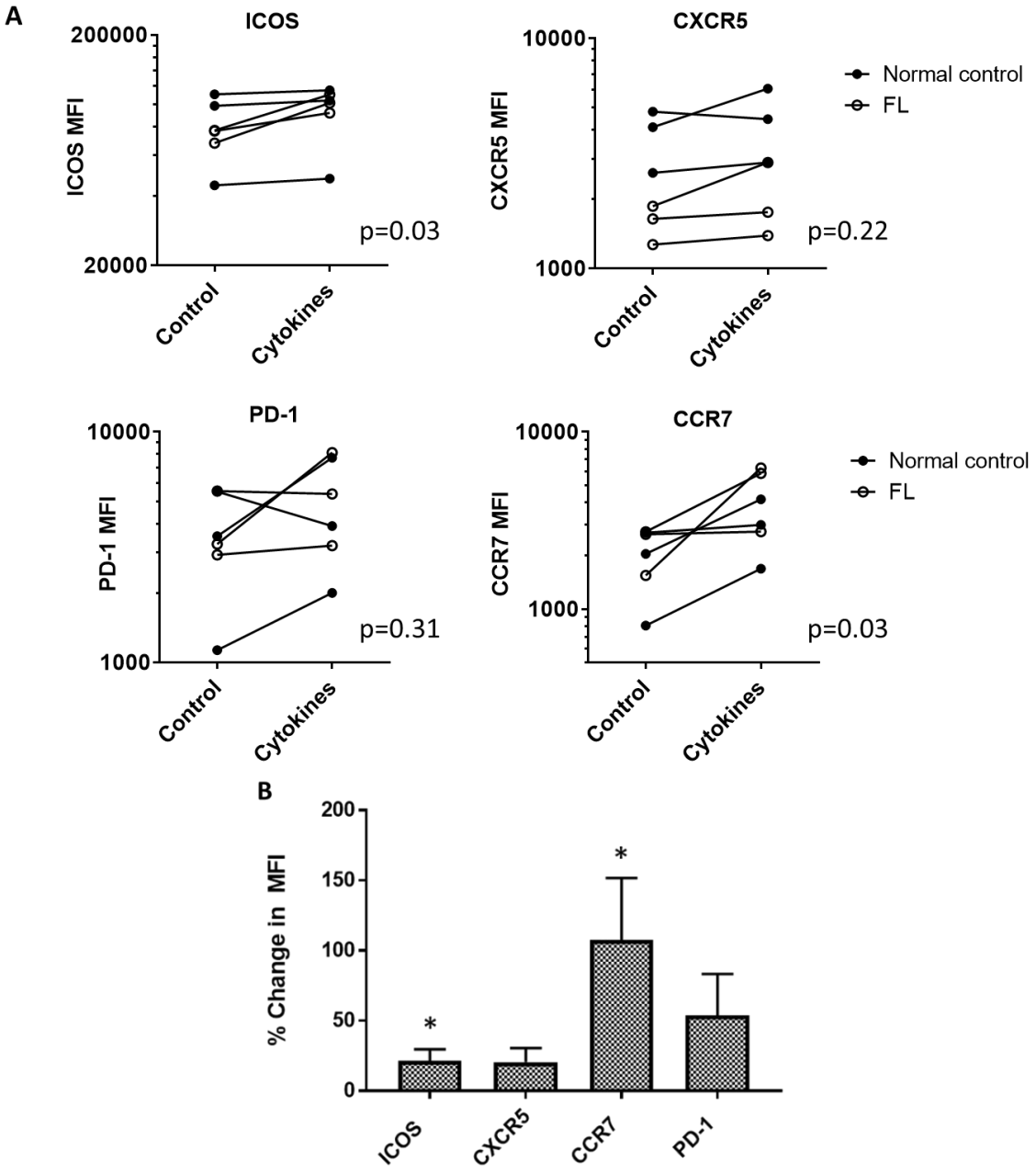

Figure 3.14. Effect of stimulation with T_{FH} cytokines on naïve T-cell phenotype. A) *Graphs compare expression of ICOS, CXCR5, PD-1 and CCR7 in naive $CD4^+$ T-cells stimulated for 72h either with or without the addition of T_{FH} cytokines: IL-12, IL-1β, IL-6 and TGFβ1.* ***B)*** *Summary histogram illustrates the mean increase in antigen expression in naïve $CD4^+$ T-cells stimulated for 72h with T_{FH} cytokines, relative to $CD4^+$ T-cells cultured without additional cytokines. Vertical bars represent standard error. *p=0.03*

There are multiple potential explanations for these discordant results:

1) Lack of T_{FH} polarisation: ICOS and CXCR5 are also both activation markers and are not specific to T_{FH}. The majority of T_{FH}-like cells produced by Schmitt *et al* co-expressed the Th17-defining transcription factor ROR-γt, in addition to BCL6 therefore may not be fully lineage-committed (Schmitt*, et al* 2014c). TGFβ1, IL-6 and IL-1β have all been used in protocols to generate Th17 cells *in vitro*, which also express CCR7, therefore these cells may have been more skewed more towards to a Th17 phenotype (Wang*, et al* 2009).
2) Methodological differences: although unlikely, it is possible that the reagents used, such as cytokine brand and anti-CD3/CD28 beads may alter efficacy. There is also the potential for small quantities of cytokines or other growth factors in FBS that may influence T_{FH} differentiation; some groups use serum-free culture systems (Locci*, et al* 2016).
3) Optimum cytokine combination: there are conflicting reports in the literature regarding the effect of various cytokines on T_{FH} differentiation (Eto*, et al* 2011, Lu*, et al* 2011). Other groups investigating human T_{FH} development have stimulated naïve T-cells with IL-12, either alone or in combination with TGFβ and/or Activin A (Locci*, et al* 2016, Ma*, et al* 2009). Some studies have used blocking agents to inhibit cytokines that inhibit T_{FH} development, such as IL-2 and IFNγ (Locci*, et al* 2016, Lu*, et al* 2011).
4) Need for cell contact: other studies have shown that contact-dependent factors are critical for T_{FH} differentiation *in vivo*, with DCs priming early T_{FH} development and cognate B-cells driving later T_{FH} development (Crotty 2014, Johnston*, et al* 2009). It is therefore unlikely that cytokine stimulation alone is sufficient to produce a full T_{FH} phenotype. Although it has been shown T-cells primed with IL-12 (with or without other cytokines) can enhance secretion of T_{FH}-related cytokines, immunoglobulin production and plasmablast differentiation, it remains unclear whether they are able to support these functions to the same magnitude as LN-derived T_{FH} (Locci*, et al* 2016, Ma*, et al* 2009, Schmitt*, et al* 2014c).

There is scope to optimise this work further, by trialling different culture media, cytokine combinations and IL-2 depletion. Gene expression profiling would enable better characterisation of these cytokine-stimulated cells, particularly with respect to expression of BCL6 and other major T-cell transcription factors. Ultimately, proof that these generated T_{FH}-like cells truly resemble LN-derived T_{FH} would require a range of functional studies with healthy autologous B-cells, prior to any FL experiments. This extensive work is outside of the scope of this thesis. We chose not to pursue this avenue, given a) our inability to generate cells with a

clear T_{FH} phenotype in these preliminary experiments and b) our success in obtaining T_{FH} from other sources, particularly LN FNA. In addition, PBMCs do not contain significant numbers of FL B-cells in most patients, therefore additional LN or BM tissue would still be required for co-culture experiments. FL LN cells derived from both disaggregated LN and FNAs were therefore used for all subsequent culture studies.

CHAPTER 4: *IN VITRO* CHARACTERISATION OF T_{FH}:B-CELL INTERACTIONS IN FOLLICULAR LYMPHOMA

4.1. Introduction

Having established and characterised FL LN cell suspensions from disaggregated LN and FNA, the initial goal was to use these to establish a co-culture system with T_{FH} and FL B-cells. Although FL cells do not survive in long-term *in vitro* cultures, short-term FL culture (up to 5-10 days) is feasible (Amé-Thomas*, et al* 2015, Myklebust*, et al* 2013, Yang*, et al* 2015a). A variety of additives have been used in published studies to enhance survival of FL cells, including CD40L, IL-4 and stromal cells (either fibroblast or FDC cell lines). Similarly, T_{FH} do not survive in long-term culture. Published studies have used additional stimulation with low-dose anti-CD3 and anti-CD28 to support survival of T_{FH} in short-term cultures with FL B-cells (Boice*, et al* 2016, Espeli and Linterman 2015). However, none of these methods can induce long-term survival of either FL B-cells or T_{FH} in culture.

Other studies have explored interactions between FL B-cells and autologous T-cells without using any additional B- or T-cell stimulation (Ramsay*, et al* 2009). T_{FH} can provide key survival signals for FL B-cells, such as CD40, IL-4 and IL-21, and are able to support the survival of autologous FL B-cells without exogenous stimulation (Ame-Thomas*, et al* 2012, Yang*, et al* 2015a). Indeed, the presence of T_{FH} has a similar effect on FL B-cell survival to culturing FL cells with a 'stimulation cocktail' comprising IL-4, IL-2 and CD40L (Amé-Thomas*, et al* 2015). Similarly, healthy B-cells alone are able to support T_{FH} survival through cognate TCR stimulation and expression of co-stimulatory molecules, such as ICOS-L and CD86 (Choi*, et al* 2011, Weber*, et al* 2015). However, it is not known whether FL B-cells are able to support T_{FH} survival to the same extent.

Due to the restricted availability of LN cell suspensions, it was not possible to trial multiple different culture systems as part of this thesis. A simple FL B-cell:T_{FH} co-culture system was developed using RPMI-1640 medium without additional growth factors or stromal cells. This was adopted because use of exogenous stimulation could potentially overwhelm more subtle levels of stimulation that T_{FH} or FL B-cells may be able to provide and thus mask evidence of mutual interactions.

The central hypothesis of this work is that T_{FH} play a key role in driving FL progression. The aim was to use LN cell cultures to explore the nature of interactions between T_{FH} and FL B-cells that

may facilitate FL growth. It has already been shown in multiple studies that T_{FH} can prevent apoptosis in FL B-cells *in vitro* and promote expression of the activation marker CD86 (Ame-Thomas*, et al* 2012, Yang*, et al* 2015a). As a first step, it was necessary to demonstrate that it was possible to recapitulate the work of others by demonstrating that T_{FH} support FL B-cell survival in order to: 1) validate the culture methods used and 2) serve as proof of principle in support of our primary hypothesis.

It has been established that FL creates a supportive TME for T_{FH} but published studies primarily focus on the ability of FL B-cells to stimulate T_{FH} through indirect means, such as the recruitment and activation of stromal cells (Boice*, et al* 2016, Brady*, et al* 2014). It is not known whether FL B-cells are able to directly maintain the presence and survival of T_{FH} in isolation. T_{FH} support in reactive GCs is critically dependent on three stimuli provided by GC B-cells: 1) cognate TCR interactions and CD3 signalling, 2) CD28 stimulation by CD86 and 3) ICOS signalling (Choi*, et al* 2011, Crotty 2014, Weber*, et al* 2015, Wing*, et al* 2014). However, FL B-cells are reported to express much lower levels of ICOS-L compared with reactive GC B-cells (Le*, et al* 2016), MHC expression is downregulated in many FL tumours (Green*, et al* 2015), and it is unknown whether cognate TCR interactions occur in FL. This chapter therefore also explores the dynamics of ICOS-L and HLA-DR expression *in vitro* and investigates whether FL B-cells are able to support T_{FH} survival and maintenance of the T_{FH} phenotype.

We hypothesise that FL B-cells directly support the presence of T_{FH} in the FL TME, initiating a positive feedback loop, in order to derive mutually beneficial survival and activation signals. The aims of the following experiments were:

1. To establish that short term (up to 5 days) culture of FL cells and T_{FH} is feasible without additional stimulation
2. To explore the effect of T_{FH} on FL B-cell survival and phenotype, particularly with respect to CD86, HLA-DR and ICOS-L expression
3. To investigate the influence of FL B-cells on T_{FH} survival and phenotype

4.2. Methods

For most cultures described here (except where indicated), FL LN cell suspensions were split into 3 parts and cultured either unmodified, or after selective B-cell or T-cell depletion. To assess the effect of FL B-cells on T_{FH} phenotype and survival, immunomagnetic $CD19^+$ B-cell depletion was used (see Section 2.5). To assess the effect of T_{FH} on FL B-cell phenotype and survival, immunomagnetic $CD3^+$ T-cell depletion was used. CD3-depletion was preferred over more

selective $CD4^+$ T-cell depletion to avoid leaving in $CD8^+$ T-cells that may, when unhindered by regulatory T-cells, have deleterious effects on FL B-cell survival (Laurent*, et al* 2011). Cells were cultured at a density of 1 $x10^6$ cells/ml in RPMI-1640 medium as described in Section 2.6. Cell death and apoptosis were assessed by flow cytometry through uptake of Fixable Viability Dye and the Annexin V, respectively (see Sections 2.1 and 2.7).

Importantly, this approach allowed for the use of FL FNAs, where low cell numbers do not allow for isolation of T_{FH} and other T-cell subsets by flow-sorting. By characterising FL B-cells in both T-replete and T-deplete cultures, it was possible to obtain surrogate evidence of the effect of T_{FH} in FL, although it was not possible to fully differentiate whether observed effects were T_{FH}-specific or partly influenced by the presence other T-cell subsets.

Therefore, where cell numbers allowed, cell cultures were repeated using flow-sorted FL B-cells, T_{FH} and non-T_{FH} $CD4^+$ T-cells. The method used for fluorescence-activated cell sorting is detailed in Section 2.7.8. FL B- and T-cells were either cultured alone in RPMI-1640 medium or mixed at a 1:1 ratio. There is inevitable cell loss during the sorting process and lymphocytes often have reduced viability in subsequent *in vitro* cultures. Therefore, only 2 LN samples had enough viable cells (at least 10^7) to enable cell sorting. These experiments were intended to support the findings from the B- and T-cell depletion studies above and were repeated on 3 separate occasions for each of two LN samples (N=6). However, given that samples were derived from only 2 patients, no formal statistical comparison has been performed.

4.3. Results

4.3.1. Patients and Lymph Node Samples

LN cell suspensions were obtained from 10 patients (6 by FNA, 4 from disaggregated LN tissue) amongst the patient cohort described in Section 3.2.3. Median age was 53.9 years (range 36.7 – 78.2). Clinical details are listed in Table 4.1.

Table 4.1. Patient characteristics

Patient ID	Tissue	Age (years)	Sex	Stage	Grade	Treatment
FL005	FNA	36.7	M	3	2	First relapse
FL006	FNA	40.3	F	3	2	W&W
FL018	FNA	78	M	1	2	First relapse
FL023	FNA	54	M	4	3A	Second relapse
FL024	FNA	74.2	M	4	Unk	First relapse
FL028	FNA	55.4	F	4	2	Pre-treatment
FL014*	LN	60.9	M	4	1	W&W
FL021	LN	54.3	F	4	1	Pre-treatment
FL022	LN	71.4	F	3	3A	Pre-treatment
FL027*	LN	78.2	M	3	1	W&W

**indicates patients that had LN tissue available for flow sorting experiments*

FNA: fine needle aspirate; LN: disaggregated lymph node tissue; unk: unknown; W&W: watch and wait

CD20 and CD4 were used as B- and T-cell markers to assess the efficacy of B- and T-cell depletion, respectively, as expression would not be altered by the presence of CD19 or CD3 selection beads (n=10). The median reduction in $CD20^+$ B-cells with immunomagnetic B-cell depletion was 95.5% (range 75.4 – 99.9%). The median reduction in $CD4^+$ T-cells with immunomagnetic T-cell depletion was 96.2% (range 86.0 – 99.6%). Only 1 sample (10%) had suboptimal (i.e. <90%) B-cell depletion and 1 sample had suboptimal T-cell depletion. These samples were still considered relatively B- and T-deplete with a CD20:CD3 ratio of 1:4 and a CD19:CD4 ratio of 8:1, respectively, therefore these samples were not excluded from this study.

The gating strategy for fluorescence associated cell sorting is shown in Figure 4.1. All cell subsets were sorted to at least 98% purity.

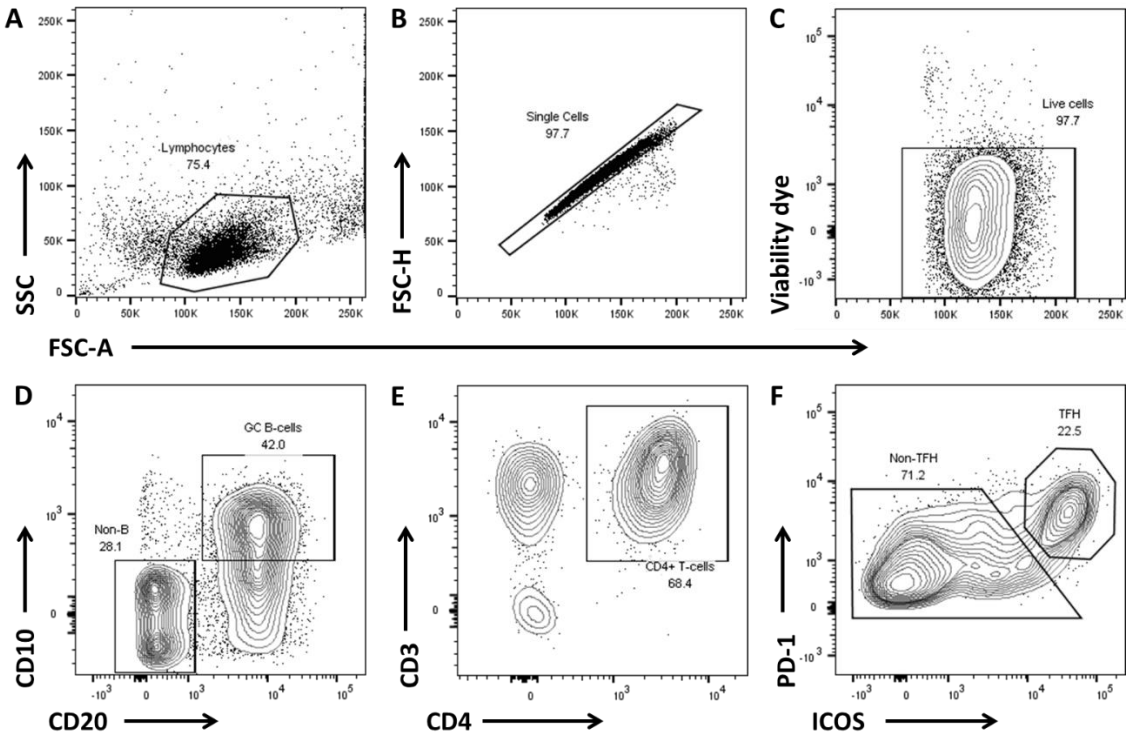

Figure 4.1. Gating strategy for fluorescence-activated cell sorting*. Representative flow plots show sequential identification of* ***A)*** *lymphocytes,* ***B)*** *single cells and* ***C)*** *viable cells.* ***D)*** *viable lymphocytes were gated according to CD19/CD10 expression to identify FL B-cells.* ***E)*** *Non-B-cells were subsequently gated by CD3/CD4 expression and* ***F)*** *$CD4^+$ T-cells were gated according to PD-1 and ICOS expression into T_{FH} and non-T_{FH}.*

4.3.2. Effect of T-Cell Depletion on FL Survival

To assess whether T_{FH} support FL B-cell viability, apoptosis and cell death were measured in FL B-cells in paired T-deplete and T-replete cultures. The flow cytometry gating strategy used is shown in Figure 4.2.

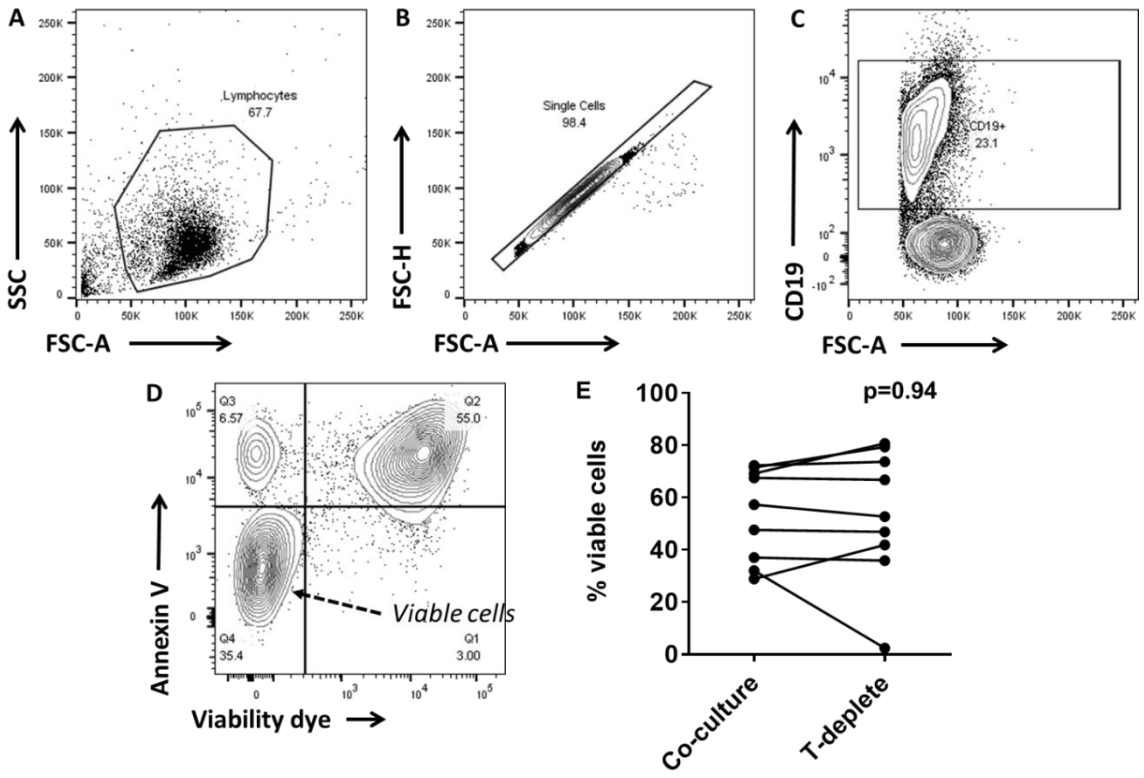

Figure 4.2: Assessment of FL B-cell apoptosis by flow cytometry. A) *Forward scatter (FSC) and side scatter (SSC) properties allowed identification of the lymphocyte population, using a wide gate to incorporate apoptotic cells with lower FSC.* ***B)*** *Lymphocytes were gated to exclude cell doublets and then (**C)** to identify CD19⁺ B-cells.* ***D)*** *A combination of Annexin V and Fixable Viability Dye were used to identify apoptotic and dead cells, respectively, allowing quantification of the proportion of CD19⁺ B-cells that remained viable.* ***E)*** *Graph shows the proportion of FL B-cells that remained viable after 5 days in T-replete (co-culture) and T-deplete culture.*

There was no difference in the proportion of viable FL B-cells between T-replete and T-deplete cultures after 5 days in culture, with 53.7% ± 5.9 and 53.4% ± 8.2 of FL B-cells remaining viable, respectively (p=0.94, N=9; Figure 4.2E). Therefore, we were unable to demonstrate that T-cells reduce apoptosis and support FL B-cell survival by this method. Just over half of cells remained viable, demonstrating that FL B-cells were able to survive in culture without extra stimulation, whilst there was sufficient cell death to allow a difference to be assessed. The failure to detect a difference in FL B-cell survival may represent a failure of the co-culture system, where the influence of other (non-T_{FH}) T-cells on cell survival counteracted any pro-survival effect of T_{FH}. However, there are also limitations to this method of quantifying B-cell survival, which assesses relative change in cell death but does not quantify the absolute number of viable B-cells remaining. Apoptotic or dead cells often have altered or aberrant expression of basic cell surface

markers and may fall outside of expected cell gates. Some dead cells may have fully fragmented and thus not been included in the initial, wide lymphocyte gate.

Therefore, in later culture experiments, the absolute number of viable FL cells was quantified at each time point using counting beads (see Section 2.7.6). Compared with baseline FL B-cell counts, there was a greater reduction in the number of viable FL cells after 5 days in T-deplete cultures than in T-replete co-cultures for all 5 samples assessed (p=0.063, N=5; see Figure 4.3). The mean proportion of FL B-cells remaining at day 5 was 43.9 ± 9.6% in T-replete co-cultures and 30.5 ± 9.1% in T-deplete cultures. CD19 is universally expressed by GC B-cells and is necessary for their survival (Otero*, et al* 2003), therefore any reduction in the number of $CD19^+$ B-cells is likely to represent cell loss or death, rather than a change in phenotype. These data suggest that the presence of T-cells enhances FL B-cell survival *in vitro*. These findings are consistent with published data showing that T_{FH} can support FL B-cell survival and that T-cells are required for FL engraftment and survival *in vivo*, although larger sample numbers are required to reach statistical significance (Ame-Thomas*, et al* 2012, Burack*, et al* 2017, Yang*, et al* 2015a). However, it is not possible to ascertain whether these changes were T_{FH}-dependent, or whether the presence of other $CD4^+$ and $CD8^+$ T-cell subsets was contributory.

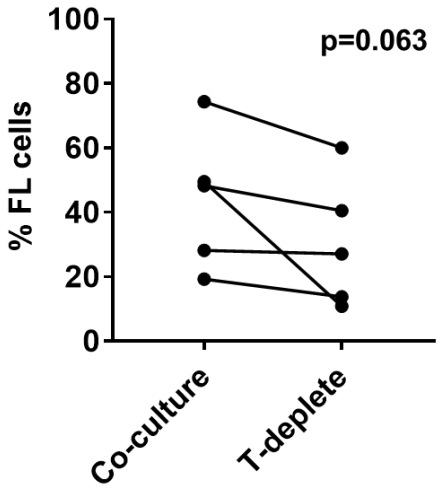

Figure 4.3. Effect of T-cell depletion on FL B-cell viability. *Graph compares the proportion of viable FL B-cells remaining after 5 days of culture under T-cell replete and T-cell deplete conditions. Viable cells were identified by exclusion of Annexin V and Fixable Viability Dye, and absolute cell numbers were quantified using counting beads.*

4.3.3. Effect of T-Cell Depletion on FL B-Cell Phenotype

The next step was to investigate whether FL T_{FH} promote activation of FL B-cells, focussing primarily on stimulatory and co-stimulatory molecules that confer the ability to interact with and support T_{FH} within the TME. HLA-DR was expressed in almost all FL B-cells at baseline (92.9 ± 2.6%, n=7), whilst CD86 expression was more heterogeneous; 44.8 ± 10.1% were $CD86^+$. Expression of both activation markers declined during *in vitro* culture for FL B-cells cultured in the absence of T-cells, although HLA-DR expression declined to a greater extent (Figure 4.4).

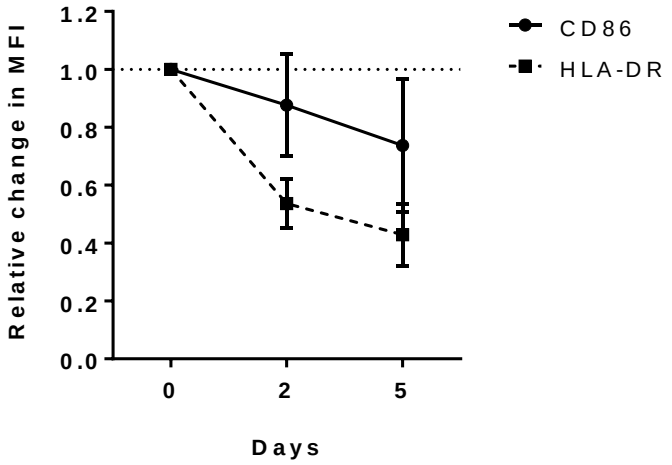

Figure 4.4: Expression of B-cell activation markers during in vitro culture. *Graph shows the change in intensity of CD86 and HLA-DR expression for FL B-cells cultured without T-cells for up to 5 days (n=7).*

After 2 days, CD86 expression on FL B-cells was higher in T-replete cultures than in T-deplete cultures for 4 of 5 samples assessed, although the differences were small: 55.0% ± 7.0 and 51.4% ± 6.2 of FL B-cells were $CD86^+$, respectively (p=0.31; Figure 4.5A). However, T_{FH} comprise a minority of $CD3^+$ T-cells, therefore any pro-tumoural role of T_{FH} may be counteracted by inhibitory elements, such as T_{regs} and $CD8^+$ T-cells. In support of this theory, the differences were more marked using flow-sorted lymphocytes: compared with FL B-cells cultured alone, co-culture with sorted T_{FH} induced a median 2.9-fold increase (range 1.3 – 5.9) in the intensity of CD86 expression after 2 days (N=6; Figure 4.5B/C). This change was T_{FH}-dependent, as there was no increase in CD86 expression in FL B-cells co-cultured with other, non-T_{FH} $CD4^+$ T-cells. Despite the small sample number, these results corroborate the findings of others and were reproducible in repeated experiments, therefore they are significant.

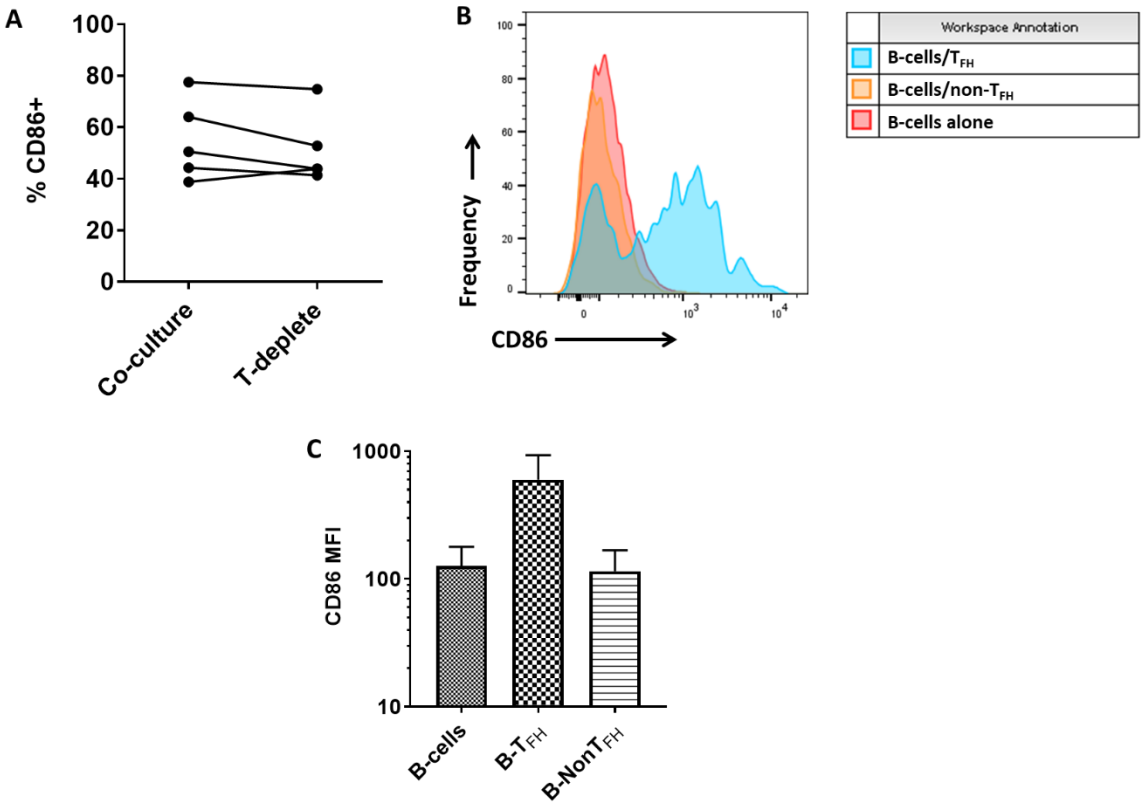

Figure 4.5. CD86 expression on FL B-cells in co-culture studies. A) *Graph shows the proportion of FL B-cells expressing CD86 in paired T-replete and T-deplete cultures after 2 days (N=5).* ***B)*** *Representative flow plot shows CD86 expression in flow-sorted FL B-cells, cultured with or without flow-sorted T_{FH} for 2 days.* ***C)*** *Histogram shows the median fluorescence intensity (MFI) of CD86 on flow-sorted FL B-cells cultured either alone, in the presence of T_{FH} or with non-T_{FH} $CD4^+$ T-cells. Horizontal bars represent mean values plus standard error, of 6 experiments using samples from 2 patients.*

FL B-cell HLA-DR expression was marginally higher in T-replete cultures than in T-deplete cultures for all 5 samples assessed, corresponding to a median 11.5% increase in HLA-DR intensity (range 8.1 – 30.9, p=0.063; Figure 4.6A). Again, these changes were much more pronounced in flow-sorted FL B- cells when co-cultured with T_{FH}, whilst the presence of non-T_{FH} $CD4^+$ T-cells did not influence HLA-DR expression (Figure 4.6B/C). HLA-DR expression was 2.7-fold higher (range 1.01 – 11.2, N=6) in FL B-cells co-cultured with T_{FH} than without. Although larger sample numbers are needed, these data provide further evidence that T_{FH} are principle drivers of FL B-cells activation.

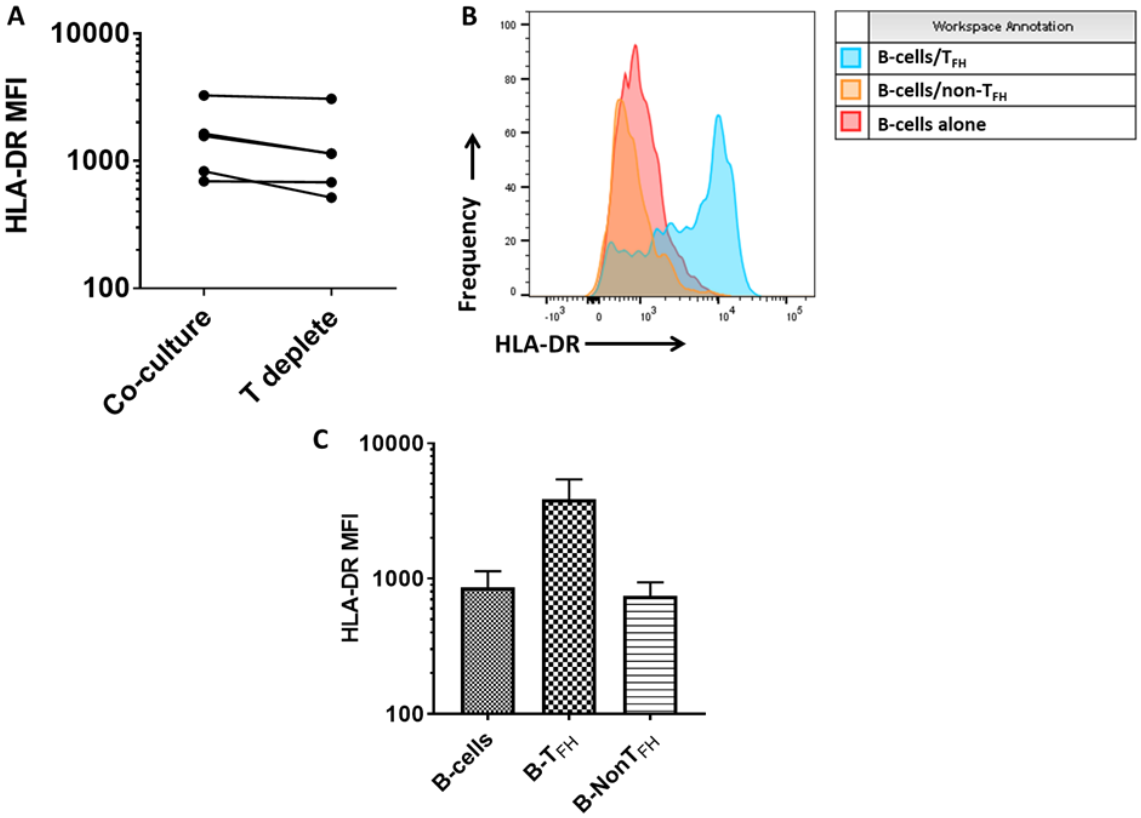

Figure 4.6. HLA-DR expression on FL B-cells in co-culture studies. *A) Graph shows the proportion of FL B-cells expressing HLA-DR in paired T-replete and T-deplete cultures (N=5). B) Representative flow plot shows HLA-DR expression in flow-sorted FL B-cells, cultured with or without T-cells for 2 days. C) Histogram shows the median fluorescence intensity (MFI) of HLA-DR on flow-sorted FL B-cells cultured either alone, in the presence of T_{FH} or with non-T_{FH} $CD4^+$ T-cells. Horizontal bars represent mean values plus standard error, of 6 experiments using samples from 2 patients.*

The majority of FL B-cells did not express ICOS-L: only 19.8 ± 7.5% of FL B-cells expressed low levels of ICOS-L at baseline (N=10). However, ICOS-L expression increased during *in vitro* culture (Figure 4.7A), consistent with published data reporting that FL B-cells rapidly upregulate ICOS-L in culture (Le*, et al* 2016). The effect of T-cell depletion on ICOS-L expression was the opposite of HLA-DR and CD86, with greater ICOS-L expression in the absence of T-cells. In T-cell deplete cultures, 56.3 ± 5.6% FL B-cells expressed ICOS-L after 2 days in culture, compared with 41.7 ± 5.7% in T-replete co-cultures ($p<0.001$; Figure 4.7B/C). Similar differences remained after 5 days: 45.7 ± 5.9% and 32.6 ± 5.9% of FL B-cells were ICOS-L^+ in T-deplete and T-replete cultures, respectively ($p=0.001$). These findings were confirmed with flow-sorted cell cultures, where ICOS-L expression was lowest in FL B-cells co-cultured with T_{FH}. Compared with FL B-cells

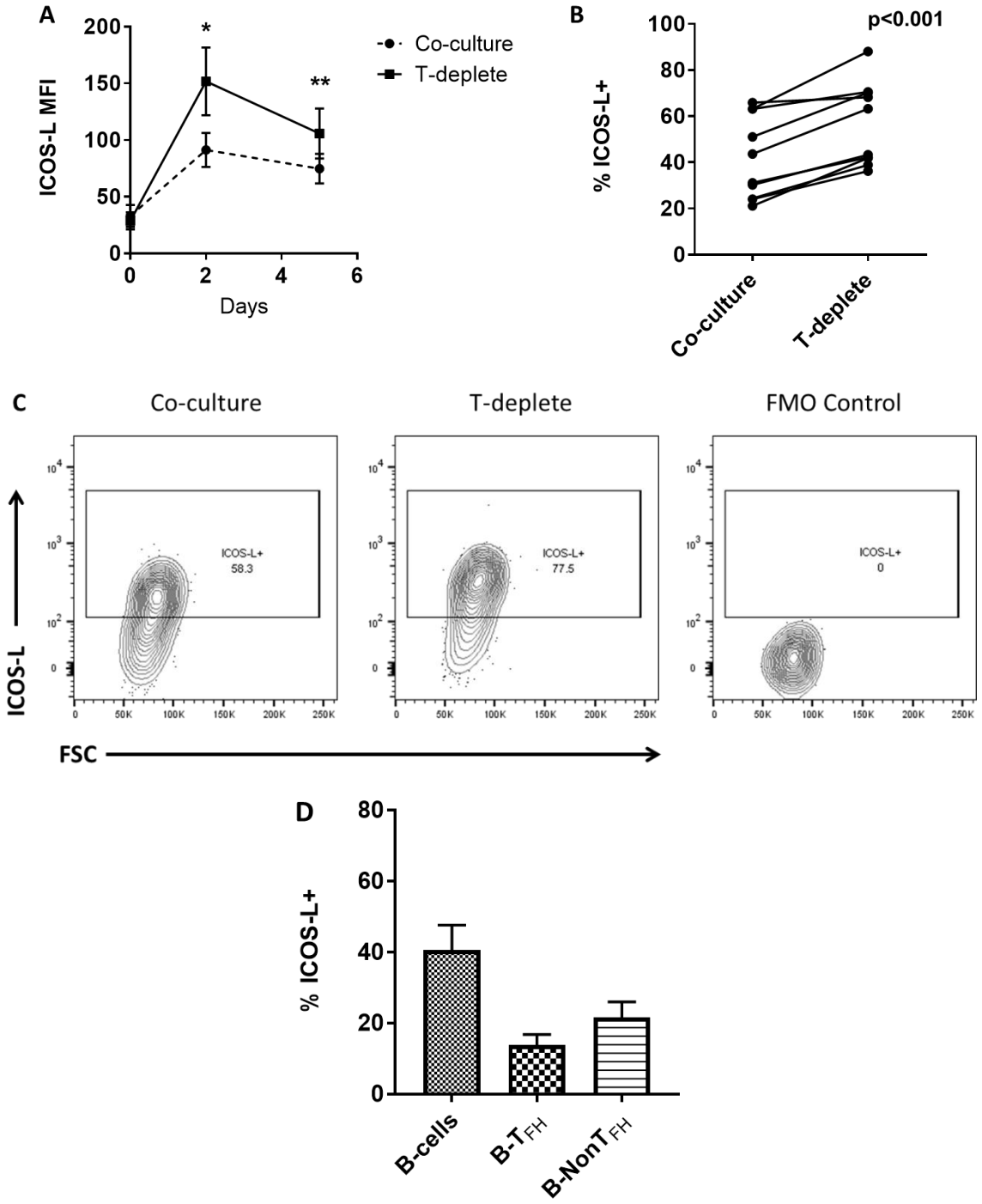

Figure 4.7. Influence of T-cells on ICOS-L expression in FL B-cells. *A) kinetics of ICOS-L expression in culture with or without T-cells. Data represent mean values ± standard error. *p<0.001; **p=0.025. B) graph shows the proportion of FL B-cells expressing ICOS-L after culture for 2 days with (co-culture) or without T-cells (T-deplete). C) representative flow plots show ICOS-L expression in FL B-cells after 2 days in T-replete and T-deplete culture, plus an FMO (fluorescence minus one) negative control. D) Bar chart shows the proportion of flow-sorted FL B-cells expressing ICOS-L when cultured with or without different CD4+ T-cell subsets. Horizontal bars represent mean value and standard error.*

cultured alone, ICOS-L expression was also reduced in B-cells co- cultured with non-T_{FH} $CD4^+$ T-cells, although to a much lesser extent than with T_{FH} (Figure 4.7D). Engagement of ICOS by ICOS-L is known to trigger rapid cleavage of surface ICOS-L on B-cells (Lownik*, et al* 2017), therefore this T_{FH}-dependent reduction in ICOS-L expression signifies the presence of dynamic ICOS/ICOS-L interactions between FL B-cells and T_{FH}.

4.3.4. Effect of FL B-Cells on T_{FH} Survival

Having demonstrated that FL B-cells can provide a source of ICOS-L, HLA-DR and CD86, the next step was to assess whether this translated to an ability to support T_{FH} *in vitro*, to recapitulate findings in healthy lymphoid tissue.

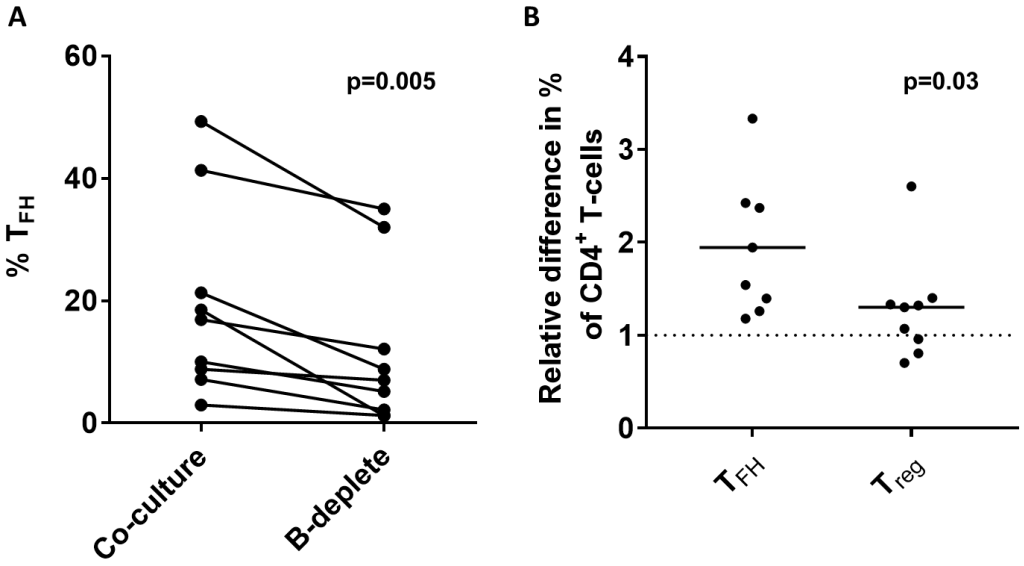

Figure 4.8. Influence of FL B-cells on $CD4^+$ T-cell composition. A) *Shows the proportion of $CD4^+$ T-cells that had a PD-$1^{hi}ICOS^+$ T_{FH} phenotype after 5 days of culture in either B-replete or B-deplete conditions (N=9). B) Graph shows the relative difference in the proportion of $CD4^+$ T-cells that had a T_{FH} and T_{reg} phenotype after 5 days in culture with FL B-cells, compared with B-deplete cultures (N=9). Horizontal bars represent median values.*

Firstly, in the presence of FL B-cells, the proportion of viable $CD4^+$ T-cells that had a T_{FH} phenotype was significantly higher than in a B-cell-deplete environment. At baseline, 30.2 ± 6.1% of $CD4^+$ T-cells had a T_{FH} phenotype, but after 5 days in culture only 11.6 ± 4.3% of $CD4^+$ T-

cells cultured in B-deplete conditions had a T_{FH} phenotype, compared with 19.6 ± 5.3% in B-replete co-cultures (p=0.005, N=9; Figure 4.8A). To assess whether this change was specific to T_{FH}, or whether the prevalence of other T-cell subsets was also altered by the presence of FL B-cells, we assessed whether there were any parallel changes in the proportion of $CD25^{+}CD127^{lo}$ T_{regs}. The proportion of $CD4^{+}$ T-cells that had a T_{reg} phenotype after 5 days was not significantly different in B-replete co-cultures compared with B-deplete cultures (p=0.19; Figure 4.8B).

These findings were confirmed by quantifying the absolute number of viable T_{FH} and other $CD4^{+}$ T-cells at each time point using counting beads. Compared with baseline T_{FH} counts, by day 5 only 15.6 ± 8.0% of T_{FH} remained in B-deplete cultures, whilst 37.0 ± 14.9% of T_{FH} remained in cultures where FL B-cells were present (p=0.06, N=5; Figure 4.9A). There was also a reduction in the absolute number of T_{regs} and $CD4^{+}$ T-cells remaining by day 5 under B-deplete conditions compared with B-replete co-cultures (p=0.06 and p=0.13, respectively, N=5), although to a lesser degree than seen with T_{FH} (Figure 4.9B). This suggests that T_{FH} are more dependent on FL B-cell support than other $CD4^{+}$ T-cells. However, a larger sample number is required to confirm these findings.

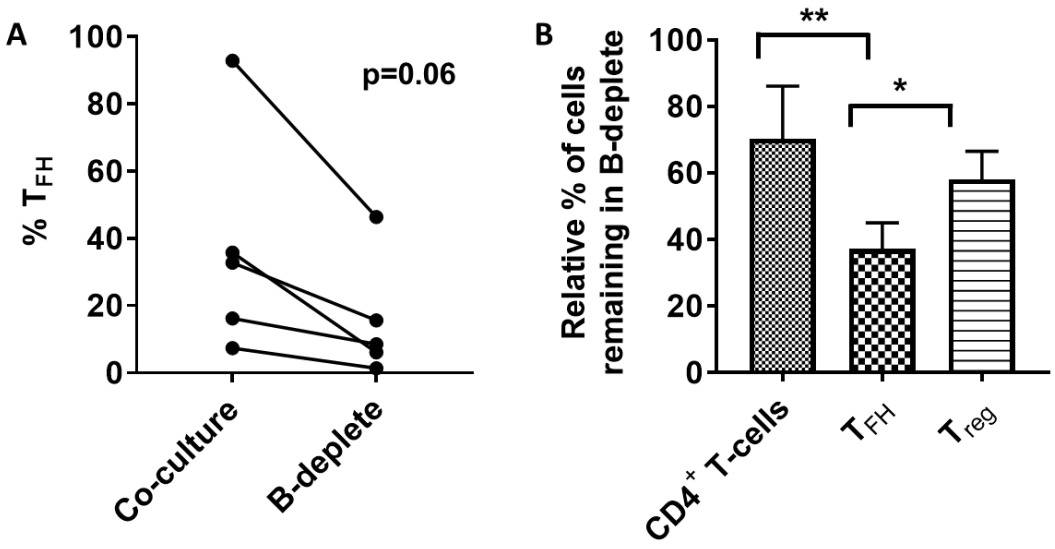

Figure 4.9. Effect of B-cell depletion on T-cell survival. *A) Graph shows the proportion of viable T_{FH} remaining after 5 days of culture compared to baseline in B-replete co-cultures and paired B-deplete cultures (N=5). B) Histogram shows the proportion of $CD4^{+}$ T-cell subsets remaining after 5 days in B-deplete cultures, relative to the proportion surviving in paired B-replete co-cultures (N=5). Bars show mean values plus standard error. *p=0.06; **p=0.13.*

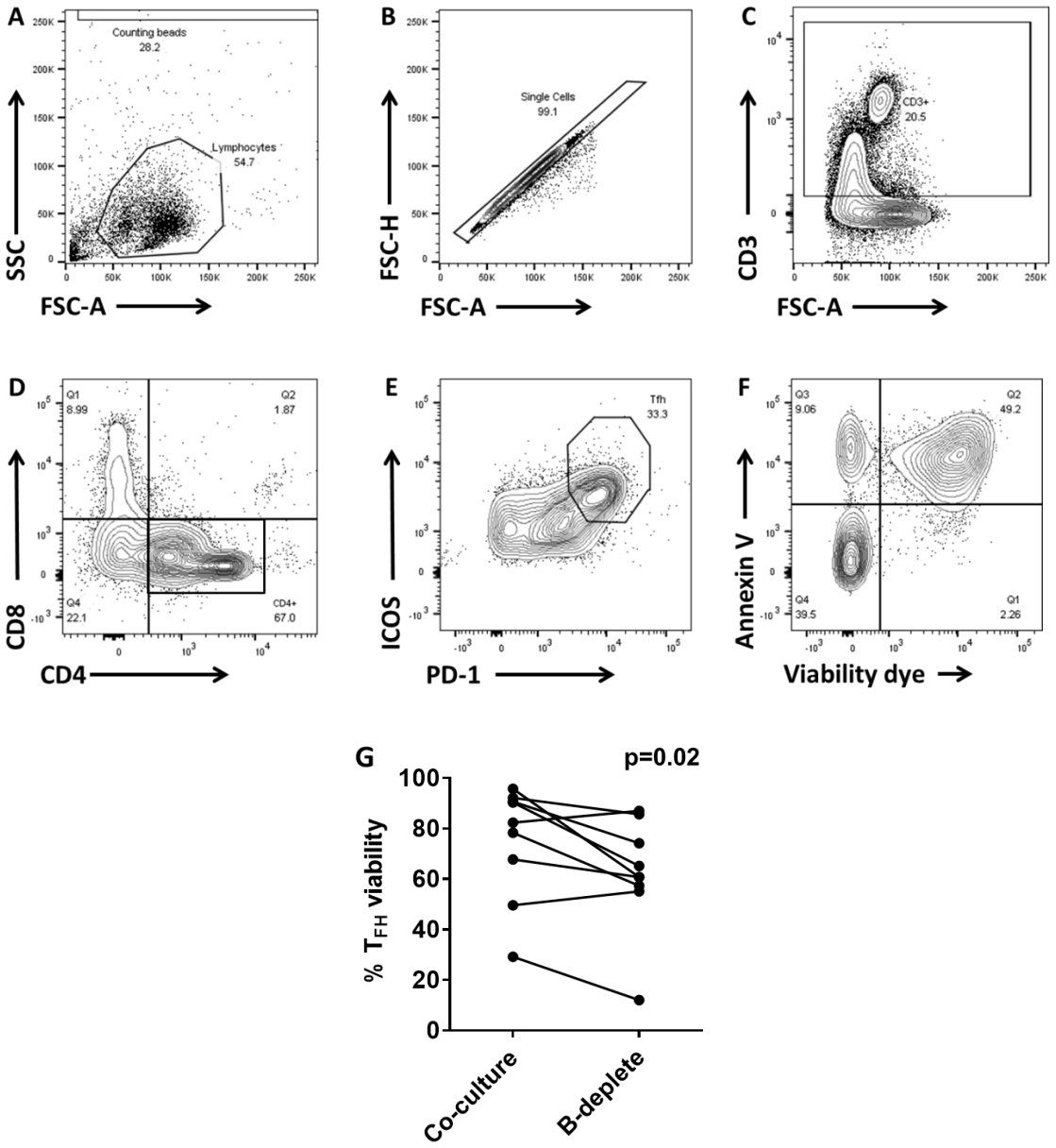

Figure 4.10. Influence of FL B-cells on T_{FH} viability. A-F) *Representative flow plots show sequential gating strategy to quantify apoptosis in T_{FH}:* ***A)*** *lymphocyte gate,* ***B)*** *doublet exclusion,* ***C)*** *$CD3^+$ T-cells,* ***D)*** *$CD4^+CD8^-$ T-cells,* ***E)*** *PD-$1^{hi}ICOS^+$ T_{FH}. Wide lymphocyte and T-cell gates were used to incorporate apoptotic cells. F) Annexin V and Fixable Viability Dye identify apoptotic and dead T_{FH}, respectively.* ***G)*** *Comparison between the proportion of T_{FH} that were viable after 5 days in culture with or without autologous FL B-cells (N=9).*

These data show that FL B-cells support T_{FH} *in vitro*, although they do not indicate whether the loss of T_{FH} in B-deplete cultures is due to increased T_{FH} cell death or loss of the T_{FH} phenotype in viable T-cells. To assess whether FL B-cell support T_{FH} viability, apoptosis and cell death were

measured in T_{FH} cells in paired B-deplete and B-replete cultures. The flow gating strategy used to quantify apoptosis and cell viability is shown in Figure 4.10. T_{FH} viability was higher in the presence of FL B-cells; 24.8 ± 7.5% of T_{FH} were dead or apoptotic in B-replete cultures compared with 38.0 ± 7.4% in B-deplete co-cultures, p=0.02; Figure 4.10G), demonstrating that FL B-cells support T_{FH} survival. However, it is also noteworthy that the majority of T_{FH} remained viable, even under B-deplete conditions. Therefore, the striking reduction in the number of T_{FH} in B-deplete cultures is not accounted for by apoptosis alone, suggesting that loss of the T_{FH} phenotype may also play a role.

4.3.5. Effect of FL B-Cells on the T_{FH} Phenotype

In healthy germinal centres, T_{FH} require interactions with GC B-cells and ICOS stimulation to maintain expression of CXCR5 and the overall T_{FH} phenotype (Choi*, et al* 2011, Weber*, et al* 2015). There are no published data assessing whether FL T_{FH} are dependent on the presence of FL B-cells to the same extent.

Following 2 days of *in vitro* culture, there was a clear reduction in PD-1 and CXCR5 expression on T_{FH} in B-deplete cultures, which was more pronounced after 5 days and corresponded to a reduction in the overall proportion of T_{FH} (Figure 4.11). In the absence of B-cells, 14.0 ± 5.1% of $CD4^+$ T-cells expressed high levels of PD-1 after 2 days in culture, compared with 23.2 ± 6.1% in B-replete co-cultures (p=0.002, N=10; Figure 4.12A). Similarly, only 35.7 ± 5.0% of $CD4^+$ T-cells were $CXCR5^{hi}$ in B-deplete cultures, compared with 45.8 ± 5.4% in the presence of FL B-cells (p=0.001; Figure 4.12B). These data demonstrate that FL T_{FH} lose their phenotype in the absence of FL B-cell support and suggest that FL B-cells actively promote the persistence of T_{FH}.

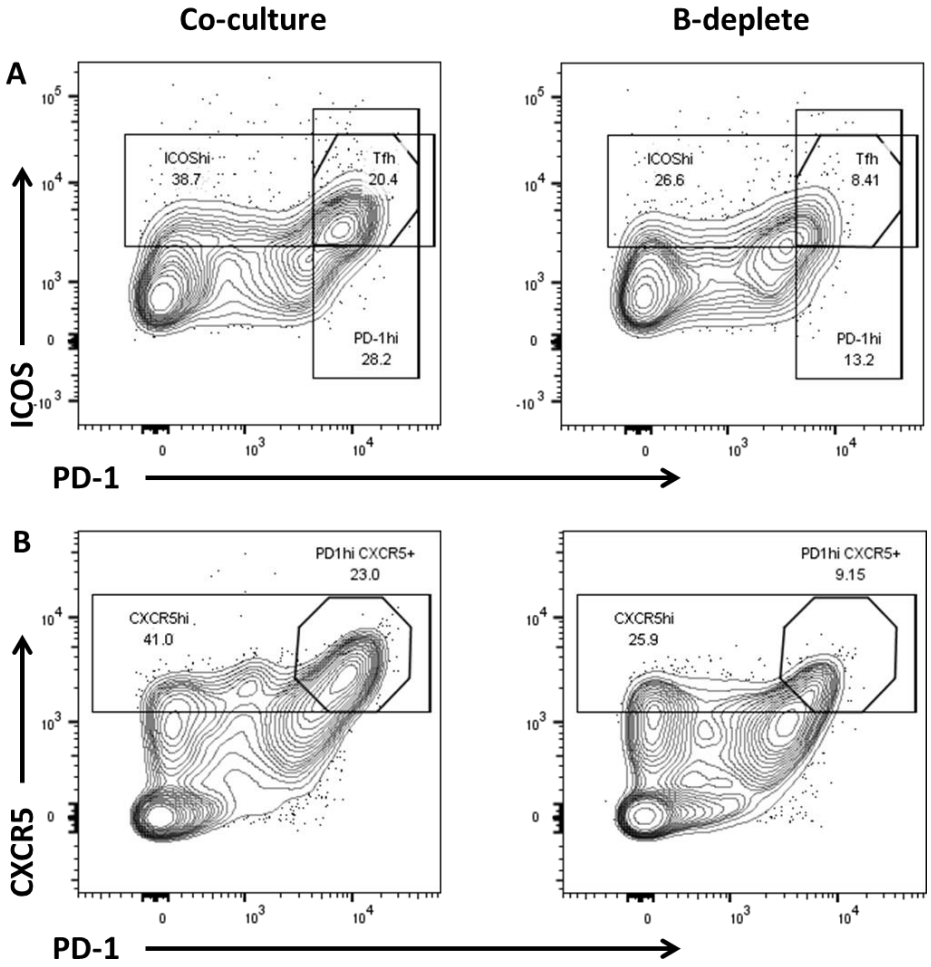

Figure 4.11. FL B-cells support maintenance of the T_{FH} phenotype. *Representative flow plots show CD4⁺ T-cells from FL LNs cultured either with, or without, FL B-cells for 5 days.* ***A)*** *demonstrates a shift PD-1 and ICOS expression in B-deplete samples, with a subsequent reduction in the proportion of T_{FH}, whilst* ***(B)*** *shows parallel shifts in CXCR5 expression.*

However, there was no overall change in the proportion of CD4⁺ T-cells that expressed high levels of ICOS (p=0.87; Figure 4.12C/D). Interaction with ICOS-L induces internalisation of ICOS, therefore the relative stability of ICOS expression despite partial loss of the T_{FH} phenotype may be due to reduced ICOS-L binding in the absence of FL B-cells. This provides further evidence to suggest the presence of dynamic ICOS/ICOS-L interactions between T_{FH} and FL B-cells.

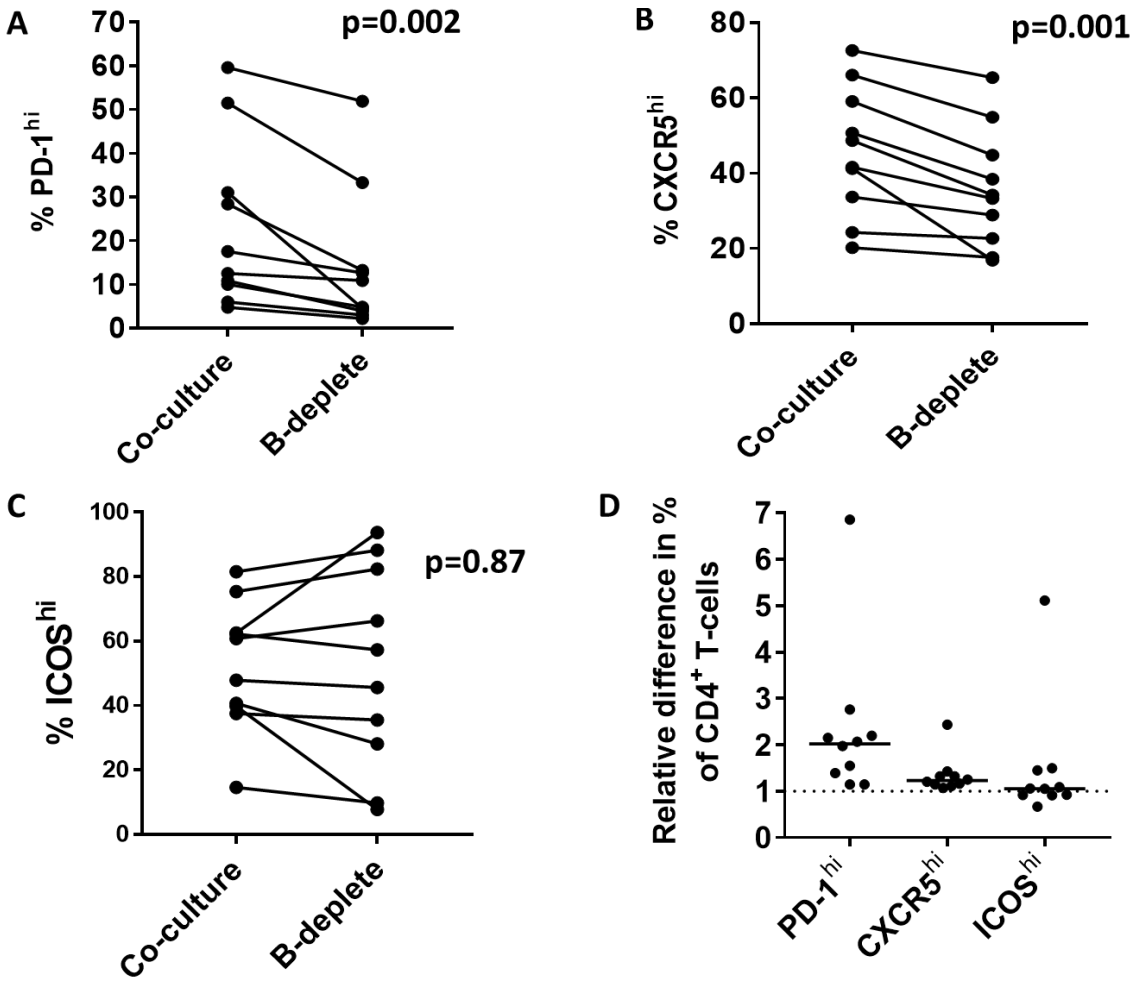

Figure 4.12. Influence of FL B-cells on T_{FH} phenotype. *Graphs show the proportion of $CD4^+$ T-cells that expressed high levels of* ***A)*** *PD-1,* ***B)*** *CXCR5 and* ***C)*** *ICOS after 2 days of culture in either B-replete or B-deplete conditions (N=10).* ***D)*** *Summary graph shows the relative change in the proportion of CD4+ T-cells expressing high levels of PD-1, CXCR5 and ICOS when co-cultured with FL B-cells, compared with B-deplete conditions (N=10). Horizontal bars represent median values.*

The changes in PD-1 and CXCR5 expression were confirmed in flow-sorted T_{FH} cultured either with or without FL B-cells. Non-T_{FH} $CD4^+$ T-cells did not show any B-cell-dependent shift in PD-1 or CXCR5 expression, suggesting that these phenotypic changes are specific to T_{FH}, although larger patient numbers are required to confirm these findings.

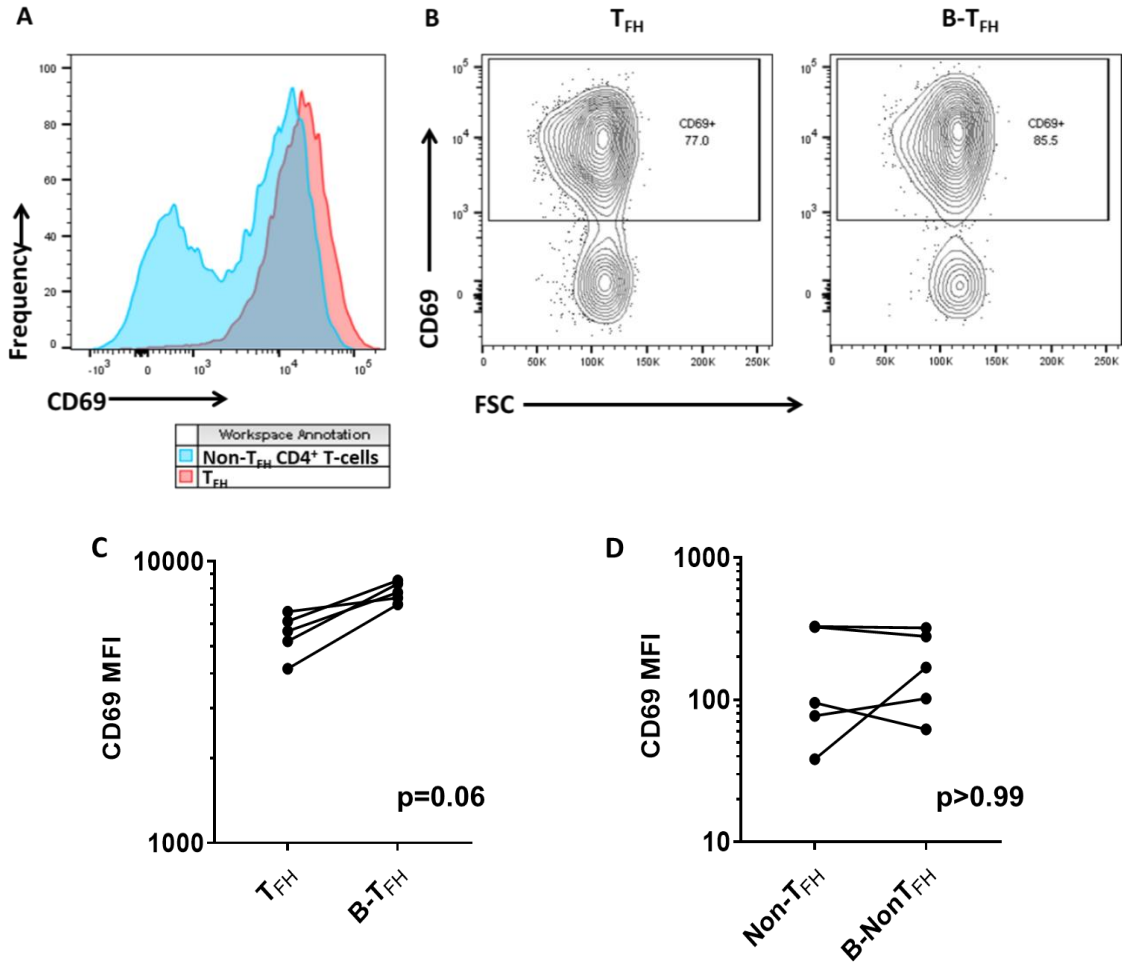

Figure 4.13. FL B-cells induce activation of T_{FH}. A) *Representative flow plot compares basal CD69 expression in flow-sorted CD4⁺ T-cell subsets.* ***B)*** *Representative flow plots show CD69 expression in T_{FH} cultured either alone or with FL B-cells.* ***C-D)*** *Graphs shows the intensity of CD69 expression in flow-sorted T_{FH} (C) and non-T_{FH} CD4⁺ T-cells (D) cultured for 2 days either in the presence or absence of FL B-cells. N=5, from 2 patients.*

T-cell activation markers were also assessed in flow-sorted T-cells to investigate whether FL B-cells support reciprocal activation of T_{FH}. CD69 is an early marker of lymphocyte activation and is rapidly upregulated in response to TCR ligation (Yamashita*, et al* 1993). Baseline expression of CD69 was higher in T_{FH} than in other CD4⁺ T-cells, in the small number of samples analysed (n=5, from 2 patients (Figure 4.13A), consistent with data published by other groups (Lee*, et al* 2015). The presence of FL B-cells supported expression of CD69 in T_{FH}: after 2 days in culture, the intensity of CD69 expression was 43.6% higher (range 12.1 – 59.9) in T_{FH} co-cultured with FL B-cells compared with T_{FH} cultured in isolation (Figure 4.13A/B). The presence of FL B-cells did not appear to alter CD69 expression in non-T_{FH} CD4⁺ T-cells (Figure 4.13C).

CD25 is also recognised as a T-cell activation marker but its expression in T_{FH} usually signifies transition to a T_{FR} phenotype. It is known that FL-T_{FH} can acquire T_{FR}-like properties under certain conditions and that FL B-cells can induce a T_{reg} phenotype in TILs (Brady*, et al* 2014, Le*, et al* 2016). Therefore, it was important to assess whether B-cell-induced T_{FH} activation was accompanied by an increase in CD25 expression. After 2 days in culture with FL B-cells, a slightly higher proportion of T_{FH} expressed CD25 than in B-deplete cultures, although the magnitude of change was small: only 6.66 ± 1.8% and 4.8 ± 1.5% of T_{FH} had a T_{FR}-like phenotype in B-replete and B-deplete culture respectively (p=0.01, N=10; Figure 4.14A). The majority of FL T_{FH} expressed high levels of CD69 but negligible levels of CD25 after 2 days in culture, unlike non-T_{FH} $CD4^+$ T cells, where CD25 and CD69 were usually co-expressed (Figure 4.14B). Therefore, FL B-cells do not induce a major shift towards a regulatory phenotype but rather promote the presence of phenotypically-active T_{FH}.

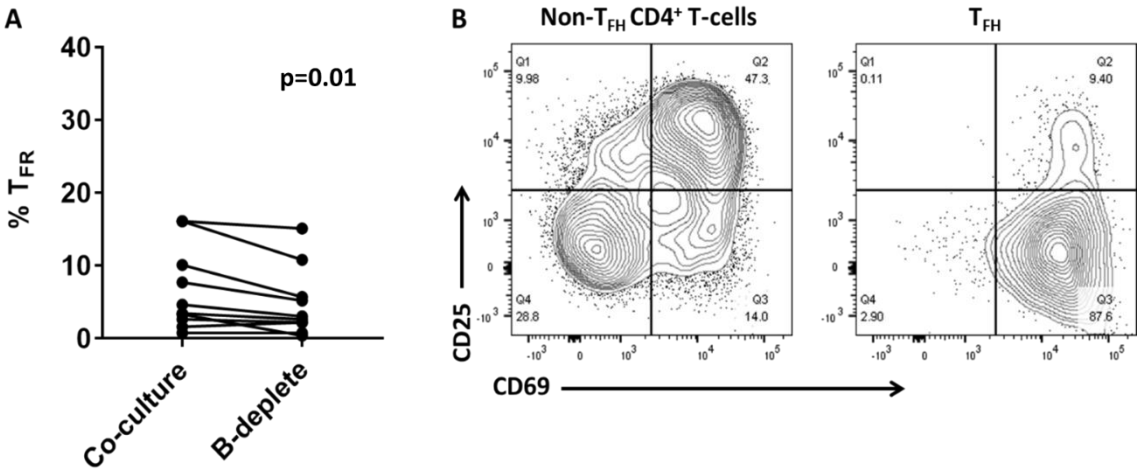

Figure 4.14. Influence of FL B-cells on T_{FR}. ***A)*** *Graph shows the proportion of T_{FH} that have a $CD25^+$ T_{FR} phenotype after 2 days of in vitro culture in B-replete (co-culture) and B-deplete conditions.* ***B)*** *Representative flow plots show expression of CD25 and CD69 in flow-sorted $CD4^+$ T-cell subsets after 2 days of in vitro culture with FL B-cells.*

4.4. Discussion

These data demonstrate that T_{FH} and FL B-cells form mutually supportive interactions that promote cell survival and activation. T_{FH} increased expression of the activation markers CD86 and HLA-DR on FL B-cells in culture, whilst FL B-cells were able to stimulate reciprocal T_{FH}

activation. The changes in CD86 expression confirm the findings of other groups (Ame-Thomas*, et al* 2012, Yang*, et al* 2015a), whilst the influence of T_{FH} on HLA-DR expression is a novel finding that has not previously been reported to our knowledge, although HLA-DR expression is known to be more heterogeneous than other B-cell markers in FL (Green*, et al* 2015, Wogsland*, et al* 2017). The functional significance of HLA-DR and CD86 expression is an increased capacity to provide reciprocal T-cell stimulation through both CD3 and CD28, respectively.

The ability of T_{FH} to enhance HLA-DR expression in FL B-cells is of particular interest, as it signifies that these FL B-cells may possess enhanced capacity to present antigen to T_{FH} and other T-cells. The ability of FL B-cells to promote activation and survival of T_{FH}, mirroring findings in reactive lymphoid tissue, also suggests that cognate TCR interactions may exist between FL B-cells and T_{FH}. This is supported by evidence that intrafollicular FL T-cells (in which T_{FH} predominate) have greater TCR clonality than extrafollicular T-cells (Townsend*, et al* 2019), suggesting they have undergone antigen-dependent expansion. However, further work is necessary to confirm whether this observation is specifically attributable to T_{FH}. Exploring the nature of these FL-TCR interactions and the antigens that drive them may offer insights into the pathogenesis of FL and constitutes an important area for future study. As a first step, the effect of blocking MHC-TCR interactions could be evaluated in FL B-T_{FH} co-cultures, to assess whether TCR signalling is necessary for T_{FH} survival in FL.

In contrast to other B-cell activation markers, the presence of T_{FH} resulted in lower expression of ICOS-L on FL B-cells. ICOS-L is a downstream target of CD40 signalling therefore T_{FH} interaction would be expected to increase ICOS-L gene expression (Watanabe*, et al* 2008). However, other mechanisms influence surface ICOS-L expression in reactive GCs, where expression of ICOS-L is tightly regulated to maintain homeostasis (Watanabe*, et al* 2008). Engagement of ICOS by ICOS-L leads to rapid cleavage of surface ICOS-L on healthy B-cells and moderate internalisation of ICOS on T-cells (Lownik*, et al* 2017). Therefore, the upregulation of ICOS-L expression in culture and T_{FH}-dependent decrease in ICOS-L expression suggest the presence of dynamic ICOS/ICOS-L interactions, mirroring those present in reactive lymphoid tissue. The persistence of ICOS expression on T_{FH} in B-cell-deplete cultures, despite a loss of expression of other T_{FH} markers, provides further evidence of these reciprocal interactions. We considered assessing expression of ICOS and ICOS-L in FL tissue, to corroborate these findings, however there were no commercially available anti-ICOS-L antibodies that were suitable for use in FFPE tissue. Similar to our results, Le *et al* demonstrated that the presence of T_{regs}, which express variable levels of ICOS, can partially inhibit ICOS-L expression on FL B-cells during *in vitro* culture (Le*, et al* 2016).

T_{FH} express greater levels of ICOS than other $CD4^+$ T-cells within the FL TME and our data demonstrate that they are the prime modulators of ICOS-L expression on FL B-cells.

ICOS/ICOS-L interactions are beneficial to both T_{FH} and FL B-cells. ICOS signalling is particularly critical for T_{FH} survival and plays a greater role in supporting T_{FH} in reactive GCs that CD28 co-stimulation (Weber*, et al* 2015). In reactive lymphoid tissue, ICOS/ICOS-L interaction stimulates upregulation of CD40L expression by T_{FH} and facilitates stable 'entanglement' between healthy GC B-cells and T_{FH}, through which additional bi-directional stimulation, by CD40 ligation and cytokine release, is able to occur (Liu*, et al* 2014, Papa*, et al* 2017). Other data, published as an abstract, suggest that ICOS-L signalling can directly sustain GC B-cell survival (Zheng*, et al* 2015). The next step in this work would be to repeat B-T_{FH} co-cultures in the presence of ICOS-blocking antibodies to assess whether FL T_{FH} are dependent on ICOS signalling. It would also be of interest to assess whether the addition of ICOS to CD40L and IL-4/IL-21 can enhance FL B-cell survival. Importantly, it is possible to therapeutically target ICOS/ICOS-L interactions. Blocking antibodies against ICOS-L have already shown signs of efficacy for treatment of autoimmune disease in early phase clinical studies (Cheng*, et al* 2018).

FL B-cells directly supported the maintenance of T_{FH} in culture, by both enhancing T_{FH} survival and maintaining expression of T_{FH} surface markers, demonstrating that T_{FH} remain dependent on B-cell support in FL (Choi*, et al* 2011, Crotty 2014). This mirrors findings in reactive lymphoid tissue where, without engagement of ICOS, T_{FH} rapidly lose expression of PD-1 and CXCR5 and revert to a non-T_{FH} effector phenotype (Bossaller*, et al* 2006, Weber*, et al* 2015). This has not been previously demonstrated in FL and implies that T_{FH} are directly co-opted by FL B-cells to support tumour growth.

To support this hypothesis, it is necessary to demonstrate that this mutual support translates into a survival benefit for FL B-cells. Indeed, a greater absolute number of FL B-cells survived in T-replete cultures than in T-deplete cultures, consistent with other studies demonstrating that T_{FH} can enhance FL viability (Amé-Thomas*, et al* 2015, Yang*, et al* 2015a). However, the inability to detect a proportional difference in apoptosis between T-replete and T-deplete co-cultures highlights the limitation of using global T-cell depletion to provide insights into T_{FH} biology. T_{FH} represent a minority of T-cells, therefore these results will reflect the competing influences of multiple other T-cell subsets, such as T_{regs} and $CD8^+$ T-cells, that potentially have a deleterious effect on FL B-cell survival (Ame-Thomas and Tarte 2014). Other investigators have found that FL B-cells can successfully be cultured with autologous T_{FH} alone, but additional stimulation is required when other T-cell subsets are present (K Tarte, personal communication).

Flow-sorting was the only way to obtain purified T_{FH} for *in vitro* experiments and is widely used for T_{FH} co-culture studies (Amé-Thomas*, et al* 2015, Boice*, et al* 2016, Espeli and Linterman 2015). However, there are several limitations, including a reduction in subsequent cell viability and the difficulty in using low cell numbers for culture studies. It is also important to consider whether the antibodies used for flow-sorting may have exerted an influence on B- and T-cell phenotype. The C398.4A ICOS antibody does not block ICOS-ICOS ligand interactions but has been reported to have a stimulatory effect on T-cells (Arimura*, et al* 2004). T_{FH} have higher ICOS expression than other $CD4^+$ T-cells, therefore may be stimulated to a greater degree. The EH12.2H7 anti-PD-1 antibody has been reported to block PD-1 activity (Tan*, et al* 2012). It is not clear what effect this would have on FL B-T_{FH} interactions, given that the majority of FL B-cells do not express PD-1 ligands and PD-L1-expressing stromal cells are usually not extracted by mechanical tissue disaggregation (Gravelle*, et al* 2017). Nevertheless, this is an important consideration when comparing different T-cell subsets, such as T_{FH} and non-T_{FH} $CD4^+$ T-cells, with different levels of PD-1 and ICOS expression; it is less relevant when comparing T_{FH} under different culture conditions (i.e. with or without FL B-cells).

There are a number of other antigens that play a significant role in FL-T_{FH} interactions that were not evaluated here, such as CD40/CD40L and HVEM/BTLA. This work was limited by the number of antigens that could easily be assessed simultaneously by flow cytometry and we prioritised T-cell antigens that defined the T_{FH} phenotype. Up to 10 colours were used in each flow panel, to avoid the need for complex compensations and large numbers of control tubes, where available cell numbers were often low. Use of mass cytometry, or CyTOF, technology can overcome these limitations by allowing simultaneous assessment of over 40 antigens, thus facilitating highly-multiplexed assessment of lymphocyte composition (Wogsland*, et al* 2017, Yang*, et al* 2019). Future studies will greatly benefit from this technology, particularly when working with restricted numbers of cells, as with FNAs.

In summary, FL B-cells directly support T_{FH} and form mutually supportive interactions to promote reciprocal activation and survival. These data strongly imply that T_{FH} are not GC bystanders but actively cooperate to provide support for FL growth. The signalling pathways that provide T_{FH} support remain intact in FL, providing potential targets for therapeutic manipulation. A key future direction of this work would be to use these culture studies as a platform to assess the effect of novel therapeutics on T_{FH} function in FL.

CHAPTER 5: INSIGHTS FROM CONFOCAL IMMUNOFLUORESCENCE MICROSCOPY STUDIES

5.1. Introduction

The co-culture studies described in the previous chapter provide evidence of functional, mutually-supportive interactions between FL B-cells and T_{FH} in FL. However, these experiments were performed in an artificial, *in vitro* environment, where tissue architecture and follicular structure were disrupted. Intra- and interfollicular areas usually contain very different T-cell subsets that do not come into direct contact *in vivo*. In addition, adherent stromal cells that can modulate T_{FH} and B-cell activity, such as FDCs and FSCs, are not usually present in disaggregated LN tissue or FNAs. Therefore, culture studies cannot replicate the multi-directional interactions within the TME that occur in FL *in vivo*. Imaging studies of FL tissue are necessary to provide information about *in situ* interactions within the FL TME and often complement *in vitro* studies.

The initial aim of the data presented in this chapter was to use confocal imaging on archival FL tissue to confirm findings from *in vitro* culture studies (Chapter 4). We considered assessing apoptosis in FL B-cells and T_{FH} *in situ*, but cleaved caspase-3 expression was found to be extremely sparse when 4 FL tissue sections were assessed by IHC (<1% cells) as a preliminary step, and this was not taken further. The lack of cleaved caspase-3 may reflect the transient nature of apoptosis, where tissue captures a snapshot of a single point in time, but it is also unclear to what extent cell death limits FL progression *in vivo* (i.e. the net effect of proliferation versus death).

Tissue imaging studies can also be hypothesis-generating and used to inform future culture studies, given that archival FFPE tissue is a much more readily available resource than viable LN cells. Previous confocal imaging work from our group has demonstrated a strong spatial correlation between T_{FH} and FL proliferation (Townsend*, et al* 2019). MYC is a master regulator of transcription that is frequently upregulated in human cancers, has wide-ranging effects on tumour growth and is linked with GC B-cell proliferation (Luo*, et al* 2018, Stine*, et al* 2015). Physiological MYC expression in reactive GC B-cells requires CD40L stimulation, which is predominantly provided by T_{FH} within GCs. MYC upregulation then triggers shuttling of cognate GC B-cells to the LN dark zone and rapid clonal expansion (Dominguez-Sola*, et al* 2012, Luo*, et al* 2018). In FL, the acquisition of mutations and translocations involving the *MYC* proto-oncogene is associated with disease transformation (Aukema*, et al* 2017, Pasqualucci*, et al* 2014); a point at which FL B-cells proliferate more rapidly and become less dependent on the non-malignant TME. The role of MYC in untransformed FL has been relatively underexplored,

largely because it has been considered a MYC-negative malignancy. However, data published during the conduct of this thesis showed that MYC expression is detectable in a minority of B-cells in most FL samples (Aukema*, et al* 2017). We therefore hypothesised that T_{FH} have a role in inducing MYC expression and thereby driving proliferation of FL B-cells.

One major unanswered question is whether the number or location of T_{FH} influences the clinical phenotype of FL. Single-parameter IHC studies have yielded conflicting results regarding the prognostic influence of intrafollicular $CD4^+$ T-cells and PD-1 expression (see Section 1.3.7). Flow cytometry studies using disaggregated LN tissue have not demonstrated a correlation between T_{FH} and survival, although these studies do not account for tissue localisation and sample numbers were small (Yang*, et al* 2019, Yang*, et al* 2015b). One possible explanation for the lack of observed effect is that the balance between tumour-promoting and inhibitory elements within the TME may be more important in regulating the behaviour of FL than the predominance of any individual cell subset.

Another important observation from our group's previous work is that regulatory T-cells are more prominent within FL follicles than reactive GCs (Townsend*, et al* 2019), a finding that has also been noted by other groups (Tarte*, et al* 2017). T_{FR} are present within FL tissue and are able to suppress T_{FH} activity, including T_{FH}-induced activation of FL B-cells (Tarte*, et al* 2017). Intrafollicular FoxP3 expression by single-parameter IHC, which reflects T_{FR} in part, has been associated with favourable outcomes in FL (Wahlin*, et al* 2010), although this data requires independent verification. There is overlap in T-cell clonality between T_{FH} and T_{FR} in FL, suggesting a common origin, and it has been shown that T_{FH} can convert to T_{FR} *in vitro* (Brady*, et al* 2014, Tarte*, et al* 2017). However, little is known about the localisation of T_{FR} and the balance between T_{FH} and T_{FR} *in vivo*. We hypothesised that the balance between T_{FH} and T_{FR} influences the clinical phenotype of FL.

Confocal imaging of FL tissue was therefore used to investigate two exploratory hypotheses regarding the regulation and function of T_{FH} in FL. The aims of this work were:

1) To investigate whether there is a spatial relationship between T_{FH} and MYC expression in FL
2) To investigate whether the balance or interaction between T_{FH} and regulatory T-cells correlates with clinical phenotype

5.2. Tissue Sections and Patient Characteristics

Methods for tissue staining, image acquisition and data analysis are described in Section 2.8.

Archival FFPE tissue was obtained from selected patients with extremes of clinical outcome and long-term follow-up data (at least 4 years). An aggressive phenotype was defined as disease progression within 24 months of initial immunochemotherapy. Good-risk patients had indolent disease, either not requiring treatment within 24 months of diagnosis or without progression for at least 5 years after initial immunochemotherapy. Positive control tissue was obtained from patients with reactive lymphoid hyperplasia.

Table 5.1. Patient characteristics

Patient ID	Age (y)	Prior lines of therapy	Management	Stage	Grade	
HR-1	45.9	1	CIT	IV	2	2nd progression within 2y, received alloSCT, alive at 10y
HR-2	70.7	1	CIT	III	2	2nd progression and death within 1y
HR-3	48.0	2	CIT plus autoSCT	IV	1	No progression after 6y
HR-4	57.7	0	CIT	IV	1	Relapse within 1y, death within 2y
HR-5	59.8	1	CIT plus alloSCT	IV	1-2	No progression after 22m
HR-6	59.4	0	CIT	III	3a	Refractory disease, relapse after alloSCT and death within 4y
LR-1	60.3	0	W&W	III	1	Remains untreated after 6y
LR-2	56.5	0	CIT	IV	2	No progression after 5y
LR-3	54.7	0	W&W	III	2	Remains untreated after 4y
LR-4	63.7	0	CIT	III	3a	No progression after 10y

LR-5	38.2	0	W&W	III	1-2	Remains untreated after 5y
LR-6	32.1	0	W&W	IV	3a	Remains untreated after 6y

AlloSCT: allogeneic stem cell transplant; autoSCT: high-dose therapy and autologous stem cell transplant; CIT: chemoimmunotherapy; HR: high-risk; LR: low-risk; W&W: watch and wait

Characteristics for the 12 FL patients are described in Table 5.1. The median age was 55.6 years (range 32.1 – 63.7) for good-risk patient and 58.7 years (range 45.9 – 70.7) for poor-risk patients. Four poor-risk patients had relapsed after prior immunchemotherapy; none had received bendamustine or purine analogue therapy.

5.3. MYC and T_{FH}

5.3.1. Results

The aim of this section was to investigate whether there is a correlation between T_{FH} and MYC expression by FL B-cells, both in terms of spatial interactions and cell number.

A four-colour imaging panel was used to identify Pax5, MYC, PD-1 and CD4 expression (see Figure 5.1). Pax5 was included to allow localisation of MYC expression to B-cells. T_{FH} were identified as $CD4^{+}PD\text{-}1^{hi}$ cells; it has previously been shown by our group, using the same methodology, that the majority of these cells co-express ICOS and are true T_{FH} (Townsend*, et al* 2019). Details of reagents used, including primary and secondary antibodies, are provided in Section 2.8.

Variable levels of background autofluorescence were seen in the yellow-green channel, on which MYC expression was assessed, in part due to the variability in quality and age of tissue sections imaged. For most tissue sections, it was possible to use negative control slides to set a threshold to set a level defining MYC positivity that excluded any background staining (see Figure 2.6). However, in 2 sections it was not possible to clearly differentiate nuclear MYC staining over background fluorescence; both were excluded from this analysis. Therefore, 10 FL tissue sections were assessed in total; 6 with good-risk and 4 with high-risk disease. Five high-powered images (x60 objective) were analysed for each tissue section; this number was determined principally by the number of good-quality images obtainable for all tissue samples.

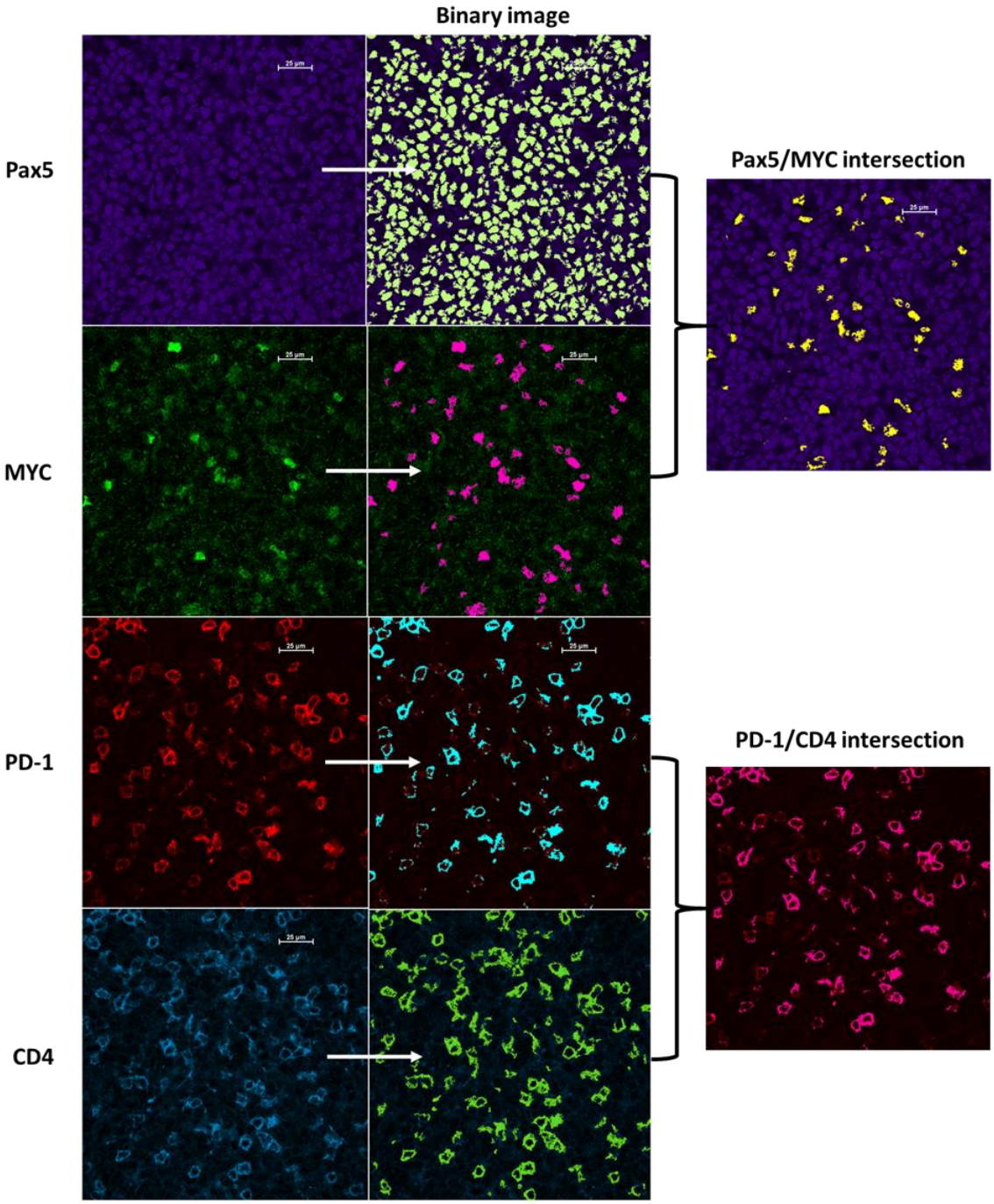

Figure 5.1. Immunofluorescence panel for assessment of T_{FH} and MYC expression. *Representative high-power (x60 objective) CIFM images show expression of Pax5 (purple), MYC (green), PD-1 (red) and CD4 (blue) in FFPE FL tissue. Scale bars measure 25µm. Right-handed panels show binary images defining expression of each individual antigen. Note that for PD-1 (red), the binary layer (pink) excludes low levels of PD-1 expression. The intersection of the PD-1 and CD4 binary layers (far right) was used to identify T_{FH}.*

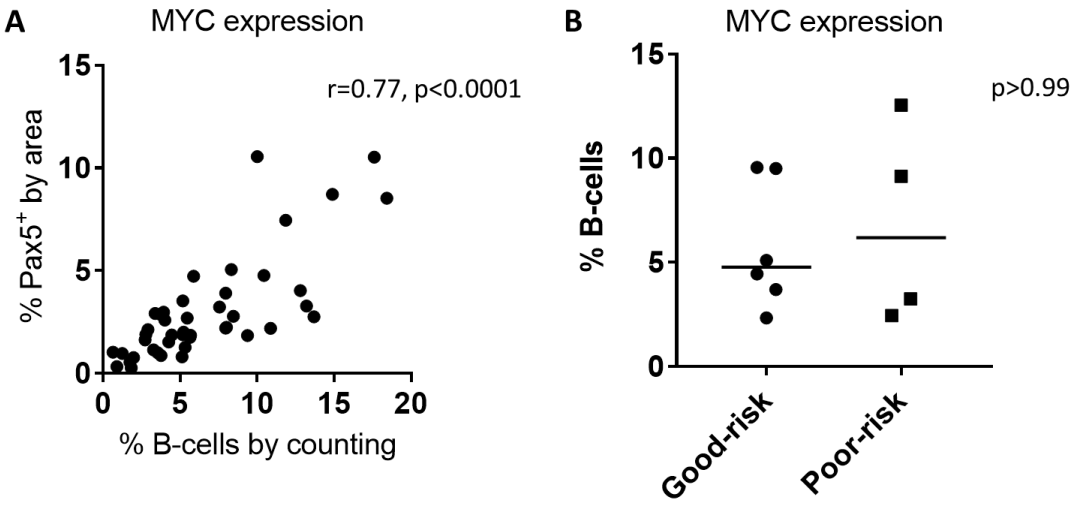

Figure 5.2. MYC expression in FL B-cells. A) *Scatter plot shows the correlation between 2 different methods of quantifying MYC expression in FL tissue. The percentage of Pax5⁺ B-cells that were MYC⁺ was assessed by counting of individual cells (x axis) and by area analysis (y axis). N=50, from 10 samples.* ***B)*** *Graph compares the proportion of FL B-cells that expressed MYC by cell count in good-risk (N=6) and poor risk (N=4) FL tissue. Horizontal bars represent median values.*

MYC expression was quantified by 2 methods: 1) by directly counting Pax5⁺ B-cells that were MYC⁺ and MYC⁻ in a 100µm² area of each image and B) by semi-automated image analysis, assessing the total area of both the Pax5 binary layer and Pax5/MYC intersection. There was a good correlation between the proportion of B-cells that were identified as MYC⁺ by both methods (r=0.77, p<0.0001; Figure 5.2A). A mean of 6.57 ± 0.66% of FL B-cells were MYC⁺ by cell count (N=50 images, from 10 patients), which is consistent with a previous IHC study reporting that 4-6% of FL B-cells express MYC (Aukema*, et al* 2017). There was no clear difference between median MYC expression between good- and poor-risk disease, although the sample number was small (Figure 5.2B).

It was evident on low-power images that there was a close spatial correlation between MYC expression and T_{FH}, both of which localised to intra- or perifollicular regions in all 12 samples, mirroring the pattern of MYC expression in reactive LN positive control tissue (Figure 5.3). On high-power images, the majority of MYC⁺ B-cells were seen to be in close contact with T_{FH} (Figure 5.4). The proportion of MYC⁺ and MYC⁻ B-cells (Pax5⁺) that were in direct contact with T_{FH} was quantified by counting cells within a 100 µm² intra/perifollicular area of each image. MYC-expressing B-cells were more likely to be in direct contact with T_{FH} than other B-cells, with 67.6

± 2.2% adjacent to T_{FH} compared with 49.7 ± 2.7% of MYC^- B-cells (p=0.0001; Figure 5.5A). It was not possible to use automated analysis techniques for this, as the Nikon Elements software was not adequately able to distinguish and segregate $Pax5^+$ B-cells within densely-packed FL tissue.

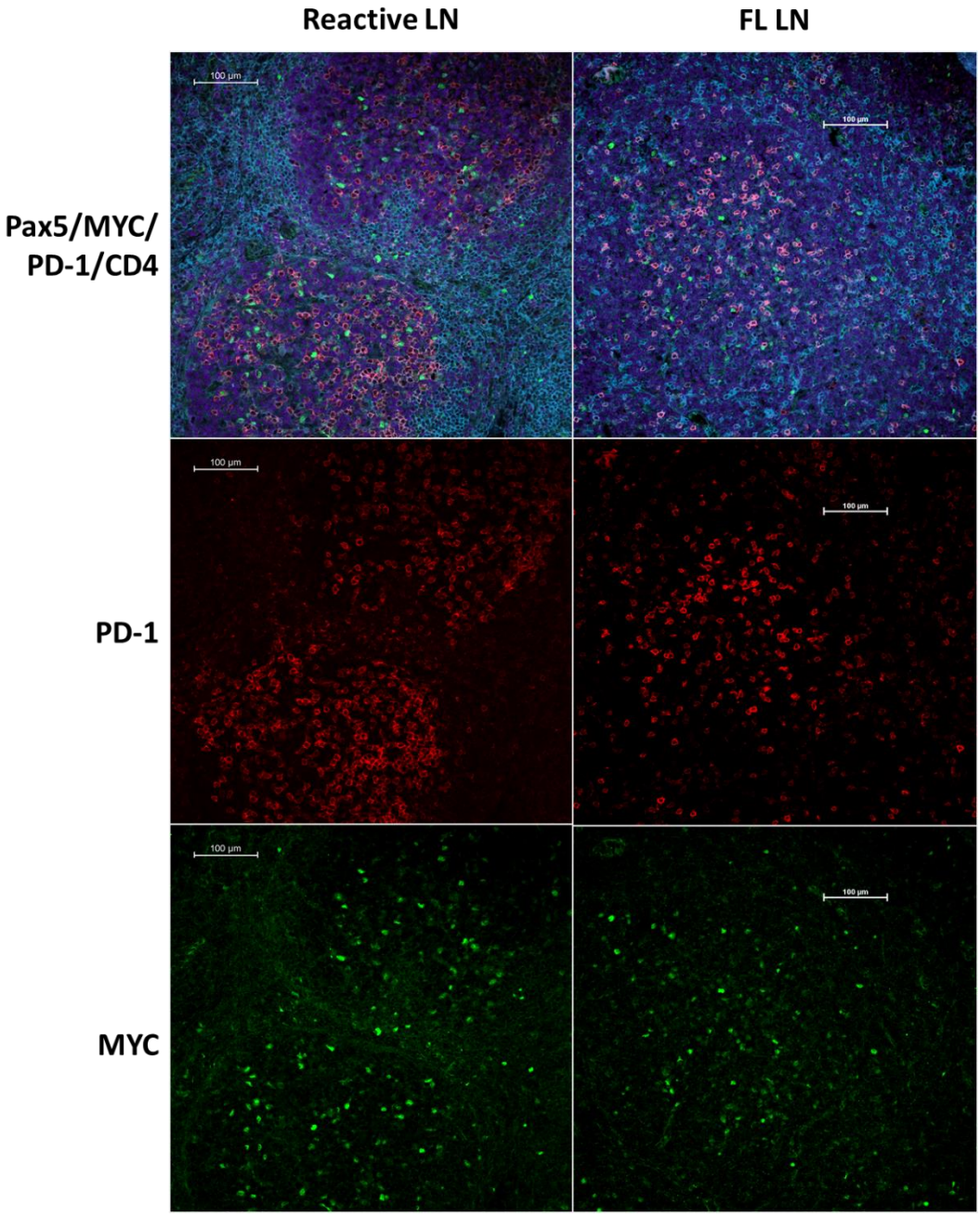

Figure 5.3. Distribution of T_{FH} and MYC expression. *Representative low-power (x20 objective) CIFM images show the distribution of Pax5 (purple), PD-1 expression (red), MYC (green) and CD4 expression (blue) in both reactive LN (left) and FL LN tissue (right). The majority of MYC expression is seen within GCs and follicles, in a similar distribution to PD-1^{hi} T-cells. Scale bars measure 100µm.*

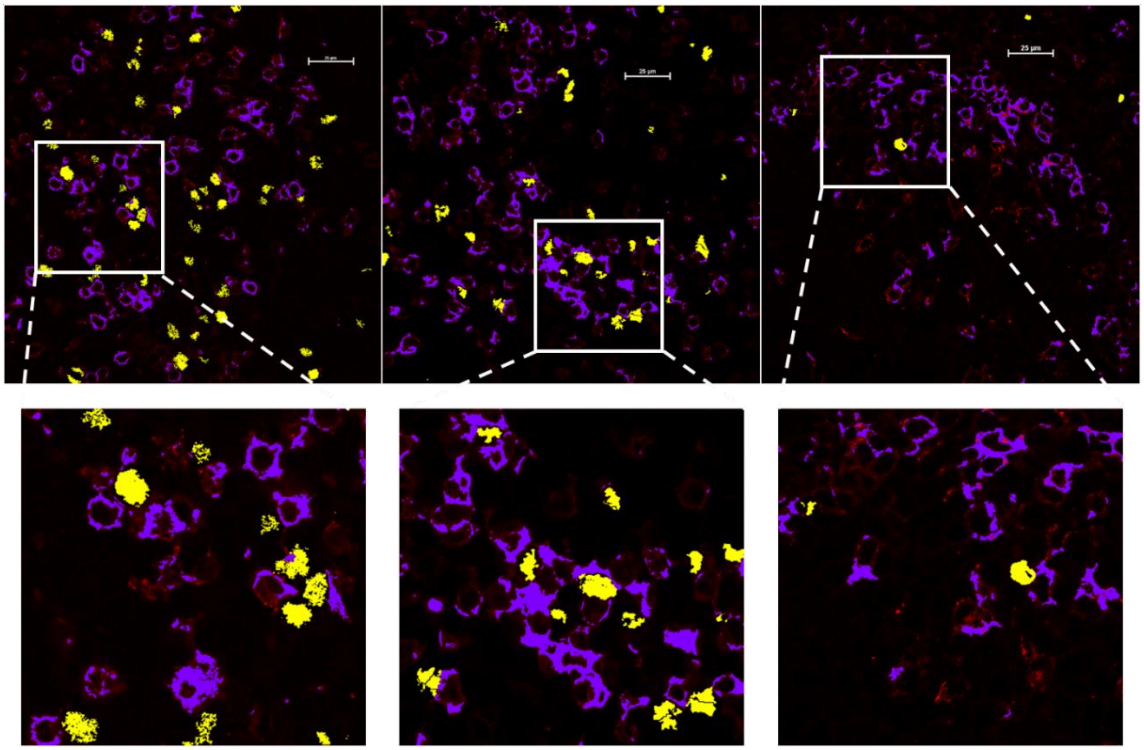

Figure 5.4. Spatial interaction between T_{FH} and MYC^+ B-cells. *High-power images (x60 objective) of FL tissue show close contact between MYC^+Pax5^+ B-cells (yellow) and $CD4^+PD\text{-}1^{hi}$ T_{FH} (purple). These representative images, taken from 3 patients with poor-risk (left) and good-risk FL (centre and right), also highlight interpatient variation in MYC expression.*

MYC expression was extremely variable in both good-risk and poor-risk FL tissue (Figure 5.2 & 5.4). As a result, there was no correlation seen between the number of T_{FH} and number of MYC^+ B-cells, assessed by quantifying the areas of the PD-1/CD4 and Pax5/MYC intersections, respectively (r=0.17, p=0.27; Figure 5.5B). This suggests that other factors may limit MYC expression. Indeed, in reactive LN tissue, both BCR and CD40L signalling are required to upregulate MYC, therefore it is likely that additional stimulation is also required in FL B-cells (Luo*, et al* 2018).

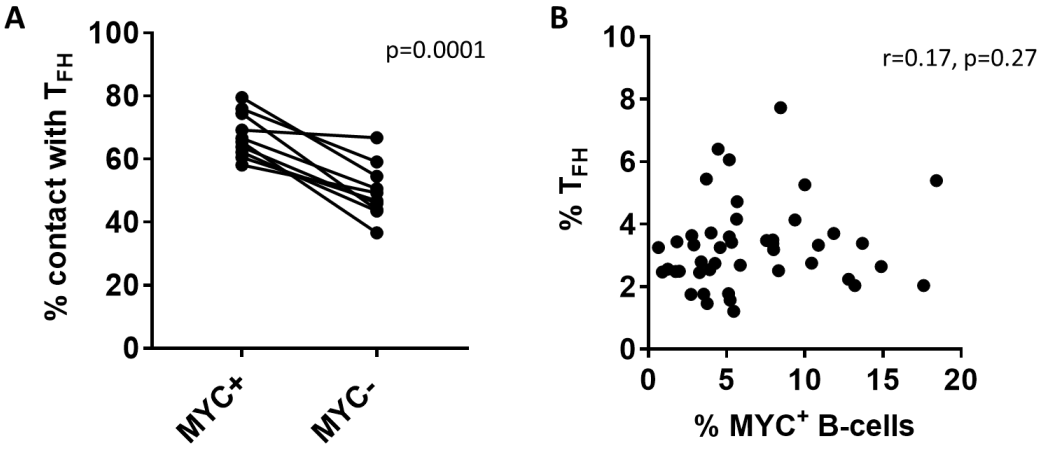

Figure 5.5. Relationship between T_{FH} and MYC expression. ***A)*** *Graph compares the proportion of MYC^+ and MYC^- B-cells that were in direct contact with $CD4^+PD\text{-}1^{hi}$ T_{FH} in FL tissue (N=10).* ***B)*** *Graph shows the correlation between the number of MYC-expressing B-cells (x axis) and T_{FH} (y axis), quantified according the areas of the Pax5/MYC and CD4/PD-1 binary layers, respectively. N=50 images from 10 patients.*

5.3.2. Discussion

These findings correlate with our knowledge of MYC expression in healthy GCs and suggest that T_{FH} can also enhance MYC expression in FL B-cells. This provides a further potential mechanistic link between T_{FH} and FL growth and proliferation. There was evidence of a strong spatial link between T_{FH} and MYC expression, even if it is not clear whether there is a correlation between number of T_{FH} and MYC^+ cells. These novel findings are therefore hypothesis-generating and require further validation.

The strength of the MYC signal by CIFM was generally weak, requiring fairly high laser power settings, and only just above background in some samples. Given that background autofluorescence was variable, it is possible that weak MYC expression may have been missed in samples with higher background staining. Other, more sensitive techniques are required to validate these results, such as RT-PCR or flow cytometry.

Visual assessment and cell counting can be open to observer bias. A repeat cell count, performed by a second, independent observer, would have strengthened these analyses, with hindsight. However, the close correlation between visual counts and automated assessment of MYC expression, and similarity with other FL studies (Aukema*, et al* 2017), both validate the analysis techniques used. Cell counting was, however, time consuming and is not suitable for assessing large numbers of samples. However, moving forward, it is potentially feasible to

automate all parts of this analysis. This would involve more complex algorithms, multiple software packages and rigorous validation, all of which were outside of the scope of this exploratory work.

A larger sample size would be necessary to fully assess whether there is any correlation between T_{FH} number and MYC expression, for example. However, *in vitro* studies are likely to provide more information than expanding sample numbers in this study. The next step should be to determine whether T_{FH} alone can increase MYC expression in FL B-cells in co-culture studies. Such experiments were not possible here due to the limited availability of fresh LN tissue and time restraints but are an important direction of future study.

5.4. Regulatory T-cells and T_{FH}

5.4.1. Results

The aim of this section is to assess whether the balance between T_{FH} and intrafollicular regulatory T-cells (including T_{FR} and other T_{regs}), both in terms of cell numbers and cell-to-cell contact, influences the clinical phenotype of FL.

A 4-colour panel was used to assess expression of PD-1, ICOS, FoxP3 and CD3 (see Figure 5.6). The combination of available primary antibodies did not allow for incorporation of CD4 into the same panel. CD3 was used instead, although on the blue channel (Dylight 405), where there were high levels of background fluorescence, therefore it was not used as part of the final analysis. T_{FH} were identified as PD-$1^{hi}$$ICOS^{+}$$FoxP3^{-}$ cells; our group has previously demonstrated that the vast majority of these represent true $CD4^{+}$ T_{FH} using the same methodology (Townsend*, et al* 2019). The threshold for high PD-1 expression was set at a level that excluded the majority of extrafollicular PD-1 expression (Figure 2.6). T_{FR} were classified as PD-$1^{hi}$$ICOS^{+}$$FoxP3^{+}$ cells. T_{regs} were identified using FoxP3 expression alone. In separate experiments, we confirmed that 96.2 ± 0.6% of these were indeed $CD4^{+}CD8^{-}$ T-cells (N=24 images, from 6 patients; Figure 5.7).

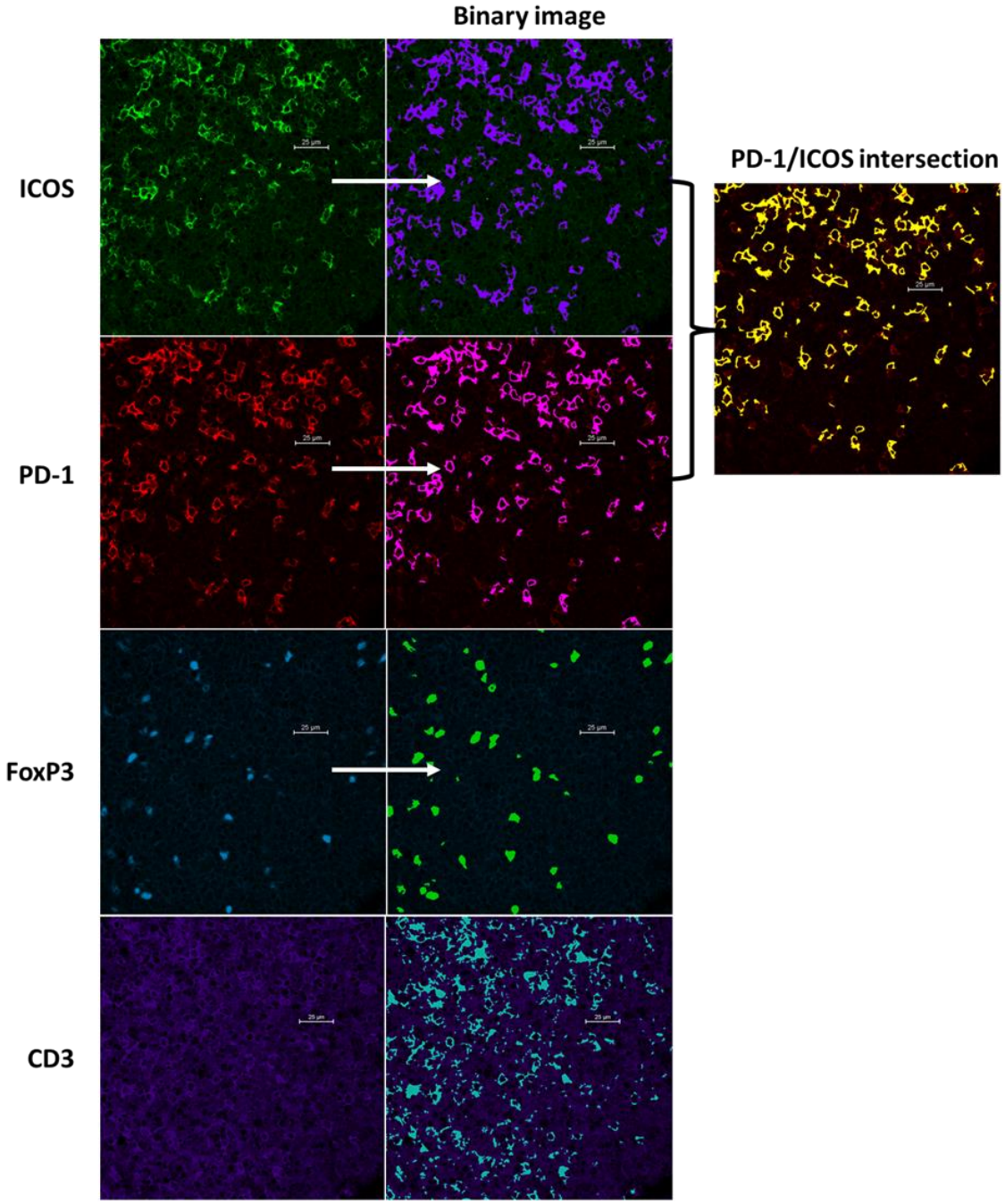

Figure 5.6. Immunofluorescence panel for visualisation of T_{FH} and T_{regs}. *Representative high-power (x60 objective) CIFM images show expression of ICOS (green), PD-1 (red), FoxP3 (blue) and CD3 (purple) in FFPE FL tissue. Scale bars measure 25µm. Right-handed panels show binary images defining expression of each individual antigen. Due to high levels of background fluorescence, it was not possible to form an accurate binary layer for CD3. The intersection of the ICOS and PD-1 binary layers (far right, yellow) was used to identify T_{FH} and T_{FR}.*

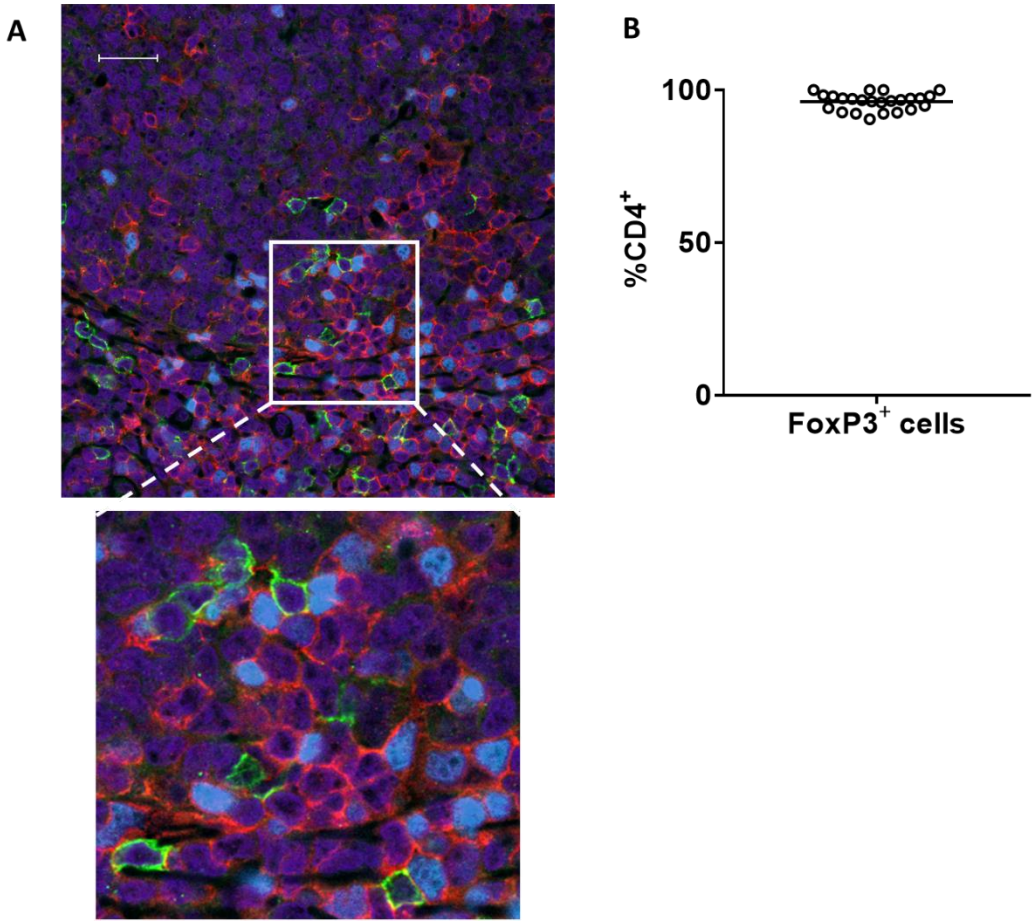

Figure 5.7. FoxP3⁺ cells are CD4⁺ T-cells. ***A)*** *Representative images show FoxP3 (blue), CD4 (x) and CD8 (y) expression in FL tissue. Almost all FoxP3+ cells are seen to co-express CD4 but not CD8.* ***B)*** *Graph shows the proportion of FoxP3⁺ T-cells that were CD4⁺ (N=24 images, from 6 patients). Horizontal bar represents mean value.*

T_{FH} localised almost exclusively to intra- and peri-follicular areas, whilst FoxP3⁺ Tregs were predominantly inter- or peri-follicular (Figure 5.8). Given that the aim was to assess the regulation of T_{FH} activity, this analysis focussed solely on the composition of T-cells in intra- and peri-follicular T-cells. A 'region of interest' was set for each image that excluded extrafollicular T-cells more than 25µm away from T_{FH} and the follicular border (Figure 5.9A).

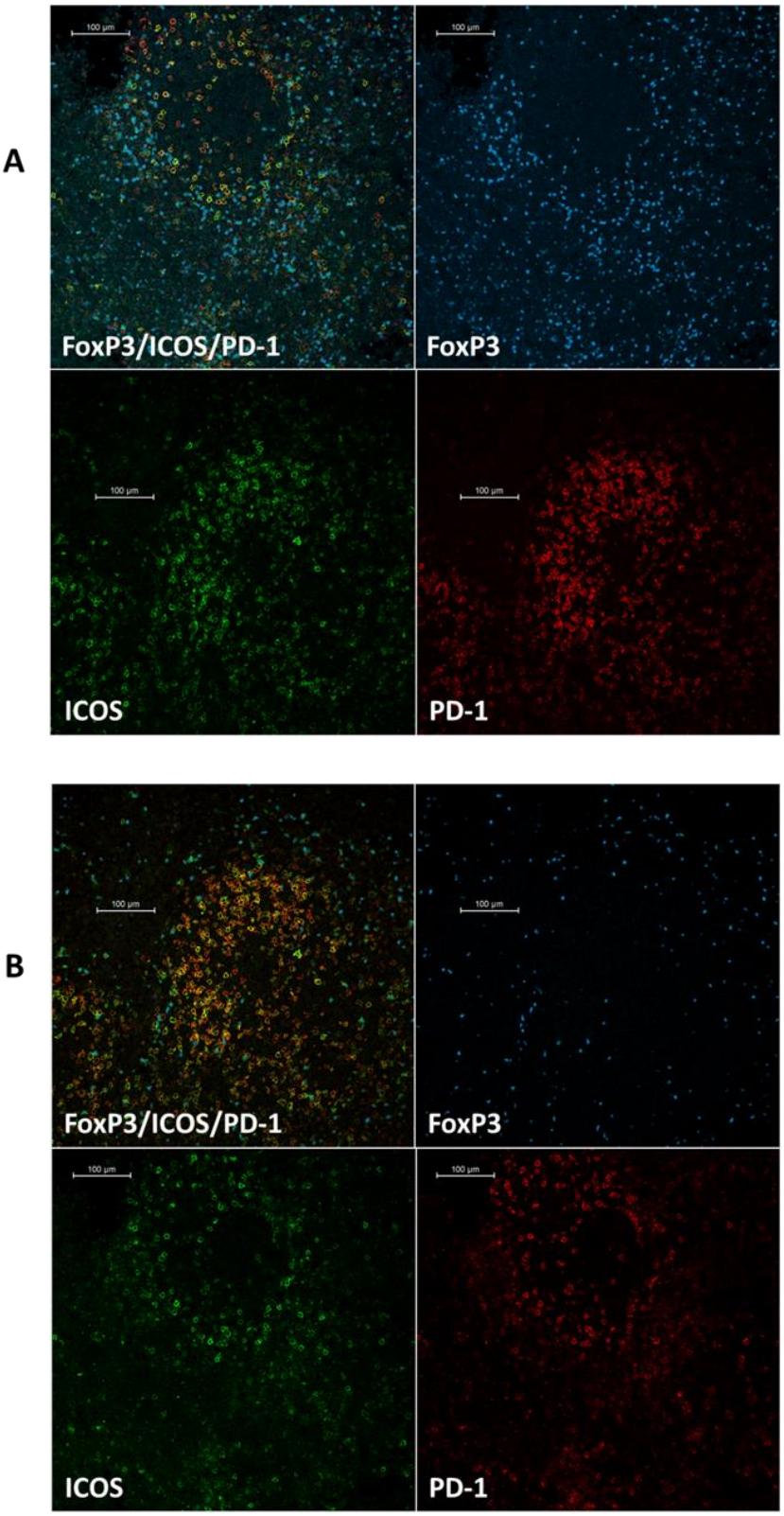

Figure 5.8. Distribution of T_{FH} and T_{regs} in FL tissue. *Representative low-power (x20 objective) CIFM images show the distribution of FoxP3 (blue), ICOS (green) and PD-1 expression (red) in FL LN tissue:* ***A)*** *predominantly perifollicular distribution of FoxP3 and* ***B)*** *Interfollicular FoxP3 expression. Scale bars measure 100µm.*

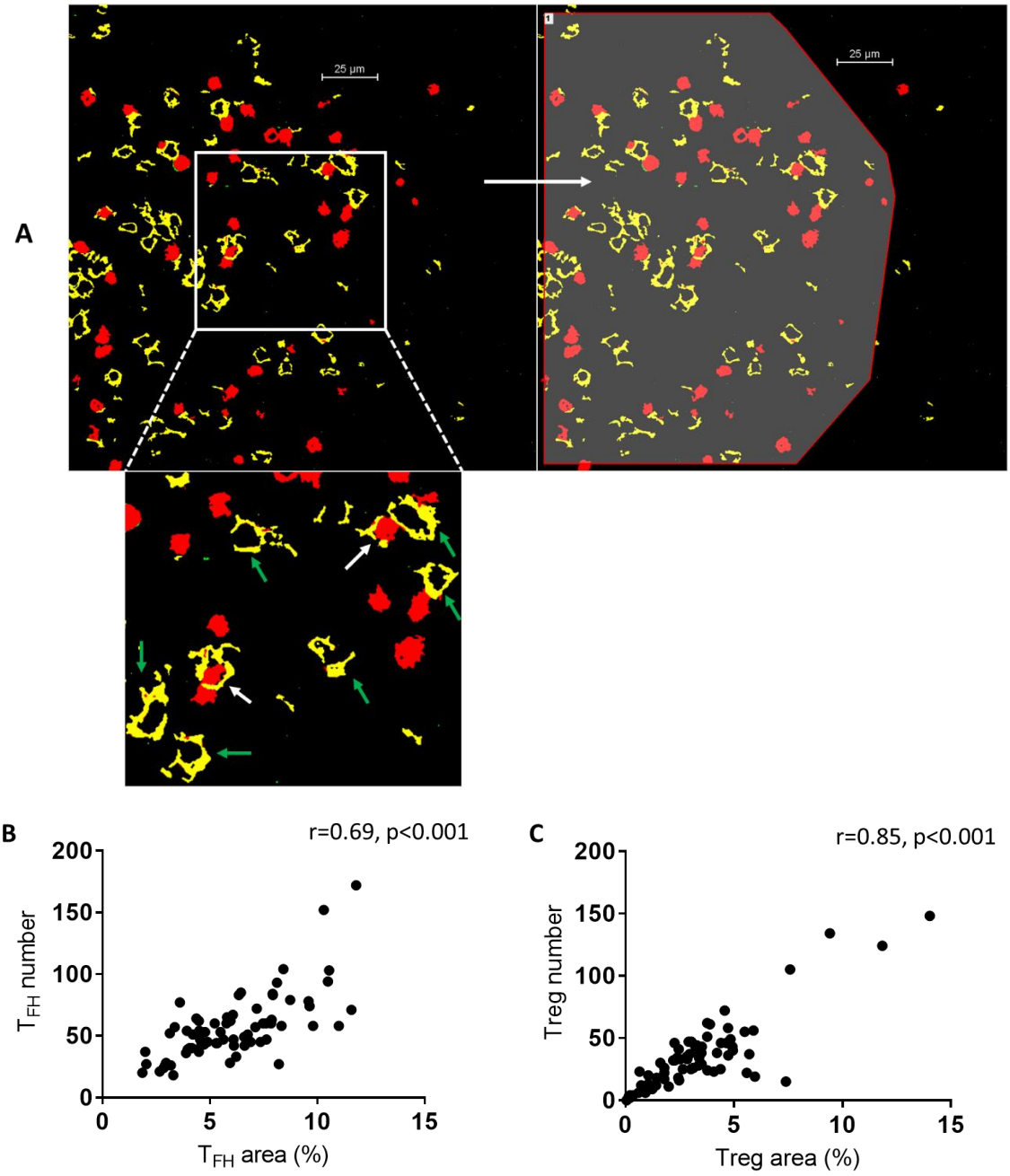

Figure 5.9. Correlation between T_{FH} and T_{FR} in FL tissue. A) *High-power image (x60 objective) of FL tissue shows binary layers representing PD-1/ICOS co-expression (yellow) and FoxP3 (red) at the periphery of an FL follicle. The expanded panel below demonstrates identification of FoxP3$^+$ T_{FR} (white arrows) and FoxP3$^-$ T_{FH} (green arrows), both with >50% circumferential PD-1/ICOS co-expression. The panel on the right shows the region of interest encircling the follicle used for both cell counting and semi-automated image analysis. Scale bars measure 25µm.* ***B)*** *Scatter plots show the correlation between cell quantification by absolute cell count and semi-automated analysis of binary layer area (expressed as a percentage of total area imaged) for PD-1^{hi}ICOS$^+$ cells and* ***C)*** *FoxP3$^+$ cells. N=72 images, from 12 patients.*

Two methods of analysis were used. Firstly, the number of T_{FH}, T_{FR} and T_{regs} were counted in each image. Cells were identified as T_{FH} and T_{FR} if more than 50% of the cell circumference was PD-$1^{hi}$$ICOS^{+}$ (Figure 5.9A). Although laborious and potentially open to observer bias, this was the most straightforward way to differentiate T_{FR} from T_{FH}. Secondly, the total areas of FoxP3 positivity and PD-1/ICOS co-expression were calculated from their respective binary layers by semi-automated image analysis, as a more objective, surrogate method of quantifying cell numbers. There was a strong correlation between the cell counts and semi-automated area analysis for measurement of both PD-$1^{hi}$$ICOS^{+}$ cells and FoxP3 expression (Figure 5.9B/C).

T_{FR} were infrequent in all 12 samples examined, comprising only 4.53 ± 1.47% of PD-$1^{hi}$$ICOS^{+}$ cells. This was very similar to findings with LN cell suspensions, where $FoxP3^{+}$ T_{regs} accounted for 7.38 ± 2.01% of PD-$1^{hi}$$ICOS^{+}$ T_{FH}-like cells by flow cytometry (N=8, p=0.21; Figure 5.10A), providing validation of the image analysis methods and cell counting. There was no detectable correlation between the number of T_{FH} and number of T_{FR} (N=12, r=-0.15, p=0.67), although the number of T_{FR} was small- 50% of images had 0-1 T_{FR} in total- so there was a relatively wide variation in T_{FR}:T_{FH} ratio due to only small differences in cell count.

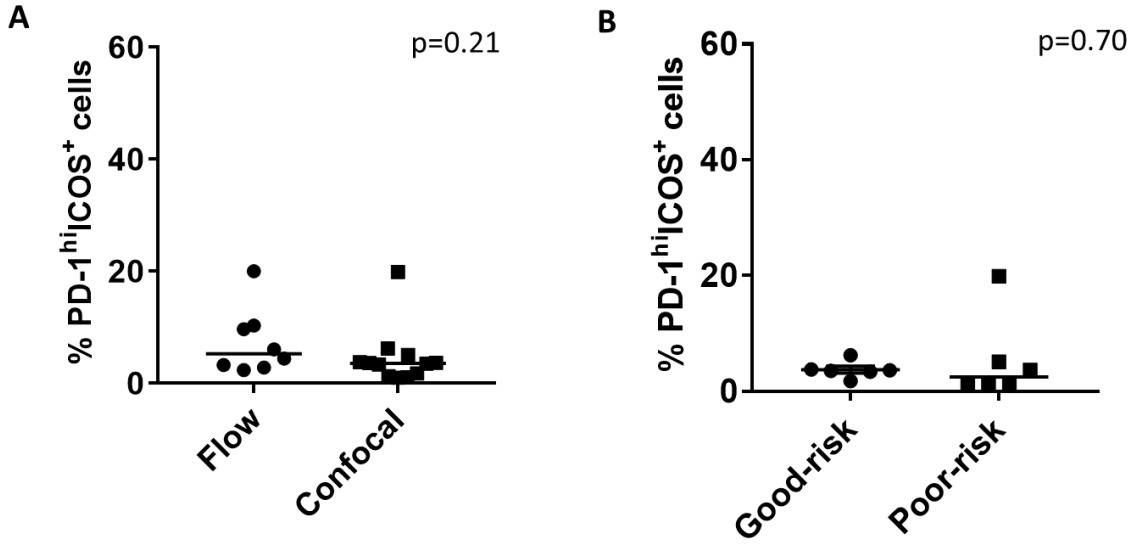

Figure 5.10. Correlation between T_{FR} and clinical outcomes in FL. ***A)*** *Graph shows the percentage of PD-$1^{hi}$$ICOS^{+}$ cells that expressed FoxP3, and thus had a T_{FR} phenotype, by both intracellular flow cytometry of FL LN cells suspensions (N=8) and CIFM of FL LN tissue (N=12).* ***B)*** *Graph compares the percentage of PD-$1^{hi}$$ICOS^{+}$ cells that had a $FoxP3^{+}$ T_{FR} phenotype in good-risk (N=6) and poor-risk FL (N=6).* ***C)*** *Graph compares the ratio of T_{FR}:T_{FH} between the same good-risk and poor-risk FL samples. Horizontal bars represent median values*

There was no detectable difference in the proportion of PD-1^{hi}ICOS^{+} T-cells that had a FoxP3^{+} T_{FR} phenotype between good- and poor-risk disease (Figure 5.10B), nor in the ratio of T_{FR}:T_{FH} (data not shown). Therefore, we were unable to detect any signal to suggest that there is a correlation between the balance of T_{FH}/T_{FR} and clinical phenotype in this small cohort. These data confirm the observations made in Chapter 3.3.5, that T_{FR} are rare in FL and therefore are unlikely to exert a dominant influence on FL phenotype.

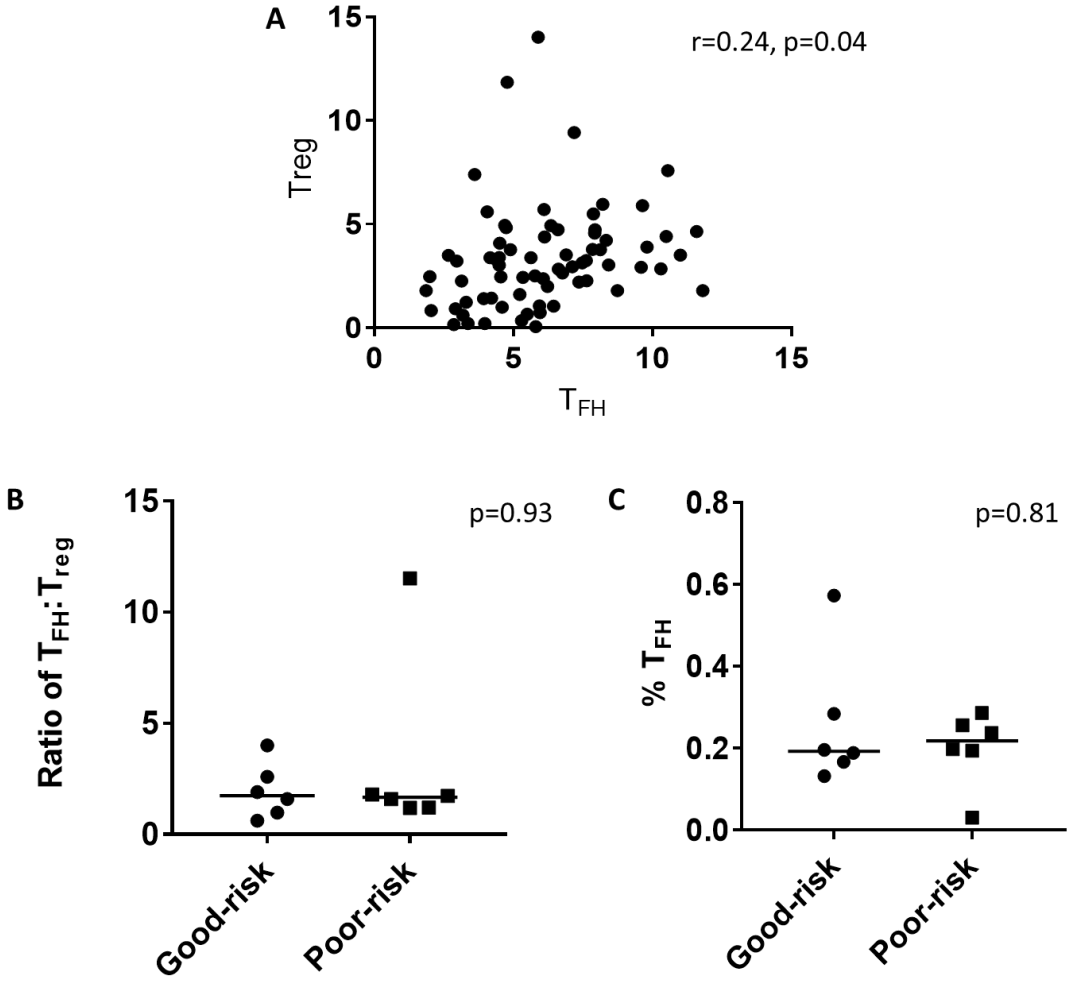

Figure 5.11. Clinical outcomes according to the balance between follicular T_{FH} and T_{reg}. A) *Scatter plot shows the correlation between the number of T_{FH} and T_{regs} in FL follicles, measured by the area of the FoxP3 and PD-1/ICOS binary layers, respectively. Results are expressed as a percentage of the total area analysed (N=72, from 12 patients).* ***B)*** *Graph compares the ratio of T_{FH}:T_{regs} in good-risk (N=6) and poor-risk FL (N=6).* ***C)*** *Graph shows the proportion of T_{FH} that were in direct contact with T_{regs} in good-risk (N=6) and poor-risk FL (N=6). Horizontal bars represent median values*

The majority of follicular regulatory T-cells were not T_{FR}; only 8.03 ± 2.15% of FoxP3$^+$ T-cells had a T_{FR} phenotype (N=12), suggesting that other T_{reg} subsets may have a greater influence on the TME within FL follicles. More than a fifth (22.89 ± 3.72%) of T_{FH} were seen to be in direct contact with FoxP3$^+$ Tregs, noting that this 2-dimensional analysis is likely to underestimate the extent of direct T_{FH}-T_{reg} interactions on a 3-dimensional level *in vivo*. There was only a weak correlation between the number of T_{reg} and T_{FH}, quantified according to the area of the FoxP3 and PD-1/ICOS binary layers, respectively (r=0.24, p=0.04; Figure 5.12A), therefore there was wide variation in the T_{FH}/T_{reg} ratio (median 1.67, range 0.62 – 11.52). However, we didn't find any evidence to suggest a relationship between the balance of T_{FH}/T_{reg} and clinical phenotype. There was no detectable difference in the ratio of T_{FH}:T_{regs} or in the proportion of T_{FH} that were in direct contact with T_{regs} between good- and poor-risk disease (Figure 5.11B-C).

5.4.2. Discussion

To our knowledge, this is the first study to explore the distribution and *in situ* interactions of T_{FR} in FL. These results demonstrate that T_{FR} represent a minority of both PD-1^{hi}ICOS$^+$ T-cells and suggest that follicular T_{regs} are unlikely to exert an influence on clinical phenotype. Whilst others have reported that T_{FR} are slightly more prevalent in FL than in reactive tonsillar tissue, they agree with our findings that T_{FR} are still represent a small minority of T-cells in FL (Tarte*, et al* 2017). Although T_{FR} are able to suppress T_{FH} activity *in vitro*, these experiments were performed by co-culture using supra-physiological ratios of T_{FR} and do not reflect *in vivo* conditions (Tarte*, et al* 2017). It is therefore unclear how much of a role T_{FR} have in regulating T_{FH} activity in FL.

Very little is known about the distribution and function of T_{FR} *in vivo*. Sayin *et al* recently explored the distribution of T_{FR} in reactive mesenteric lymphoid tissue and reported that most were located at the T:B-cell border, distant from reactive GCs (Sayin*, et al* 2018). The authors concluded that T_{FR} were unlikely to suppress GC T_{FH} activity directly *in vivo*, in agreement with our findings. However, the definition of T_{FR} in this recent study- according to CD3, CD25 and FoxP3 expression only- was questionable; whilst most 'T_{FR}' expressed CXCR5, only a minority expressed PD-1, at lower levels than PD-1^{hi} T_{FH}. Functionally, T_{FR} did not suppress T_{FH}-stimulated IgG production by GC B-cells *in vitro* to any greater extent that other T_{regs} (Sayin*, et al* 2018). Despite the limitations of this study, it is the first to explore the *in-situ* interactions of T_{FR} in human LNs and serves to highlight our lack of understanding of this rare T-cell subset.

Our analyses assume that all T_{FR} are PD-1^{hi}, which is contentious, as the definitions of T_{FR} vary between studies (Espeli and Linterman 2015, Sayin*, et al* 2018). However, FoxP3 is generally

considered to be a regulatory T-cell-defining marker and there was no suggestion of a link between clinical phenotype and the balance between T_{FH} and FoxP3-expressing T_{regs} either.

These were a number of factors that limited the ability to draw firm conclusions from the comparisons between good-risk and poor-risk disease, including sample size and patient heterogeneity. Over 80% of previously-untreated FL patients receiving frontline immunochemotherapy experience disease remission lasting more than 24 months, therefore are classified as good-risk disease by the definitions applied here (Casulo*, et al* 2015). It is therefore more difficult to obtain good-quality tissue from poor-risk FL patients, due to both the relative scarcity of poor-risk patients and the increasing preference for use of diagnostic needle core biopsy over whole LN excision. As a result, sample numbers were small, and the poor-risk population included a heterogeneous mix of treatment-naïve and relapsed FL. This illustrates the need to obtain tissue from larger biobanks with linked outcome data, ideally treated uniformly within the context of clinical trials. Nevertheless, this analysis was intended to be exploratory in nature and was not deemed to be worth pursuing, given the lack of any evidence to suggest that the balance between T-cell subsets was associated with clinical phenotype. To extend this work with CIFM would therefore require a much larger sample number and would only be feasible with further automation of image analysis.

This analysis does not consider other factors that potentially regulate T_{FH} activity in FL. In particular, PD-1 ligands are likely to play a key role in T_{FH} homeostasis, given that uniquely high levels of PD-1 expression define T_{FH} (Crotty 2014). Gene expression profiling suggests that PD-L2 expression is more strongly linked with prognosis than PD-L1, although both are expressed within the FL TME (Laurent*, et al* 2015, Myklebust*, et al* 2013, Tobin*, et al* 2019). We hoped to explore this further, but it was not possible to find an effective, commercially available anti-PD-L2 antibody, despite trialling multiple different antigen retrieval conditions, blocking methods and primary antibody concentrations. To fully explore the cumulative relevance of multiple such competing pro- and anti-tumour factors in the FL TME will require highly-multiplexed data analysis techniques, that incorporate more parameters than can be assessed by standard CIFM. Alternative imaging methods are required to facilitate such analyses; imaging mass cytometry is one example and is the focus of the following chapter.

CHAPTER 6: IMAGING MASS CYTOMETRY AS A TOOL TO EXPLORE THE FOLLICULAR LYMPHOMA TUMOUR MICROENVIRONMENT

6.1. Introduction

Multiple studies have established that the composition of the FL TME correlates with prognosis, but it has not yet been determined which cell subsets are responsible for this observation (Ame-Thomas and Tarte 2014, Dave*, et al* 2004, Tobin*, et al* 2019). Many of these findings are derived from tumour gene expression profiling, where cellular and spatial information is lost. A large number of IHC studies have attempted to link single cell markers with prognosis, but these studies lack the ability to identify complex cell subsets within the FL TME (Ame-Thomas and Tarte 2014). The clinical phenotype of FL is likely to reflect the net effect of multiple interactions between FL B-cells and various non-malignant cells. Therefore, to fully characterise T_{FH} and their interactions within the TME requires multiplexed assessment of FL tissue.

CIFM produces high-resolution images and can facilitate semi-automated analysis of antigen expression within FFPE tissue. However, a number of factors limit the ability of CIFM to assess multiple antigens simultaneously, and thus explore interactions between complex cell subtypes within the TME. Firstly, the CIFM technique described in the previous chapter is reliant on the use of fluorescent anti-species secondary antibodies to amplify antigen signal. The majority of primary antibodies are raised in either mice or rabbits, with limited availability of goat- and rat-derived antibodies. Choice of primary antibody is therefore restricted by species diversity and it was not possible to use more than 4 different antibodies simultaneously. Ideally, 2-3 of these are required to identify T_{FH} alone. In order to increase the repertoire of antigens studied, other researchers within our institution have attempted to use directly fluorochrome-conjugated primary antibodies but found that image quality was poor without signal amplification. In addition, although the confocal microscope can in theory assess up to 6 distinct fluorochromes simultaneously, this will only increase the potential for background staining, spectral overlap and the complexity of image analysis.

Imaging mass cytometry (IMC) is an imaging technique that can overcome many of the limitations of CIFM by enabling simultaneous assessment of more than 32 antigens (Giesen*, et al* 2014). The technique relies on staining of tissue with metal-conjugated primary antibodies, principally using stable lanthanide metal isotopes that are not present within the normal environment. The presence of these isotopes is detected by mass spectrometry and used to construct 2-dimensional images of antigen expression (Figure 6.1).

The aim of this chapter was to investigate the feasibility and utility of this novel imaging technique for highly multiplexed assessment of the TME in FL. This work focuses primarily on development and validation of IMC methodology.

The main objectives were:

1. To assess whether it is possible to assess >15 antigens simultaneously in FL tissue by IMC
2. To assess whether T_{FH} can be identified by IMC
3. To develop an automated pipeline for image analysis, that can be used to investigate cellular networks within the FL TME
4. To investigate whether IMC can replicate the findings of other tissue imaging studies

This work aims to provide proof of principle for future projects that will explore the prognostic influence of cellular networks within the FL TME, after completion of this thesis.

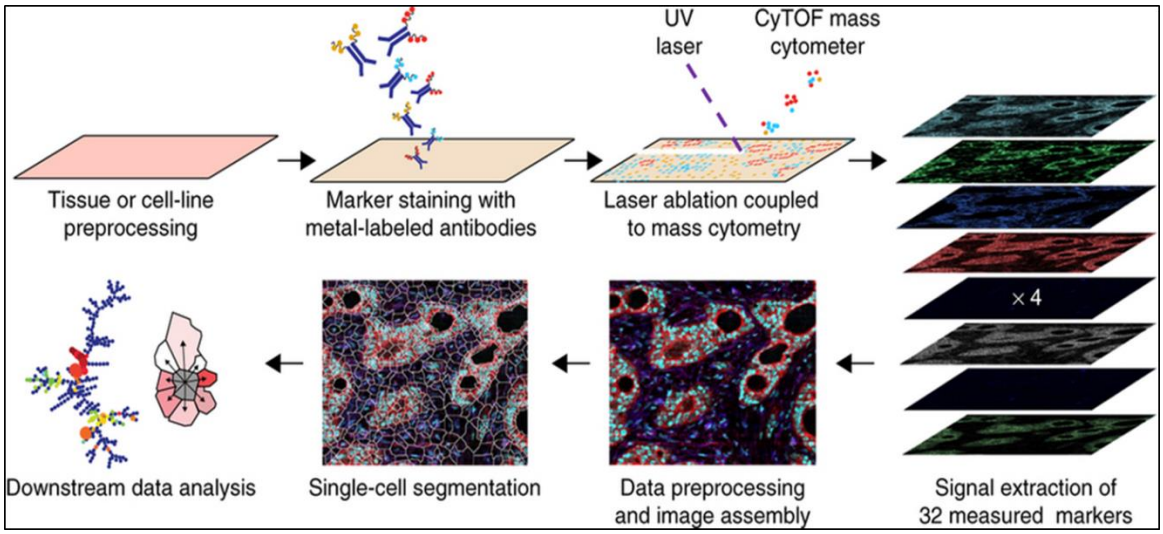

Figure 6.1. Overview of Imaging Mass Cytometry. *Image summarises the pathway for highly-mutliplexed spatial assessment of cell subsets in tissue sections. Reprinted by permission from Springer Nature: Highly multiplexed imaging of tumor tissues with subcellular resolution by mass cytometry, Giesen et al, Nature Methods 2014;11:417–422 ©.*

6.2. Methods

6.2.1. Tissue Processing and Primary Antibody Staining

Protocols for tissue deparaffinisation, antigen retrieval and tissue staining were developed by Drs Katrina Todd and Richard Ellis at the Biomedical Research Council Flow Core at Guy's

Hospital, London, and were adapted from published Fluidigm tissue processing protocols (California, USA). In brief, tissue sections were cut to a thickness of 5µm and floated onto Superfrost Plus slides (Thermofisher). Tissue was deparaffinised in 2 changes of 100% xylene, followed by 50% xylene/50% ethanol, for 10 minutes each. Samples were then rehydrated through graded ethanol solutions (96%, 90%, 80% and 70%) for 5 minutes each, then transferred to Dulbecco's PBS (DPBS; Thermofisher). Antigen retrieval was performed in pre-warmed Antigen Retrieval Solution pH 9.0 (R&D Systems, Minneapolis, USA) in a 96°C water bath for 30 minutes. Tissue was blocked using Superblock solution (Thermofisher) containing 5% BSA and 5% Trustain FcR Block (Biolegend) for 2 hours.

Table 6.1. List of metal-conjugated antibodies for IMC. *cCasp3: cleaved caspase-3. *Indicates antibody not included in final antibody panel due to poor staining characteristics.*

Channel	Element	Target	Clone	Concentration	Manufacturer
141	Pr	**AID***	ZA001	1:50	Fisher Scientific
142	Nd	**Pax5**	1H9	1:50	Biolegend
143	Nd	**PD-L2***	176611	1:100	Fisher Scientific
146	Nd	**BCL2**	EPR17509	1:200	Fluidigm
147	Sm	**BCL6**	K11291	1:50	Fisher Scientific
148	Nd	**ICOS**	D1KT	1:50	New England Biolabs
150	Nd	**PD-L1**	130021	1:75	R&D Systems
151	Eu	**CD31**	Polyclonal	1:400	Abcam
153	Eu	**CD16**	EPR16784	1:400	Abcam
154	Sm	**Tim3**	D5D5R	1:100	Fluidigm
155	Gd	**FoxP3**	236A/E7	1:50	Fisher Scientific
156	Gd	**CD4**	EPR6855	1:100	Abcam
158	Gd	**pSTAT3***	4/P-STAT3	1:50	Fluiidigm
159	Tb	**CD68**	KP1	1:800	Fluidigm
161	Dy	**CD20**	H1	1:500	Fluidigm
162	Dy	**CD8**	C8/144B	1:800	Fluidigm
164	Dy	**CD21**	EP3093	1:1000	Abcam
166	Er	**PD-1**	EPR4877(2)	1:50	Abcam
168	Er	**Ki67**	B56	1:500	Fluidigm
170	Er	**CD3**	Polyclonal	1:400	Fluidigm
172	Yb	**cCasp3**	5A1E	1:100	Fluidigm
174	Yb	**CD74**	LN2	1:200	Biolegend
175	Lu	**MYC***	Y69	1:50	Abcam
176	Yb	**Tbet**	4B10	1:50	Biolegend
191/193	Ir	**DNA**	N/A	1:250	Fluidigm

Metal-conjugated primary antibodies (initial protein concentration 0.5mg/ml) were diluted to the desired concentration (see Table 6.1) in the same blocking solution, applied to the tissue section and incubated overnight at 4°C. Tissue sections were washed in DPBS containing 0.1% Tween surfactant. Iridium was diluted to a concentration of 2μM in distilled water and applied to tissue sections for 30 minutes. Slides were washed in DPBS and water, then air-dried for at least 24h. Slides are stable at this point and can be imaged at any point from days to months in the future. It is also possible to return to stained sections and ablate additional areas.

To avoid non-specific background staining, it was important to avoid any heavy metal contamination at any stage during tissue processing, therefore ultrapure water was obtained through a Milli-Q Purification System (Merck Millipore, Massachusetts, USA) and, at all stages, dedicated plastic/glassware was used that had not come into contact with detergent or other unknown chemicals.

6.2.2. Antibody Selection, Optimisation and Panel Design

Most isotope-conjugated primary antibodies were purchased directly from Fluidigm and had already been validated for use in FFPE tissue. Alternatively, protein-free primary antibodies were conjugated to selected metal isotopes using the Maxpar Antibody Labelling Kit (Fluidigm) according to manufacturer's instructions by Dr Cynthia Bishop at the Biomedical Research Council (BRC) Flow Core at Guy's Hospital, London. These antibodies were validated by IHC, using the both conjugated and unconjugated forms of the primary antibody, to ensure that metal conjugation had not altered staining characteristics (Figure 6.2). A list of antigens, antibody clones and corresponding metal isotopes is provided in Table 6.1.

Most antibodies were initially trialled at dilutions of 1:100 and 1:400 (or 1:250 and 1:1000 for certain strong antigens) on both FL tissue and reactive LN, and concentrations adjusted for subsequent experiments on the basis of the results.

There are 2 main sources of overlap between detection channels in IMC (Chevrier*, et al* 2018). Firstly, if an antigen and isotope are very abundant, there may be some carryover into immediately adjacent detection channels by time-of-flight, although, in practice we did not observe this, even with strong antigens. Secondly, there is variation in the purity of different metal isotopes. This is an important consideration when using multiple isotopes of the same element but is predictable and quantifiable: for example, neodynium-143 contains 2.2% neodymium-144 (Table 6.2). Selection of metal isotopes was therefore dependent on: a) the expected abundance of target antigen and b) purity of the metal isotope. Antigens with

significant overlap in expression, such as CD3 and CD4, were not placed next to each other so it was easy to visually assess if significant spill over was occurring. We also used a smaller number of antibodies (maximum 22 simultaneously) than the number of available channels (35), so that channels could be left vacant where spill over was predicted to occur. Finally, compensation algorithms developed by the BRC Flow Core were applied during image analysis to remove crosstalk between channels. Unlike liquid mass cytometry, IMC is performed in a dry atmosphere where metal oxidation does not occur.

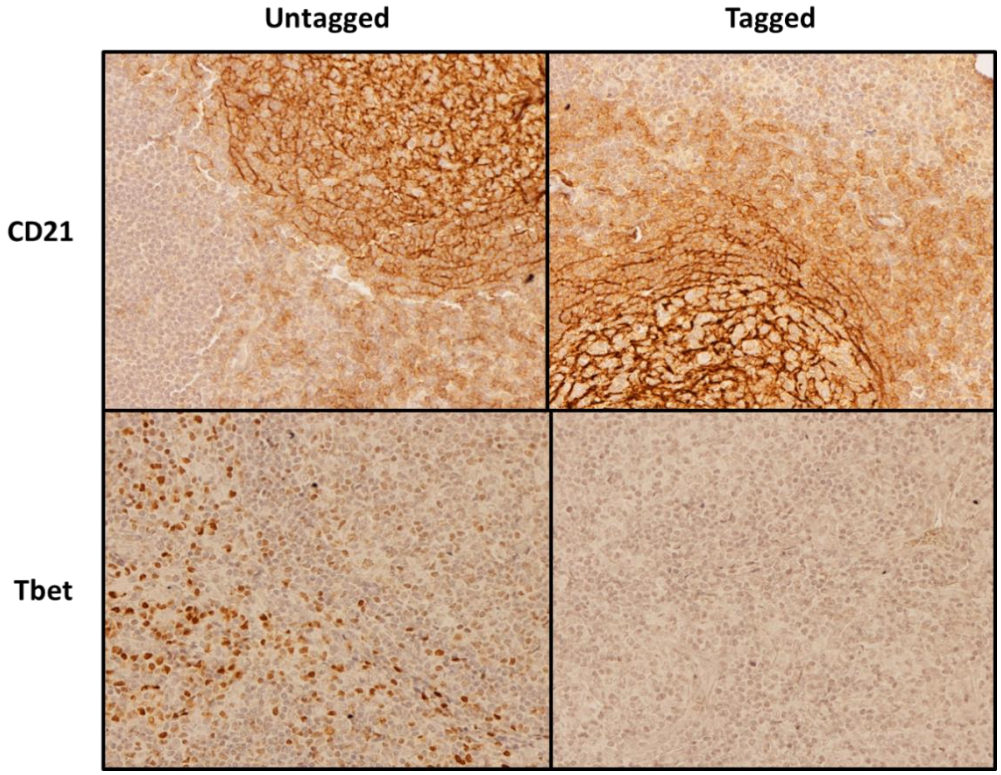

Figure 6.2. Antibody validation after metal tagging. *Images show assessment of antigen expression in reactive LN tissue by IHC using metal-tagged (right) and untagged (left) primary antibodies from the same clone and batch (x20 objective lens). CD21 staining (top) is not altered by antibody tagging, whilst Tbet staining (EPR9302, Abcam; bottom) is lost, presumably due to disruption of the binding epitope. An alternative Tbet clone (4B10, Fluidigm) was used for subsequent experiments.*

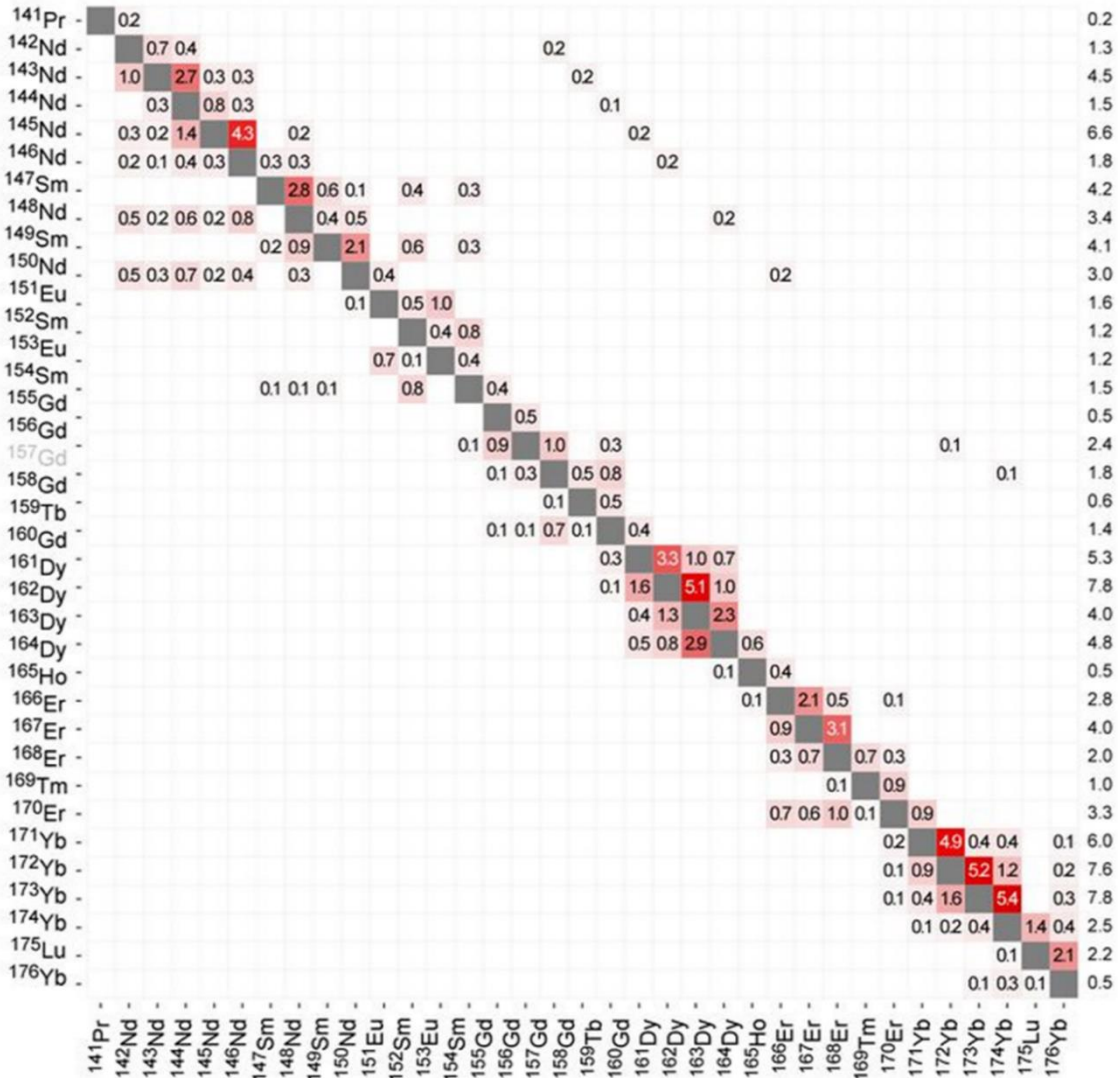

Table 6.2. Metal isotope purity matrix. *Table shows the percentage spillover for each metal isotype (x axis) and the amount of signal it contributes to adjacent channels (y axis). The total amount of spillover received for each channel is quantified in the right-hand column. Image from Chevrier et al., 2018, Cell Systems 6, 612–620 (Elsevier Inc.), DOI: 10.1016/j.cels.2018.02.010*

6.2.3. Controls

Control slides were not used for most IMC experiments for several reasons. Firstly, secondary antibodies are not used for IMC, thereby eliminating a major potential source of non-specific background staining. Secondly, there is significantly less overlap between mass cytometry channels than there is with immunofluorescence (Chevrier*, et al* 2018). The main sources of overlap between channels in IMC are predictable, quantifiable and can be mitigated by panel design. Thirdly, there should be no natural background signal with the lanthanide metal isotopes used. Cost and resource use were also important considerations, which are significantly higher with IMC than with CIFM or IHC. Therefore, IHC was used where antibody testing and validation

were required. Initially, sections of reactive LN tissue were stained alongside FL tissue as a positive control to ensure equivalent staining patterns in both tissues.

6.2.3. Image Acquisition and Analysis

Images were acquired on a Hyperion imaging mass cytometer (Fluidigm), operated by Dr Richard Ellis at the BRC Flow Core. Samples were first imaged by light microscopy to select an area for imaging with a clear follicular structure. IMC slides were placed within a pressurised imaging chamber. The tissue was ablated in 1μm^2 areas by laser beam to produce an aerosolised plume of tissue. Flow of argon gas within the chamber directs the plume through inductively-couple plasma to atomise and ionise the constituents, which are then detected according to time-of-flight by a mass cytometer. A total area of 1mm^2 was ablated, with an acquisition time of 2 hours, for each tissue section.

Raw image files were viewed and exported using MCD Viewer software version 1 (Fluidigm). Subsequent image analysis was principally performed by Dr Nedyalko Petrov and Dr Filomena Spada at the BRC Flow Core, using a mixture of in-house tools and commercial image analysis tools. After applying in-house compensation algorithms, image stacks were transferred to CellProfiler software (Broad Institute, Massachusetts, USA), where artefactual 'hot' pixels with aberrant signal were removed (Figure 6.3A). Images were then transferred to Ilastik software (Berg*, et al* 2019), where the pixel classification tool used machine learning to generate a probability map for expression of each marker (Figure 6.3B). These outputs were then exported back into CellProfiler, where the probability value for each pixel was attributed to the original object and used to generate segmentation masks to identify cells as single objects (Figure 6.3C). Data on cell number and area were extracted directly at this point. Distances between different cell types were calculated using Matlab software (MathWorks, Massachusetts, USA).

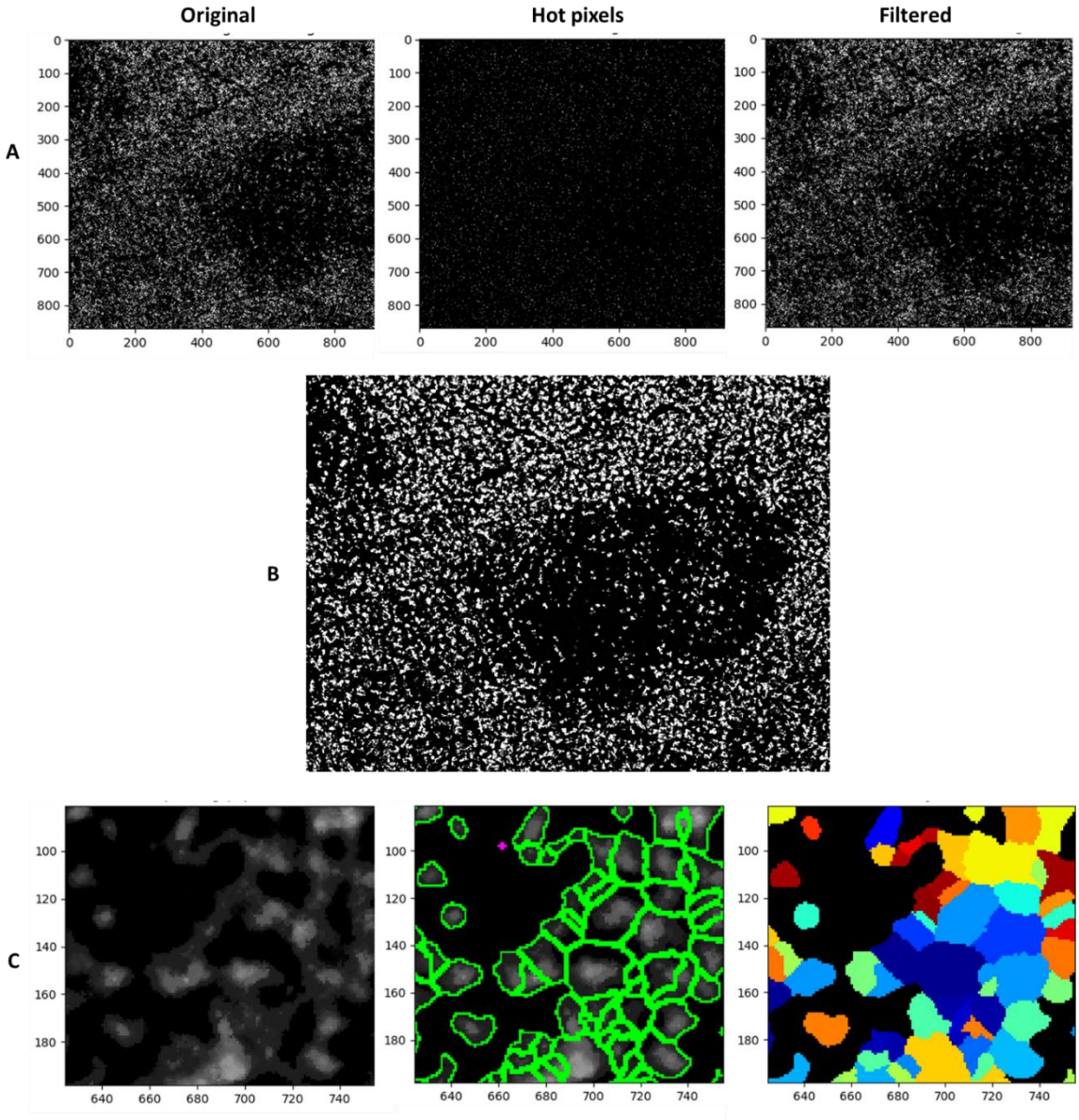

Figure 6.3. Imaging Mass Cytometry analysis and cell segmentation. A) *Representative images of FL tissue show original output for CD3 expression (left). Using CellProfiler image analysis software, aberrant hot pixels were filtered out (centre panel) to produce a clean image for CD3 (right).* ***B)*** *Filtered images were then used to generate a probability map for CD3 expression using Ilastik software.* ***C)*** *The same probability map was applied to the original images in CellProfiler software, where image contours were smoothed (left panel). Membrane CD3 staining was used to produce a cell segmentation mask (binary layer, green; centre panel), which facilitated automated cell segmentation and CD3⁺ object identification (right; colours demonstrate segregation of cellular objects). Axes show distance in µm.*

6.3. Results

6.3.1. Multiparameter Assessment of FL Tissue and Identification of T_{FH}

The same 12 FFPE FL tissue sections were stained as detailed in Section 5.2, from extremes of clinical outcome, allowing for comparison of IMC and CIFM results. These samples had already been well characterised and were known to have detectable T_{FH}.

The final panel included 20 antibodies, including markers of proliferation, activation and exhaustion, alongside basic lineage markers (Table 6.1 and Figure 6.4). Successful multiparameter imaging by IMC was possible in all 12 tissue samples to a maximum resolution of 1µm (Figure 6.4). The brightest signal was seen for membranous lineage markers, such as CD3, CD20, CD31 and CD68. The signal for most nuclear antigens, such as FoxP3, Pax5, BCL6 and Tbet was weaker. Without a secondary antibody amplification step, several weak antigens that were identifiable by IHC and CIFM, were not detectable by IMC, including MYC, AID and phospho-STAT3 (data not shown). The PD-1 signal was also weak but was detectable within follicular regions by IMC. The distribution and pattern of PD-1 expression suggests that only follicular PD-1^{hi} cells, i.e. T_{FH}, were identified, but not other PD-1-expressing cells (Figure 6.5). In one FL sample, it was not possible to identify true PD-1 expression above levels of background staining; this sample has been excluded from these analyses.

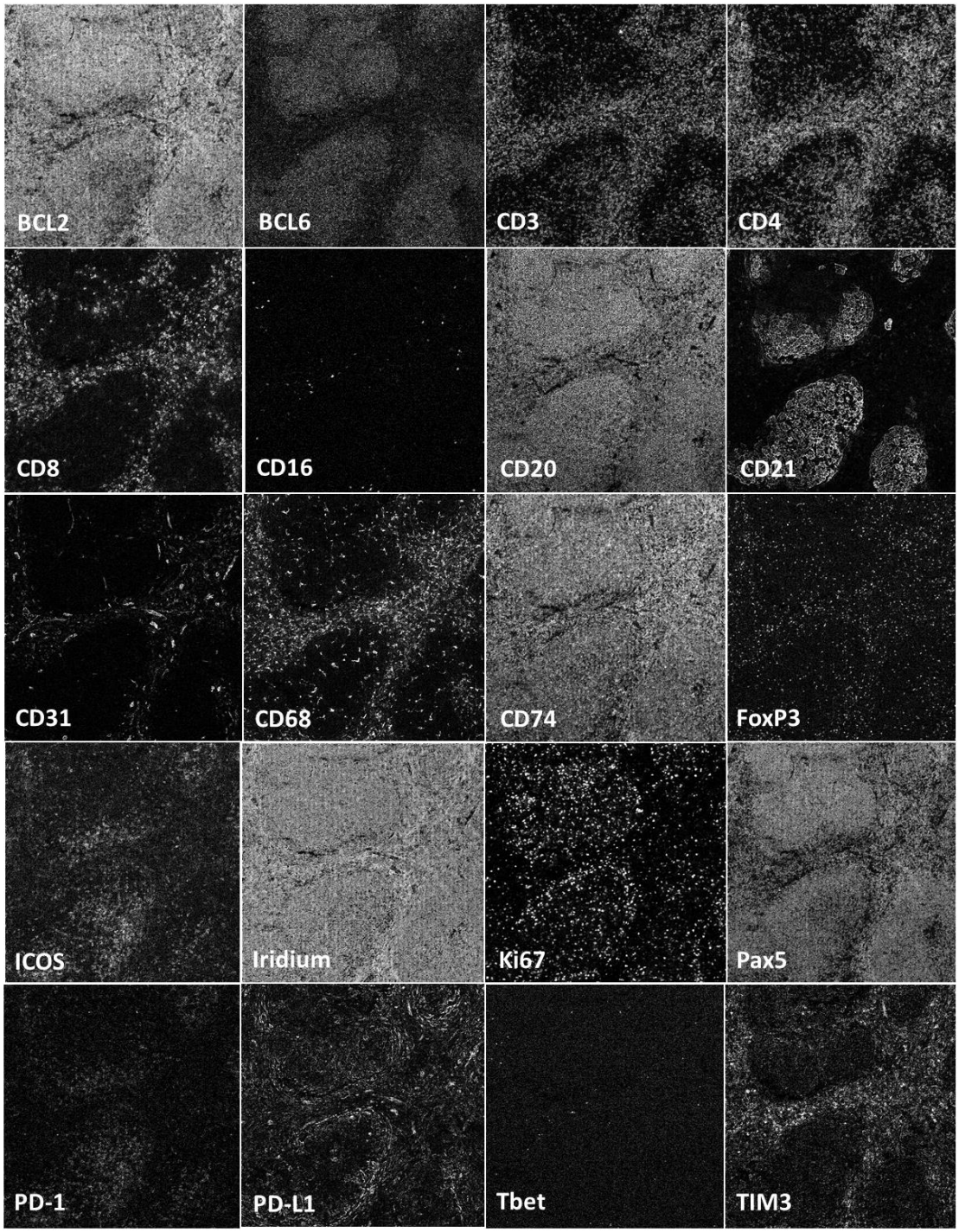

Figure 6.4. Multiparameter assessment of FL tissue by IMC. *Figure shows unmanipulated images of 20 tissue markers obtained simultaneously from the same FL tissue section by imaging mass cytometry. Images measure 1mm by 1mm.*

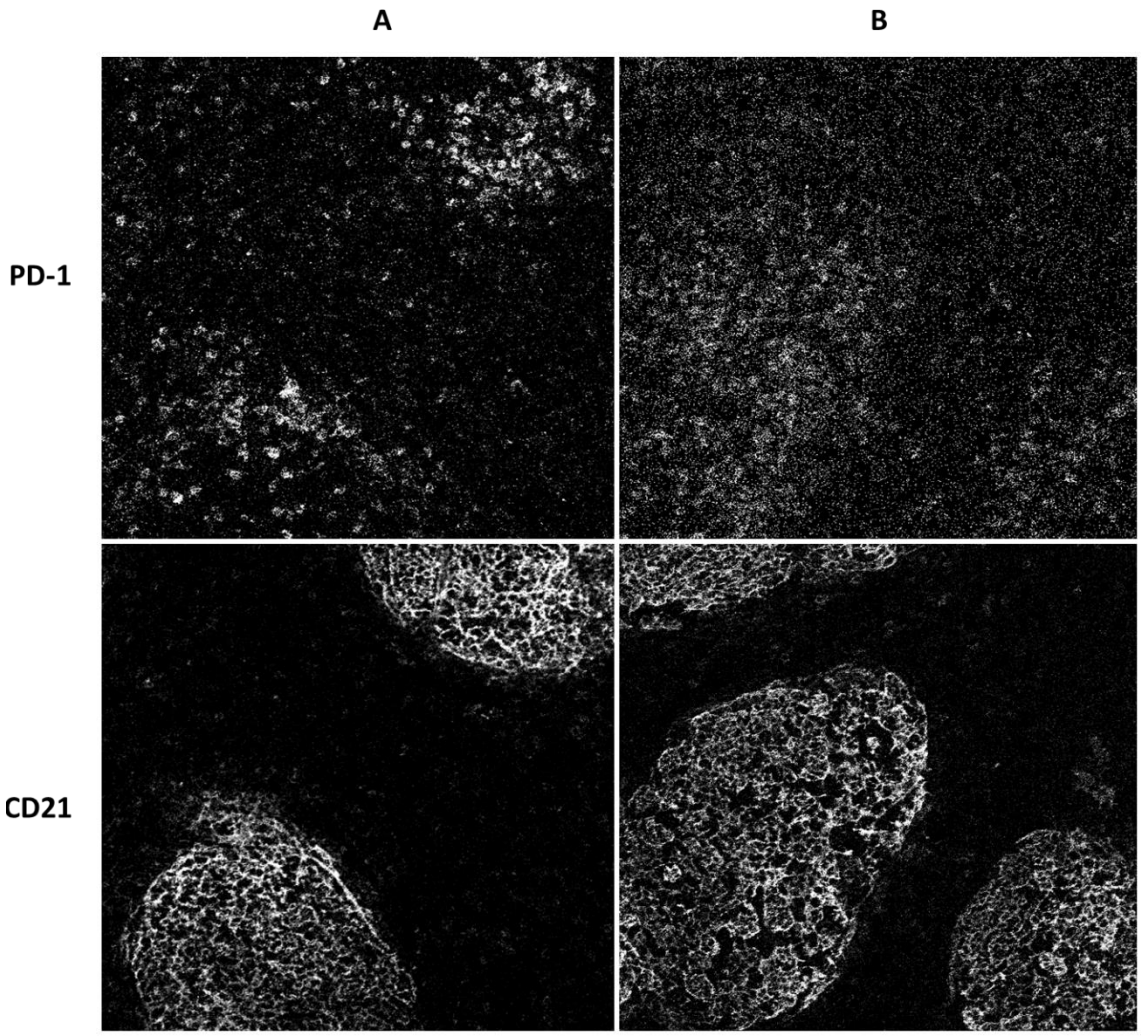

Figure 6.5. Follicular PD-1 staining by Imaging Mass Cytometry. *Representative IMC images of FL tissue show that PD-1 expression (top) is primarily seen within follicular regions, highlighted by CD21 (bottom). Low-level interfollicular PD-1 expression is not clearly detectable by IMC. Significant variability in staining was seen, with very clear definition of PD-1$^+$ cells in image A (left) but poor definition in image B, only just above levels of background uptake.*

Probability maps showing co-expression of CD3, CD4, PD-1 and ICOS were used to identify T_{FH} (Figure 6.6A–D). Intrafollicular CD3 and CD4 expression were relatively weak, partly because there are fewer T-cells than in interfollicular areas, but also because activated T-cells, such as T_{FH}, usually express lower levels of both antigens (Townsend*, et al* 2019). These were predominantly within follicular/perifollicular areas in all 11 samples, consistent with the distribution seen by CIFM. Other cell groups identified for this analysis were CD20$^+$Ki67$^+$ proliferating B-cells, CD3$^+$CD8$^+$ cytotoxic T-cells and non-T_{FH} CD3$^+$CD4$^+$ T-cells (Figure 6.6E–F)

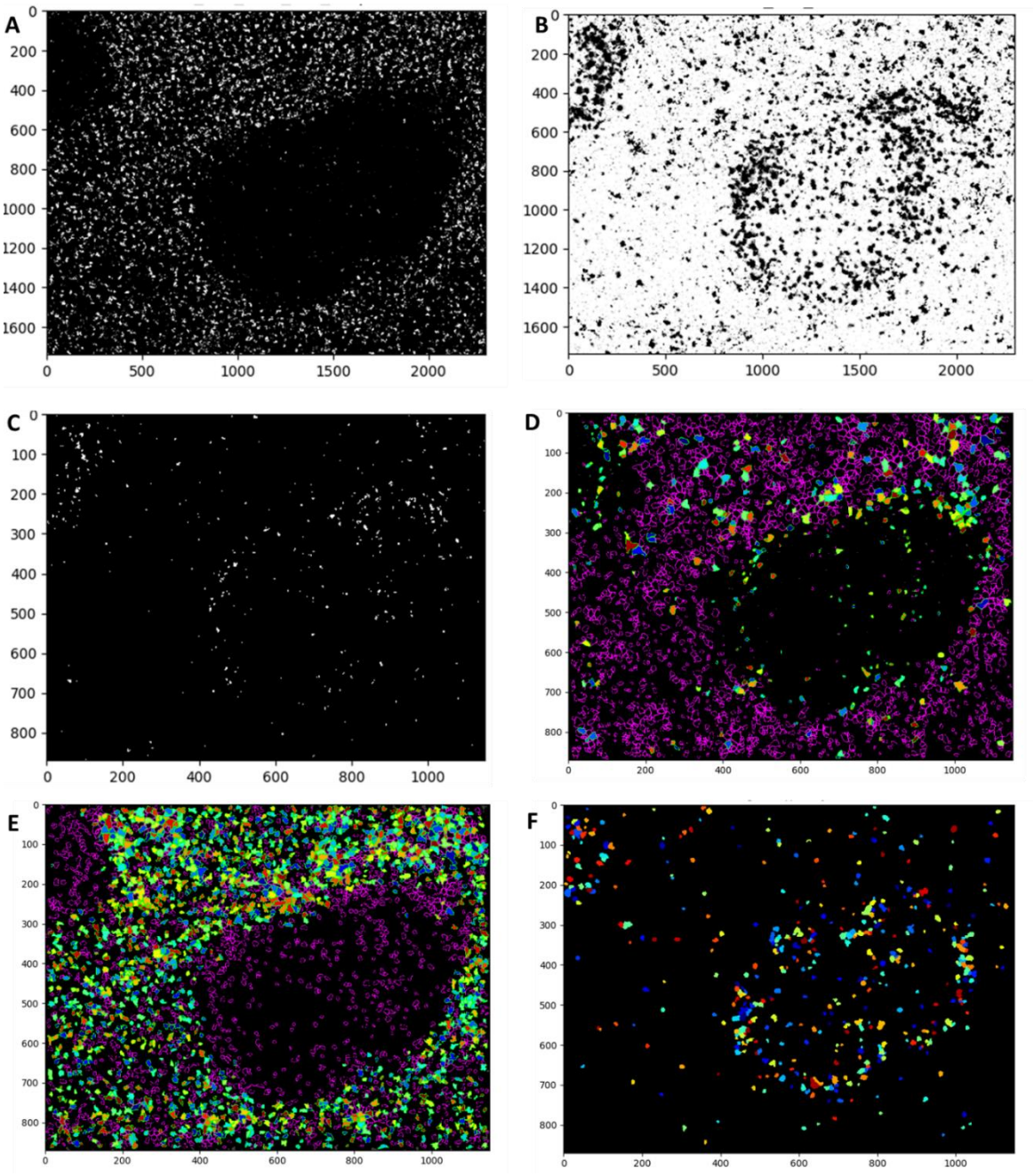

Image 6.6. Identification of T-cells and proliferating B-cells by IMC. *Probability maps show areas of CD3/CD4 co-expression* ***(A)****, and PD-1/ICOS co-expression* ***(B)*** *in FL tissue. These two probability maps were combined in* ***(C)*** *to identify* $CD3^+CD4^+PD\text{-}1^+ICOS^+$ *expression. This was then mapped onto the original image in* ***(D)*** *to identify* $CD3^+CD4^+PD\text{-}1^+ICOS^+$ T_{FH} *cells.* $CD3^+$ *cells are outlined in magenta. Image B was deducted from Image A to identify* $CD3^+CD4^+$ *T-cells with a non-*T_{FH} *phenotype, shown in* ***(E)****. Probability maps for CD20 and Ki67 were combined to identify proliferating B-cells, shown in image* ***(F)****. Axes show distance in µm.*

6.3.2. Correlation with Confocal Imaging Results

Importantly, through IMC it was possible to recreate 2 key findings from previous CIFM studies by our research group (Townsend*, et al* 2019). Firstly, there was a clear correlation between the number of proliferating B-cells and the number of T_{FH} (r=0.63, p=0.04, N=11; Figure 6.7A). Secondly, there was a close spatial relationship between T_{FH} and proliferation, with smaller distances between proliferating B-cells and T_{FH} than with other T-cells. The mean distance from $CD3^+$ T-cells to the nearest $Ki67^+CD20^+$ cell was 22.0 ± 1.9µm for T_{FH}, 34.8 ± 2.6µm for non-T_{FH} $CD4^+$ T-cells and 36.7 ± 3.4µm for $CD8^+$ T-cells (n=11; Figure 6.7B). These results provide important validation of the IMC analysis pipeline.

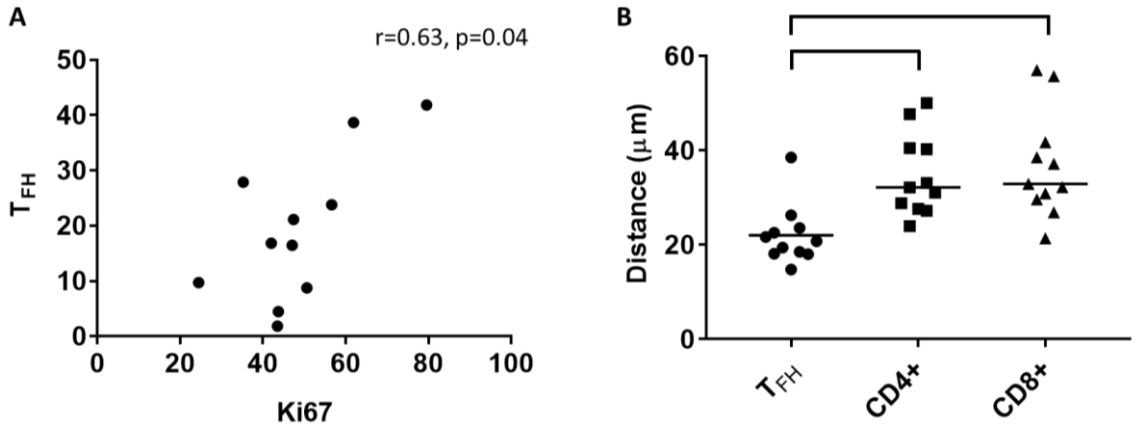

Figure 6.7. Relationship between T_{FH} and proliferating B-cells. A) *Scatter plot shows the correlation between the area of proliferating B-cells ($CD20^+Ki67^+$; x axis) and T_{FH} ($CD3^+CD4^+PD\text{-}1^+ICOS^+$; y axis) in IMC images from 11 FL patients. Values indicate the area of each cell type in $\mu m^2 x10^3$, within a $1mm^2$ image.* ***B)*** *Graph shows the mean distance from T-cells to the nearest proliferating B-cell (N=11). $CD4^+$ T-cells were defined as $CD3^+CD4^+$ cells without PD-1/ICOS co-expression. Horizontal bars represent mean values. *p<0.0001 for both comparisons.*

There was no clear evidence of a correlation between the number of T_{FH} assessed by IHC and CIFM in the same tissue samples (see Figure 6.8). This was not entirely unexpected, given that the CIFM analysis focussed solely on follicular areas, whereas the IMC analysis included both follicular and interfollicular areas. However, this may, in part, be due to the very weak PD-1 signal or insufficient detection of follicular CD4 by IMC, which may miss T_{FH} in some samples. Two samples had a very low T_{FH} area measurements by IMC (<5µm^2) but with moderate

expression of PD-1 and ICOS by CIFM, suggesting that T_{FH} identification by IMC may have been suboptimal.

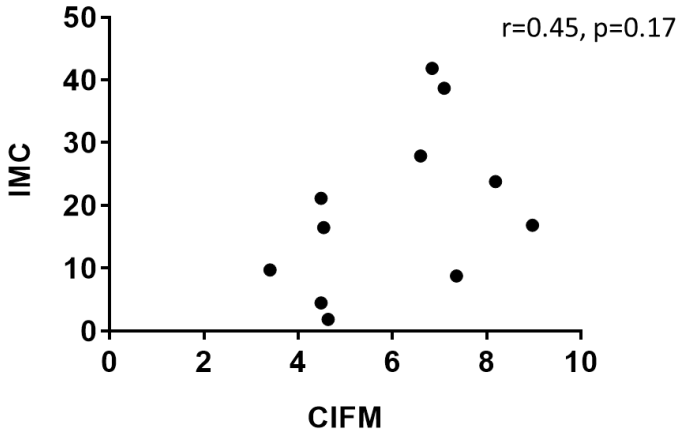

Figure 6.8. Correlation between T_{FH} numbers by CIFM and IMC. *The x axis shows the area of PD-1/ICOS co-expression by CIFM assessment of FL tissue (N=11), expressed as a percentage of the total image area (see Section 5.4.2). The y axis shows the area of CD3⁺CD4⁺PD-1⁺ICOS+ cells by IMC in µm x10³, in the same tissue blocks.*

6.4. Discussion

This preliminary work shows that highly multiplexed tissue imaging by IMC is feasible in archival FL tissue and can identify T_{FH}. It was possible to demonstrate a clear correlation between T_{FH} and FL proliferation by IMC, thus reproducing findings with other tissue imaging methods (Townsend*, et al* 2019). IMC has mostly been studied in breast carcinoma to date (Giesen*, et al* 2014, Schapiro*, et al* 2017, Schulz*, et al* 2018). To our knowledge, there are no published reports validating its use in lymphoma, where cells are tightly packed, and tissue architecture differs from solid organ malignancies.

This work is part of an ongoing project, with plans to analyse all 20 antigens and expand patient numbers in future. Follicular and interfollicular areas, defined by CD21 expression, may need to be considered separately, given the very different cellular composition in these areas. IMC will enable measurement of the distance between multiple different cell types, extending the data shown in Figure 6.7B, to produce a 'neighbourhood analysis' in order to identify and characterise cell networks (Giesen*, et al* 2014, Schapiro*, et al* 2017). This technology offers the opportunity to perform a global analysis of the FL TME in single tissue sections and may facilitate discovery

of non-malignant cell networks that can influence the clinical phenotype of FL, overcoming the limitations of IHC and other more limited tissue imaging techniques.

The preliminary data presented here highlight several limitations of IMC. There is no secondary signal antibody amplification step and therefore the antigen detection threshold is higher: IMC can detect 100-500 primary antibodies per pixel, compared with 20-200 for CIFM (Bodenmiller 2016). Therefore, IMC was not sensitive enough to detect expression of weak antigens, such as MYC and AID, which restricted our ability to assess the relationship between T_{FH} and B-cell phenotype. One potential solution may be to use novel techniques to assess mRNA expression by IMC, which include multiple signal amplification steps (Schulz*, et al* 2018). Tissue staining protocols for other antigens will also need to be optimised going forwards, particularly for PD-1, in order to more reliably identify T_{FH}. This may involve using entirely different anti-PD-1 antibody, such as the polyclonal anti-PD-1 antibody used for CIFM, or combining 2 clones together to amplify signal.

Spatial resolution is lower with IMC than with CIFM, with a maximum resolution of 1µm, compared with 0.2µm for the confocal studies in the previous chapter. IMC therefore cannot replace higher-resolution imaging techniques in assessing cell synapse formation or subcellular structures. However, IMC can be used as a platform to screen and identify key markers that can then be assessed by higher-resolution, limited-parameter techniques, where required. Resolution may improve as the technology evolves but is currently limited by the minimum area of tissue that the laser is able to ablate. Cost and resource utilisation are other important considerations. Image acquisition takes 2 hours for each $1mm^2$ section. Each slide needs to be set up manually beforehand, which takes an additional hour. It is therefore advantageous to fit as many tissue sections as possible onto each slide to limit set-up time and expense; tissue microarrays are ideal in this respect.

This preliminary work has been used to successfully apply for and obtain tissue microarrays from a large, international, phase 3 clinical trial in FL with linked clinical outcome and gene expression data. Following on from this MD, this will be used to explore some of these findings from this thesis, such as the relationship between T_{FH} and B-cell phenotype, and identify prognostic cell networks within the FL TME.

CHAPTER 7: CONCLUSIONS AND FUTURE WORK

This work adds to the growing body of evidence that T_{FH} play a key role in supporting FL B-cells. The experiments described in Chapter 4 demonstrate a mutual dependence of T_{FH} and FL B-cells for survival and activation, which strongly implies that T_{FH} may have a central role in the pathogenesis of FL. Whilst it has previously been published that T_{FH} can support FL B-cell survival (Ame-Thomas*, et al* 2012, Yang*, et al* 2015a), it has not to our knowledge been shown that FL B-cells actively support T_{FH} survival and activation.

It is important to understand the factors that drive the recruitment and persistence of T_{FH} in FL tissue, in order to provide insights into disease pathogenesis and identify potential targets for therapeutic intervention. Here, we show that the three key stimuli that are necessary for T_{FH} support in reactive lymphoid tissue- TCR, CD28 and ICOS stimulation- can all be provided by FL B-cells. Furthermore, T_{FH} are able to support expression of both HLA-DR and CD86 in FL B-cells, suggesting that they may derive cognate stimulation in return. There is evidence of dynamic ICOS/ICOS-L interactions between T_{FH} and FL B-cells, which are likely to be critical for maintaining the T_{FH} phenotype (Bossaller*, et al* 2006, Weber*, et al* 2015). All these factors strongly suggest that FL is driven by a positive feedback loop involving both the tumour cells and T_{FH}.

This work raises a number of important questions for future study. Firstly, are T_{FH} dependent on antigen-dependent stimulation in FL tissue? The next step would be to repeat FL-T_{FH} co-culture studies in the presence and absence of agents that block HLA-DR/TCR interactions to assess whether FL T_{FH} are indeed dependent on TCR stimulation. If this proves to be correct, future experiments could elute and characterise the peptides presented by FL B-cells, to identify the nature of any antigenic stimulus driving T_{FH} expansion.

Secondly, the importance of ICOS stimulation in supporting T_{FH} activity requires further exploration. Studies in reactive LN tissue have shown blocking ICOS stimulation results in rapid and complete loss of T_{FH} (Bossaller*, et al* 2006, Weber*, et al* 2015). T_{FH}-FL B-cell co-cultures performed in the presence and absence of ICOS or ICOS-L blockade would ascertain whether the same applies to FL T_{FH}. This may be a means to therapeutically target T_{FH} in FL tissue, given that pharmacological agents targeting ICOS-L are already being used in clinical trials for other diseases such as systemic lupus erythematosus (Cheng*, et al* 2018). However, ICOS expression is not unique to T_{FH} and therapeutic manipulation may potentially inhibit anti-tumour T-cell immunity, such as activated cytotoxic T-cells. Mixed co-culture assays, such as the CD3 depletion model described in Chapter 4, would enable evaluation of the net effect of ICOS blockade on FL B-cell activation and survival.

The confocal immunofluorescence microscopy studies presented here demonstrate a very close spatial correlation between T_{FH} and MYC expression. These novel findings are preliminary and require further validation with *in vitro* studies to demonstrate a direct relationship between T_{FH} and MYC expression. However, the plausibility of these results is supported by recent studies showing that CD40L stimulation is necessary for MYC expression in reactive GC B-cells (Luo*, et al* 2018). Induction of MYC expression by T_{FH} would provide a mechanistic link between the TME and tumour growth and explain why TME-dependence is lost in transformed disease.

One limitation of this work is the low sample number for some experiments, particularly where disaggregated LN tissue was required. The difficulty in obtaining fresh LN tissue was partly mitigated by using FNA to obtain FL cell suspensions. This work demonstrates that this relatively non-invasive technique can provide sufficient cells to conduct successful co-culture experiments. The distribution of lymphocytes obtained by FNA reflected those present in disaggregated whole LN tissue. However, whilst some patients were willing to undergo up to 3 FNAs over a 4-year period, it is not ethical or feasible to expect most patients to undergo repeated FNA altruistically. To broaden this research will require either a larger patient base or more disaggregated LN tissue. Preliminary studies here using PB and BM T-cells demonstrated that it is only possible to obtain cells with a clear T_{FH} phenotype from secondary lymphoid tissue.

One of the main priorities in FL research is identifying the factors that determine the marked clinical heterogeneity and drive more aggressive disease phenotypes. Whilst it is hypothesised that T_{FH} directly induce FL proliferation and acquisition of genomic changes that facilitate disease progression and transformation, it remains uncertain whether T_{FH} correlate with clinical outcomes. Single parameter IHC studies and multiparameter flow cytometry studies have not demonstrated a link between T_{FH} and clinical phenotype, but these studies are limited either in their ability to accurately identify T_{FH}, or to assess spatial interactions within FL tissue, respectively (Ame-Thomas and Tarte 2014). This thesis demonstrates that it is possible to image archival FL tissue by IMC to enable highly multiplexed assessment of the TME *in situ*. More work needs to be done to optimise quality of staining and image analysis, but IMC holds great promise to assess the spatial interactions of T_{FH} with FL B-cells and the wider TME and can overcome the limitations of other methodologies. This technology may finally be able to untangle the effect of complex effects of cell subsets and networks within the TME. As a direct result of this work, we have obtained tissue microarrays with linked outcome data from a large, international clinical trial in FL. Once techniques have been optimised, this vital resource will be used to develop a TME prognostic signature and assess whether T_{FH} have a prognostic role in FL.

Many of the T_{FH} interactions highlighted by this work mirror those seen in reactive LN tissue. This is consistent with previous work by our group showing that the number, distributions and interactions of T_{FH} in FL tissue reflect those seen in reactive GCs (Townsend*, et al* 2019). However, there are known phenotypic differences between T_{FH} in reactive LN and FL tissue that are not explained by the findings above, such as overexpression of IL-4 (Amé-Thomas*, et al* 2015, Calvo*, et al* 2008, Pangault*, et al* 2010). Pathological interruption of HVEM/BTLA interactions is a key feature in FL and may account for changes in gene expression in FL T_{FH} (Boice*, et al* 2016). Such qualitative differences in T_{FH} phenotype, rather than quantitative changes in T_{FH} number, may also be important in FL pathogenesis and may need to be considered in future T_{FH} studies.

However, T_{FH} do not need to have prognostic effect to have clinical relevance in FL. If they are indeed integral to the development of FL and maintenance of malignant follicles, in a similar way to reactive GCs, then they are a clear therapeutic target. Indeed, the correlation between T_{FH} and Ki67, demonstrated here by IMC, suggests that T_{FH} may determine the rate of FL proliferation (Townsend*, et al* 2019). Whilst T_{FH} are likely to encourage the acquisition of deleterious mutations in FL, as the disease evolves and transforms these genomic changes may result in reliance on the FL TME being lost. Therefore, any correlation between T_{FH} and outcomes may be obscured when including very poor-risk, advanced cases.

There is a clear need to identify the effect of novel therapeutics on T_{FH}, rather than just considering all $CD4^+$ T-cells together as a whole. This work highlights that T_{FH} comprise a minority of $CD4^+$ T-cells but have distinct effects of FL B-cell activation and survival. Given their activated phenotype and intrafollicular location, T_{FH} may have a disproportionate influence on FL biology compared with most other T-cell subsets. Several recent studies have highlighted the potential for novel agents, such as PI3K and PD-1 inhibitors, to have unintended pro-tumoural effects (Compagno*, et al* 2017, Ratner*, et al* 2018). It is imperative that the effect on T_{FH} biology is considered when introducing new immunomodulatory therapies for FL. Better understanding of T_{FH} biology and the influence of the wider TME on FL phenotype will assist in the design of rational, targeted therapeutic approaches, with the hope of improving clinical outcomes for patients in future.

APPENDIX: ANTIGEN RETRIEVAL BUFFERS FOR FFPE TISSUE

Citrate buffer:

900ml distilled water

2.1g sodium citrate

25ml 1M NaOH

Titrated to pH 6.1 with further NaOH

0.5ml Tween-20

Tris-EDTA buffer:

1000ml distilled water

1.21g Tris added to 1L distilled H2O

0.37g EDTA

Titrated to pH 9.0 with 1M NaOH or HCl, if needed

0.5ml Tween 20

REFERENCES

Ahearne, M.J., Willimott, S., Pinon, L., Kennedy, D.B., Miall, F., Dyer, M.J. & Wagner, S.D. (2013) Enhancement of CD154/IL4 proliferation by the T follicular helper (Tfh) cytokine, IL21 and increased numbers of circulating cells resembling Tfh cells in chronic lymphocytic leukaemia. *Br J Haematol,* **162,** 360-370.

Alexandrov, L.B., Nik-Zainal, S., Wedge, D.C., Aparicio, S.A., Behjati, S., Biankin, A.V., Bignell, G.R., Bolli, N., Borg, A., Borresen-Dale, A.L., Boyault, S., Burkhardt, B., Butler, A.P., Caldas, C., Davies, H.R., Desmedt, C., Eils, R., Eyfjord, J.E., Foekens, J.A., Greaves, M., Hosoda, F., Hutter, B., Ilicic, T., Imbeaud, S., Imielinski, M., Jager, N., Jones, D.T., Jones, D., Knappskog, S., Kool, M., Lakhani, S.R., Lopez-Otin, C., Martin, S., Munshi, N.C., Nakamura, H., Northcott, P.A., Pajic, M., Papaemmanuil, E., Paradiso, A., Pearson, J.V., Puente, X.S., Raine, K., Ramakrishna, M., Richardson, A.L., Richter, J., Rosenstiel, P., Schlesner, M., Schumacher, T.N., Span, P.N., Teague, J.W., Totoki, Y., Tutt, A.N., Valdes-Mas, R., van Buuren, M.M., van 't Veer, L., Vincent-Salomon, A., Waddell, N., Yates, L.R., Australian Pancreatic Cancer Genome, I., Consortium, I.B.C., Consortium, I.M.-S., PedBrain, I., Zucman-Rossi, J., Futreal, P.A., McDermott, U., Lichter, P., Meyerson, M., Grimmond, S.M., Siebert, R., Campo, E., Shibata, T., Pfister, S.M., Campbell, P.J. & Stratton, M.R. (2013) Signatures of mutational processes in human cancer. *Nature,* **500,** 415-421.

Amé-Thomas, P., Hoeller, S., Artchounin, C., Misiak, J., Braza, M.S., Jean, R., Le Priol, J., Monvoisin, C., Martin, N., Gaulard, P. & Tarte, K. (2015) CD10 delineates a subset of human IL-4 producing follicular helper T cells involved in the survival of follicular lymphoma B cells. *Blood,* **125,** 2381-2385.

Ame-Thomas, P., Le Priol, J., Yssel, H., Caron, G., Pangault, C., Jean, R., Martin, N., Marafioti, T., Gaulard, P., Lamy, T., Fest, T., Semana, G. & Tarte, K. (2012) Characterization of intratumoral follicular helper T cells in follicular lymphoma: role in the survival of malignant B cells. *Leukemia,* **26,** 1053-1063.

Ame-Thomas, P., Maby-El Hajjami, H., Monvoisin, C., Jean, R., Monnier, D., Caulet-Maugendre, S., Guillaudeux, T., Lamy, T., Fest, T. & Tarte, K. (2007) Human mesenchymal stem cells isolated from bone marrow and lymphoid organs support tumor B-cell growth: role of stromal cells in follicular lymphoma pathogenesis. *Blood,* **109,** 693-702.

Ame-Thomas, P. & Tarte, K. (2014) The yin and the yang of follicular lymphoma cell niches: role of microenvironment heterogeneity and plasticity. *Semin Cancer Biol,* **24,** 23-32.

Amin, R., Mourcin, F., Uhel, F., Pangault, C., Ruminy, P., Dupré, L., Guirriec, M., Marchand, T., Fest, T., Lamy, T. & Tarte, K. (2015) DC-SIGN–expressing macrophages trigger activation of mannosylated IgM B-cell receptor in follicular lymphoma. *Blood,* **126,** 1911-1920.

Anderson, J.R., Armitage, J.O., Weisenburger, D.D. & Project, f.t.N.-H.s.L.C. (1998) Epidemiology of the non-Hodgkin's lymphomas: Distributions of the major subtypes differ by geographic locations. *Annals of Oncology,* **9,** 717-720.

Ardeshna, K.M., Smith, P., Norton, A., Hancock, B.W., Hoskin, P.J., MacLennan, K.A., Marcus, R.E., Jelliffe, A., Vaughan, G., Hudson, Linch, D.C. & British National Lymphoma, I. (2003) Long-term effect of a watch and wait policy versus immediate systemic treatment for asymptomatic advanced-stage non-Hodgkin lymphoma: a randomised controlled trial. *Lancet,* **362,** 516-522.

Arimura, Y., Shiroki, F., Kuwahara, S., Kato, H., Dianzani, U., Uchiyama, T. & Yagi, J. (2004) Akt is a neutral amplifier for Th cell differentiation. *J Biol Chem,* **279,** 11408-11416.

Attridge, K., Kenefeck, R., Wardzinski, L., Qureshi, O.S., Wang, C.J., Manzotti, C., Okkenhaug, K. & Walker, L.S.K. (2014) IL-21 Promotes CD4 T Cell Responses by Phosphatidylinositol 3-

Kinase–Dependent Upregulation of CD86 on B Cells. *The Journal of Immunology,* **192,** 2195-2201.

Aukema, S.M., van Pel, R., Nagel, I., Bens, S., Siebert, R., Rosati, S., van den Berg, E., Bosga-Bouwer, A.G., Kibbelaar, R.E., Hoogendoorn, M., van Imhoff, G.W., Kluin-Nelemans, H.C., Kluin, P.M. & Nijland, M. (2017) MYC expression and translocation analyses in low-grade and transformed follicular lymphoma. *Histopathology,* **71,** 960-971.

Bachy, E., Maurer, M.J., Habermann, T.M., Gelas-Dore, B., Maucort-Boulch, D., Estell, J.A., Van den Neste, E., Bouabdallah, R., Gyan, E., Feldman, A.L., Bargay, J., Delmer, A., Slager, S.L., Gomes da Silva, M., Fitoussi, O., Belada, D., Maisonneuve, H., Intragumtornchai, T., Ansell, S.M., Lamy, T., Dartigues, P., Link, B.K., Seymour, J.F., Cerhan, J.R. & Salles, G. (2018) A simplified scoring system in de novo follicular lymphoma treated initially with immunochemotherapy. *Blood,* **132,** 49-58.

Beguelin, W., Popovic, R., Teater, M., Jiang, Y., Bunting, K.L., Rosen, M., Shen, H., Yang, S.N., Wang, L., Ezponda, T., Martinez-Garcia, E., Zhang, H., Zheng, Y., Verma, S.K., McCabe, M.T., Ott, H.M., Van Aller, G.S., Kruger, R.G., Liu, Y., McHugh, C.F., Scott, D.W., Chung, Y.R., Kelleher, N., Shaknovich, R., Creasy, C.L., Gascoyne, R.D., Wong, K.K., Cerchietti, L., Levine, R.L., Abdel-Wahab, O., Licht, J.D., Elemento, O. & Melnick, A.M. (2013) EZH2 is required for germinal center formation and somatic EZH2 mutations promote lymphoid transformation. *Cancer Cell,* **23,** 677-692.

Beltran, B.E., Quinones, P., Morales, D., Alva, J.C., Miranda, R.N., Lu, G., Shah, B.D., Sotomayor, E.M. & Castillo, J.J. (2013) Follicular lymphoma with leukemic phase at diagnosis: a series of seven cases and review of the literature. *Leuk Res,* **37,** 1116-1119.

Berg, S., Kutra, D., Kroeger, T., Straehle, C.N., Kausler, B.X., Haubold, C., Schiegg, M., Ales, J., Beier, T., Rudy, M., Eren, K., Cervantes, J.I., Xu, B., Beuttenmueller, F., Wolny, A., Zhang, C., Koethe, U., Hamprecht, F.A. & Kreshuk, A. (2019) ilastik: interactive machine learning for (bio)image analysis. *Nature Methods*.

Bindea, G., Mlecnik, B., Tosolini, M., Kirilovsky, A., Waldner, M., Obenauf, A.C., Angell, H., Fredriksen, T., Lafontaine, L., Berger, A., Bruneval, P., Fridman, W.H., Becker, C., Pages, F., Speicher, M.R., Trajanoski, Z. & Galon, J. (2013) Spatiotemporal dynamics of intratumoral immune cells reveal the immune landscape in human cancer. *Immunity,* **39,** 782-795.

Blaker, Y.N., Spetalen, S., Brodtkorb, M., Lingjaerde, O.C., Beiske, K., Ostenstad, B., Sander, B., Wahlin, B.E., Melen, C.M., Myklebust, J.H., Holte, H., Delabie, J. & Smeland, E.B. (2016) The tumour microenvironment influences survival and time to transformation in follicular lymphoma in the rituximab era. *Br J Haematol,* **175,** 102-114.

Bodenmiller, B. (2016) Multiplexed Epitope-Based Tissue Imaging for Discovery and Healthcare Applications. *Cell Systems,* **2,** 225-238.

Bognar, A., Csernus, B., Bodor, C., Reiniger, L., Szepesi, A., Toth, E., Kopper, L. & Matolcsy, A. (2005) Clonal selection in the bone marrow involvement of follicular lymphoma. *Leukemia,* **19,** 1656-1662.

Boice, M., Salloum, D., Mourcin, F., Sanghvi, V., Amin, R., Oricchio, E., Jiang, M., Mottok, A., Denis-Lagache, N., Ciriello, G., Tam, W., Teruya-Feldstein, J., de Stanchina, E., Chan, W.C., Malek, S.N., Ennishi, D., Brentjens, R.J., Gascoyne, R.D., Cogne, M., Tarte, K. & Wendel, H.G. (2016) Loss of the HVEM Tumor Suppressor in Lymphoma and Restoration by Modified CAR-T Cells. *Cell,* **167,** 405-418 e413.

Bolen, C.R., Hiddemann, W., Marcus, R., Herold, M., Huet, S., Salles, G., Mattiello, F., Nielsen, T., Mir, F., Venstrom, J.M. & Oestergaard, M.Z. (2019) TREATMENT-DEPENDENCE OF HIGH-RISK GENE EXPRESSION SIGNATURES IN DE NOVO FOLLICULAR LYMPHOMA. *Hematological Oncology,* **37,** 193-194.

Bossaller, L., Burger, J., Draeger, R., Grimbacher, B., Knoth, R., Plebani, A., Durandy, A., Baumann, U., Schlesier, M., Welcher, A.A., Peter, H.H. & Warnatz, K. (2006) ICOS Deficiency Is

Associated with a Severe Reduction of CXCR5⁺CD4 Germinal Center Th Cells. *The Journal of Immunology,* **177,** 4927-4932.

Brady, M.T., Hilchey, S.P., Hyrien, O., Spence, S.A. & Bernstein, S.H. (2014) Mesenchymal stromal cells support the viability and differentiation of follicular lymphoma-infiltrating follicular helper T-cells. *PLoS One,* **9,** e97597.

Brice, P., Bastion, Y., Lepage, E., Brousse, N., Haïoun, C., Moreau, P., Straetmans, N., Tilly, H., Tabah, I. & Solal-Céligny, P. (1997) Comparison in low-tumor-burden follicular lymphomas between an initial no-treatment policy, prednimustine, or interferon alfa: a randomized study from the Groupe d'Etude des Lymphomes Folliculaires. Groupe d'Etude des Lymphomes de l'Adulte. *Journal of Clinical Oncology,* **15,** 1110-1117.

Brusa, D., Serra, S., Coscia, M., Rossi, D., D'Arena, G., Laurenti, L., Jaksic, O., Fedele, G., Inghirami, G., Gaidano, G., Malavasi, F. & Deaglio, S. (2013) The PD-1/PD-L1 axis contributes to T cell dysfunction in chronic lymphocytic leukemia. *Haematologica*.

Burack, R., Shenoy, G., Spence, J.M., Spence, S., Rock, P., Shultz, L., Bankert, R. & Bernstein, S. (2016) A Patient-Derived Xenograft Model of Marginal Zone and Follicular Lymphomas Demonstrates a Key Role of CD4+ T Cells. *Blood,* **128,** 916-916.

Burack, W.R., Spence, J.M., Spence, J.P., Spence, S.A., Rock, P.J., Shenoy, G.N., Shultz, L.D., Bankert, R.B. & Bernstein, S.H. (2017) Patient-derived xenografts of low-grade B-cell lymphomas demonstrate roles of the tumor microenvironment. *Blood advances,* **1,** 1263-1273.

Caeser, R., Di Re, M., Krupka, J.A., Gao, J., Lara-Chica, M., Dias, J.M.L., Cooke, S.L., Fenner, R., Usheva, Z., Runge, H., Beer, P.A., Eldaly, H., Pak, H.-K., Park, C.-S., Vassiliou, G., Huntly, B.J.P., Mupo, A., Bashford-Rogers, R.J. & Hodson, D.J. (2019) Genetic modification of primary human B cells generates translationally-relevant models of high-grade lymphoma. *bioRxiv***,** 618835.

Calvo, K.R., Dabir, B., Kovach, A., Devor, C., Bandle, R., Bond, A., Shih, J.H. & Jaffe, E.S. (2008) IL-4 protein expression and basal activation of Erk in vivo in follicular lymphoma. *Blood,* **112,** 3818-3826.

Canioni, D., Salles, G., Mounier, N., Brousse, N., Keuppens, M., Morchhauser, F., Lamy, T., Sonet, A., Rousselet, M.-C., Foussard, C. & Xerri, L. (2008) High Numbers of Tumor-Associated Macrophages Have an Adverse Prognostic Value That Can Be Circumvented by Rituximab in Patients With Follicular Lymphoma Enrolled Onto the GELA-GOELAMS FL-2000 Trial. *Journal of Clinical Oncology,* **26,** 440-446.

Carreras, J., Lopez-Guillermo, A., Roncador, G., Villamor, N., Colomo, L., Martinez, A., Hamoudi, R., Howat, W.J., Montserrat, E. & Campo, E. (2009) High numbers of tumor-infiltrating programmed cell death 1-positive regulatory lymphocytes are associated with improved overall survival in follicular lymphoma. *J Clin Oncol,* **27,** 1470-1476.

Casulo, C., Byrtek, M., Dawson, K.L., Zhou, X., Farber, C.M., Flowers, C.R., Hainsworth, J.D., Maurer, M.J., Cerhan, J.R., Link, B.K., Zelenetz, A.D. & Friedberg, J.W. (2015) Early Relapse of Follicular Lymphoma After Rituximab Plus Cyclophosphamide, Doxorubicin, Vincristine, and Prednisone Defines Patients at High Risk for Death: An Analysis From the National LymphoCare Study. *J Clin Oncol,* **33,** 2516-2522.

Cha, S.-C., Qin, H., Kannan, S., Rawal, S., Watkins, L.S., Baio, F.E., Wu, W., Ong, J., Wei, J., Kwak, B., Kim, S., Popescu, M.S., Paick, D.S., Kim, K., Luong, A., Davis, R.E., Schroeder, H.W., Kwak, L.W. & Neelapu, S.S. (2013) Nonstereotyped Lymphoma B Cell Receptors Recognize Vimentin as a Shared Autoantigen. *The Journal of Immunology,* **190,** 4887-4898.

Cheng, L.E., Amoura, Z., Cheah, B., Hiepe, F., Sullivan, B.A., Zhou, L., Arnold, G.E., Tsuji, W.H., Merrill, J.T. & Chung, J.B. (2018) Brief Report: A Randomized, Double-Blind, Parallel-Group, Placebo-Controlled, Multiple-Dose Study to Evaluate AMG 557 in Patients With

Systemic Lupus Erythematosus and Active Lupus Arthritis. *Arthritis & Rheumatology,* **70,** 1071-1076.

Cheung, K.-J.J., Johnson, N.A., Affleck, J.G., Severson, T., Steidl, C., Ben-Neriah, S., Schein, J., Morin, R.D., Moore, R., Shah, S.P., Qian, H., Paul, J.E., Telenius, A., Relander, T., Lam, W., Savage, K., Connors, J.M., Brown, C., Marra, M.A., Gascoyne, R.D. & Horsman, D.E. (2010) Acquired TNFRSF14 Mutations in Follicular Lymphoma Are Associated with Worse Prognosis. *Cancer Research,* **70,** 9166-9174.

Chevrier, S., Crowell, H., Zanotelli, V., Engler, S., Robinson, M.D. & Bodenmiller, B. (2017) Channel crosstalk correction in suspension and imaging mass cytometry. *bioRxiv***,** 185744.

Chevrier, S., Crowell, H.L., Zanotelli, V.R.T., Engler, S., Robinson, M.D. & Bodenmiller, B. (2018) Compensation of Signal Spillover in Suspension and Imaging Mass Cytometry. *Cell Systems,* **6,** 612-620.e615.

Chiu, H., Trisal, P., Bjorklund, C., Carrancio, S., Toraño, E.G., Guarinos, C., Papazoglou, D., Hagner, P.R., Beldi-Ferchiou, A., Tarte, K., Delfau-Larue, M.-H., Morschhauser, F., Ramsay, A.G. & Gandhi, A.K. (2019) Combination lenalidomide-rituximab immunotherapy activates anti-tumour immunity and induces tumour cell death by complementary mechanisms of action in follicular lymphoma. *British journal of haematology,* **185,** 240-253.

Choi, Y.S., Kageyama, R., Eto, D., Escobar, T.C., Johnston, R.J., Monticelli, L., Lao, C. & Crotty, S. (2011) ICOS receptor instructs T follicular helper cell versus effector cell differentiation via induction of the transcriptional repressor Bcl6. *Immunity,* **34,** 932-946.

Choi, Y.S., Yang, J.A., Yusuf, I., Johnston, R.J., Greenbaum, J., Peters, B. & Crotty, S. (2013) Bcl6 expressing follicular helper CD4 T cells are fate committed early and have the capacity to form memory. *J Immunol,* **190,** 4014-4026.

Christopoulos, P., Pfeifer, D., Bartholomé, K., Follo, M., Timmer, J., Fisch, P. & Veelken, H. (2011) Definition and characterization of the systemic T-cell dysregulation in untreated indolent B-cell lymphoma and very early CLL. *Blood,* **117,** 3836-3846.

Coelho, V., Krysov, S., Ghaemmaghami, A.M., Emara, M., Potter, K.N., Johnson, P., Packham, G., Martinez-Pomares, L. & Stevenson, F.K. (2010) Glycosylation of surface Ig creates a functional bridge between human follicular lymphoma and microenvironmental lectins. *Proceedings of the National Academy of Sciences,* **107,** 18587-18592.

Compagno, M., Wang, Q., Pighi, C., Cheong, T.-C., Meng, F.-L., Poggio, T., Yeap, L.-S., Karaca, E., Blasco, R.B., Langellotto, F., Ambrogio, C., Voena, C., Wiestner, A., Kasar, S.N., Brown, J.R., Sun, J., Wu, C.J., Gostissa, M., Alt, F.W. & Chiarle, R. (2017) Phosphatidylinositol 3-kinase δ blockade increases genomic instability in B cells. *Nature,* **542,** 489-493.

Correia, C., Schneider, P.A., Dai, H., Dogan, A., Maurer, M.J., Church, A.K., Novak, A.J., Feldman, A.L., Wu, X., Ding, H., Meng, X.W., Cerhan, J.R., Slager, S.L., Macon, W.R., Habermann, T.M., Karp, J.E., Gore, S.D., Kay, N.E., Jelinek, D.F., Witzig, T.E., Nowakowski, G.S. & Kaufmann, S.H. (2015) BCL2 mutations are associated with increased risk of transformation and shortened survival in follicular lymphoma. *Blood,* **125,** 658-667.

Cortes, J.R., Ambesi-Impiombato, A., Couronné, L., Quinn, S.A., Kim, C.S., da Silva Almeida, A.C., West, Z., Belver, L., Martin, M.S., Scourzic, L., Bhagat, G., Bernard, O.A., Ferrando, A.A. & Palomero, T. (2018) RHOA G17V Induces T Follicular Helper Cell Specification and Promotes Lymphomagenesis. *Cancer Cell,* **33,** 259-273.e257.

Cottereau, A.S., Versari, A., Chartier, L., Dupuis, J., Tarantino, V., Casasnovas, R.-O., Franceschetto, A., Itti, E., Tilly, H., Haioun, C., Federico, M., Berriolo, A., Salles, G.A., Luminari, S., Meignan, M. & Trotman, J. (2016) Low Suvmax Measured on Baseline FDG-PET/CT and Elevated β2 Microglobulin Are Negative Predictors of Outcome in High Tumor Burden Follicular Lymphoma Treated By Immunochemotherapy: A Pooled Analysis of Three Prospective Studies. *Blood,* **128,** 1101-1101.

Cozzolino, I., Rocco, M., Villani, G. & Picardi, M. (2016) Lymph Node Fine-Needle Cytology of Non-Hodgkin Lymphoma: Diagnosis and Classification by Flow Cytometry. *Acta Cytologica,* **60,** 302-314.

Crotty, S. (2014) T follicular helper cell differentiation, function, and roles in disease. *Immunity,* **41,** 529-542.

Crotty, S. (2015) A brief history of T cell help to B cells. *Nat Rev Immunol,* **15,** 185-189.

Crotty, S. (2019) T Follicular Helper Cell Biology: A Decade of Discovery and Diseases. *Immunity,* **50,** 1132-1148.

Cubas, R.A., Mudd, J.C., Savoye, A.L., Perreau, M., van Grevenynghe, J., Metcalf, T., Connick, E., Meditz, A., Freeman, G.J., Abesada-Terk, G., Jr., Jacobson, J.M., Brooks, A.D., Crotty, S., Estes, J.D., Pantaleo, G., Lederman, M.M. & Haddad, E.K. (2013) Inadequate T follicular cell help impairs B cell immunity during HIV infection. *Nat Med,* **19,** 494-499.

Dan, J.M., Lindestam Arlehamn, C.S., Weiskopf, D., da Silva Antunes, R., Havenar-Daughton, C., Reiss, S.M., Brigger, M., Bothwell, M., Sette, A. & Crotty, S. (2016) A Cytokine-Independent Approach To Identify Antigen-Specific Human Germinal Center T Follicular Helper Cells and Rare Antigen-Specific CD4⁺ T Cells in Blood. *The Journal of Immunology,* **197,** 983-993.

Dave, S.S., Wright, G., Tan, B., Rosenwald, A., Gascoyne, R.D., Chan, W.C., Fisher, R.I., Braziel, R.M., Rimsza, L.M., Grogan, T.M., Miller, T.P., LeBlanc, M., Greiner, T.C., Weisenburger, D.D., Lynch, J.C., Vose, J., Armitage, J.O., Smeland, E.B., Kvaloy, S., Holte, H., Delabie, J., Connors, J.M., Lansdorp, P.M., Ouyang, Q., Lister, T.A., Davies, A.J., Norton, A.J., Muller-Hermelink, H.K., Ott, G., Campo, E., Montserrat, E., Wilson, W.H., Jaffe, E.S., Simon, R., Yang, L., Powell, J., Zhao, H., Goldschmidt, N., Chiorazzi, M. & Staudt, L.M. (2004) Prediction of survival in follicular lymphoma based on molecular features of tumor-infiltrating immune cells. *N Engl J Med,* **351,** 2159-2169.

Davids, M.S., Roberts, A.W., Seymour, J.F., Pagel, J.M., Kahl, B.S., Wierda, W.G., Puvvada, S., Kipps, T.J., Anderson, M.A., Salem, A.H., Dunbar, M., Zhu, M., Peale, F., Ross, J.A., Gressick, L., Desai, M., Kim, S.Y., Verdugo, M., Humerickhouse, R.A., Gordon, G.B. & Gerecitano, J.F. (2017) Phase I First-in-Human Study of Venetoclax in Patients With Relapsed or Refractory Non-Hodgkin Lymphoma. *J Clin Oncol,* **35,** 826-833.

de Leval, L., Rickman, D.S., Thielen, C., Reynies, A., Huang, Y.L., Delsol, G., Lamant, L., Leroy, K., Briere, J., Molina, T., Berger, F., Gisselbrecht, C., Xerri, L. & Gaulard, P. (2007) The gene expression profile of nodal peripheral T-cell lymphoma demonstrates a molecular link between angioimmunoblastic T-cell lymphoma (AITL) and follicular helper T (TFH) cells. *Blood,* **109,** 4952-4963.

De Silva, N.S. & Klein, U. (2015) Dynamics of B cells in germinal centres. *Nat Rev Immunol,* **15,** 137-148.

Deenick, E.K., Chan, A., Ma, C.S., Gatto, D., Schwartzberg, P.L., Brink, R. & Tangye, S.G. (2010) Follicular Helper T Cell Differentiation Requires Continuous Antigen Presentation that Is Independent of Unique B Cell Signaling. *Immunity,* **33,** 241-253.

Dolken, G., Illerhaus, G., Hirt, C. & Mertelsmann, R. (1996) BCL-2/J(H) rearrangements in circulating B cells of healthy blood donors and patients with nonmalignant diseases. *Journal of Clinical Oncology,* **14,** 1333-1344.

Dominguez-Sola, D., Victora, G.D., Ying, C.Y., Phan, R.T., Saito, M., Nussenzweig, M.C. & Dalla-Favera, R. (2012) The proto-oncogene MYC is required for selection in the germinal center and cyclic reentry. *Nature Immunology,* **13,** 1083.

Dubovsky, J.A., Beckwith, K.A., Natarajan, G., Woyach, J.A., Jaglowski, S., Zhong, Y., Hessler, J.D., Liu, T.M., Chang, B.Y., Larkin, K.M., Stefanovski, M.R., Chappell, D.L., Frissora, F.W., Smith, L.L., Smucker, K.A., Flynn, J.M., Jones, J.A., Andritsos, L.A., Maddocks, K., Lehman, A.M., Furman, R., Sharman, J., Mishra, A., Caligiuri, M.A., Satoskar, A.R., Buggy, J.J.,

Muthusamy, N., Johnson, A.J. & Byrd, J.C. (2013) Ibrutinib is an irreversible molecular inhibitor of ITK driving a Th1-selective pressure in T lymphocytes. *Blood,* **122,** 2539-2549.

Egle, A., Harris, A.W., Bath, M.L., O'Reilly, L. & Cory, S. (2004a) VavP-Bcl2 transgenic mice develop follicular lymphoma preceded by germinal center hyperplasia. *Blood,* **103,** 2276-2283.

Egle, A., Harris, A.W., Bath, M.L., O'Reilly, L. & Cory, S. (2004b) VavP-Bcl2 transgenic mice develop follicular lymphoma preceded by germinal center hyperplasia. *Blood,* **103,** 2276-2283.

Espeli, M. & Linterman, M. (2015) *T Follicular Helper Cells: Methods and Protocols.* Springer Protocols.

Eto, D., Lao, C., DiToro, D., Barnett, B., Escobar, T.C., Kageyama, R., Yusuf, I. & Crotty, S. (2011) IL-21 and IL-6 are critical for different aspects of B cell immunity and redundantly induce optimal follicular helper CD4 T cell (Tfh) differentiation. *Plos One,* **6,** e17739.

Farinha, P., Roncador, G., Al-Tourah, A., Connors, J.M. & Gascoyne, R.D. (2008) Combined FOXP3⁺ and PD1⁺ T Cell Density and Architectural Patterns Predict Overall Survival and Risk of Transformation in Uniformly Treated Patients with Follicular Lymphoma. *Blood,* **112,** 2815-2815.

Federico, M., Bellei, M., Marcheselli, L., Luminari, S., Lopez-Guillermo, A., Vitolo, U., Pro, B., Pileri, S., Pulsoni, A., Soubeyran, P., Cortelazzo, S., Martinelli, G., Martelli, M., Rigacci, L., Arcaini, L., Raimondo, F.D., Merli, F., Sabattini, E., McLaughlin, P. & Solal-Céligny, P. (2009) Follicular Lymphoma International Prognostic Index 2: A New Prognostic Index for Follicular Lymphoma Developed by the International Follicular Lymphoma Prognostic Factor Project. *Journal of Clinical Oncology,* **27,** 4555-4562.

Fessas, P., Lee, H., Ikemizu, S. & Janowitz, T. (2017) A molecular and preclinical comparison of the PD-1-targeted T-cell checkpoint inhibitors nivolumab and pembrolizumab. *Seminars in oncology,* **44,** 136-140.

Flinn, I.W., Miller, C.B., Ardeshna, K.M., Tetreault, S., Assouline, S.E., Zinzani, P.L., Mayer, J., Merli, M., Lunin, S.D., Pettitt, A.R., Nagy, Z., Tournilhac, O., Abou-Nassar, K.E., Crump, M., Jacobsen, E.D., de Vos, S., Santabarbara, P., Shi, W., Steelman, L. & Wagner-Johnston, N.D. (2016) Dynamo: A Phase 2 Study Demonstrating the Clinical Activity of Duvelisib in Patients with Relapsed Refractory Indolent Non-Hodgkin Lymphoma. *Blood,* **128,** 1218-1218.

Fowler, N.H., Davis, R.E., Rawal, S., Nastoupil, L., Hagemeister, F.B., McLaughlin, P., Kwak, L.W., Romaguera, J.E., Fanale, M.A., Fayad, L.E., Westin, J.R., Shah, J., Orlowski, R.Z., Wang, M., Turturro, F., Oki, Y., Claret, L.C., Feng, L., Baladandayuthapani, V., Muzzafar, T., Tsai, K.Y., Samaniego, F. & Neelapu, S.S. (2014) Safety and activity of lenalidomide and rituximab in untreated indolent lymphoma: an open-label, phase 2 trial. *Lancet Oncol,* **15,** 1311-1318.

Fu, W., Liu, X., Lin, X., Feng, H., Sun, L., Li, S., Chen, H., Tang, H., Lu, L., Jin, W. & Dong, C. (2018) Deficiency in T follicular regulatory cells promotes autoimmunity. *The Journal of Experimental Medicine,* **215,** 815-825.

Giesen, C., Wang, H.A.O., Schapiro, D., Zivanovic, N., Jacobs, A., Hattendorf, B., Schüffler, P.J., Grolimund, D., Buhmann, J.M., Brandt, S., Varga, Z., Wild, P.J., Günther, D. & Bodenmiller, B. (2014) Highly multiplexed imaging of tumor tissues with subcellular resolution by mass cytometry. *Nature Methods,* **11,** 417.

Gitlin, A.D., Shulman, Z. & Nussenzweig, M.C. (2014) Clonal selection in the germinal centre by regulated proliferation and hypermutation. *Nature,* **509,** 637.

Glas, A.M., Knoops, L., Delahaye, L., Kersten, M.J., Kibbelaar, R.E., Wessels, L.A., Laar, R.v., Krieken, J.H.J.M.v., Baars, J.W., Raemaekers, J., Kluin, P.M., Veer, L.J.v.t. & Jong, D.d. (2007) Gene-Expression and Immunohistochemical Study of Specific T-Cell Subsets and

Accessory Cell Types in the Transformation and Prognosis of Follicular Lymphoma. *Journal of Clinical Oncology,* **25,** 390-398.

Good-Jacobson, K.L., Song, E., Anderson, S., Sharpe, A.H. & Shlomchik, M.J. (2012) CD80 expression on B cells regulates murine T follicular helper development, germinal center B cell survival, and plasma cell generation. *J Immunol,* **188,** 4217-4225.

Good-Jacobson, K.L., Szumilas, C.G., Chen, L., Sharpe, A.H., Tomayko, M.M. & Shlomchik, M.J. (2010) PD-1 regulates germinal center B cell survival and the formation and affinity of long-lived plasma cells. *Nat Immunol,* **11,** 535-542.

Gopal , A.K., Kahl , B.S., de Vos , S., Wagner-Johnston , N.D., Schuster , S.J., Jurczak , W.J., Flinn , I.W., Flowers , C.R., Martin , P., Viardot , A., Blum , K.A., Goy , A.H., Davies , A.J., Zinzani , P.L., Dreyling , M., Johnson , D., Miller , L.L., Holes , L., Li , D., Dansey , R.D., Godfrey , W.R. & Salles , G.A. (2014) PI3Kδ Inhibition by Idelalisib in Patients with Relapsed Indolent Lymphoma. *New England Journal of Medicine,* **370,** 1008-1018.

Gopal, A.K., Schuster, S.J., Fowler, N.H., Trotman, J., Hess, G., Hou, J.-Z., Yacoub, A., Lill, M., Martin, P., Vitolo, U., Spencer, A., Radford, J., Jurczak, W., Morton, J., Caballero, D., Deshpande, S., Gartenberg, G.J., Wang, S.-S., Damle, R.N., Schaffer, M., Balasubramanian, S., Vermeulen, J., Cheson, B.D. & Salles, G. (2018) Ibrutinib as Treatment for Patients With Relapsed/Refractory Follicular Lymphoma: Results From the Open-Label, Multicenter, Phase II DAWN Study. *Journal of Clinical Oncology,* **36,** 2405-2412.

Gravelle, P., Burroni, B., Péricart, S., Rossi, C., Bezombes, C., Tosolini, M., Damotte, D., Brousset, P., Fournié, J.-J. & Laurent, C. (2017) Mechanisms of PD-1/PD-L1 expression and prognostic relevance in non-Hodgkin lymphoma: a summary of immunohistochemical studies. *Oncotarget,* **8,** 44960-44975.

Gravelle, P., Do, C., Franchet, C., Mueller, S., Oberic, L., Ysebaert, L., Larocca, L.M., Hohaus, S., Calmels, M.-N., Frenois, F.-X., Kridel, R., Gascoyne, R.D., Laurent, G., Brousset, P., Valitutti, S. & Laurent, C. (2016) Impaired functional responses in follicular lymphoma CD8(+)TIM-3(+) T lymphocytes following TCR engagement. *Oncoimmunology,* **5,** e1224044-e1224044.

Green, M.R., Gentles, A.J., Nair, R.V., Irish, J.M., Kihira, S., Liu, C.L., Kela, I., Hopmans, E.S., Myklebust, J.H., Ji, H., Plevritis, S.K., Levy, R. & Alizadeh, A.A. (2013) Hierarchy in somatic mutations arising during genomic evolution and progression of follicular lymphoma. *Blood*.

Green, M.R., Kihira, S., Liu, C.L., Nair, R.V., Salari, R., Gentles, A.J., Irish, J., Stehr, H., Vicente-Dueñas, C., Romero-Camarero, I., Sanchez-Garcia, I., Plevritis, S.K., Arber, D.A., Batzoglou, S., Levy, R. & Alizadeh, A.A. (2015) Mutations in early follicular lymphoma progenitors are associated with suppressed antigen presentation. *Proceedings of the National Academy of Sciences,* **112,** E1116-E1125.

Gribben, J.G., Fowler, N. & Morschhauser, F. (2015) Mechanisms of Action of Lenalidomide in B-Cell Non-Hodgkin Lymphoma. *J Clin Oncol,* **33,** 2803-2811.

Grimbacher, B., Hutloff, A., Schlesier, M., Glocker, E., Warnatz, K., Drager, R., Eibel, H., Fischer, B., Schaffer, A.A., Mages, H.W., Kroczek, R.A. & Peter, H.H. (2003) Homozygous loss of ICOS is associated with adult-onset common variable immunodeficiency. *Nat Immunol,* **4,** 261-268.

Gu-Trantien, C., Loi, S., Garaud, S., Equeter, C., Libin, M., de Wind, A., Ravoet, M., Le Buanec, H., Sibille, C., Manfouo-Foutsop, G., Veys, I., Haibe-Kains, B., Singhal, S.K., Michiels, S., Rothe, F., Salgado, R., Duvillier, H., Ignatiadis, M., Desmedt, C., Bron, D., Larsimont, D., Piccart, M., Sotiriou, C. & Willard-Gallo, K. (2013) CD4(+) follicular helper T cell infiltration predicts breast cancer survival. *J Clin Invest,* **123,** 2873-2892.

Guadagnolo, B.A., Li, S., Neuberg, D., Ng, A., Hua, L., Silver, B., Stevenson, M.A. & Mauch, P. (2006) Long-term outcome and mortality trends in early-stage, Grade 1-2 follicular lymphoma treated with radiation therapy. *Int J Radiat Oncol Biol Phys,* **64,** 928-934.

Guilloton, F., Caron, G., Ménard, C., Pangault, C., Amé-Thomas, P., Dulong, J., De Vos, J., Rossille, D., Henry, C., Lamy, T., Fouquet, O., Fest, T. & Tarte, K. (2012) Mesenchymal stromal cells orchestrate follicular lymphoma cell niche through the CCL2-dependent recruitment and polarization of monocytes. *Blood,* **119,** 2556-2567.

Hale, J.S., Youngblood, B., Latner, D.R., Mohammed, A.U., Ye, L., Akondy, R.S., Wu, T., Iyer, S.S. & Ahmed, R. (2013) Distinct memory CD4+ T cells with commitment to T follicular helper- and T helper 1-cell lineages are generated after acute viral infection. *Immunity,* **38,** 805-817.

Hams, E., McCarron, M.J., Amu, S., Yagita, H., Azuma, M., Chen, L. & Fallon, P.G. (2011) Blockade of B7-H1 (Programmed Death Ligand 1) Enhances Humoral Immunity by Positively Regulating the Generation of T Follicular Helper Cells. *The Journal of Immunology,* **186,** 5648-5655.

Hanahan, D. & Weinberg, R.A. (2011) Hallmarks of cancer: the next generation. *Cell,* **144,** 646-674.

Hardianti, M.S., Tatsumi, E., Syampurnawati, M., Furuta, K., Saigo, K., Nakamachi, Y., Kumagai, S., Ohno, H., Tanabe, S., Uchida, M. & Yasuda, N. (2004) Activation-induced cytidine deaminase expression in follicular lymphoma: association between AID expression and ongoing mutation in FL. *Leukemia,* **18,** 826-831.

Havenar-Daughton, C., Carnathan, D.G., Torrents de la Peña, A., Pauthner, M., Briney, B., Reiss, S.M., Wood, J.S., Kaushik, K., van Gils, M.J., Rosales, S.L., van der Woude, P., Locci, M., Le, K.M., de Taeye, S.W., Sok, D., Mohammed, A.U.R., Huang, J., Gumber, S., Garcia, A., Kasturi, S.P., Pulendran, B., Moore, J.P., Ahmed, R., Seumois, G., Burton, D.R., Sanders, R.W., Silvestri, G. & Crotty, S. (2016) Direct Probing of Germinal Center Responses Reveals Immunological Features and Bottlenecks for Neutralizing Antibody Responses to HIV Env Trimer. *Cell Reports,* **17,** 2195-2209.

He, J., Tsai, L.M., Leong, Y.A., Hu, X., Ma, C.S., Chevalier, N., Sun, X., Vandenberg, K., Rockman, S., Ding, Y., Zhu, L., Wei, W., Wang, C., Karnowski, A., Belz, G.T., Ghali, J.R., Cook, M.C., Riminton, D.S., Veillette, A., Schwartzberg, P.L., Mackay, F., Brink, R., Tangye, S.G., Vinuesa, C.G., Mackay, C.R., Li, Z. & Yu, D. (2013) Circulating precursor CCR7(lo)PD-1(hi) CXCR5(+) CD4(+) T cells indicate Tfh cell activity and promote antibody responses upon antigen reexposure. *Immunity,* **39,** 770-781.

Hiddemann, W., Barbui, A.M., Canales, M.A., Cannell, P.K., Collins, G.P., Dürig, J., Forstpointner, R., Herold, M., Hertzberg, M., Klanova, M., Radford, J., Seymour, J.F., Tobinai, K., Trotman, J., Burciu, A., Fingerle-Rowson, G., Wolbers, M., Nielsen, T. & Marcus, R.E. (2018) Immunochemotherapy With Obinutuzumab or Rituximab for Previously Untreated Follicular Lymphoma in the GALLIUM Study: Influence of Chemotherapy on Efficacy and Safety. *Journal of Clinical Oncology,* **36,** 2395-2404.

Hiddemann, W., Kneba, M., Dreyling, M., Schmitz, N., Lengfelder, E., Schmits, R., Reiser, M., Metzner, B., Harder, H., Hegewisch-Becker, S., Fischer, T., Kropff, M., Reis, H.E., Freund, M., Wormann, B., Fuchs, R., Planker, M., Schimke, J., Eimermacher, H., Trumper, L., Aldaoud, A., Parwaresch, R. & Unterhalt, M. (2005) Frontline therapy with rituximab added to the combination of cyclophosphamide, doxorubicin, vincristine, and prednisone (CHOP) significantly improves the outcome for patients with advanced-stage follicular lymphoma compared with therapy with CHOP alone: results of a prospective randomized study of the German Low-Grade Lymphoma Study Group. *Blood,* **106,** 3725-3732.

Hilchey, S.P., De, A., Rimsza, L.M., Bankert, R.B. & Bernstein, S.H. (2007) Follicular Lymphoma Intratumoral CD4⁺CD25⁺GITR⁺ Regulatory T

Cells Potently Suppress CD3/CD28-Costimulated Autologous and Allogeneic CD8⁺CD25[−] and CD4⁺CD25[−] T Cells. *The Journal of Immunology,* **178,** 4051-4061.

Hilchey, S.P., Rosenberg, A.F., Hyrien, O., Secor-Socha, S., Cochran, M.R., Brady, M.T., Wang, J.C., Sanz, I., Burack, W.R., Quataert, S.A. & Bernstein, S.H. (2011) Follicular lymphoma tumor-infiltrating T-helper (T(H)) cells have the same polyfunctional potential as normal nodal T(H) cells despite skewed differentiation. *Blood,* **118,** 3591-3602.

Huet, S., Tesson, B., Jais, J.-P., Feldman, A.L., Magnano, L., Thomas, E., Traverse-Glehen, A., Albaud, B., Carrère, M., Xerri, L., Ansell, S.M., Baseggio, L., Reyes, C., Tarte, K., Boyault, S., Haioun, C., Link, B.K., Feugier, P., Lopez-Guillermo, A., Tilly, H., Brice, P., Hayette, S., Jardin, F., Offner, F., Sujobert, P., Gentien, D., Viari, A., Campo, E., Cerhan, J.R. & Salles, G. (2018) A gene-expression profiling score for prediction of outcome in patients with follicular lymphoma: a retrospective training and validation analysis in three international cohorts. *The Lancet Oncology,* **19,** 549-561.

Huet, S., Xerri, L., Tesson, B., Mareschal, S., Taix, S., Mescam-Mancini, L., Sohier, E., Carrère, M., Lazarovici, J., Casasnovas, O., Tonon, L., Boyault, S., Hayette, S., Haioun, C., Fabiani, B., Viari, A., Jardin, F. & Salles, G. (2017) EZH2 alterations in follicular lymphoma: biological and clinical correlations. *Blood cancer journal,* **7,** e555-e555.

Irish, J.M., Czerwinski, D.K., Nolan, G.P. & Levy, R. (2006) Altered B-cell receptor signaling kinetics distinguish human follicular lymphoma B cells from tumor-infiltrating nonmalignant B cells. *Blood,* **108,** 3135-3142.

Irish, J.M., Myklebust, J.H., Alizadeh, A.A., Houot, R., Sharman, J.P., Czerwinski, D.K., Nolan, G.P. & Levy, R. (2010) B-cell signaling networks reveal a negative prognostic human lymphoma cell subset that emerges during tumor progression. *Proceedings of the National Academy of Sciences,* **107,** 12747-12754.

Ise, W., Fujii, K., Shiroguchi, K., Ito, A., Kometani, K., Takeda, K., Kawakami, E., Yamashita, K., Suzuki, K., Okada, T. & Kurosaki, T. (2018) T Follicular Helper Cell-Germinal Center B Cell Interaction Strength Regulates Entry into Plasma Cell or Recycling Germinal Center Cell Fate. *Immunity,* **48,** 702-715.e704.

Jäger, U., Böcskör, S., Le, T., Mitterbauer, G., Bolz, I., Chott, A., Kneba, M., Mannhalter, C. & Nadel, B. (2000) Follicular lymphomas' BCL-2/IgH junctions contain templated nucleotide insertions: novel insights into the mechanism of t(14;18) translocation. *Blood,* **95,** 3520-3529.

Johl, A., Lengfelder, E., Hiddemann, W., Klapper, W. & Group, t.G.L.-g.L.S. (2016) Core needle biopsies and surgical excision biopsies in the diagnosis of lymphoma—experience at the Lymph Node Registry Kiel. *Annals of Hematology,* **95,** 1281-1286.

Johnston, R.J., Choi, Y.S., Diamond, J.A., Yang, J.A. & Crotty, S. (2012) STAT5 is a potent negative regulator of TFH cell differentiation. *J Exp Med,* **209,** 243-250.

Johnston, R.J., Poholek, A.C., DiToro, D., Yusuf, I., Eto, D., Barnett, B., Dent, A.L., Craft, J. & Crotty, S. (2009) Bcl6 and Blimp-1 are reciprocal and antagonistic regulators of T follicular helper cell differentiation. *Science,* **325,** 1006-1010.

Junlen, H.R., Peterson, S., Kimby, E., Lockmer, S., Linden, O., Nilsson-Ehle, H., Erlanson, M., Hagberg, H., Radlund, A., Hagberg, O. & Wahlin, B.E. (2015) Follicular lymphoma in Sweden: nationwide improved survival in the rituximab era, particularly in elderly women: a Swedish Lymphoma Registry study. *Leukemia,* **29,** 668-676.

Jurinovic, V., Kridel, R., Staiger, A.M., Szczepanowski, M., Horn, H., Dreyling, M.H., Rosenwald, A., Ott, G., Klapper, W., Zelenetz, A.D., Barr, P.M., Friedberg, J.W., Ansell, S., Sehn, L.H., Connors, J.M., Gascoyne, R.D., Hiddemann, W., Unterhalt, M., Weinstock, D.M. & Weigert, O. (2016) Clinicogenetic risk models predict early progression of follicular lymphoma after first-line immunochemotherapy. *Blood,* **128,** 1112-1120.

Kagami, Y., Jung, J., Choi, Y.S., Osumi, K., Nakamura, S., Morishima, Y. & Seto, M. (2001) Establishment of a follicular lymphoma cell line (FLK-1) dependent on follicular dendritic cell-like cell line HK. *Leukemia,* **15,** 148-156.

Kiaii, S., Clear, A.J., Ramsay, A.G., Davies, D., Sangaralingam, A., Lee, A., Calaminici, M., Neuberg, D.S. & Gribben, J.G. (2013) Follicular lymphoma cells induce changes in T-cell gene expression and function: potential impact on survival and risk of transformation. *J Clin Oncol,* **31,** 2654-2661.

Klapper, W., Hoster, E., Rölver, L., Schrader, C., Janssen, D., Tiemann, M., Bernd, H.-W., Determann, O., Hansmann, M.-L., Möller, P., Feller, A., Stein, H., Wacker, H.-H., Dreyling, M., Unterhalt, M., Hiddemann, W. & Ott, G. (2007) Tumor Sclerosis but Not Cell Proliferation or Malignancy Grade Is a Prognostic Marker in Advanced-Stage Follicular Lymphoma: The German Low Grade Lymphoma Study Group. *Journal of Clinical Oncology,* **25,** 3330-3336.

Konforte, D., Simard, N. & Paige, C.J. (2009) IL-21: An Executor of B Cell Fate. *The Journal of Immunology,* **182,** 1781-1787.

Launay, E., Pangault, C., Bertrand, P., Jardin, F., Lamy, T., Tilly, H., Tarte, K., Bastard, C. & Fest, T. (2012) High rate of TNFRSF14 gene alterations related to 1p36 region in de novo follicular lymphoma and impact on prognosis. *Leukemia,* **26,** 559-562.

Laurent, C., Charmpi, K., Gravelle, P., Tosolini, M., Franchet, C., Ysebaert, L., Brousset, P., Bidaut, A., Ycart, B. & Fournie, J.J. (2015) Several immune escape patterns in non-Hodgkin's lymphomas. *Oncoimmunology,* **4,** e1026530.

Laurent, C., Müller, S., Do, C., Al-Saati, T., Allart, S., Larocca, L.M., Hohaus, S., Duchez, S., Quillet-Mary, A., Laurent, G., Brousset, P. & Valitutti, S. (2011) Distribution, function, and prognostic value of cytotoxic T lymphocytes in follicular lymphoma: a 3-D tissue-imaging study. *Blood,* **118,** 5371-5379.

Le, K.-S., Thibult, M.-L., Just-Landi, S., Pastor, S., Gondois-Rey, F., Granjeaud, S., Broussais, F., Bouabdallah, R., Colisson, R., Caux, C., Ménétrier-Caux, C., Leroux, D., Xerri, L. & Olive, D. (2016) Follicular B Lymphomas Generate Regulatory T Cells via the ICOS/ICOSL Pathway and Are Susceptible to Treatment by Anti-ICOS/ICOSL Therapy. *Cancer Research,* **76,** 4648-4660.

Lee, J.-Y., Skon, C.N., Lee, Y.J., Oh, S., Taylor, J.J., Malhotra, D., Jenkins, M.K., Rosenfeld, M.G., Hogquist, K.A. & Jameson, S.C. (2015) The transcription factor KLF2 restrains $CD4^+$ T follicular helper cell differentiation. *Immunity,* **42,** 252-264.

Lefebvre, J.S. & Haynes, L. (2012) Aging of the CD4 T Cell Compartment. *Open Longev Sci,* **6,** 83-91.

Leonard, J.P., Trneny, M., Izutsu, K., Fowler, N.H., Hong, X., Zhu, J., Zhang, H., Offner, F., Scheliga, A., Nowakowski, G.S., Pinto, A., Re, F., Fogliatto, L.M., Scheinberg, P., Flinn, I.W., Moreira, C., Cabeçadas, J., Liu, D., Kalambakas, S., Fustier, P., Wu, C., Gribben, J.G. & Investigators, f.t.A.T. (2019) AUGMENT: A Phase III Study of Lenalidomide Plus Rituximab Versus Placebo Plus Rituximab in Relapsed or Refractory Indolent Lymphoma. *Journal of Clinical Oncology,* **37,** 1188-1199.

Lesokhin, A.M., Ansell, S.M., Armand, P., Scott, E.C., Halwani, A., Gutierrez, M., Millenson, M.M., Cohen, A.D., Schuster, S.J., Lebovic, D., Dhodapkar, M., Avigan, D., Chapuy, B., Ligon, A.H., Freeman, G.J., Rodig, S.J., Cattry, D., Zhu, L., Grosso, J.F., Garelik, M.B.B., Shipp, M.A., Borrello, I. & Timmerman, J. (2016) Nivolumab in Patients With Relapsed or Refractory Hematologic Malignancy: Preliminary Results of a Phase Ib Study. *Journal of Clinical Oncology,* **34,** 2698-2704.

Limpens, J., Stad, R., Vos, C., Devlaam, C., Dejong, D., Vanommen, G.J.B., Schuuring, E. & Kluin, P.M. (1995) Lymphoma-Associated Translocation T(14-18) in Blood B-Cells of Normal Individuals. *Blood,* **85,** 2528-2536.

Link, B.K., Maurer, M.J., Nowakowski, G.S., Ansell, S.M., Macon, W.R., Syrbu, S.I., Slager, S.L., Thompson, C.A., Inwards, D.J., Johnston, P.B., Colgan, J.P., Witzig, T.E., Habermann, T.M. & Cerhan, J.R. (2013) Rates and outcomes of follicular lymphoma transformation in the immunochemotherapy era: a report from the University of Iowa/MayoClinic Specialized Program of Research Excellence Molecular Epidemiology Resource. *J Clin Oncol,* **31,** 3272-3278.

Linterman, M.A., Pierson, W., Lee, S.K., Kallies, A., Kawamoto, S., Rayner, T.F., Srivastava, M., Divekar, D.P., Beaton, L., Hogan, J.J., Fagarasan, S., Liston, A., Smith, K.G.C. & Vinuesa, C.G. (2011) Foxp3+ follicular regulatory T cells control the germinal center response. *Nature Medicine,* **17,** 975.

Liu, D., Xu, H., Shih, C., Wan, Z., Ma, X., Ma, W., Luo, D. & Qi, H. (2014) T–B-cell entanglement and ICOSL-driven feed-forward regulation of germinal centre reaction. *Nature,* **517,** 214.

Liu, Y.F., Hernandez, A.M., Shibata, D. & Cortopassi, G.A. (1994) Bcl2 Translocation Frequency Rises with Age in Humans. *Proceedings of the National Academy of Sciences of the United States of America,* **91,** 8910-8914.

Locci, M., Wu, J.E., Arumemi, F., Mikulski, Z., Dahlberg, C., Miller, A.T. & Crotty, S. (2016) Activin A programs the differentiation of human TFH cells. *Nature Immunology,* **17,** 976.

Loeffler, M., Kreuz, M., Haake, A., Hasenclever, D., Trautmann, H., Arnold, C., Winter, K., Koch, K., Klapper, W., Scholtysik, R., Rosolowski, M., Hoffmann, S., Ammerpohl, O., Szczepanowski, M., Herrmann, D., Küppers, R., Pott, C. & Siebert, R. (2014) Genomic and epigenomic co-evolution in follicular lymphomas. *Leukemia,* **29,** 456.

Lownik, J.C., Luker, A.J., Damle, S.R., Cooley, L.F., El Sayed, R., Hutloff, A., Pitzalis, C., Martin, R.K., El Shikh, M.E.M. & Conrad, D.H. (2017) ADAM10-Mediated ICOS Ligand Shedding on B Cells Is Necessary for Proper T Cell ICOS Regulation and T Follicular Helper Responses. *The Journal of Immunology,* **199,** 2305-2315.

Lu, K.T., Kanno, Y., Cannons, J.L., Handon, R., Bible, P., Elkahloun, A.G., Anderson, S.M., Wei, L., Sun, H., O'Shea, J.J. & Schwartzberg, P.L. (2011) Functional and epigenetic studies reveal multistep differentiation and plasticity of in vitro-generated and in vivo-derived follicular T helper cells. *Immunity,* **35,** 622-632.

Luo, W., Weisel, F. & Shlomchik, M.J. (2018) B Cell Receptor and CD40 Signaling Are Rewired for Synergistic Induction of the c-Myc Transcription Factor in Germinal Center B Cells. *Immunity,* **48,** 313-326.e315.

Ma, C.S. & Deenick, E.K. (2014) Human T follicular helper (Tfh) cells and disease. *Immunology and Cell Biology,* **92,** 64-71.

Ma, C.S., Suryani, S., Avery, D.T., Chan, A., Nanan, R., Santner-Nanan, B., Deenick, E.K. & Tangye, S.G. (2009) Early commitment of naive human CD4(+) T cells to the T follicular helper (T-FH) cell lineage is induced by IL-12. *Immunology and Cell Biology,* **87,** 590-600.

Mac Manus, M.P. & Hoppe, R.T. (1996) Is radiotherapy curative for stage I and II low-grade follicular lymphoma? Results of a long-term follow-up study of patients treated at Stanford University. *J Clin Oncol,* **14,** 1282-1290.

Mamand, S., Carr, M., Allchin, R.L., Ahearne, M.J. & Wagner, S.D. (2019) Interleukin-2-inducible T-cell kinase inhibitors modify functional polarization of human peripheral T-cell lymphoma cells. *Blood advances,* **3,** 705-710.

Marafioti, T., Copie-Bergman, C., Calaminici, M., Paterson, J.C., Shende, V.H., Liu, H., Baia, M., Ramsay, A.D., Agostinelli, C., Briere, J., Clear, A., Du, M.Q., Piccaluga, P.P., Masir, N., Nacheva, E.P., Sujobert, P., Shanmugam, K., Grogan, T.M., Brooks, S.P., Khwaja, A., Ardeshna, K., Townsend, W., Pileri, S.A., Haioun, C., Linch, D., Gribben, J.G., Gaulard, P. & Isaacson, P.G. (2013) Another look at follicular lymphoma: immunophenotypic and molecular analyses identify distinct follicular lymphoma subgroups. *Histopathology,* **62,** 860-875.

Marcus, R., Davies, A., Ando, K., Klapper, W., Opat, S., Owen, C., Phillips, E., Sangha, R., Schlag, R., Seymour, J.F., Townsend, W., Trněný, M., Wenger, M., Fingerle-Rowson, G., Rufibach, K., Moore, T., Herold, M. & Hiddemann, W. (2017) Obinutuzumab for the First-Line Treatment of Follicular Lymphoma. *New England Journal of Medicine,* **377,** 1331-1344.

Marcus, R., Imrie, K., Solal-Celigny, P., Catalano, J.V., Dmoszynska, A., Raposo, J.C., Offner, F.C., Gomez-Codina, J., Belch, A., Cunningham, D., Wassner-Fritsch, E. & Stein, G. (2008) Phase III study of R-CVP compared with cyclophosphamide, vincristine, and prednisone alone in patients with previously untreated advanced follicular lymphoma. *J Clin Oncol,* **26,** 4579-4586.

Martin, A., Bardwell, P.D., Woo, C.J., Fan, M., Shulman, M.J. & Scharff, M.D. (2002) Activation-induced cytidine deaminase turns on somatic hypermutation in hybridomas. *Nature,* **415,** 802-806.

Maurer, M.J., Bachy, E., Ghesquières, H., Ansell, S.M., Nowakowski, G.S., Thompson, C.A., Inwards, D.J., Allmer, C., Chassagne-Clément, C., Nicolas-Virelizier, E., Sebban, C., Lebras, L., Sarkozy, C., Macon, W.R., Feldman, A.L., Syrbu, S.I., Traverse-Glehan, A., Coiffier, B., Slager, S.L., Weiner, G.J., Witzig, T.E., Habermann, T.M., Salles, G., Cerhan, J.R. & Link, B.K. (2016) Early event status informs subsequent outcome in newly diagnosed follicular lymphoma. *American Journal of Hematology,* **91,** 1096-1101.

McDonnell, T.J. & Korsmeyer, S.J. (1991) Progression from lymphoid hyperplasia to high-grade malignant lymphoma in mice transgenic for the t(14; 18). *Nature,* **349,** 254-256.

McGuire, H.M., Vogelzang, A., Warren, J., Loetsch, C., Natividad, K.D., Chan, T.D., Brink, R., Batten, M. & King, C. (2015) IL-21 and IL-4 Collaborate To Shape T-Dependent Antibody Responses. *The Journal of Immunology,* **195,** 5123-5135.

Meignan, M., Cottereau, A.S., Versari, A., Chartier, L., Dupuis, J., Boussetta, S., Grassi, I., Casasnovas, R.-O., Haioun, C., Tilly, H., Tarantino, V., Dubreuil, J., Federico, M., Salles, G., Luminari, S. & Trotman, J. (2016) Baseline Metabolic Tumor Volume Predicts Outcome in High–Tumor-Burden Follicular Lymphoma: A Pooled Analysis of Three Multicenter Studies. *Journal of Clinical Oncology,* **34,** 3618-3626.

Menter, T., Bodmer-Haecki, A., Dirnhofer, S. & Tzankov, A. (2016) Evaluation of the diagnostic and prognostic value of PDL1 expression in Hodgkin and B-cell lymphomas. *Hum Pathol,* **54,** 17-24.

Mintz, M.A., Felce, J.H., Chou, M.Y., Mayya, V., Xu, Y., Shui, J.-W., An, J., Li, Z., Marson, A., Okada, T., Ware, C.F., Kronenberg, M., Dustin, M.L. & Cyster, J.G. (2019) The HVEM-BTLA Axis Restrains T Cell Help to Germinal Center B Cells and Functions as a Cell-Extrinsic Suppressor in Lymphomagenesis. *Immunity*.

Morin, R.D., Mendez-Lago, M., Mungall, A.J., Goya, R., Mungall, K.L., Corbett, R.D., Johnson, N.A., Severson, T.M., Chiu, R., Field, M., Jackman, S., Krzywinski, M., Scott, D.W., Trinh, D.L., Tamura-Wells, J., Li, S., Firme, M.R., Rogic, S., Griffith, M., Chan, S., Yakovenko, O., Meyer, I.M., Zhao, E.Y., Smailus, D., Moksa, M., Chittaranjan, S., Rimsza, L., Brooks-Wilson, A., Spinelli, J.J., Ben-Neriah, S., Meissner, B., Woolcock, B., Boyle, M., McDonald, H., Tam, A., Zhao, Y., Delaney, A., Zeng, T., Tse, K., Butterfield, Y., Birol, I., Holt, R., Schein, J., Horsman, D.E., Moore, R., Jones, S.J., Connors, J.M., Hirst, M., Gascoyne, R.D. & Marra, M.A. (2011) Frequent mutation of histone-modifying genes in non-Hodgkin lymphoma. *Nature,* **476,** 298-303.

Morita, R., Schmitt, N., Bentebibel, S.E., Ranganathan, R., Bourdery, L., Zurawski, G., Foucat, E., Dullaers, M., Oh, S., Sabzghabaei, N., Lavecchio, E.M., Punaro, M., Pascual, V., Banchereau, J. & Ueno, H. (2011) Human blood CXCR5(+)CD4(+) T cells are counterparts of T follicular cells and contain specific subsets that differentially support antibody secretion. *Immunity,* **34,** 108-121.

Morschhauser, F., Fowler, N.H., Feugier, P., Bouabdallah, R., Tilly, H., Palomba, M.L., Fruchart, C., Libby, E.N., Casasnovas, R.-O., Flinn, I.W., Haioun, C., Maisonneuve, H., Ysebaert, L., Bartlett, N.L., Bouabdallah, K., Brice, P., Ribrag, V., Daguindau, N., Le Gouill, S., Pica, G.M., Martin Garcia-Sancho, A., López-Guillermo, A., Larouche, J.-F., Ando, K., Gomes da Silva, M., André, M., Zachée, P., Sehn, L.H., Tobinai, K., Cartron, G., Liu, D., Wang, J., Xerri, L. & Salles, G.A. (2018) Rituximab plus Lenalidomide in Advanced Untreated Follicular Lymphoma. *New England Journal of Medicine,* **379,** 934-947.

Mourcin, F., Pangault, C., Amin-Ali, R., Ame-Thomas, P. & Tarte, K. (2012) Stromal cell contribution to human follicular lymphoma pathogenesis. *Front Immunol,* **3,** 280.

Munoz-Fontela, C., Mandinova, A., Aaronson, S.A. & Lee, S.W. (2016) Emerging roles of p53 and other tumour-suppressor genes in immune regulation. *Nat Rev Immunol,* **16,** 741-750.

Muramatsu, M., Kinoshita, K., Fagarasan, S., Yamada, S., Shinkai, Y. & Honjo, T. (2000) Class switch recombination and hypermutation require activation-induced cytidine deaminase (AID), a potential RNA editing enzyme. *Cell,* **102,** 553-563.

Myklebust, J.H., Irish, J.M., Brody, J., Czerwinski, D.K., Houot, R., Kohrt, H.E., Timmerman, J., Said, J., Green, M.R., Delabie, J., Kolstad, A., Alizadeh, A.A. & Levy, R. (2013) High PD-1 expression and suppressed cytokine signaling distinguish T cells infiltrating follicular lymphoma tumors from peripheral T cells. *Blood,* **121,** 1367-1376.

Ng, K.W., Marshall, E.A., Enfield, K.S.S., Martin, S.D., Milne, K., Pewarchuk, M.E., Abraham, N. & Lam, W.L. (2018) Somatic mutation-associated T follicular helper cell elevation in lung adenocarcinoma. *Oncoimmunology,* **7,** e1504728.

Nurieva, R.I., Chung, Y., Martinez, G.J., Yang, X.O., Tanaka, S., Matskevitch, T.D., Wang, Y.H. & Dong, C. (2009) Bcl6 mediates the development of T follicular helper cells. *Science,* **325,** 1001-1005.

Nurieva, R.I., Chuvpilo, S., Wieder, E.D., Elkon, K.B., Locksley, R., Serfling, E. & Dong, C. (2007) A Costimulation-Initiated Signaling Pathway Regulates NFATc1 Transcription in T Lymphocytes. *The Journal of Immunology,* **179,** 1096-1103.

O'Shea, D., O'Riain, C., Taylor, C., Waters, R., Carlotti, E., MacDougall, F., Gribben, J., Rosenwald, A., Ott, G., Rimsza, L.M., Smeland, E.B., Johnson, N., Campo, E., Greiner, T.C., Chan, W.C., Gascoyne, R.D., Wright, G., Staudt, L.M., Lister, T.A. & Fitzgibbon, J. (2008) The presence of TP53 mutation at diagnosis of follicular lymphoma identifies a high-risk group of patients with shortened time to disease progression and poorer overall survival. *Blood,* **112,** 3126-3129.

Okosun, J., Bodor, C., Wang, J., Araf, S., Yang, C.Y., Pan, C., Boller, S., Cittaro, D., Bozek, M., Iqbal, S., Matthews, J., Wrench, D., Marzec, J., Tawana, K., Popov, N., O'Riain, C., O'Shea, D., Carlotti, E., Davies, A., Lawrie, C.H., Matolcsy, A., Calaminici, M., Norton, A., Byers, R.J., Mein, C., Stupka, E., Lister, T.A., Lenz, G., Montoto, S., Gribben, J.G., Fan, Y., Grosschedl, R., Chelala, C. & Fitzgibbon, J. (2014) Integrated genomic analysis identifies recurrent mutations and evolution patterns driving the initiation and progression of follicular lymphoma. *Nat Genet,* **46,** 176-181.

Ortega-Molina, A., Boss, I.W., Canela, A., Pan, H., Jiang, Y., Zhao, C., Jiang, M., Hu, D., Agirre, X., Niesvizky, I., Lee, J.E., Chen, H.T., Ennishi, D., Scott, D.W., Mottok, A., Hother, C., Liu, S., Cao, X.J., Tam, W., Shaknovich, R., Garcia, B.A., Gascoyne, R.D., Ge, K., Shilatifard, A., Elemento, O., Nussenzweig, A., Melnick, A.M. & Wendel, H.G. (2015) The histone lysine methyltransferase KMT2D sustains a gene expression program that represses B cell lymphoma development. *Nat Med,* **21,** 1199-1208.

Otero, D.C., Anzelon, A.N. & Rickert, R.C. (2003) CD19 Function in Early and Late B Cell Development: I. Maintenance of Follicular and Marginal Zone B Cells Requires CD19-Dependent Survival Signals. *The Journal of Immunology,* **170,** 73-83.

Pandey, S., Mourcin, F., Marchand, T., Nayar, S., Guirriec, M., Pangault, C., Monvoisin, C., Amé-Thomas, P., Guilloton, F., Dulong, J., Coles, M., Fest, T., Mottok, A., Barone, F. & Tarte,

K. (2017) IL-4/CXCL12 loop is a key regulator of lymphoid stroma function in follicular lymphoma. *Blood*.

Pangault, C., Ame-Thomas, P., Ruminy, P., Rossille, D., Caron, G., Baia, M., De Vos, J., Roussel, M., Monvoisin, C., Lamy, T., Tilly, H., Gaulard, P., Tarte, K. & Fest, T. (2010) Follicular lymphoma cell niche: identification of a preeminent IL-4-dependent T(FH)-B cell axis. *Leukemia,* **24,** 2080-2089.

Papa, I., Saliba, D., Ponzoni, M., Bustamante, S., Canete, P.F., Gonzalez-Figueroa, P., McNamara, H.A., Valvo, S., Grimbaldeston, M., Sweet, R.A., Vohra, H., Cockburn, I.A., Meyer-Hermann, M., Dustin, M.L., Doglioni, C. & Vinuesa, C.G. (2017) TFH-derived dopamine accelerates productive synapses in germinal centres. *Nature,* **547,** 318.

Pasikowska, M., Walsby, E., Apollonio, B., Cuthill, K., Phillips, E., Coulter, E., Longhi, M.S., Ma, Y., Yallop, D., Barber, L.D., Patten, P., Fegan, C., Ramsay, A.G., Pepper, C., Devereux, S. & Buggins, A.G. (2016) Phenotype and immune function of lymph node and peripheral blood CLL cells are linked to transendothelial migration. *Blood,* **128,** 563-573.

Pasqualucci, L., Bhagat, G., Jankovic, M., Compagno, M., Smith, P., Muramatsu, M., Honjo, T., Morse, H.C., 3rd, Nussenzweig, M.C. & Dalla-Favera, R. (2008) AID is required for germinal center-derived lymphomagenesis. *Nat Genet,* **40,** 108-112.

Pasqualucci, L., Bhagat, G., Jankovic, M., Compagno, M., Smith, P., Muramatsu, M., Honjo, T., Morse Iii, H.C., Nussenzweig, M.C. & Dalla-Favera, R. (2007) AID is required for germinal center–derived lymphomagenesis. *Nature Genetics,* **40,** 108.

Pasqualucci, L., Khiabanian, H., Fangazio, M., Vasishtha, M., Messina, M., Holmes, A.B., Ouillette, P., Trifonov, V., Rossi, D., Tabbo, F., Ponzoni, M., Chadburn, A., Murty, V.V., Bhagat, G., Gaidano, G., Inghirami, G., Malek, S.N., Rabadan, R. & Dalla-Favera, R. (2014) Genetics of follicular lymphoma transformation. *Cell Rep,* **6,** 130-140.

Pastore, A., Jurinovic, V., Kridel, R., Hoster, E., Staiger, A.M., Szczepanowski, M., Pott, C., Kopp, N., Murakami, M., Horn, H., Leich, E., Moccia, A.A., Mottok, A., Sunkavalli, A., Van Hummelen, P., Ducar, M., Ennishi, D., Shulha, H.P., Hother, C., Connors, J.M., Sehn, L.H., Dreyling, M., Neuberg, D., Möller, P., Feller, A.C., Hansmann, M.L., Stein, H., Rosenwald, A., Ott, G., Klapper, W., Unterhalt, M., Hiddemann, W., Gascoyne, R.D., Weinstock, D.M. & Weigert, O. (2015) Integration of gene mutations in risk prognostication for patients receiving first-line immunochemotherapy for follicular lymphoma: a retrospective analysis of a prospective clinical trial and validation in a population-based registry. *The Lancet Oncology,* **16,** 1111-1122.

Petersen, P.M., Gospodarowicz, M., Tsang, R., Pintilie, M., Wells, W., Hodgson, D., Sun, A., Crump, M., Patterson, B. & Bailey, D. (2004) Long-term outcome in stage I and II follicular lymphoma following treatment with involved field radiation therapy alone. *Journal of Clinical Oncology,* **22,** 6521-6521.

Pott, C., Hoster, E., Kehden, B., Unterhalt, M., Herold, M., van der Jagt, R.H., Janssens, A., Kneba, M., Mayer, J., Pocock, C., Danesi, N., Fingerle-Rowson, G., Harbron, C., Mundt, K., Marcus, R.E. & Hiddemann, W. (2016) Minimal Residual Disease in Patients with Follicular Lymphoma Treated with Obinutuzumab or Rituximab As First-Line Induction Immunochemotherapy and Maintenance in the Phase 3 GALLIUM Study. *Blood,* **128,** 613-613.

Qi, H., Cannons, J.L., Klauschen, F., Schwartzberg, P.L. & Germain, R.N. (2008) SAP-controlled T-B cell interactions underlie germinal centre formation. *Nature,* **455,** 764-769.

Rajnai, H., Bodor, C., Balogh, Z., Gagyi, E., Csomor, J., Krenacs, T., Toth, E. & Matolcsy, A. (2012) Impact of the reactive microenvironment on the bone marrow involvement of follicular lymphoma. *Histopathology,* **60,** E66-75.

Ramiro, A.R., Jankovic, M., Eisenreich, T., Difilippantonio, S., Chen-Kiang, S., Muramatsu, M., Honjo, T., Nussenzweig, A. & Nussenzweig, M.C. (2004) AID is required for c-myc/IgH chromosome translocations in vivo. *Cell,* **118,** 431-438.

Ramsay, A.G., Clear, A.J., Kelly, G., Fatah, R., Matthews, J., Macdougall, F., Lister, T.A., Lee, A.M., Calaminici, M. & Gribben, J.G. (2009) Follicular lymphoma cells induce T-cell immunologic synapse dysfunction that can be repaired with lenalidomide: implications for the tumor microenvironment and immunotherapy. *Blood,* **114,** 4713-4720.

Ratner, L., Waldmann, T.A., Janakiram, M. & Brammer, J.E. (2018) Rapid Progression of Adult T-Cell Leukemia–Lymphoma after PD-1 Inhibitor Therapy. *New England Journal of Medicine,* **378,** 1947-1948.

Revy, P., Muto, T., Levy, Y., Geissmann, F., Plebani, A., Sanal, O., Catalan, N., Forveille, M., Dufourcq-Labelouse, R., Gennery, A., Tezcan, I., Ersoy, F., Kayserili, H., Ugazio, A.G., Brousse, N., Muramatsu, M., Notarangelo, L.D., Kinoshita, K., Honjo, T., Fischer, A. & Durandy, A. (2000) Activation-induced cytidine deaminase (AID) deficiency causes the autosomal recessive form of the Hyper-IgM syndrome (HIGM2). *Cell,* **102,** 565-575.

Richendollar, B.G., Pohlman, B., Elson, P. & Hsi, E.D. (2011) Follicular programmed death 1-positive lymphocytes in the tumor microenvironment are an independent prognostic factor in follicular lymphoma. *Hum Pathol,* **42,** 552-557.

Rohr, J., Guo, S., Huo, J., Bouska, A., Lachel, C., Li, Y., Simone, P.D., Zhang, W., Gong, Q., Wang, C., Cannon, A., Heavican, T., Mottok, A., Hung, S., Rosenwald, A., Gascoyne, R., Fu, K., Greiner, T.C., Weisenburger, D.D., Vose, J.M., Staudt, L.M., Xiao, W., Borgstahl, G.E.O., Davis, S., Steidl, C., McKeithan, T., Iqbal, J. & Chan, W.C. (2016) Recurrent activating mutations of CD28 in peripheral T-cell lymphomas. *Leukemia,* **30,** 1062-1070.

Rolf, J., Bell, S.E., Kovesdi, D., Janas, M.L., Soond, D.R., Webb, L.M., Santinelli, S., Saunders, T., Hebeis, B., Killeen, N., Okkenhaug, K. & Turner, M. (2010) Phosphoinositide 3-kinase activity in T cells regulates the magnitude of the germinal center reaction. *J Immunol,* **185,** 4042-4052.

Rummel, M.J., Niederle, N., Maschmeyer, G., Banat, G.A., von Grunhagen, U., Losem, C., Kofahl-Krause, D., Heil, G., Welslau, M., Balser, C., Kaiser, U., Weidmann, E., Durk, H., Ballo, H., Stauch, M., Roller, F., Barth, J., Hoelzer, D., Hinke, A., Brugger, W. & Study group indolent, L. (2013) Bendamustine plus rituximab versus CHOP plus rituximab as first-line treatment for patients with indolent and mantle-cell lymphomas: an open-label, multicentre, randomised, phase 3 non-inferiority trial. *Lancet,* **381,** 1203-1210.

Sage, P.T., Francisco, L.M., Carman, C.V. & Sharpe, A.H. (2013) The receptor PD-1 controls follicular regulatory T cells in the lymph nodes and blood. *Nat Immunol,* **14,** 152-161.

Sakata-Yanagimoto, M., Enami, T., Yoshida, K., Shiraishi, Y., Ishii, R., Miyake, Y., Muto, H., Tsuyama, N., Sato-Otsubo, A., Okuno, Y., Sakata, S., Kamada, Y., Nakamoto-Matsubara, R., Tran, N.B., Izutsu, K., Sato, Y., Ohta, Y., Furuta, J., Shimizu, S., Komeno, T., Sato, Y., Ito, T., Noguchi, M., Noguchi, E., Sanada, M., Chiba, K., Tanaka, H., Suzukawa, K., Nanmoku, T., Hasegawa, Y., Nureki, O., Miyano, S., Nakamura, N., Takeuchi, K., Ogawa, S. & Chiba, S. (2014) Somatic RHOA mutation in angioimmunoblastic T cell lymphoma. *Nature Genetics,* **46,** 171.

Salek-Ardakani, S., Choi, Y.S., Rafii-El-Idrissi Benhnia, M., Flynn, R., Arens, R., Shoenberger, S., Crotty, S., Croft, M. & Salek-Ardakani, S. (2011) B Cell-Specific Expression of B7-2 Is Required for Follicular Th Cell Function in Response to Vaccinia Virus. *The Journal of Immunology,* **186,** 5294-5303.

Salles, G., Seymour, J.F., Offner, F., Lopez-Guillermo, A., Belada, D., Xerri, L., Feugier, P., Bouabdallah, R., Catalano, J.V., Brice, P., Caballero, D., Haioun, C., Pedersen, L.M., Delmer, A., Simpson, D., Leppa, S., Soubeyran, P., Hagenbeek, A., Casasnovas, O., Intragumtornchai, T., Ferme, C., da Silva, M.G., Sebban, C., Lister, A., Estell, J.A., Milone, G., Sonet, A., Mendila, M., Coiffier, B. & Tilly, H. (2011) Rituximab maintenance for 2 years in patients with high tumour burden follicular lymphoma responding to rituximab plus chemotherapy (PRIMA): a phase 3, randomised controlled trial. *Lancet,* **377,** 42-51.

Sant, M., Minicozzi, P., Mounier, M., Anderson, L.A., Brenner, H., Holleczek, B., Marcos-Gragera, R., Maynadie, M., Monnereau, A., Osca-Gelis, G., Visser, O., De Angelis, R. & Group, E.-W. (2014) Survival for haematological malignancies in Europe between 1997 and 2008 by region and age: results of EUROCARE-5, a population-based study. *Lancet Oncol,* **15,** 931-942.

Sarkozy, C., Link, B., Ghesquieres, H., Maurer, M., Nicolas-Virelizier, E., Thompson, C., Traverse-Glehen, A., Feldman, A., Allmer, C., Slager, S., Ansell, S., Habermann, T., Bachy, E., Cerhan, J. & Salles, G. (2017) CAUSE OF DEATH IN FOLLICULAR LYMPHOMA IN THE RITUXIMAB ERA: A POOLED ANALYSIS OF FRENCH AND US COHORTS. *Hematological Oncology,* **35,** 34-35.

Sarkozy, C., Trneny, M., Xerri, L., Wickham, N., Feugier, P., Leppa, S., Brice, P., Soubeyran, P., Gomes Da Silva, M., Mounier, C., Offner, F., Dupuis, J., Caballero, D., Canioni, D., Paula, M., Delarue, R., Zachee, P., Seymour, J., Salles, G. & Tilly, H. (2016) Risk Factors and Outcomes for Patients With Follicular Lymphoma Who Had Histologic Transformation After Response to First-Line Immunochemotherapy in the PRIMA Trial. *J Clin Oncol,* **34,** 2575-2582.

Sayin, I., Radtke, A.J., Vella, L.A., Jin, W., Wherry, E.J., Buggert, M., Betts, M.R., Herati, R.S., Germain, R.N. & Canaday, D.H. (2018) Spatial distribution and function of T follicular regulatory cells in human lymph nodes. *The Journal of Experimental Medicine,* **215,** 1531-1542.

Schaerli, P., Willimann, K., Lang, A.B., Lipp, M., Loetscher, P. & Moser, B. (2000) Cxc Chemokine Receptor 5 Expression Defines Follicular Homing T Cells with B Cell Helper Function. *The Journal of Experimental Medicine,* **192,** 1553-1562.

Schapiro, D., Jackson, H.W., Raghuraman, S., Fischer, J.R., Zanotelli, V.R.T., Schulz, D., Giesen, C., Catena, R., Varga, Z. & Bodenmiller, B. (2017) histoCAT: analysis of cell phenotypes and interactions in multiplex image cytometry data. *Nature Methods,* **14,** 873.

Scherer, F., Navarrete, M.A., Bertinetti-Lapatki, C., Boehm, J., Schmitt-Graeff, A. & Veelken, H. (2016) Isotype-switched follicular lymphoma displays dissociation between activation-induced cytidine deaminase expression and somatic hypermutation. *Leuk Lymphoma,* **57,** 151-160.

Schmitt, N., Bentebibel, S.-E. & Ueno, H. (2014a) Phenotype and functions of memory Tfh cells in human blood. *Trends in Immunology,* **35,** 436-442.

Schmitt, N., Bentebibel, S.E. & Ueno, H. (2014b) Phenotype and functions of memory Tfh cells in human blood. *Trends Immunol,* **35,** 436-442.

Schmitt, N., Liu, Y., Bentebibel, S.E., Munagala, I., Bourdery, L., Venuprasad, K., Banchereau, J. & Ueno, H. (2014c) The cytokine TGF-beta co-opts signaling via STAT3-STAT4 to promote the differentiation of human TFH cells. *Nat Immunol,* **15,** 856-865.

Schulz, D., Zanotelli, V.R.T., Fischer, J.R., Schapiro, D., Engler, S., Lun, X.-K., Jackson, H.W. & Bodenmiller, B. (2018) Simultaneous Multiplexed Imaging of mRNA and Proteins with Subcellular Resolution in Breast Cancer Tissue Samples by Mass Cytometry. *Cell Systems,* **6,** 25-36.e25.

Shi, J., Hou, S., Fang, Q., Liu, X., Liu, X. & Qi, H. (2018a) PD-1 Controls Follicular T Helper Cell Positioning and Function. *Immunity,* **49,** 264-274.e264.

Shi, Q., Flowers, C.R., Hiddemann, W., Marcus, R., Herold, M., Hagenbeek, A., Kimby, E., Hochster, H., Vitolo, U., Peterson, B.A., Gyan, E., Ghielmini, M., Nielsen, T., Bedout, S.D., Fu, T., Valente, N., Fowler, N.H., Hoster, E., Ladetto, M., Morschhauser, F., Zucca, E., Salles, G. & Sargent, D.J. (2017) Thirty-Month Complete Response as a Surrogate End Point in First-Line Follicular Lymphoma Therapy: An Individual Patient-Level Analysis of Multiple Randomized Trials. *Journal of Clinical Oncology,* **35,** 552-560.

Shi, W., Dong, L., Sun, Q., Ding, H., Meng, J. & Dai, G. (2018b) Follicular helper T cells promote the effector functions of CD8+ T cells via the provision of IL-21, which is downregulated

due to PD-1/PD-L1-mediated suppression in colorectal cancer. *Experimental Cell Research,* **372,** 35-42.

Shirota, H., Klinman, D.M., Ito, S.-e., Ito, H., Kubo, M. & Ishioka, C. (2017) IL4 from T Follicular Helper Cells Downregulates Antitumor Immunity. *Cancer Immunology Research,* **5,** 61-71.

Smeltzer, J.P., Jones, J.M., Ziesmer, S.C., Grote, D.M., Xiu, B., Ristow, K.M., Yang, Z.Z., Nowakowski, G.S., Feldman, A.L., Cerhan, J.R., Novak, A.J. & Ansell, S.M. (2014) Pattern of CD14⁺ Follicular Dendritic Cells and PD1⁺ T Cells Independently Predicts Time to Transformation in Follicular Lymphoma. *Clinical Cancer Research,* **20,** 2862-2872.

Smith, A., Crouch, S., Lax, S., Li, J., Painter, D., Howell, D., Patmore, R., Jack, A. & Roman, E. (2015) Lymphoma incidence, survival and prevalence 2004-2014: sub-type analyses from the UK's Haematological Malignancy Research Network. *Br J Cancer,* **112,** 1575-1584.

Sohani, A.R., Pitcher, B., Chadburn, A., Said, J.W., Martin, P., Czuczman, M.S., Bartlett, N.L., Rosenbaum, C.A., Leonard, J.P., Cheson, B.D. & Hsi, E.D. (2015) Interfollicular CD10 Expression and Follicular PD1 Tumor-Infiltrating Lymphocytes As Biologic Risk Factors in Patients with Previously Untreated Follicular Lymphoma Receiving Rituximab-Based Biologic Therapy: An Alliance Correlative Science Study (CALGB 50901, 50402, 50701, 50803, 50401). *Blood,* **126,** 334-334.

Solal-Céligny, P., Roy, P., Colombat, P., White, J., Armitage, J.O., Arranz-Saez, R., Au, W.Y., Bellei, M., Brice, P., Caballero, D., Coiffier, B., Conde-Garcia, E., Doyen, C., Federico, M., Fisher, R.I., Garcia-Conde, J.F., Guglielmi, C., Hagenbeek, A., Haïoun, C., LeBlanc, M., Lister, A.T., Lopez-Guillermo, A., McLaughlin, P., Milpied, N., Morel, P., Mounier, N., Proctor, S.J., Rohatiner, A., Smith, P., Soubeyran, P., Tilly, H., Vitolo, U., Zinzani, P.-L., Zucca, E. & Montserrat, E. (2004) Follicular Lymphoma International Prognostic Index. *Blood,* **104,** 1258-1265.

Stine, Z.E., Walton, Z.E., Altman, B.J., Hsieh, A.L. & Dang, C.V. (2015) MYC, Metabolism, and Cancer. *Cancer Discovery,* **5,** 1024-1039.

Stone, E.L., Pepper, M., Katayama, C.D., Kerdiles, Y.M., Lai, C.Y., Emslie, E., Lin, Y.C., Yang, E., Goldrath, A.W., Li, M.O., Cantrell, D.A. & Hedrick, S.M. (2015) ICOS coreceptor signaling inactivates the transcription factor FOXO1 to promote Tfh cell differentiation. *Immunity,* **42,** 239-251.

Strasser, A., Harris, A.W. & Cory, S. (1993) E mu-bcl-2 transgene facilitates spontaneous transformation of early pre-B and immunoglobulin-secreting cells but not T cells. *Oncogene,* **8,** 1-9.

Sungalee, S., Mamessier, E., Morgado, E., Gregoire, E., Brohawn, P.Z., Morehouse, C.A., Jouve, N., Monvoisin, C., Menard, C., Debroas, G., Faroudi, M., Mechin, V., Navarro, J.M., Drevet, C., Eberle, F.C., Chasson, L., Baudimont, F., Mancini, S.J., Tellier, J., Picquenot, J.M., Kelly, R., Vineis, P., Ruminy, P., Chetaille, B., Jaffe, E.S., Schiff, C., Hardwigsen, J., Tice, D.A., Higgs, B.W., Tarte, K., Nadel, B. & Roulland, S. (2014) Germinal center reentries of BCL2-overexpressing B cells drive follicular lymphoma progression. *J Clin Invest,* **124,** 5337-5351.

Sureda, A., Zhang, M.-J., Dreger, P., Carreras, J., Fenske, T., Finel, H., Schouten, H., Montoto, S., Robinson, S., Smith, S.M., Boumedil, A., Hamadani, M. & Pasquini, M.C. (2018) Allogeneic hematopoietic stem cell transplantation for relapsed follicular lymphoma: A combined analysis on behalf of the Lymphoma Working Party of the EBMT and the Lymphoma Committee of the CIBMTR. *Cancer,* **124,** 1733-1742.

Swerdlow, S.H., Campo, E., Harris, N.L., Jaffe, E.S., Pileri, S.A., Stein, H., Thiele, J. & Vardiman, J.W. (2008) *WHO classification of tumours of haematopoietic and lymphoid tissues.* . IARC, Lyon, France:.

Swerdlow, S.H., Campo, E., Pileri, S.A., Harris, N.L., Stein, H., Siebert, R., Advani, R., Ghielmini, M., Salles, G.A., Zelenetz, A.D. & Jaffe, E.S. (2016) The 2016 revision of the World Health Organization classification of lymphoid neoplasms. *Blood,* **127,** 2375-2390.

Tan, C.S., Bord, E., Broge, T.A.J., Glotzbecker, B., Mills, H., Gheuens, S., Rosenblatt, J., Avigan, D. & Koralnik, I.J. (2012) Increased Program Cell Death–1 Expression on T Lymphocytes of Patients With Progressive Multifocal Leukoencephalopathy. *JAIDS Journal of Acquired Immune Deficiency Syndromes,* **60,** 244-248.

Tarte, K., Rodriguez, S., Ame-Thomas, P., Saintamand, A., Alizadeh, M., Monvoisin, C., Subero, I.M. & Lamy, T. (2017) Follicular Lymphoma Regulatory T Cell Function and Origin. *Blood,* **130,** 2762-2762.

Taskinen, M., Karjalainen-Lindsberg, M.-L., Nyman, H., Eerola, L.-M. & Leppä, S. (2007) A High Tumor-Associated Macrophage Content Predicts Favorable Outcome in Follicular Lymphoma Patients Treated with Rituximab and Cyclophosphamide-Doxorubicin-Vincristine-Prednisone. *Clinical Cancer Research,* **13,** 5784-5789.

Thijssen, R., Slinger, E., Weller, K., Geest, C.R., Beaumont, T., van Oers, M.H., Kater, A.P. & Eldering, E. (2015) Resistance to ABT-199 induced by microenvironmental signals in chronic lymphocytic leukemia can be counteracted by CD20 antibodies or kinase inhibitors. *Haematologica,* **100,** e302-306.

Tobin, J.W.D., Keane, C., Gunawardana, J., Mollee, P., Birch, S., Hoang, T., Lee, J., Li, L., Huang, L., Murigneux, V., Fink, J.L., Matigian, N., Vari, F., Francis, S., Kridel, R., Weigert, O., Haebe, S., Jurinovic, V., Klapper, W., Steidl, C., Sehn, L.H., Law, S.-C., Wykes, M.N. & Gandhi, M.K. (2019) Progression of Disease Within 24 Months in Follicular Lymphoma Is Associated With Reduced Intratumoral Immune Infiltration. *Journal of Clinical Oncology,* **0,** JCO.18.02365.

Townsend, W., Pasikowska, M., Yallop, D., Phillips, E.H., Patten, P.E.M., Salisbury, J.R., Marcus, R., Pepper, A. & Devereux, S. (2019) The architecture of neoplastic follicles in follicular lymphoma; analysis of the relationship between the tumor and follicular helper T-cells. *Haematologica***,** haematol.2019.220160.

Travert, M., Ame-Thomas, P., Pangault, C., Morizot, A., Micheau, O., Semana, G., Lamy, T., Fest, T., Tarte, K. & Guillaudeux, T. (2008) CD40 Ligand Protects from TRAIL-Induced Apoptosis in Follicular Lymphomas through NF-κB Activation and Up-Regulation of c-FLIP and Bcl-x_L. *The Journal of Immunology,* **181,** 1001-1011.

Trotman, J., Fournier, M., Lamy, T., Seymour, J.F., Sonet, A., Janikova, A., Shpilberg, O., Gyan, E., Tilly, H., Estell, J., Forsyth, C., Decaudin, D., Fabiani, B., Gabarre, J., Salles, B., Van Den Neste, E., Canioni, D., Garin, E., Fulham, M., Vander Borght, T. & Salles, G. (2011) Positron emission tomography-computed tomography (PET-CT) after induction therapy is highly predictive of patient outcome in follicular lymphoma: analysis of PET-CT in a subset of PRIMA trial participants. *J Clin Oncol,* **29,** 3194-3200.

Tsujimoto, Y., Gorham, J., Cossman, J., Jaffe, E. & Croce, C. (1985) The t(14;18) chromosome translocations involved in B-cell neoplasms result from mistakes in VDJ joining. *Science,* **229,** 1390-1393.

Vendel, A.C., Calemine-Fenaux, J., Izrael-Tomasevic, A., Chauhan, V., Arnott, D. & Eaton, D.L. (2009) B and T Lymphocyte Attenuator Regulates B Cell Receptor Signaling by Targeting Syk and BLNK. *The Journal of Immunology,* **182,** 1509-1517.

Wahlin, B.E., Aggarwal, M., Montes-Moreno, S., Gonzalez, L.F., Roncador, G., Sanchez-Verde, L., Christensson, B., Sander, B. & Kimby, E. (2010) A Unifying Microenvironment Model in Follicular Lymphoma: Outcome Is Predicted by Programmed Death-1–Positive, Regulatory, Cytotoxic, and Helper T Cells and Macrophages. *Clinical Cancer Research,* **16,** 637-650.

Wahlin, B.E., Yri, O.E., Kimby, E., Holte, H., Delabie, J., Smeland, E.B., Sundström, C., Christensson, B. & Sander, B. (2012) Clinical significance of the WHO grades of follicular

lymphoma in a population-based cohort of 505 patients with long follow-up times. *British Journal of Haematology,* **156,** 225-233.

Wallin, E.F., Jolly, E.C., Suchánek, O., Bradley, J.A., Espéli, M., Jayne, D.R.W., Linterman, M.A. & Smith, K.G.C. (2014) Human T-follicular helper and T-follicular regulatory cell maintenance is independent of germinal centers. *Blood,* **124,** 2666-2674.

Wang, C., Kang, S.G., Lee, J., Sun, Z. & Kim, C.H. (2009) The roles of CCR6 in migration of Th17 cells and regulation of effector T-cell balance in the gut. *Mucosal Immunol,* **2,** 173-183.

Wang, C.J., Heuts, F., Ovcinnikovs, V., Wardzinski, L., Bowers, C., Schmidt, E.M., Kogimtzis, A., Kenefeck, R., Sansom, D.M. & Walker, L.S.K. (2015) CTLA-4 controls follicular helper T-cell differentiation by regulating the strength of CD28 engagement. *Proceedings of the National Academy of Sciences,* **112,** 524-529.

Watanabe, M., Takagi, Y., Kotani, M., Hara, Y., Inamine, A., Hayashi, K., Ogawa, S., Takeda, K., Tanabe, K. & Abe, R. (2008) Down-Regulation of ICOS Ligand by Interaction with ICOS Functions as a Regulatory Mechanism for Immune Responses. *The Journal of Immunology,* **180,** 5222-5234.

Weber, J.P., Fuhrmann, F., Feist, R.K., Lahmann, A., Al Baz, M.S., Gentz, L.-J., Vu Van, D., Mages, H.W., Haftmann, C., Riedel, R., Grün, J.R., Schuh, W., Kroczek, R.A., Radbruch, A., Mashreghi, M.-F. & Hutloff, A. (2015) ICOS maintains the T follicular helper cell phenotype by down-regulating Krüppel-like factor 2. *The Journal of Experimental Medicine,* **212,** 217-233.

Weinstein, J.S., Herman, E.I., Lainez, B., Licona-Limón, P., Esplugues, E., Flavell, R. & Craft, J. (2016) TFH cells progressively differentiate to regulate the germinal center response. *Nature Immunology,* **17,** 1197.

Westin, J.R., Chu, F., Zhang, M., Fayad, L.E., Kwak, L.W., Fowler, N., Romaguera, J., Hagemeister, F., Fanale, M., Samaniego, F., Feng, L., Baladandayuthapani, V., Wang, Z., Ma, W., Gao, Y., Wallace, M., Vence, L.M., Radvanyi, L., Muzzafar, T., Rotem-Yehudar, R., Davis, R.E. & Neelapu, S.S. (2014) Safety and activity of PD1 blockade by pidilizumab in combination with rituximab in patients with relapsed follicular lymphoma: a single group, open-label, phase 2 trial. *Lancet Oncol,* **15,** 69-77.

Wing, James B., Ise, W., Kurosaki, T. & Sakaguchi, S. (2014) Regulatory T Cells Control Antigen-Specific Expansion of Tfh Cell Number and Humoral Immune Responses via the Coreceptor CTLA-4. *Immunity,* **41,** 1013-1025.

Wogsland, C.E., Greenplate, A.R., Kolstad, A., Myklebust, J.H., Irish, J.M. & Huse, K. (2017) Mass Cytometry of Follicular Lymphoma Tumors Reveals Intrinsic Heterogeneity in Proteins Including HLA-DR and a Deficit in Nonmalignant Plasmablast and Germinal Center B-Cell Populations. *Cytometry B Clin Cytom,* **92,** 79-87.

Yamashita, I., Nagata, T., Tada, T. & Nakayama, T. (1993) CD69 cell surface expression identifies developing thymocytes which audition for T cell antigen receptor-mediated positive selection. *Int Immunol,* **5,** 1139-1150.

Yang, L. & Zhang, Y. (2017) Tumor-associated macrophages: from basic research to clinical application. *Journal of Hematology & Oncology,* **10,** 58.

Yang, Z.-Z., Kim, H.J., Villasboas, J.C., Price-Troska, T., Jalali, S., Wu, H., Luchtel, R.A., Polley, M.-Y.C., Novak, A.J. & Ansell, S.M. (2019) Mass Cytometry Analysis Reveals that Specific Intratumoral CD4⁺ T Cell Subsets Correlate with Patient Survival in Follicular Lymphoma. *Cell Reports,* **26,** 2178-2193.e2173.

Yang, Z.Z., Grote, D.M., Ziesmer, S.C., Niki, T., Hirashima, M., Novak, A.J., Witzig, T.E. & Ansell, S.M. (2012) IL-12 upregulates TIM-3 expression and induces T cell exhaustion in patients with follicular B cell non-Hodgkin lymphoma. *J Clin Invest,* **122,** 1271-1282.

Yang, Z.Z., Grote, D.M., Ziesmer, S.C., Xiu, B., Novak, A.J. & Ansell, S.M. (2015a) PD-1 expression defines two distinct T-cell sub-populations in follicular lymphoma that differentially impact patient survival. *Blood Cancer J,* **5,** e281.

Yang, Z.Z., Grote, D.M., Ziesmer, S.C., Xiu, B., Novak, A.J. & Ansell, S.M. (2015b) PD-1 expression defines two distinct T-cell sub-populations in follicular lymphoma that differentially impact patient survival. *Blood cancer journal,* **5,** e281-e281.

Yildiz, M., Li, H., Bernard, D., Amin, N.A., Ouillette, P., Jones, S., Saiya-Cork, K., Parkin, B., Jacobi, K., Shedden, K., Wang, S., Chang, A.E., Kaminski, M.S. & Malek, S.N. (2015) Activating STAT6 mutations in follicular lymphoma. *Blood,* **125,** 668-679.

Yoo, H.Y., Kim, P., Kim, W.S., Lee, S.H., Kim, S., Kang, S.Y., Jang, H.Y., Lee, J.-E., Kim, J., Kim, S.J., Ko, Y.H. & Lee, S. (2016) Frequent CTLA4-CD28 gene fusion in diverse types of T-cell lymphoma. *Haematologica,* **101,** 757-763.

Zan, H. & Casali, P. (2013) Regulation of Aicda expression and AID activity. *Autoimmunity,* **46,** 83-101.

Zhang, J., Dominguez-Sola, D., Hussein, S., Lee, J.E., Holmes, A.B., Bansal, M., Vlasevska, S., Mo, T., Tang, H., Basso, K., Ge, K., Dalla-Favera, R. & Pasqualucci, L. (2015) Disruption of KMT2D perturbs germinal center B cell development and promotes lymphomagenesis. *Nat Med,* **21,** 1190-1198.

Zheng, B., Xu, G., Chen, X., Marinova, E. & Han, S. (2015) ICOSL-mediated signaling is essential for the survival and functional maturation of germinal center B cells through the classical NF-κB pathway (IRM10P.611). *The Journal of Immunology,* **194,** 131.139-131.139.

Zhou, M., Zou, R., Gan, H., Liang, Z., Li, F., Lin, T., Luo, Y., Cai, X., He, F. & Shen, E. (2014) The effect of aging on the frequency, phenotype and cytokine production of human blood CD4 + CXCR5 + T follicular helper cells: comparison of aged and young subjects. *Immunity & Ageing,* **11,** 12.